Preface: International Congress on Renewable Energy

(ICORE-2021)

. The conference organized on 27/11/2021 by the school of Electrical and Electronics Engineering, REVA University has provided a platform to share and exchange the recent innovations and developments in the area of Renewable Energy. This conference proceedings contains the full version of the articles presented by researchers during the conference.

The conference attracted 75 articles and out of which only 22 articles were selected after screening by esteemed reviewers. Quality and relevance were the two main screening objectives for the selection of the articles. The conference provided an excellent platform for researchers and experts from industries across the globe to deliberate on various themes of global interests. The conference had three key-note lectures by eminent experts from abroad and five parallel sessions. The participants appreciated all the key-note lectures and interacted well with the experts.

The organizing members of ICORE-2021 would like to express their sincere gratitude to all the authors for their dedicated contributions to this proceeding. We are very grateful to the International/National advisory committee, keynote speakers, reviewers and session chairs for all the support. Our sincere thanks to the members of various committees, office & technical staff for sparing their valuable time in organizing the conference successfully. Last but not the least, we are thankful for the enormous support of River Publishers for supporting us in every step of our journey toward successful conduction of this conference.

Edited by:

Dr. Vivekanandan Subburaj
Dr. Ritesh Dash
Dr. K Jyotheeswara Reddy

A Bridge Type DC-DC Converter with Dual Input for Hybrid Energy System

[1]Sivaprasad Athikkal, [2]Ravi Eswar Kodumur Meesala, [3]Vivekanandan Subburaj

[1-2]Department of EEE, SRM IST, Kattankulathur, India.

[3]School of Electrical and Electronics Engineering, Reva University, Bangalore, India

sivanuday@gmail.com

Abstract

A proper power electronic circuit is critical in the hybridization of various sources of energy as their relevance is reached a milestone in the area of hybrid energy application. A dual input bridge type DC-DC converter to incorporate various energy sources is introduced in this paper. The proposed converter is better suited for all the basic modes of operations like buck, buck-boost etc. In this paper experimental and simulation validation of the converter is performed for buck-boost operation. Performance evaluation with other reported topologies is done based on the various aspects such as efficiency, component count etc. It clearly reveals that the given converter holds large voltage conversion ratio, fewer number of components and a good efficiency profile.

Keywords. Hybrid energy integration, multi input DC-DC converters, DIBC converter.

1. INTRODUCTION

Due to increasing demand of non-conventional sources in the power generation scenario, the hybridization of various energy sources has gained more attention. Hybrid Energy System (HES) is a key answer intended for the problems associated with the power generation from the individual energy sources. These renewable sources and storages like a battery are greatly utilised to structure an HES [1-2]. In conventional method, multiple numbers of DC-DC converters with single input are coupled in parallel manner and it marks in high intricacy in controller part, high cost, and reduction in the compactness and low efficiency profile. To surpass these drawbacks, the perception of multi input DC-DC converters (MICs) is discussed. Major attractive features of MICs are reduced complexity, cost and good efficiency profile [4-6]. Since MICs have several advantages compared to single input converters, their application is radically increased in the recent HES applications. Many MICs are previously reported in the literature [4-14], where they classified in to isolated and non-isolated MICs. In isolated topologies, the existence of transformers with multiple winding to provide isolation enhances the cost of the system and also enhances the complexity. A

MIC with flux additivity feature is discussed in [7]. Various MICs and their identification methods are described in [8-10]. A two input converter is introduced for distinct sources addition in [11]. A new MIC that can be applied for renewable applications is introduced in [12].

The converters discussed in the literature can be used for a variety of applications. But some of the converter [3], [12] are restricted for the simultaneous power supply from the input sources. Even though some MICs [4] are well suited for both individual and simultaneous power supply, large number of components present in these converters increases the complexity and reduces the efficiency. Many of the reported MICs are only capable for unidirectional operation; hence they are not appropriate for specific applications such as electric vehicle where bi-directional operation is an essential criterion. Thus, in this paper, an effort is done to propose a Dual input Bridge type DC-DC (DIBC) converter that is skilful of parallel and series energy supply capacity from input sources without any compromise in efficiency and cost. The operating principle and functioning states of DIBC converter are described in subsequent sections.

2. DUAL INPUT BRIDGE TYPE DC-DC (DIBC) CONVERTER

The idea of DIBC converter is conceived from the concept of normal DC-DC converter. The structure of DIBC converter topology is displayed in Figure 1. The circuit has diodes (D_1&D_2) and power switches (S_1-S_m) along with the inductor and capacitor. With the proper control of S_1, S_2 and S_3, the individual, concurrent operation of the inputs can be realized. The conduction of diodes and S_m decides the possible operating modes. With respect to switching scheme opted, four working states are present in buck-boost mode as revealed in Figure 2 (a-d).Four functioning states of DIBC converter are mentioned below:

***State 1*:** Figure 2a shows the equivalent circuit of state 1. Here S_1 and S_m are ON, where the other devices are non-conducting. Thus V_1 energizes the inductor and energy to the load is provided by the capacitor.

***State 2*:** Figure 2b shows the equivalent circuit of state 1. Here, the ON devices are S_2 and S_m and all other devices are turned OFF. Here, energy to the load is given by the capacitor, source V_2 charges the inductor.

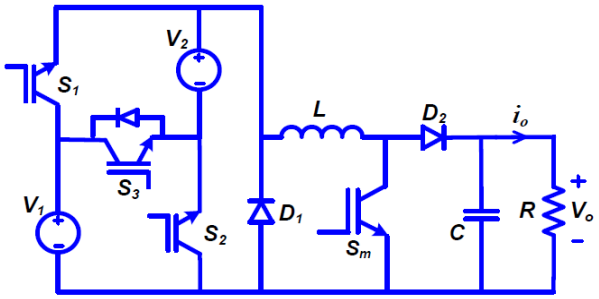

Figure 1. Basic circuit of DIBC converter.

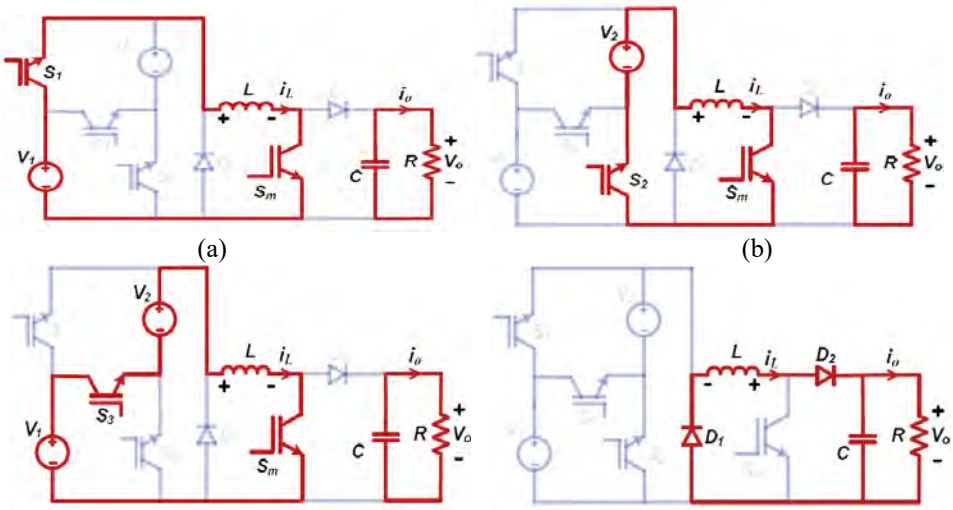

Figure 2.States of DIBC converter (a) V_1 is delivering the power (b)V_2 is delivering the power (c) V_1 and V_2 simultaneously supplies the power (d) Freewheeling state.

***State 3*:** Figure 2c displays, the converter circuit in state 3. The conducting devices are S_3 and S_m, and all other devices are in non-conducting state. S_3conduction supports to realize the series supply of inputs. Here, the inductor is energized simultaneously by both input sources.

***State 4*:** Figure 2d shows the structure of the converter in state 4. Only diodes are conducting in this state and the inductor energy is freewheeled through D_1 and D_2.

2.1. DIBC Converter Analysis

The Detailed converter analysis is conducted in CCM of the inductor for buck-boost operation. Based on the concept of volt-second balance, a DC-DC converter should have zero average inductor voltage which can be expressed as

$$V_1 d_1 + V_2 d_2 + (V_1 + V_2) d_3 - V_0(1 - d_1 - d_2 - d_3) = 0 \quad (1)$$

Hence the expression for the output voltage is

$$V_0 = \frac{V_1 d_1 + V_2 d_2 + (V_1 + V_2) d_3}{(1 - d_1 - d_2 - d_3)} \quad (2)$$

The value of the inductor can be determined from the below expression;

$$L = \frac{V_0(1 - (d_1 + d_2 + d_3)}{\Delta i_L f} \quad (3)$$

Similarly, the capacitor value can be determined as

$$C = \frac{V_o(d_1 + d_2 + d_3)}{R \Delta V_o f} \quad (4)$$

3. SIMULATION ANALYSIS AND DISCUSSION

The converter simulation is performed in MATLAB/Simulink platform. The specifications chosen are revealed in Table 1. Waveforms of DIBC converter in buck-boost state for a total duty ratio of greater than 0.5 are depicted in Figure 3. From Figure 3(b), it is observed that the inductor is energized with a voltage of 90 V and 70 V for first two working states. Then it is energized with 160 V (V_1+V_2) for d_3 and is de-energized with -240 V (-Vo).

Table 1. Simulation parameters of DIBC converter.

Input 1 (V)	Input 2 (V)	L (mH)	C (µF)	F (kHz)	Vo (V) Buck-boost
90	70	5	470	20	240/80

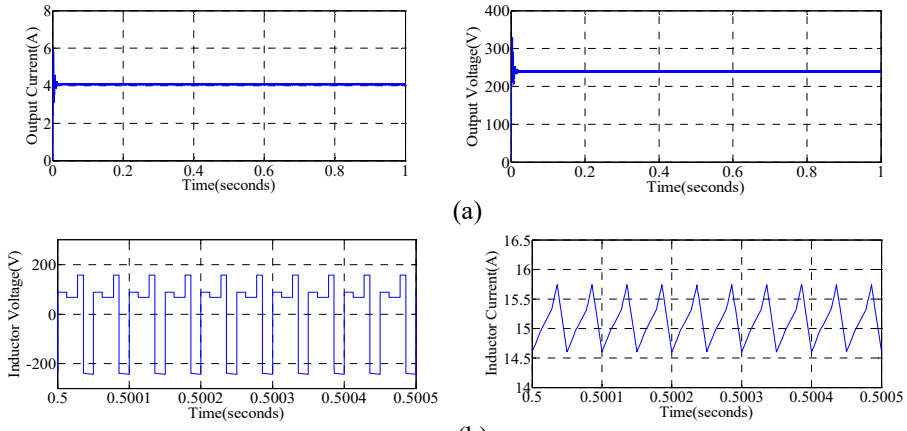

Figure 3. Simulation wave form: (a) output voltage, current (b) inductor voltage, current (d > 0.5).

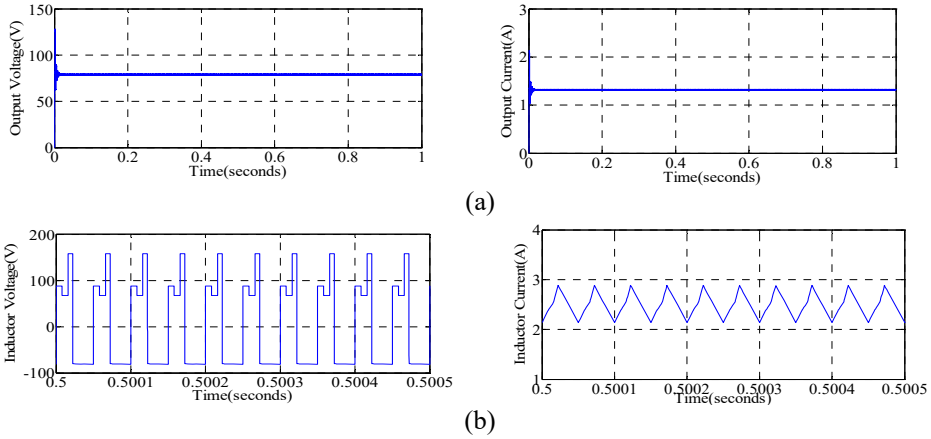

Figure 4. Simulation wave forms: (a) Load voltage, current (b) voltage, current of inductor (d < 0.5).

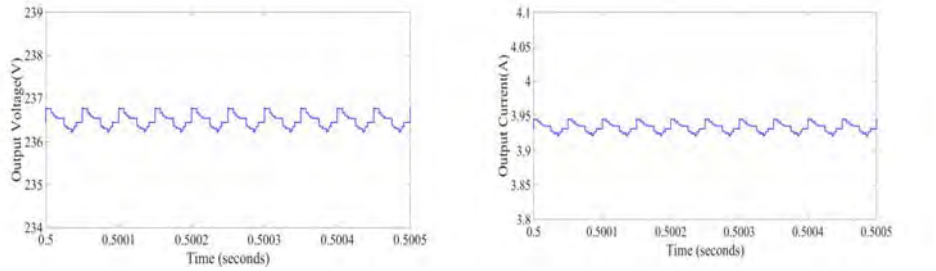

Figure 5. Ripple content in load voltage and current in steady state condition.

Simulation waveforms of the converter for a total duty ratio of less than 0.5 in buck-boost mode are illustrated in Figure 4. The inductor is charged by 90 V, 70 V and 160 V for d_1, d_2 and d_3 correspondingly. Finally, it is de-energized by V (-Vo). The simulation of DIBC converter is done with ideal components, due to which the results are so closer to theoretical investigation of the converter. Figure 5 shows the ripple contents presents in the output current and voltage. From the analysis it is verified that the amount of ripple contents are within the permissible limit.

4. EXPERIMENTAL RESULTS

To verify the practicability of DIBC converter in real time condition, a hardware prototype is built. Using LabVIEW 2013 software, gate pulses are generated by a frequency of 20 kHz. The switches of DIBC converter are realised with IRFP 460 MOSET and MUR 860 diodes are also used. The specifications considered for the analysis are already tabulated in Table 1. Various waveforms such as output voltage, inductor voltage etc., are recorded and are illustrated in Figure 6 (a-b). For a duty ratio lesser than 0.5, the voltage obtained at the output is 77 V (Figure 6(a)), and for a duty ratio of greater than 0.5, the measured output voltage is 200 V (Figure 6(b)). Here the experimental and simulation results are well matched each other. From these results it is inferred that, the DIBC converter is well appropriate for the hybrid energy source incorporation and is competent to deliver energy to the load in individual and simultaneous manner. The efficiency values are plotted with respect to the power variation as given in Figure 7. From the figure, it can be summarised that the efficiency range of DIBC converter is good. Quantitative comparison of the DIBC converter with other converters is conducted based on the parameters like, efficiency, count of switching devices etc., and are described in Table 2.

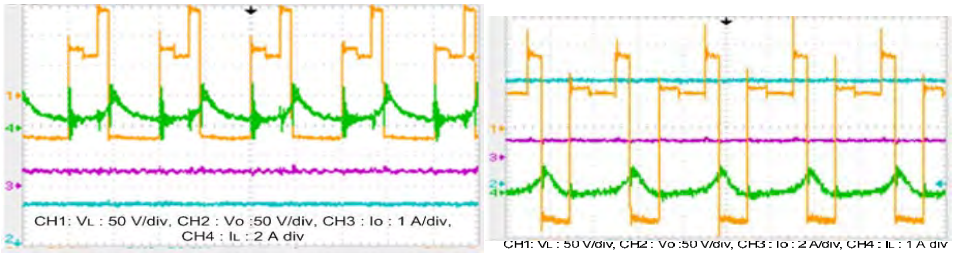

(a) (b)

Figure 6. Hardware waveforms of voltage, current of the inductor, output voltage and current (a) for duty ratio less than 0.5(b) for duty ratio greater than 0.5.

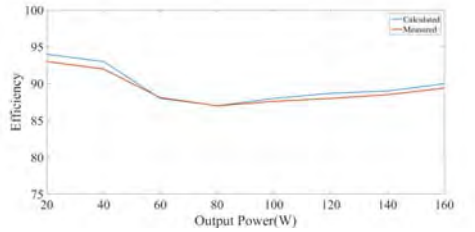

Figure 7. Efficiency analysis of DIBC converter.

Table 2. Comparison of DIBC converter and other reported MICs.

Converter proposed	Switching Devices	Inductor	Capacitor	Voltage stress	Efficiency (%)
Converter in [4]	2n	n	1	V_o	78-91
Converter in [6]	n+4	1	1	V_n	80-92
DIBC converter	n+4	1	1	V_n	88-93

n: Number of inputs

5. CONCLUSION

A two input bridge type DC-DC converter is proposed in this article to include two input sources. Complete converter analysis is performed for buck-boost operation. The hardware evaluation of DIBC converter is conducted to confirm the correctness of simulation outcomes. From the analyses, the converter operation is found acceptable. The efficiency analysis of the DIBC converter is conducted to confirm the superior performance DIBC converter. From the overall analysis, it is noticed that the DIBC converter has certain merits such as optimized structure, low voltage stresses and lower component count due to which the converter efficiency is good. These merits definitely boost up the significance of DIBC converter in the specific applications such as renewable energy incorporation, microgrid, and hybrid electric vehicle.

6. REFERENCES

[1] Cao and A. Emadi, 'A New Battery/UltraCapacitor Hybrid Energy Storage System for Electric, Hybrid, and Plug-In Hybrid Electric Vehicles', in IEEE Transactions on Power Electronics, vol. 27, no. 1, pp. 122-132, Jan. 2012.

[2] S. Kumar and H. P. Ikkurti, 'Design and control of novel power electronics interface for battery-ultracapacitor Hybrid Energy Storage System', International Conference on Sustainable Energy and Intelligent Systems (SEISCON 2011), pp. 236-241, 2011.

[3] A. Khaligh, J. Cao and Y. Lee, 'A Multiple-Input DC–DC Converter Topology', in IEEE Transactions on Power Electronics, vol. 24, no. 3, pp. 862-868, March 2009.

[4] Kumar, L and Jain, S., 'Multiple-input DC/DC converter topology for hybrid energy system', in IET Power Electronics, vol.6, no.8, pp.1483-1501, September 2013.

[5] Y. Li, X. Ruan, D. Yang, F. Liu and C. K. Tse, 'Synthesis of Multiple-Input DC/DC Converters', in IEEE Transactions on Power Electronics, vol. 25, no. 9, pp. 2372-2385, Sept. 2010.

[6] Y. Liu and Y. Chen, 'A Systematic Approach to Synthesizing Multi-Input DC/DC Converters', 2007 IEEE Power Electronics Specialists Conference, pp. 2626-2632, 2007.

[7] Yaow-Ming Chen, Yuan-Chuan Liu and Feng-Yu Wu, 'Multi-input DC/DC converter based on the multiwinding transformer for renewable energy applications', in IEEE Transactions on Industry Applications, vol. 38, no. 4, pp. 1096-1104, July-Aug. 2002.

[8] A. Kwasinski, 'Identification of Feasible Topologies for Multiple-Input DC–DC Converters', in IEEE Transactions on Power Electronics, vol. 24, no. 3, pp. 856-861, March 2009.

[9] S. Athikkal and K. M. R. Eswar, 'A Three Input Dual Output Boost Type Non Isolated DC-DC Converter', 2021 International Conference on Intelligent Technologies (CONIT), pp. 1-6, 2021.

[10] G. Guru Kumar, K. Sundaramoorthy, S. Athikkal and V. Karthikeyan, 'Dual input super boost DC-DC converter for solar powered electric vehicle', in IET Power Electronics, vol. 12, no. 9, pp. 2276-2284, 2019.

[11] Athikkal, S., Sundaramoorthy, K., Sankar, A, 'Development and performance analysis of dual-input DC–DC converters for DC microgrid application', IEEJ Trans. Electr. Electron. Eng., 2018, 13, (7), pp. 1034–1043.

[12] S. Athikkal, 'Performance Evaluation of A Positive Output Voltage Dual Input DC-DC Converter', 2021 2nd International Conference for Emerging Technology (INCET), pp. 1-5, 2021.

Critical Bus Ranking and Severity Prediction using Data Mining and ML Technique under n-1 Condition

Ravi V Angadi[1], Suresh Babu Daram[2], P. S Venkataramu[3]

[1, 3]Department of Electrical and Electronics Engineering, Presidency University, Bengaluru, Karnataka, India

[2]Department of Electrical and Electronics Engineering, Sree Vidyanikethan Engineering College, Tirupati, AP, India

[1]raviangadi404@gmail.com, [2]sureshbabudaram@gmail.com, [3]venkataramups1@gmail.com

Abstract.

The load dispatch centre must identify critical or weak buses for each operational situation. It is now more important than ever due to the potential of voltage instability and voltage collapse. This article explore the application of data mining and machine learning techniques to identify and to predict the critical bus ranking under n-1 condition. In the process of static steady analysis, there will be a significant amount of data will generate during the contingency analysis process, and it is critical to figure out how to transfer that data to the system's value in order to evaluate the severity of the system. Data analysis through the use of data mining and machine learning techniques helps to predict the risk that bus services may suffer in a variety of load scenarios. The study is carried on IEEE 30 bus system; the data for the study is generated by computing VCPI for different load conditions. In the analysis, the MATLAB & WEKA Data Mining Software was employed.

Keywords. Contingency analysis, VCPI, Critical Bus, Data Mining, Machine Learning, severity prediction.

1. INTRODUCTION

The possible reasons for a power outage can range from major (with a huge impact) to minor (with a small impact). To properly control and ensure power system failures, impact assessments and system contingency rankings are essential. A system which compares the losses of one machine to the others' influence is utilized to conduct a general critical load bus identification (N-1 contingency criteria). There is often a consideration for the loss of a generator, a transformer, and a transmission line in the N-1 contingency analysis. [1-3]. Increasing use of stressed power systems creates voltage stability and system security challenges. A huge issue is the impact of a power outage. It's significant since one of the main problems is the frequency of a line outage, which has a drastic influence on the system's balance (pre-contingency case) electric power demand that allows for the utility provider to adjust the frequency without instability [4].

When a line outage occurs, the system is forced to function under the contingency state for an extended period of time. To avoid voltage collapse, a previous knowledge of the load bus voltage stability margins under various contingency situations is required. This may be acquired by monitoring and taking control action against any changes in those margins. One of the major causes of voltage collapse is the system's failure to provide reactive power, as a result of a growing load [5].

The likelihood of voltage collapse occurring is strongly influenced by the maximum load a certain bus can support. Trying to raise the load past this threshold would lead to the system falling out of control, which might cause the voltage to collapse. The massive overload would seem to prove that the main system's power capacity would be unable to handle it [4-5]. The maximum loadability of a load bus in the system is estimated using VCPI. The load buses are rated according to their maximum loadability, with the lowest maximum loadability being placed first. The bus has the least amount of strength, since its

maximum load capacity is low, and the load has already overloaded the voltage to the point of failing.

Planning or operation engineers can utilize this information to ensure that the amount of equipment they install does not put the voltage stability limit at risk by beyond the maximum loadability of the system. Overloading a bus above a certain critical level leads the system to collapse unless the system is adjusted properly. The key voltage stability margin is what this study defines as the threshold for bus loading. Estimating the criticality of a bus may be done by calculating the voltage stability margin. It is important to know where to put the additional voltage support devices so as to minimize voltage instability, which is why figuring out where the key buses are is advantageous.

The planning power engineer must use this facts to correctly communicate. So, Big Data and machine learning approaches are providing a new framework that gives solutions to clean up poor data and support the power engineers in making informed decisions in the future about operation and planning [6-7]. The relevance and use of big data analytics in many areas is comprehensively discussed [8]. The simulation data is mined using a data mining tool with a j48 classification algorithm to estimate the transmission line severity [6-7] [9].

The VCPI is employed in this article to rank the buses. Data analytics tools are used to process the huge amount of data that is generated from simulation, and machine learning is used to evaluate the potential severity of the bus condition and identify conditions that could lead to it. Training data is evaluated by running the j48 classification algorithm and is fed to the machine learning, which identifies the potential risks that the bus could face.

This document has six parts. Section II describes the critical bus ranking technique. Section III introduces a data mining process. Section IV describes the proposed algorithm, whereas Section V discusses the Case Study and Results. Section VI concludes.

2. APPROACH OF CRITICAL BUS RANKING

The load dispatch centre must identify the crucial bus for a particular operational state. According to the operator's needs, these important buses will be prioritized based on load situations and voltages. Recent power systems' voltage instability and voltage collapse have made the bus ranking duty even more critical. The voltage collapse prediction indicator (VCPI) combines the voltage magnitude and voltage angle information at buses and the network admittance matrix to forecast voltage collapse [5] [10]. A successful approach of assigning importance to buses based on their capacity to tolerate voltage disturbances. The load restriction technique is used to create a ranking index for buses. The index identifies how bad things go in a bus (such as excessive voltage oscillations) if a particular situation occurs. The critical bus in the system is determined by an indication of voltage collapse [10]. The effectiveness of load monitoring may be achieved for all the load buses in the system utilizing VCPI. The model may be derived at bus k by using complex number identities, as stated in Eqn (1). When VCPI is equal to 1, the system is considered unstable [11].

$$VCPI_{kth,bus} = \left| 1 - \frac{\sum_{\substack{m=1 \\ m \neq k}}^{N} \left| V_m^{'} \right|}{V_k} \right| \quad \ldots\ldots\ldots \quad (1)$$

3. CRITICAL BUS ANALYSIS USING DATA PROCESSING AND DATA MINING

In the process of computing VCPI for various load condition, a huge volume of data will be generated dusting the steady state analysis. Handling the data is the huge problem of today because of the fast expansion of extracting data and transforming it into usable information. Data mining is a way of detecting patterns and valuable information using huge data sets. Even while organizations have seen more improvements in data management, their executives are still running into issues with scalability and automation [12]. This research analyses the relationship between data mining methods and support, and it will be possible to categorize the various methods into two distinct aims: either defining the target dataset or creating algorithms to make predictions [13].

The power engineers use data mining to identify significant information, connect patterns, and spot linkages. The typical sequence of Data mining includes four steps: establishing objectives, collecting and processing data, applying Data mining techniques, and assessing results. There are many simulations have to be done to learn the load flows of the system under different loading circumstances in order to better understand the results of contingency analysis. Many data processing steps will be needed in this process; data mining will be better suited to addressing the contingency analysis of power systems [3] [6-7].

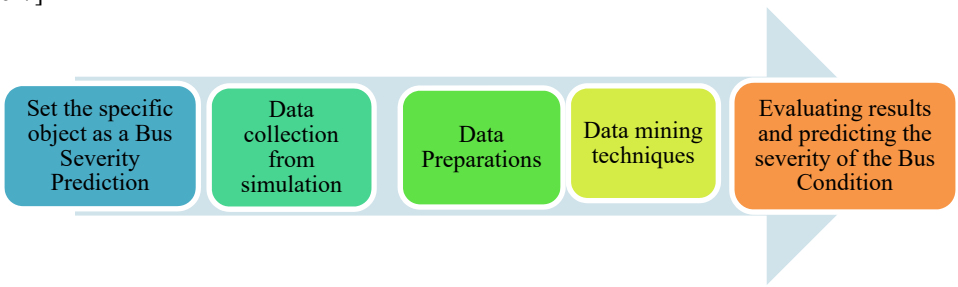

Figure 1. Data mining process applied to contingency study of power system

The schematic process flow of data mining techniques is presented in Figure 1, which illustrates the use of contingency analysis on the power system. Setting the specified object is the initial stage of data mining, and should take the least amount of time. First, data must be collected. This approach may vary depending on the system being used. Initially, three types of data are collected: Structured, unstructured, and semi-structured data.

To aid power engineers in addressing important issues, data mining collects and organizes data sets from simulation processes. Depending on the dataset, limiting the number of dimensions might further improve performance. While high frequency patterns have broader applications, data variances may be more fascinating to suggest probable severity forecasts. It is possible to apply classification algorithms based on the provided data at the fourth stage of data mining process. This is done by labelling the incoming data (supervised learning). The findings must be examined and comprehended when the data is aggregated. When finishing results, they should be valid, fresh, useful, and understandable. When these conditions are met, the suggested system may use this data to develop new techniques for successful severity prediction of bus.

4. PROPOSED ALGORITHM

The data mining approach was applied to the contingency analysis of the power system to rank the severity of the buses. The VCPI was calculated in accordance with eqn. (1). The following algorithm demonstrates the use of the constructed model; the model is shown to be effective.

Step No. 1: Read System Data.

Step No. 2: Compute the load flow solution by NR Method.

Step No. 3:	Calculate Voltage collapse proximity indicator for different load conditions.
Step No. 4:	Computed results to be saved.CSV file format.
Step No. 5:	Read the Voltage Collapse proximity indicator of each bus.
Step No. 6:	Data Processing Using Big Data Analytics tool.
Step No. 7:	Select Explorer in WEKA & Load the Data file saved in. CSV file format
Step No. 8:	Click on classification and save file in .arff format after selecting Select Classification-Tree-J48, and use training set and click on the start option to predict the severity and ranking of the each line.
Step No. 9:	Right Click for option of tree J48 which is shown on the Result List window.
Step No. 10	Print the severity and contingency ranking of bus.

Supervised learning is a machine learning technique that anticipates the input-output relationship. Supervised learning is used to determine transmission line severity under various load situations. Regression and classification models are among the most prominent groups of techniques used for control [6-7] [14]. A classification algorithm may be used in operational data mining to create models of both classification and regression. Decisions are made using a decision tree, the basis of which is a tree categorization [6-7] [15].

5. CASE STUDY AND RESULTS

The suggested method's performance is tested by using IEEE-30's bus system to run a simulation. For the active and reactive power, the convergence limit is 0.00001. The basic MVA of the system is 100 MVA. The IEEE-30 bus system consists of 1-slack buses, 5-generator buses, 24 load buses, and 41 transmission lines [3]. When it comes to finding out the root cause of power system instability, critical bus is important. The identification of the most important bus occurs by prioritizing buses by importance. A transmission-line outage was the scenario taken into account. In this scenario, you take off one transmission line at a time. Critical buses are ranked by the usage of VCPI for IEEE-30. The case studies analysed are explained by considering two different loading condition under single line transmission out age conditions.

Table.1: List of Bus Ranking under n-1 of transmission line outage with base load condition.

Bus Rank No	Bus No. when line 4 outaged	Bus No. when line 18 outaged	Bus No. when line 24 outaged	Rank No	Bus No. when line 4 outaged	Bus No. when line 18 outaged	Bus No. when line 24 outaged
1	11	11	11	16	22	20	1
2	3	13	13	17	24	19	25
3	13	12	12	18	27	6	6
4	12	2	15	19	5	5	5
5	16	17	17	20	23	24	28
6	14	16	2	21	4	15	8
7	10	21	16	22	29	18	27
8	1	9	20	23	25	29	23
9	2	1	14	24	9	8	30
10	21	3	22	25	30	25	10
11	17	14	21	26	7	30	24
12	15	22	9	27	8	10	26
13	19	27	19	28	26	23	4
14	20	11	18	29	6	26	7

15	18	13	3	30	28	4	29

The ranking for the buses was based on the computation of VCPI. The rankings are as mentioned in table 1 for different line outages and it is observed very clearly from the table 1 the bus ranking is varied for different line outage scenario. The critical bus rankings are dependent on how severe the situation is. Critically severe ranges from 1 to 10, then from 11 to 20 and 21 to 30 for the lower levels of severity as mentioned in the table.

Table.2: Critical Bus Ranking Classification

Sl. No	Condition	Ranks
1	Critical	1 to 10
2	Semi- Critical	11 to 20
3	Non-critical	21 to 30

The same analysis was carried for different loading and observed it for top 10 contingency ranking is listed. The single line outages are considered into account separately to prepare the data for different loading conditions, in all three scenarios. The data produced is firstly pre-processed and categorized with j48 classification algorithms by ranging as critical, semi-critical and non-critical.

Table. 3: Trained Data set for Base Load Condition for different line outages.

Sl. No	C No.	VCPI	Condition	Sl. No	C No.	VCPI	Condition
1	C_No_3	0.1373	Critical	31	C_No_12	0.1674	Critical
2	C_No_3	0.1340	Critical	32	C_No_12	0.1596	Critical
3	C_No_3	0.1649	Critical	33	C_No_12	0.1598	Critical
4	C_No_3	0.1026	Non Critical	34	C_No_12	0.1154	Semi Critical
5	C_No_3	0.1054	Semi Critical	35	C_No_12	0.1043	Semi Critical
6	C_No_3	0.0522	Non Critical	36	C_No_12	0.1318	Critical
7	C_No_3	0.0879	Non Critical	37	C_No_12	0.1323	Critical
8	C_No_3	0.0866	Non Critical	38	C_No_12	0.1021	Semi Critical
9	C_No_3	0.0963	Non Critical	39	C_No_12	0.1094	Semi Critical
10	C_No_3	0.1420	Critical	40	C_No_12	0.1107	Semi Critical
11	C_No_3	0.1915	Critical	41	C_No_18	0.1099	Semi Critical
12	C_No_3	0.1551	Critical	42	C_No_18	0.1307	Critical
13	C_No_3	0.1644	Critical	43	C_No_18	0.1125	Semi Critical
14	C_No_3	0.1445	Critical	44	C_No_18	0.0513	Non Critical
15	C_No_3	0.1320	Semi Critical	45	C_No_18	0.1029	Semi Critical
16	C_No_3	0.1468	Critical	46	C_No_18	0.1041	Semi Critical
17	C_No_3	0.1324	Semi Critical	47	C_No_18	0.0469	Non Critical
18	C_No_3	0.1293	Semi Critical	48	C_No_18	0.0936	Non Critical
19	C_No_3	0.1315	Semi Critical	49	C_No_18	0.1196	Semi Critical
20	C_No_3	0.1297	Semi Critical	50	C_No_18	0.0819	Non Critical
21	C_No_12	0.1199	Critical	51	C_No_18	0.1636	Critical
22	C_No_12	0.1346	Critical	52	C_No_18	0.1542	Critical
23	C_No_12	0.1166	Critical	53	C_No_18	0.1560	Critical
24	C_No_12	0.0554	Non Critical	54	C_No_18	0.1252	Critical
25	C_No_12	0.1069	Semi Critical	55	C_No_18	0.1363	Critical
26	C_No_12	0.1077	Semi Critical	56	C_No_18	0.1288	Critical
27	C_No_12	0.0506	Non Critical	57	C_No_18	0.1313	Critical
28	C_No_12	0.0976	Non Critical	58	C_No_18	0.1172	Semi Critical
29	C_No_12	0.1214	Critical	59	C_No_18	0.1194	Semi Critical
30	C_No_12	0.0816	Non Critical	60	C_No_18	0.1264	Critical

The severity was predicted based on VCPI which was computed for different line outage condition, the data generated during this phenomenon was in high volume and was processed with the help of data analytic and machine learning tools. In this analysis 65% of the data is used for training to predict the severity of the line and 35% of the data is used to test based on the training data set. Table.3 shows the training data set for the different load condition.

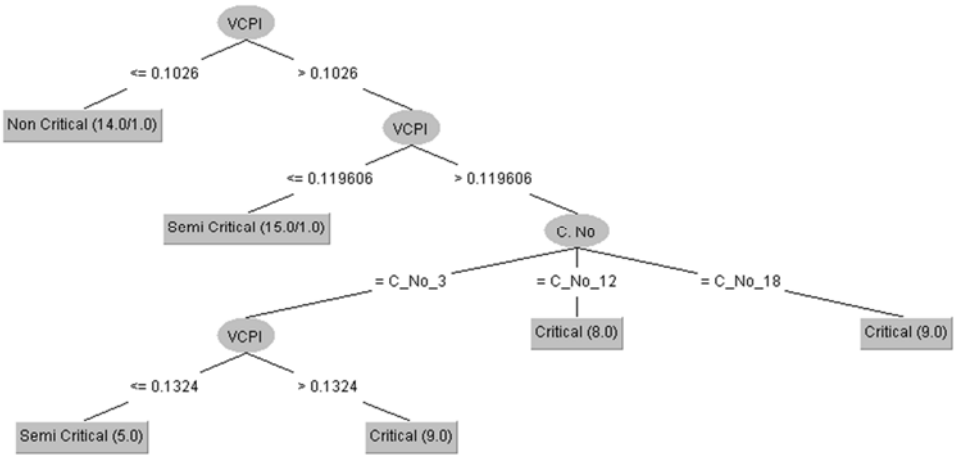

Figure 2. Decision tree for predicting the severity condition of the buses for different line outages.

Table. 4: Tested Data set for Base Load Condition for different line outages

Sl. No	C No.	VCPI	Condition	Sl. No	C No.	VCPI	Condition
1	C_No_3	0.1336	Critical	16	C_No_12	0.0705	'Non Critical'
2	C_No_3	0.126	'Semi Critical'	17	C_No_12	0.1133	'Semi Critical'
3	C_No_3	0.1034	'Semi Critical'	18	C_No_12	0.0164	'Non Critical'
4	C_No_3	0.1224	'Semi Critical'	19	C_No_12	0.0989	'Non Critical'
5	C_No_3	0.0984	'Non Critical'	20	C_No_12	0.0896	'Non Critical'
6	C_No_3	0.078	'Non Critical'	21	C_No_18	0.12	Critical
7	C_No_3	0.1173	'Semi Critical'	22	C_No_18	0.1218	Critical
8	C_No_3	0.0091	'Non Critical'	23	C_No_18	0.0894	'Non Critical'
9	C_No_3	0.1025	'Non Critical'	24	C_No_18	0.0797	'Non Critical'
10	C_No_3	0.0931	'Non Critical'	25	C_No_18	0.1057	'Semi Critical'
11	C_No_12	0.1222	Critical	26	C_No_18	0.0712	'Non Critical'
12	C_No_12	0.1146	'Semi Critical'	27	C_No_18	0.0929	'Non Critical'
13	C_No_12	0.0763	'Non Critical'	28	C_No_18	0.1003	'Non Critical'
14	C_No_12	0.1062	'Semi Critical'	29	C_No_18	0.0043	'Non Critical'
15	C_No_12	0.0905	'Non Critical'	30	C_No_18	0.0844	'Non Critical'

Figure.2 shows the decision tree chart for the basic loading condition for different line outages was illustrated. By considering the categorization, in table 4, the critical, semi-critical and non-critical ranges are tabulated and severity forecast for the buses based on the VCPI's are provided. The Figure 3 shows visualization classifier error for base load condition under different line outage. The data scattered visualization is obtained for different condition and analysed by using the visualization classifier errors. Based on the training data set, the sample missing data set conditions are predicted for the base load condition under single line outage is shown in Figure 4.

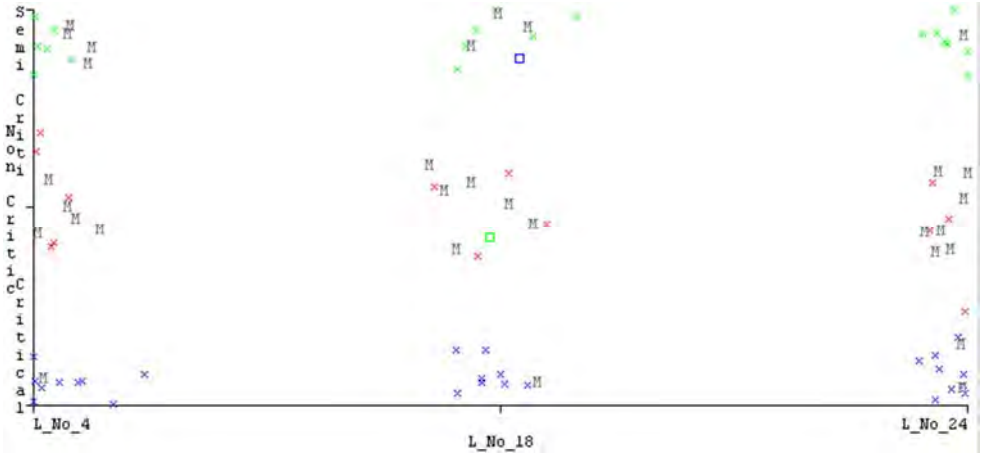

Figure 3. Visualization of Condition versus line number for base load condition for line outages

6. CONCLUSION

This study employs a classification approach to predict the critical buses by computing VCPI, and it does so depending on the ranking procedure. The J48 classification technique yielded nearly identical results to manual categorization. Using the top 10 rank index values, it was decided that rank-10 represents a serious issue, with rankings from 10 to 20 representing partially severe conditions, and ranks more than 20 representing typical conditions is achieved, the proposed method efficient to predict the severity of the busses by using the data mining technique, simulation data is processed and severity of the busses were predicted by using classification algorithm.

7. ACKNOWLEDGEMENTS

The authors like to express their gratitude to the managements of Presidency University, Bengaluru, and Sree Vidyanikethan Engineering College, Tirupati, for their continual support and provision of facilities necessary for the completion of this study.

REFERENCES

[1] N. Wannoi, N. Jirsuwankul, C. Chompoo-inwai, C. Chompoo-inwai and C. Wannoi, "Novel Techniques for Critical Load Buses Identification and Load Bus's Available Capacity Calculation to Improve Power System Stability," *2020 IEEE/IAS Industrial and Commercial Power System Asia (I&CPS Asia), 2020*, pp. 799-804, doi: 10.1109/ICPSAsia48933.2020.9208413.

[2] Ali Abdulwahhab Abdulrazzaq, "Contingency ranking of power systems using a performance index," *International Research Journal of Engineering and Technology*, vol. 02, Iss. 02, May-2015, pp. 180 -183

[3] R. V. Angadi, S. Babu Daram, D. Pravallika and P. S. Venkataramu, "Contingency Ranking Through Big Data Analytics with GIPFC in Power System under n-1Condition," *2020 IEEE 17th India Council International Conference (INDICON), 2020*, pp. 1-6, doi: 10.1109/INDICON49873.2020.9342527.

[4] Shobha Shankar, & Ananthapadmanabha. (2011). "Fuzzy Approach to Critical Bus Ranking Under Normal and Line Outage Contingencies", *International Journal on Soft Computing*, 2(1), 59–69. doi:10.5121/ijsc.2011.2106

[5] Jain, M, Venkataramu, P S, and Ananthapadmanabha, T. "Critical bus ranking under line outage contingencies", Canada: N. p., 2007. Web.

[6] R. V. Angadi, S. B. Daram and P. S. Venkataramu, "Contingency Analysis of Power System using Big Data Analytic Techniques," *2020 5th International Conference on Computing, Communication and Security (ICCCS), 2020*, pp. 1-7, doi: 10.1109/ICCCS49678.2020.9276796.

[7] R. V. Angadi, S. Babu Daram and P. S. Venkataramu, "Analysis of Power System Security using Big Data and Machine Learning Techniques," *2020 IEEE 17th India Council International Conference (INDICON), 2020*, pp. 1-8, doi: 10.1109/INDICON49873.2020.9342458.

[8] Ravi V Angadi, P. S Venkataramu and Suresh Babu Daram, "Role of Big Data Analytics in Power System Application", *2nd International Conference on Design and Manufacturing Aspects for Sustainable Energy GRIET Hyderabad India, E3S Web Conf.* 184 01017 (2020) DOI: 10.1051/e3sconf/202018401017

[9] Ravi V Angadi, P. S Venkataramu and Suresh Babu Daram, "Severity Prediction of Single Transmission Line Outage using Big Data and Machine Learning Techniques", *International Journal of Grid and Distributed Computing,* vol. 13, no. 2, pp. 1090-1108, 2020.

[10] V. Balamourougan, T. S. Sidhu and M. S. Sachdev, "Technique for Online Prediction of Voltage Collapse", *IEE Proceedings on Generation, Transmission and Distribution*, Vol. 151, No. 4, July 2004, pp. 453-460.

[11] Suresh Babu Daram, P. S. Venkataramu and M. S. Nagaraj, "Voltage Stability Index Based Critical Bus Ranking Incorporating IPFC under Single Transmission Line Outage Condition", *International Journal of Electrical Power System and Technology*, vol. 2, no. 1, pp. 12-19, 2016.

[12] https://www.ibm.com/cloud/learn/data-mining.

[13] Lior Rokach and Oded Maimon, "Data Mining with Decision Trees: Theory and Applications," *World Scientific Publishing Co. Pte. Ltd*, 2nd Edition 2014.

[14] Dr. Neeraj Bhargava, Girja Sharma, Dr. Ritu Bhargava, Manish Mathuria, "Decision Tree Analysis on J48 Algorithm for Data Mining", *International Journal of Advanced Research in Computer Science and Software Engineering*, vol 3, Iss. 6, June 2013, pp 1114 – 1119.

[15] Anand Kishor Pandey and Dharmveer Singh Rajpoot, "A comparative study of classification techniques by utilizing WEKA," IEEE-*2016 International Conference on Signal Processing and Communication, Noida*, 26-28 Dec. 2016, pp. 219-224.

Modelling, simulation and analysis of 5 MWe Linear Fresnel Collector based solar thermal energy conversion cycle with energy storage

Dr. P. Badari Narayana[1], Dr. S. Narasimha Kumar [2*]
Dr. Asheesh Kumar [3*]
[1]Associate Professor, Mahatma Gandhi Institute of Technology, Hyderabad, India
[2]Assistant Professor, Chaitanya Bharathi Institute of Technology, Hyd, India
[3] Assistant Professor, Mahatma Gandhi Institute of Technology, Hyderabad, India

Email
[1]badari.p@gmail.com , [2*] narasimha71110@gmail.com, mailasheesh@gmail.com [3*]

Abstract

Solar thermal energy conversion cycle is a preferable option for process industries both for steam generation and electricity generation. Linear Fresnel Reflector (LFR) Technology is becoming equally competitive to Parabolic Trough Technology for the past five years. It is cost effective, easy to install and requires relatively less land area. In this paper, a solar thermal energy conversion cycle with energy storage is designed based on LFR technology for a 5 MW electricity generation. Process heat generating industries in India can utilize the solar energy and power their equipment during solar and non-solar hours. Solar field based on LFR collectors is designed to heat the heat transfer fluid (HTF) flowing through the absorber tube. Solar salt in molten state is used as both the HTF and thermal energy storage (TES) material. Solar resource assessment data for a few Indian cities is mapped from National Solar Radiation Database (NSRDB) database. Length of the solar field along with different TES materials is designed for each location. The variation of mass flow rate of HTF against the plant operating hours is also analysed. The solar field area is an optimum choice between the plant equipment cost and the monthly electrical units generated. Out of ten locations analysed in this work, Ananthapuramu happens to be the best place for harnessing solar energy to generate electricity through thermal energy conversion cycle. At this place, annual energy yield of a 5 MWe Linear Fresnel solar thermal power plant is 12,500 MWH with 6 hours of storage.

Keywords: Solar thermal, Linear Fresnel Reflectors, Thermal Energy Storage, Annual Energy Yield, Molten Salt, Ananthapuramu.

1. INTRODUCTION

India is a country that has a locational advantage to capture sun energy with respect to equatorial plane. For most of the sites in India, average annual solar global radiation value is 5.75 kWh/m^2-day [1]. Solar thermal energy conversion is useful for industries for both process steam and electrical power generation. Ministry of New and Renewable Energy Sources has been trying to encourage solar thermal power for a decade in India. National Institute of Solar energy (NISE) at Gurugram has a test setup of 1 MW solar thermal power plant based on Parabolic Trough Collector (PTC) and Linear Fresnel Reflector (LFR) Technology [2]. Private developers have established these PTC based power generation units in megawatt sizes at Rajasthan and in Andhra Pradesh in during 2013-2014 [3,4]. World's largest Linear Fresnel Power plant is commissioned in India in 2014 and generates 280GWh of electrical energy per year [5]. LFR technology has crossed the demonstration stage but still not matured as PTC in terms of using it for process industries ranging from 500 kW to 5 MW in India. Telangana, Andhra Pradesh and other states have the solar thermal energy potential of 229 GW with a threshold Direct Normal Irradiance (DNI) of 1800 kWh/m^2/year and 36 GW with a threshold DNI of 1800 kWh/m^2/year [6]. There are a few important industrially popular sites in India with interesting values of DNI (with averages above 500 kW/m^2) that are favourable for LFR implementation. Such

sites have been invariably chosen to perform simulations in this work. Existing Process industries require steam for processes such as laundry, water and milk pasteurisation, automobile washing, agricultural drying, sterilization, fermentation and chemical synthesis. During the non-production times, the same plant can also feed electrical power to the grid as well or can operate on a hybrid scheme. Solar thermal projects for process heat and electricity power generation requirements can utilize the thermal energy storage (TES) to achieve a thermal backup for a discharge duration of 4 hours to 18 hours. Mount Abu, India has a solar thermal power plant with TES based on Scheffler dish that generates steam for daily cooking purposes. This plant was funded by UN Development Programme (UNDP), Global Environment Facility and Ministry of Renewable Energy Sources (MNRE), Government of India and uses a Cast Iron TES block at 450^0C to supply steam. Cast Iron and Molten Salt have only been tried in India till date as TES, where in usage of other storage materials made of Phase Change Materials (PCM) is yet to reach the commercial usage.

LFR concentrated solar thermal technology is most promising for electric energy production and process steam generation with a remarkable potential to reduce construction and maintenance costs [6]. In India, commercial LFR based solar thermal power plants cost Rs. 12 Crore per MW with an additional capital cost of Rs. 2 Crore per hour of TES [17].

Table 1 presents the list of relevant global research works on LFR performance simulation and couple of Indian commercial solar thermal power plants.

S.No	Details of the LFR plants in Literature	Techno-Commercial Performance Parameters reported
1	K.S. Reddy et al. (2012) Solar thermal power plant 100 MW Modelling & Simulation [8]	Net Energy Efficiency of 1 MWe - 16% Net Energy Efficiency of 50 MWe – 27.21% Levelized Cost of Energy (LCOE) – Rs. 10.19/ kWh Software used – Cycle Tempo
2	Deepak and Sudhakar (2017) [9]	263,973,360 kWh with the plant efficiency of 18.3 %. The capacity utilization of the proposed LFR plant is found to be 30.2%. Software Used – SAM (NREL)
3	Mokhtar Ghodbane et al.(2019) [16]	thermal efficiency of the solar reflector has reached 37.5%; absorbed tube temperature, it ranged between 264.78 and 347.78 _C; superheated steam temperature, it ranged between 233.38 and 263.73C Software Used – Numerical Analysis in FEM coded in MATLAB
4	A. Buscemi, et al. Concrete thermal energy storage for linear Fresnel collectors for a Pasta making Factory in Italy (2020) [10]	Plant area including Solar field and storage area 11000 m^2 Electricity units generated 4.3152 GWH Overall Solar field efficiency 39% with 48% of solar energy contributing to Storage. Software Used: TRNSYS
5	Reliance Solar thermal power plant 125 MW, Rajasthan, India (2014) [17]	280 GWh of electricity every year and can offset over 2.1 million tonnes of carbon dioxide for 10 years. Software used: Not Applicable.
6	LFR Solar thermal power plant Dadri Uttara Pradesh, India (2015) [19]	14MW plant developed by Thermax Ltd and Frenell GmbH, 30000 m^2 and Annual Energy Yield 14 GWh. Software used: Not Applicable.

7	Danish et al. Innovative Greenhouse-LFR concept (2021) [11]	greenhouse-LFR, the maximum thermal efficiency was 73.2% whereas for conventional-LFR it was 37.2% Modelled by SolTrace software
8	Present work	5 MWe solar thermal LFR and TES plant simulation modelling software used is SAM, NREL [18]

Table 1. Literature survey on LFR solar thermal power plants and their simulation studies

2. SOLAR THERMAL POWER PLANT MODELING

LFR technology requires improvements in terms of achieving higher optical efficiencies but has better competitive edge when compared for overall cost vs. efficiency. LFR achieves higher values of land use efficiency and wind loads can be neglected to design their low-profile structure [7]. It becomes essential to model a solar thermal energy conversion plant of LFR technology with TES for various sites in India for evaluating the feasibility of a 5 MWe sizing plant. This research work performs simulations of LFR based solar thermal plant for ten locations (cities) in India. The work is aimed at achieving following objectives:

1. Estimating the Annual Energy Yield at new potential locations in India with a 5 MW_e LFR Solar thermal power plant
2. Analysing the thermal and electrical outputs of the plant for 4 hours of thermal energy storage.

2.1. Solar resource estimation at identified sites for LFR plants:

The potential for Concentrated Solar thermal Power (CSP) in India is estimated to be 2800 GW. But for CSP projects, estimation of Direct Normal Irradiance is most important. Any deviations in the measurement of DNI leads to increase in the number of Fresnel mirrors after the commissioning of the power plant. The uncertainty in DNI values coming from Satellite data needs to be corrected with operating power plants data or through theoretical modelling. Out of the ten Indian cities (that are industrially popular and have many process industries present in and around) where data is collected from NSRDB database of NREL laboratory, basic solar radiation assessment exercise is performed so as to analyse the availability of solar radiation as per the declination angle and sun rise time. Solar declination is the angle between the earth-sun line and the equatorial plane.

Declination of any given location is given by the equation $\delta = 23.45\, Sin\left[\frac{360}{365}(284 + n)\right]$ ---(1).

Where *n* is the number of day and India, which is in Northern hemisphere, $\delta > 0$, during spring and summer (May 21st to September 21st) there is no much tracking is required as optimum tilt for an Indian location is zero for three months from May to July. And for those months where $\delta < 0$ (September 21st to March 21st) the optimum tilt angle required for the collector is ranging in between 24.290 to 560 [13]. Hence, studying the effect of declination angle with respect to sunrise time, so as to determine the tracking start time and program their values for SCADA systems is much vital for a tracking system design. There are many models to estimate the DNI values [14] and System Advisor Modelling (SAM) [18] developed by NREL, USA uses the National Solar Radiation Database (NSRDB) that has the data pertaining to various sites in India NSRDB data contains DNI, Direct Horizontal Irradiance (DHI), Dry-bulb Temperature, Dry bulb temperature (°C), Dew point temperature (°C), Relative humidity (%), Atmospheric pressure (mbar), Wind speed (only 2 metres above the ground value) (m/s), Wind direction (°E of N) and Albedo pertaining to the chosen location. . For designing the solar thermal collectors, only DNI data is significant.

2.2. Solar Thermal Power plant design

LFR based Linearly focussing systems are popular for both process steam generation and electricity power requirements due to their less construction, installation and integration costs. The reasons are - they do not have much moving joints, wind loads are lower due to near to ground mounting, least shading problems, tightly packed area with mirrors and simple-to-clean systems. Main disadvantage of LFR systems is they have optical losses. Concentrated ratios of LFR systems are 10 to 40, where as those of the Parabolic Trough systems are in between 30 to 100 [6]. Power plant for electricity generation using LFR technology has four major blocks – Linear Fresnel solar field, Storage Block,

Heat exchanger block and Power block (traditional Rankine cycle block without a boiler). In this work, The solar thermal power plant is designed and modelling is performed using SAM tool [18].

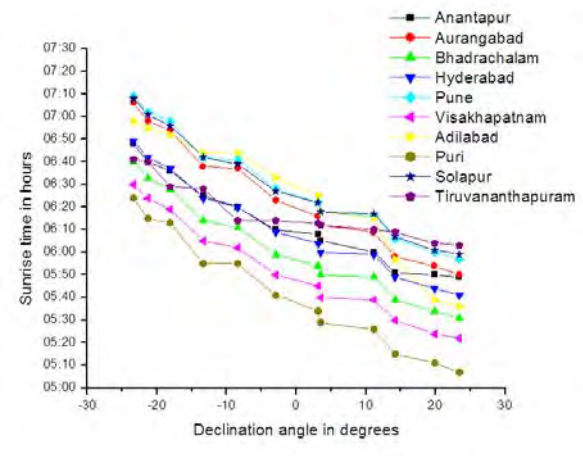

Fig 1. Variation of Sun rise time in Hours with declination angle at various locations in India

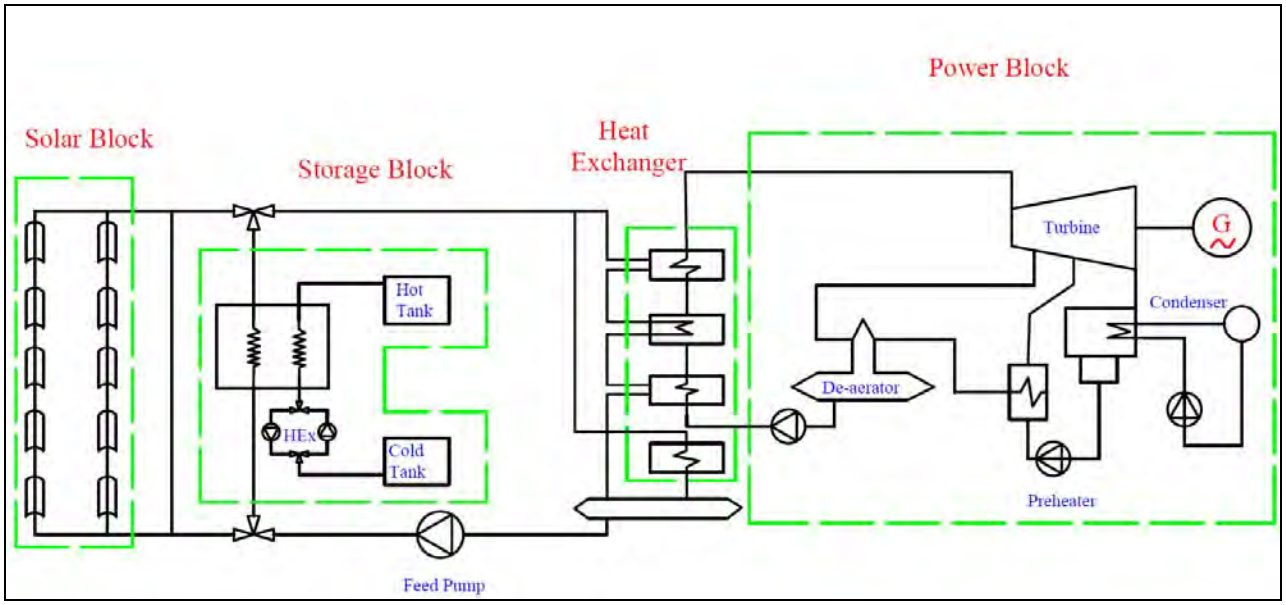

Fig 2. Block diagram of Solar Thermal Power plant with LFR and TES simulation

2.2.1. LFR Solar field array design

Linear Fresnel Reflectors are made of multiple narrow segments of mirrors concentrating the sunlight on an absorber tube above them. The absorber tube in LFR, is placed at the focal line of the Parabolic Trough. The principal advantage of LFR is they are placed near to ground, leading to minimal wind loads and less heavy structure. The basic module used in this work to design the LFR field array consists of 11 primary reflector units amounting to a total reflector surface of 22m^2 and a receiver unit [15]. The basic module is represented in the figure 2. Package density of the LFR module is defined as the ratio of aperture area to ground area. Mirror reflectivity is 95% with Scott PTR 70 receiver with direct solar absorptance 0.95 and optical efficiency of 0.635 at zenith angle. Maximum operating temperature of the absorber is 400^{0}C with a thermal loss coefficient of 0.000043W/m^2/K^2. Thermal output of the LFR module shown in the figure 3, is given by 12.3 kW/m^2 with a total installation surface area of 377 W/m^2. Single loop aperture area is 7524.8 m^2 and there are 7 such loops in the solar field. The characteristics of LFR system are defined as a function of overall efficiency of the

LFR system with respect to the temperature differential between the Heat Transfer Fluid (HTF) and the ambient temperature. It can be observed that for ambient temperatures in India, the system performance is near to its rated design efficiency value. The total collector area of 5 MW LFR power plant is 85000 m^2. Field are is 13 acres multiplied by non-solar field multiplier of 1.6.

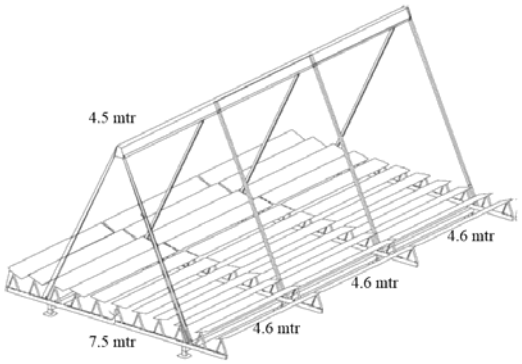

Fig.3. Drawing of the Fresnel solar collector module

Simulation block	Elements of interest	Remarks
Solar Resource Assessment	I_{bn}	Direct Normal Irradiance (data available from NSDRB data base directly) in kWh/m^2
Solar Field	Solar Collector Assembly (SCA)	Area of SCA (7.5 m X 4.6 m) = 22 m^2 Thermal output 12.3 kW per module [LF 11] 377 W/m^2 as per total installation surface area
	Conversion efficiency of the collector loop	Maximum efficiency 66.3%
	Total area of the solar field	52673.47 m^2 with Solar Multiple Value = 2.3
	Thermal energy output from solar field	30 MW_{th}
	Net-Effective land area required by the plant	85000 m^2
Heat transfer fluid (HTF)	Full load storage hours considered	4 Hours
TES	Storage volume	282.289 m^3
	Storage Tank diameter	4.23 m
	Minimum Fluid Volume	14.1144 m^3
	Thermal capacity of TES	50.38 MW_{th}
	Estimated Heat Loss	0.0436 MW_{th}
	HTF outlet temperature	525^0C
	Design inlet temperature of HTF Cycle	293^0C
	HTF mass flow rate	35.9 kg/sec
Power Block		
	Rated cycle conversion efficiency	39.7%
	Net electrical output of the plant at Nameplate	4.5 MW_e

Table. 2. Simulation parameters of Thermal Energy conversion cycle parameters of 5 MW_e.

2.2.2. HTF and TES flow arrangement:

HTF fluid selected for this simulation and modelling is molten salt and is flowing through the solar field array with 10 kg/hour that gets settled in hot and cold tanks. Hot and cold tanks are big cylindrical structures of the size of 4.23 diameter. The variation of HTF mass flow rate vs. the solar time is presented in the figure 4. It can be understood that outlet temperature of the HTF is almost directly proportional to the mass flow rate and is maximum during the noon. Field HTF is maintained at a minimum operating temperature of 238^0C and a maximum operating temperature of 593^0C. TES hot tank temperature is varying with solar time and reaches a maximum of 475^0C and at 2 PM, it starts decreasing till 465^0C up to 10 PM. The simulation tool has provision to use variety of Molten salts known as Hi-Tec Solar Salt, Therminol VP-1 and Dowtherm RP. Out of three HTFs, Hitec salt is found to be superior in performance. Hitech Salt (Solar Salt) used in solar plants consists of potassium nitrate (53% by weight), sodium nitrite $NaNO_2$ (40% by weight), and sodium nitrate (7% by weight) with a liquid temperature range of 149°C - 538°C. TES is also Hitec salt here, whose minimum storage temperature is 238^0C in the simulation cycle. For 4-hours storage, Total tank volume is 313 m^3 for a thermal capacity of 56 MW_{th}. TES fluid density is 1829.33 kg/m^3. Cold tank set point is 263^0C. The power plant design parameters are presented in table 1. The variation of mass flow rate and hourly variation of outlet temperature of HTF flowing in the receiver tubes of the solar field along with solar time is represented in the graph for Ananthapuramu Location at a mean day of the year. In between 8AM to 6PM the temperature and mass flow rate of the designed plant are around 500^0C and 160 Tonnes per hour respectively. Hourly variation of mass flow rate and HTF outlet temperature during a solar day is represented in Fig 4.

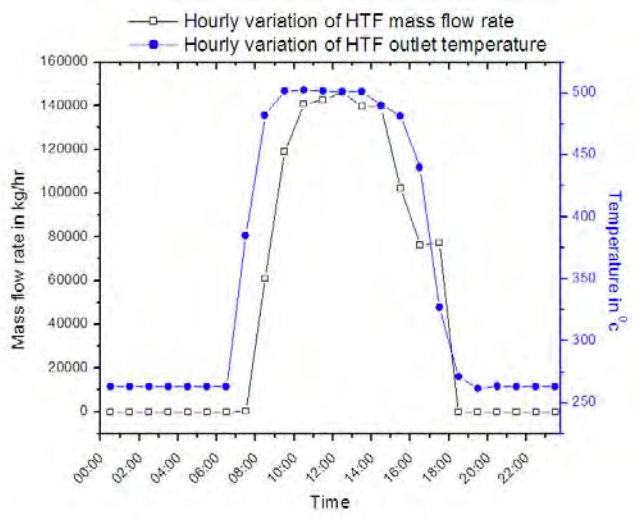

Fig. 4. Variation of Mass Flow rate of HTF during a solar day in the field

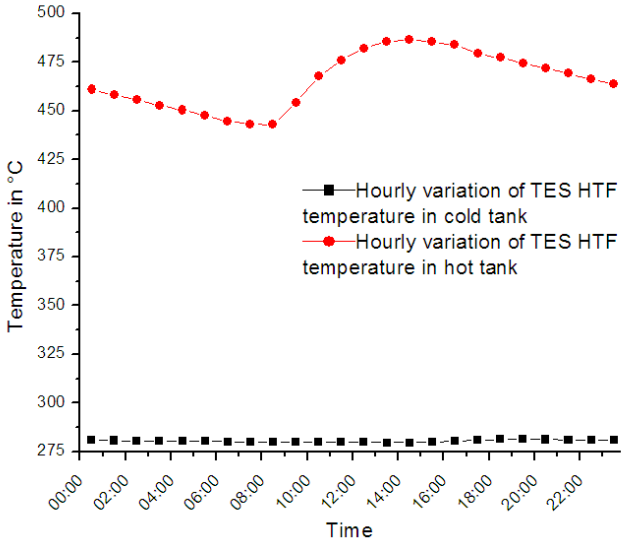

Fig. 5. Hourly variation of TES tanks temperature

Fig 5 shows the variation of TES material Molten Salt in the cold tank vs. hot tank during the solar hours or plant operation hours. It becomes crucial for the plant operation to maintain the temperatures of hot and cold tanks at a minimum of 475^0C so as to avoid the problems of HTF becoming frozen during cold climates.

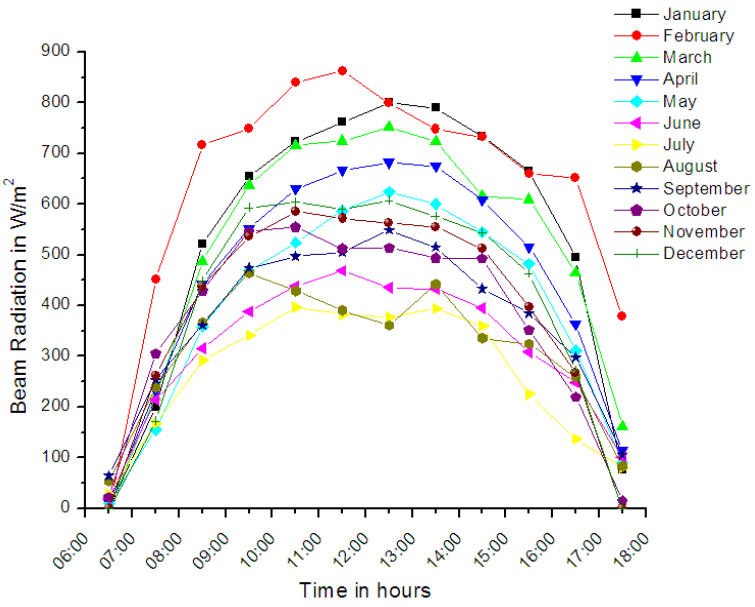

Fig 6. Distribution of Solar beam radiation in Ananthapuramu (Anantapur), India Long. Latt.

Fig 6, depicts the daily solar radiation spectrum around the year in Ananthapuramu location which happens to be highest of all the sites considered in this work. This place is the most favourable location for installing the solar thermal power plants in India.

Fig 7, displays the mean monthly net energy generation by a LFR solar thermal plant of 5 MWe capacity. The total number of electrical units generated Ananthapuramu in kWh has been found to be the highest.

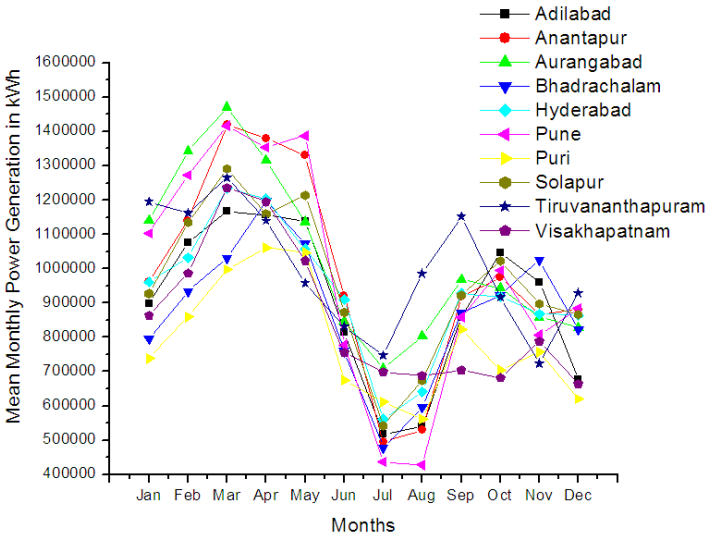

Fig 7. Mean monthly net energy generation units at various sites

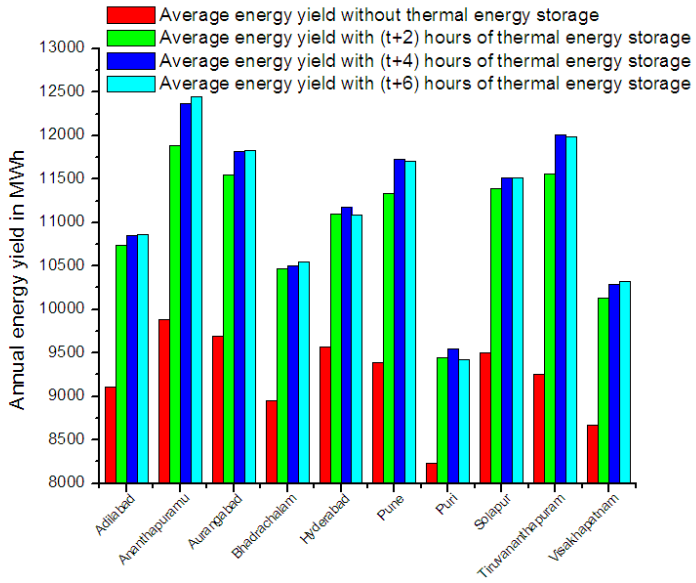

Fig.8. Annual Energy yield in kWh at various locations in India

Graph 8, compares the annual energy yield with and without storage at each location with Ananthapuramu being the location with the highest AEY.

Fig 9 and 10 show the variation of thermal and electrical power output from a 5 MW LFR plant installed at Ananthapuramu with its input Solar radiation i.e DNI. This annual average value is the point of interest to the power plant developer in preparing their detailed project report to be submitted for bankability.

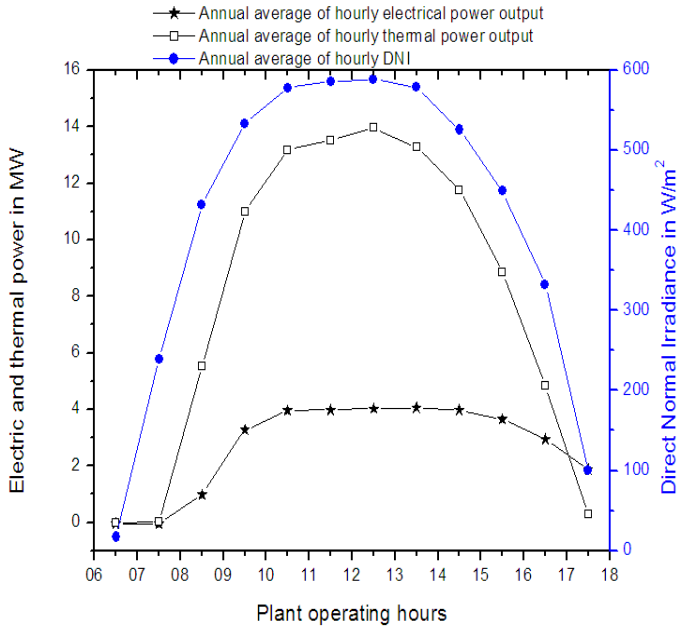

Fig.9. Electrical energy output of 5 Mwe LFR plant at Ananthapuramu location

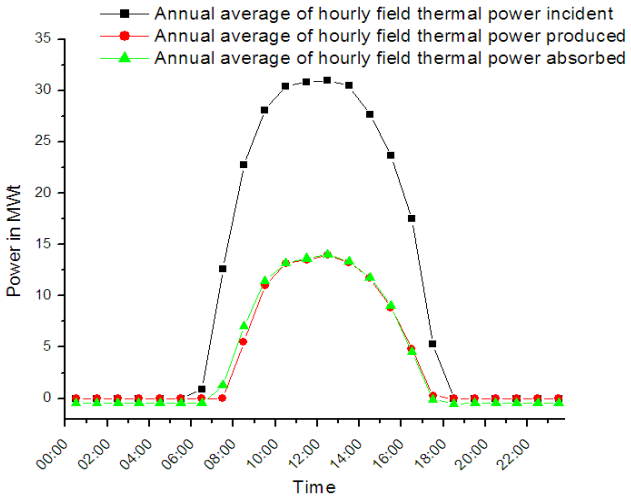

Fig. 10. Daily avaerage thermal energy output of LFR plant at Ananthapuramu

3. CONCLUSIONS

Solar thermal power plants are a preferable option to electricity where transportation of fuel is expensive such as deserts and dry arid land areas. Linear Fresnel Reflector (LFR) based solar thermal is a reliable, cost-effective technology for power generation in India. Ten industrially significant locations have been taken for analysis in this study and simulations have been performed to predict the Annual Energy Yield (in MWH_e per year) of a 5 MW_e LFR solar thermal power plant with TES, across all these locations. Out of all these locations, Ananthapuramu, Andhra Pradesh has been identified as a potential site for a 5 MW LFR plant. Ananthapuramu with the longitude and latitude values of 14.36 and 77.65N is a popular solar site with the high values of measured DNI. LFR technology has the advantage of cost vs. performance over the other concentrated solar thermal technologies. A 5 MW LFR solar thermal plant can generate 12500 MWH of Annual Energy Units at Ananthapuramu with energy storage being considered. The modelling & simulation performed in this work will be useful for analysing the daily and monthly performance of the plant with TES. This work highlights the usage of SAP modelling software for the simulation of concentrated solar thermal plants. With such analysis, power plant designers and developers can get an initial estimate on performance and can analyse the techno-commercial feasibility of the power plant in the location of interest. Currently CSP Projects in India, have been suffering with lack of policy upgradation & proper DNI assessment. Increased infrastructure costs, high maintenance costs and lack of indigenously manufactured LFR mirrors are the major hurdles for the growth of solar thermal power plants in India. More practical and industry-grade installations would ensure stabilised growth both in kW and MW scale in India. This research work is an attempt to help designing the solar thermal power plants for process industries having few acres of barren lands.

4. REFERENCES

1. Jamil, B., Siddiqui, A. T., & Akhtar, N. (2016). Estimation of solar radiation and optimum tilt angles for south-facing surfaces in Humid Subtropical Climatic Region of India. Engineering Science and Technology, an International Journal, 19(4), 1826-1835.11
2. Sharma, C., Sharma, A. K., Mullick, S. C., & Kandpal, T. C. (2015). Assessment of solar thermal power generation potential in India. Renewable and Sustainable Energy Reviews, 42, 902-912.
3. Desai, N. B., Bandyopadhyay, S., Nayak, J. K., Banerjee, R., & Kedare, S. B. (2014). Simulation of 1MWe solar thermal power plant. Energy Procedia, 57, 507-516.
4. Desai, N. B., & Bandyopadhyay, S. (2017). Line-focusing concentrating solar collector-based power plants: a review. Clean Technologies and Environmental Policy, 19(1), 9-35.
5. https://cleantechnica.com/2014/11/14/worlds-largest-linear-fresnel-csp-project-commissioned-india/

6. Karathanasis, S. (2019). Linear Fresnel Reflector Systems for Solar Radiation Concentration. Springer International Publishing.
7. Sun, J., Zhang, Z., Wang, L., Zhang, Z., & Wei, J. (2020). Comprehensive Review of Line-Focus Concentrating Solar Thermal Technologies: Parabolic Trough Collector (PTC) vs Linear Fresnel Reflector (LFR). Journal of Thermal Science, 1-28.
8. Reddy, K. S., Ravi Kumar, K., & Devaraj, V. A. (2012). Feasibility analysis of megawatt scale solar thermal power plants. Journal of Renewable and Sustainable Energy, 4(6), 063111.
9. Bishoyi, D., & Sudhakar, K. (2017). Modeling and performance simulation of 100 MW LFR based solar thermal power plant in Udaipur India. Resource-Efficient Technologies, 3(4), 365-377.
10. A. Buscemi, D. Panno, G. Ciulla, M. Beccali, V. Lo Brano, Concrete thermal energy storage for linear Fresnel collectors: Exploiting the South Mediterranean's solar potential for agri-food processes, Energy Conversion and Management,Volume 166,2018,Pages 719-734, ISSN 0196-8904, https://doi.org/10.1016/j.enconman.2018.04.075.
11. Danish, S. N., Almutairi, Z., El-Leathy, A., Al-Ansary, H., Jardan, Y., & Alaqel, S. (2021). Modeling and Performance Simulation of an Innovative Concept of Linear Fresnel Reflector based CSP System. Journal of Thermal Science, 1-11.
12. Baba, Y. F., Ajdad, H., Al Mers, A., Bouatem, A., Idrissi, B. B., & El Alj, S. (2020). Preliminary cost-effectiveness assessment of a Linear Fresnel Concentrator: Case studies. Case Studies in Thermal Engineering, 22, 100730.
13. Jamil, B., Siddiqui, A. T., & Akhtar, N. (2016). Estimation of solar radiation and optimum tilt angles for south-facing surfaces in Humid Subtropical Climatic Region of India. Engineering Science and Technology, an International Journal, 19(4), 1826-1835.
14. Mousavi Maleki, S. A., Hizam, H., & Gomes, C. (2017). Estimation of hourly, daily and monthly global solar radiation on inclined surfaces: Models re-visited. Energies, 10(1), 134.
15. Compact Linear Fresnel Reflector Technical Data sheet by Industrial Solar GmbH (www.industrial-solar.de)
16. Ghodbane, M., Boumeddane, B., Said, Z., & Bellos, E. (2019). A numerical simulation of a linear Fresnel solar reflector directed to produce steam for the power plant. Journal of cleaner production, 231, 494-508.
17. https://helioscsp.com/india-reliance-powers-dhursar-concentrated-solar-power-csp-project-nears-completion/

18. System advisor model (SAM) general description (Version 2020.11. 29). National Renewable Energy Laboratory Technical Report.
19. https://solarpaces.nrel.gov/project/dadri-iscc-plant

Ensuring energy sustainability in rural areas by the provision of solar street lighting system

[1]Arjyadhara Pradhan, [2]Lipika Nanda, [3]Babita Panda, [4]Chitralekha Jena

School of Electrical Engineering, KIIT Deemed to be University, Bhubaneswar, Odisha
arjyadhara.pradhanfel@kiit.ac.in
lnandafel@kiit.ac.in

Abstract

Odisha is a state of hills, and mountains, plains and rivers, forest, villages, and a good diversity of wildlife. Even though government of Odisha has developed many places and interconnected them with roadways and electricity, still there are places where proper communication by both roads and rail services are lagging. Streetlight facilities can someway help to overcome these problems and make life of rural people easier. Another critical problem lies in the remote areas is the communication system. Proper electric supply also has not reached these places, frequent power cuts, lack of maintenance, illiteracy, lack of technology are some of the problems faced by the people of these areas. Hence use of solar powered streetlight can solve these problems. Solar energy is freely available and only major cost is involved in the installation process. The maintenance cost is very minimal and with local technicians the maintenance work can also be done. In this paper solar street lighting system is designed using LED for ensuring energy sustainability in rural Odisha.

Keywords. Inverter, LED, Microcontroller, Photovoltaic, Rural, MPPT

1 INTRODUCTION

In the present scenario improving lighting efficiency is one of the ways of energy conservation and build sustainable energy development. The consumption of electricity from lighting sector is nearly 22% [1]. Moreover, emphasize is made on the use of renewable as it decreases the presence of carbon dioxide in the atmosphere [2]. Even use of non-conventional source helps nation to get rid of dependence on fossil fuels which causes much pollution [3]. From several years it has been seen that among various lighting systems solar streetlight using LED is more common [4]. Generating electricity from solar energy through the process of photovoltaic (PV) is safer, noise free, environmentally benign and is rugged [5]. Solar energy has the ability to enhance resilience in the communities by providing power even if the grid is not there.

In comparison to other lights LED has many advantages like provides uniform illumination, consumes less energy, comfortable to eye, hence drive compatible. Many road accidents can be avoided with proper street lighting system.A.P. Niruka designed SSL for campus environment [6] L.P. Huai compared conventional street lighting system with that of solar streetlight and found that the solar streetlight saves 64.7% of the total cost in comparison to conventional

method. He also explained that the SSL system provides greater stability and very less chance of electrocution. [7]. People are deprived of basic necessities in the remote hilly and rural areas. With the sunset life comes to a hault at these remote places. Movement of people to different places becomes difficult [8]-[9].
The main objective of this paper is to design provision of solar streetlights for illumination of village roads and open meeting grounds. The paper mainly focuses on the rural villages of Odisha like Kalahandi and Mayurbhanj districts. Village people often gather in common places for meetings and evening is the best free time for them as most of them are busy with field work during the daytime. Solar streetlights can be beneficial for them so that they can move around during off sunshine hours. Even if some villages are getting electricity supply from common grid but frequent local problems like theft, falling of trees, branches during stormy weather are common happenings in these rural areas. The critical problem lies in that once the power failure occurs for days on no service and no maintenance happens. Thus, the rural people suffer a lot. Hence solar based streetlights are standalone system which are capable to generate the own electricity sufficient to charge the LED unit. The various advantages of solar street lighting system are as follows.

- Rural electrification focusing on the streetlights powered by solar
- Convenience to village people
- Improved transport system
- Energy conservation
- Less maintenance
- Improved lifestyle of rural people.

2 SOLAR STREET LIGHT SYSTEM

Solar PV based street lighting system is a standalone application of solar energy which is used for illumination of streets, corridors, basement, and open areas. There are different types of lights which are commercially available in market like CFL, tungsten filament, mercury vapour lamp, LEDS. Among all these LEDs leads the present time in terms of light intensity, efficiency, lumens, and long life. Lighting through LEDs have been used at different places and also finds its market in street lighting systems. Solar energy is clean and green form of energy hence combination of solar energy and low power consuming LEDs provides a promising solution for streetlights [10]-[11].

The fundamental components of a solar powered street lighting system using LED consists of the following components:

- Solar Photovoltaic Module
- LED unit
- Rechargeable Battery (Deep cycle)
- Control Circuit consists of Solar charge controller
- Pole
- Supporting structures

3 COMPONENT DESCRIPTION

3.1 Solar PV Panel

Photovoltaic modules are used to convert solar energy i.e., photons to electrical energy in DC form by the principle of photoconduction. There are different types of panels like crystalline like monocrystalline, multicrystalline, thin film like, amorphous and dye-sensitized, nano based, cadmium telluride etc. While choosing solar module for the project careful selection based on material is require so that irrespective of any climate condition the efficiency will be better, and output will be more.

Table 1 Shows comparison of different types of Solar module

Solar Module	Efficiency	Lifetime	Price	Power/Area
Monocrystalline silicon	10-13%	25 years	High	High
Polycrystalline silicon	9-13%	10 years	Moderate	Moderate
Amorphous silicon	6-8%	10 years	Low	Low

3.2 Light emitting diodes

Lighting system uses lamp which converts gas or electrical energy into light energy. Depending upon the device efficiency depends on the amount of light produced. The unit of measurement of visible light is lumen. Different types of lamps are used for lighting purpose like compact fluorescent lamp, mercury vapour lamp, tungsten filament lamp, metal halide lamps, light emitting diodes, organic light emitting diodes, light emitting polymers etc. Different types of these lamps have different efficacy and different ratings. Mostly LEDS are convenient for street lighting system. LED stands for Light emitting diode. They have a better life span and higher efficiency in comparison to other lamps. LED emits more than 100 lumen per watt. For solar lighting systems LEDS are most preferred as it takes very less voltage, less heat and less power. The components are made of Gallium nitride material doped by phosphorous. LEDS does not require warm up time to

come to its full brightness. These require controlled DC supply for its operation and are affected by high temperature hence special heat sinks and cooling fans are included in its circuit.

Table 2 Specification of different types of solar street lighting system

SSLA Type	Lamp size (Watt)	PV module size (Wp)	Battery Size for Lead Acid (AH)	Battery size for Lithium Ion (AH)	Charge controller (Ampere)	Pole height (m)
1	10	50	40	30	5	7
2	20	100	60	45	10	7
3	30	150	80	60	12	7
4	40	200	100	75	15	8
5	60	300	150	115	25	8
6	80	400	200	150	30	9
7	100	500	250	180	40	10

3.3 Battery

For storing electricity generated by solar PV panels batteries are used. Battery acts like backup. During daytime electrical energy generated by the PV panels are supplied to the battery and when the load demand exceeds or during sunset these batteries supply the load. Different types of batteries are available in the market. Among them deep cycle batteries are commonly used as they can withstand deep discharges. The various rechargeable batteries include:

3.1.1 Lead-Acid (LA) Battery

Lead acid batteries finds its wide application in solar systems as its technology is matured and are also available at low cost. For extending its life they are used with low depth of discharge (DOD) i.e., 65%-80%. Basically, there are two varieties of lead acid batteries like flooded type and valve regulated lead acid batteries. These types require very less maintenance.

3.1.2 Nickel-Cadmium (Ni-Cad) Battery

Nickel batteries are costly and are also dangerous as cadmium disposal is hazardous. These batteries have many merit points like greater life span, high discharge tolerance. Foe solar powered system Nickel cadmium batteries are not often used as they are very costly and also available in limited edition.

3.1.3 Lithium-Ion (LI) or Lithium-Polymer (LP) Battery

Studies shows that lithium-ion batteries are better than Nickel cadmium batteries with high depth of discharge, more number of charging cycles and high energy. But still these are also not preferred for PV application-based lighting systems as these are available at higher price.

3.4 Charge Controller

One of the major components of solar streetlight system is the charge controller. Charging of batteries are controlled by charge controllers. Photovoltaic panels provide variable output which needs to be adjusted hence controller comes into picture as it takes the variable input from solar panels like voltage or current conditions it with its logic to fit the battery charging process. Over-charging of batteries can be prevented by the use of these charge controllers. Charge controller uses either pulse width modulation or maximum power point tracking technique to perform its operation. There are different types of MPPT techniques which can be used for the operation. The operation of charge controllers is mostly at three stages. But these stages vary depending on battery voltages.

3.5 Sensors

Sensors are essential electrical components require to sense the ON/OFF the solar powered LEDS. It makes the system economically and technically viable. There are different types of sensors available in the market to be used for PV system like infrared sensors, LDRs, ultrasonic sensors. These sensors control the LED lamp functionalities such that the system can be made more energy efficient. Depending upon the intensity of the light these sensors get activated.

4 INSTALLATIONS

Design of a solar streetlight system must be strong and robust as these are generally installed in the roadsides where it is exposed to different weather conditions like rain, pollution, dust, snow, fog, mist, sun etc. Moreover, care should be taken while its design that it should not affect the street plan and beauty of the roadways and any hindrance to the city structures.

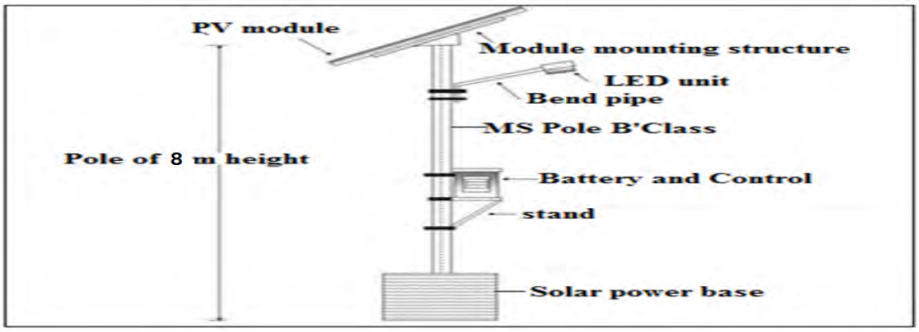

Figure 4.1. Shows pole mounted installation of solar based streetlight system

The components of the solar powered lighting system include PV module mounted on the structure. The module mounting structure is 32*32*3mm. The luminary part consists of LEDS supported with the help of bend pipe. A single pole M.S class B is used of height 8 m. Battery box along with the control circuit is positioned towards the base of the pole. The pole rests on a solid base of broader cross section area. Generally solar panels are mounted on the top to avoid any kind of shading effect on the panel and prevent ground hindrance and local dust.

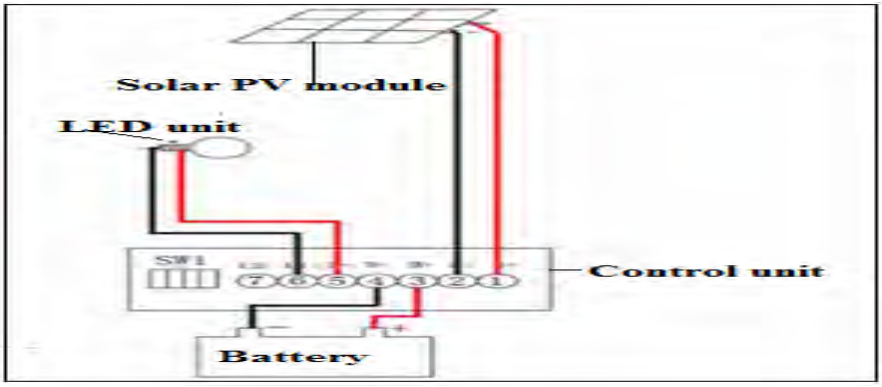

Figure 4.2. Shows the wiring connection of the solar streetlight system

The solar module provides the necessary DC current to the battery such that it gets charged during the sunshine hours. The charging and discharging of the battery is controlled by the control unit which is a solar charge controller. The LED unit is controlled by sensors i.e LDR light dependent resistor, current and voltage sensors.

5 WORKING PRINCIPLE

Solar radiations fall on the solar PV panel and by the effect of photo conduction produces electrical energy. The output of the solar panel is fed to the charge controller and the control circuit. The control circuit consists of micro controller

and two sensors one is light or dark sensor, and the other is infrared sensor. The output of the micro controller is fed to the light driver circuit and hence the light driver circuit supplies the LED lamp which glows.

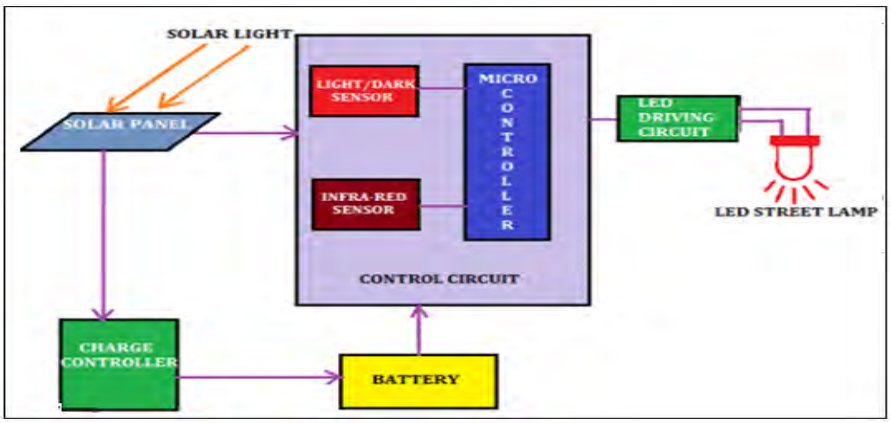

Figure 5.1. Shows the block diagram representation of the solar powered streetlights using LEDs

6 CALCULATION OF DESIGN OF SINGLE POLE

We consider the solar streetlight system consists of 1 unit of 60 watt LED lamp and 12 V Lithium battery.

Therefore, **current capacity** is given as

$$\text{Current (I)} = \text{Power (Watt)/Voltage (volt)} \quad (6.1)$$

=60W/12V=**5 A**

6.1 Battery capacity

Considering different cases like evening hour, night and rainy time the total lighting time per day is 7 hours. Hence the battery capacity can be calculated as 5A* 7 hours* 6 days= 210 Ah. Battery just discharges up to 80%. Therefore, actual battery capacity can be taken as 210Ah *125%=**262.5Ah**.

6.2 Calculation of Illumination in Lumen

Considering E= 32 Lux and d =height of the pole =6m

Illumination id defined as

$$I = E \times d^2 \quad (6.2)$$

= 32*36

=1152 lumens ~ 1200 lumens

6.3 Calculation of Power of solar panel (Wp)

The solar module has voltage 17.4 volt.

solar streetlight works for 7 hour each night. But it is observed that the solar panel takes solar radiations for 4.5 hours. Therefore, power is calculated as

$$\frac{Wp}{17.4} = \frac{5A \times 7h \times 120\%}{4.5} = 162 \text{ Watt} \quad (6.3)$$

In real case there are different constraints like power consumption of controller, connections, rectifier unit hence a little higher side PV rating is considered. Thus, we take 200-Watt PV panel. Therefore, two solar modules with 100-120Wp are best suited. This is the design for one solar powered pole. Therefore, for designing the solar powered street lighting system for the entire village we consider fifty such poles supplying electricity to the village.

7 CONCLUSION

Energy from sun is the cleanest form of renewable energy. Moreover energy suitability in the rural areas mostly villages can be ensured by provision of solar operated street lights. Use of LED in comparison to other lamps are more beneficial and also the efficiency improves by 755. Not only this there is also an increased percentage of energy saving by the use of solar streetlight system. Lifestyle of the village people can be improved with this facility, empowering them with the modern system. In this paper advantages of LED is highlighted. Design of one single solar powered LED lighting pole is done. The current, battery, power rating of the panel are calculated and thus with the calculation a rough estimation is made for the entire village.

8 REFERENCES

[1]. Aung, N. S. M., & Myint, Z. H. (2015). Design of stand-alone solar street lighting system with LED. International journal of scientific engineering and technology research, 3(17), 3518-3522.

[2]. N. Kannan and D. Vakeesan, "Solar energy for future world: - A review", Renewable and Sustainable Energy Reviews, vol. 62, pp. 1092-1105, 2016.

[3]. B. Ng and Z. Akasah, "An Overview of Malaysia Green Technology Corporation Office Building: A Showcase Energy-Efficient Building Project in Malaysia", Journal of Sustainable Development, vol. 4, no. 5, 2011.

[4]. B. Ng and Z. Akasah, "Energy-efficient buildings: an in-depth look into definitions and design problems", International Journal of Emerging Sciences, vol. 3, no. 4, 2013.

[5]. Herzog, T. Lipman, J. Edwards and D. Kammen, "Renewable Energy: A Viable Choice", Environment: Science and Policy for Sustainable Development, vol. 43, no. 10, pp. 8-20, 2001.

[6]. Acharya, A., Nanda, L., Roy, T., Misra, B.,"Boost Converter with Generalized Quadratic Boosting Cell with Reduced Capacitor Voltage Stresses", Lecture Notes in Electrical Engineering, 2021, 691, pp. 79–91, 2021

[7]. Nanda, L., Acharya, A.,"Evaluation on various Dc-Dc non-isolated maximized voltage gain converter topology",11th International Conference on Advances in Computing, Control, and Telecommunication Technologies, ACT 2020, pp. 173–178,2020

[8]. Arjyadhara Pradhan, Bhagabat Panda, "Performance analysis of Photovoltaic module at changing environmental condition using MATLAB/Simulink" International Journal of Applied Engineering Research ,ISSN 0973-4562 Volume 12, Number 13 (2017) pp. 3677- 3683

[9]. Arjyadhara Pradhan, Bhagabat Panda, "A simplified design and modeling of boost converter for photovoltaic sytem",International Journal of Electrical and Computer Engineering, 2018, 8(1), pp. 141–149.

[10]. Arjyadhara Pradhan, Bhagabat Panda, "Experimental analysis of factors affecting the power output of the PV module"International Journal of Electrical and Computer Engineering, 2017, 7(6), pp. 3190–3197.

[11]. Arjyadhara Pradhan, Babita Panda, Bhagabat Panda, Aradhana Khilo,"An Improved MPPT Technique for improving efficiency of PV module"1st International Conference on Conference on advances in electrical control and signal systems (AECSS-2019),8th-9th November 2019 SOA | SIKSHA 'O' ANUSANDHAN vol 665, pp 633-644.

1

Modeling of PWM Technique for Three Phase Voltage Source Inverter

Bansilal Bairwa, Sanjeeva Kumar, Santoshkumar Hampannavar, Raghu C N
bansilal.bairwa@reva.edu.in

School of Electrical and Electronics Engineering,REVA University,Bangalore, India 560064

Abstract

This paper deal with 3rd harmonic-based pulse width modulation techniques for 3 phase voltage source inverters. In this work DC voltage is converted in AC voltage with the help of inverter. 3rd harmonic is generated with the help of fundamental component in power supply, that is used for generating the pulse for inverter. Three phase inverters have been adopted in this work, that having the capability to generate the pure sinusoidal output voltage for load. 3Phase LC filter also proposed in this work to getting the voltage for load without any harmonics. This study have been carried out with the help of modeling and simulation with MATLAB.
Keywords: PWM, Voltage source inverter, Load, Supply.

1.1 Introduction

Harmonics definition changes to way we see the harmonics in the nature. In the harmonics for the power system say "positive integer multiples of the fundamental frequency. Harmonics are sometime these harmonics are destruction and distraction in transmission lines. Those harmonics produced

An Edited Volume, 1–7.

by the components of power electronic such as rectifiers, transistors, or but the electrical motor with unbalanced loads. Those frequently affects power quality problems in the equipment which cause the conductor heating, variable speed drives get misfired. In fundamental frequency is also 50Hz, then the second harmonics will be in 120Hz, The third will be in the range of 150Hz. In generally to know the nth harmonics then nth harmonics will be (n*50) Hz. Majorly the harmonics are classified as follows of single-phase system: (1) Current harmonics; (2) Voltage harmonics Harmonics of three phase systems can be found in following parts for current and voltage:

- Even harmonics
- Odd harmonics
- Triplen harmonics
- Non triplen odd harmonics

Basis of sequence harmonics are categorized in three major parts

- Positive sequence harmonics
- Negative sequence harmonics
- Zeros sequence harmonics

Level of harmonic distortion present in power system are measured in total harmonics distortion (THD). THD methods are either to related to current or voltage harmonics. That can be defined as ratio of RMS value of all harmonics to the RMS value of the fundamental element times 100%. Then DC component is not considered for calculating the THD in power system. The effects of harmonics on motor and communication (Telephones lines majorly effects by increasing the current in the system, In that area harmonics are always exhibits based third harmonics majorly, those will increase the harmonics in neutral lines of transmission lines. Motors will experience losses due to eddy currents and hysteresis set in the iron core of motor[1, 2, 3, 4]. If there is more harmonics then results in higher core losses in motor core. Counter electromotive force (CEMF) from 5th harmonics in larger motor which acts in opposite direction of rotation. Those CEMF is not large enough to counteract the rotation So, it does play role in rotation speed of motor Now a days telephones are become old due to evolution of wireless communication evolved. Usually, those transmitted frequency 300 and 3400Hz.It normally does not interfere with telephone communications because its frequency to low so. Inverters are widely used now a days to fulfill the need of day to day requirements of industries, offices and home appliances. AC power cannot be stored But DC can be stored using battery . Appliances we use are mostly

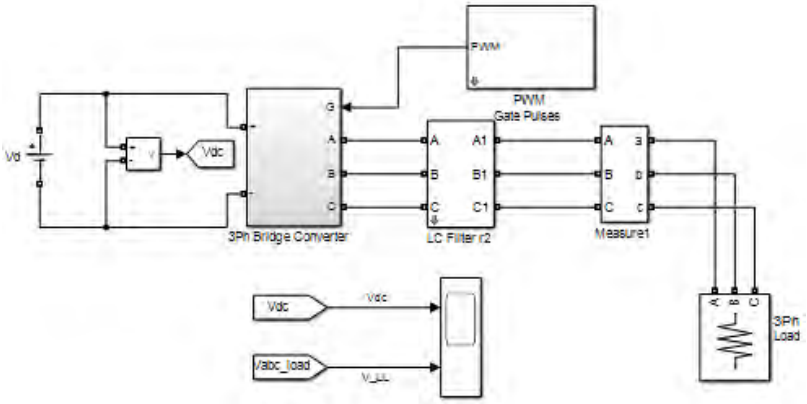

Figure 1.1 Proposed work with simulink diagram

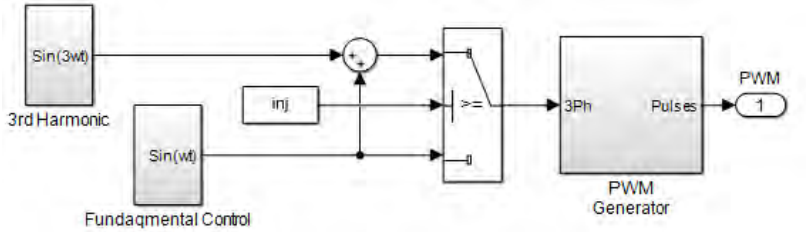

Figure 1.2 3rd harmonics generation using simulink

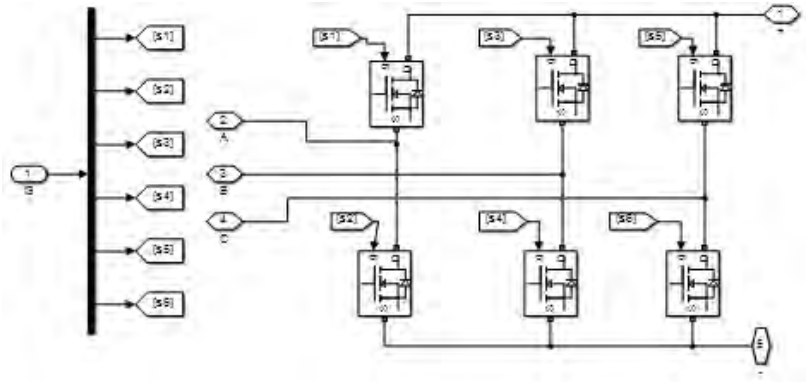

Figure 1.3 Inverter modeling in MATLAB Simulink.

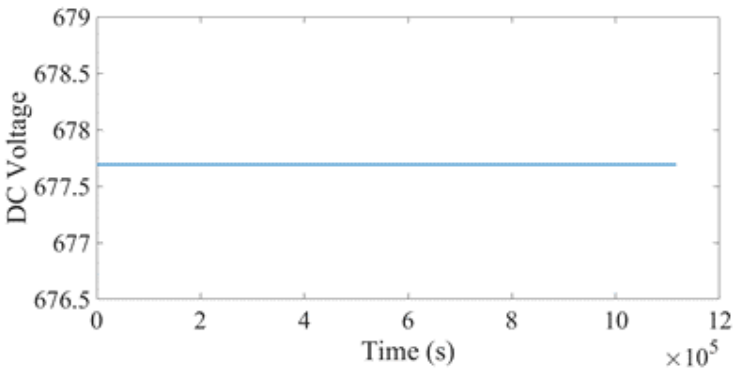

Figure 1.4 DC voltage supplied to inverter for conversion

of AC in nature. So DC is converted to AC by inverter. In the processes of converting DC to AC and depending up on the converter technology , control, type of load harmonics are introduced in the inverter[5, 6, 7, 8]. Harmonics are unwanted components which leads to distortion of current and voltage waves leading to increased power losses, hence reduced efficiency. Also reduces life of the device, components[9, 10, 11]. Harmonies are positive integer multiple of fundamental frequency like third harmonics, fifth harmonics, seventh harmonics etc. when fundamental frequency is 50hz, frequency of third fifth harmonics is 3*50=150 hz , 250hz respectively. In this proposed work, third harmonics is modeled for three phase voltage inverter using MATLAB which keeps the HD value less than the acceptable value by novel Mathematical modeling strategical control algorithm. Harmonics is an important phenomena in power system, healthy signal having the minimum total harmonics distortionḢarmonics in single phase transformer in divided in three several cases [12, 13, 14, 15]. when flux is sinusoidal and linear (B = H). In this case EMF is in sinusoidal as well as the current will also be sinusoidal, that is an ideal case.

1.2 Methodology

The proposed work consisting of the structure of three-page voltage source inverter with six pulse width modulation. The proposed work consisting of the DC voltage as input to voltage source inverter, three phase bridge converter, LC filter, PWM gate pulse and the three-phase load is discuss in the next paragraph. Figure 1.1 represents the proposed work. Primary prime application of the VSI is converting the DC input to AC output. In this work DC voltage is taken as 415*2*sqrt (2). Here 415 is considered as line-to-line voltage, the output of the voltage source inverter to feed the load that is showing in Figure 1.4. 3 Phase Bridge converter: 6 MOSFET have been used for this configuration with internal diode resistances 0.01 ohms and R on equal to 0.1 ohm, Snubber resistance is taken 1e5 for the proposed circuit that is mentioned in Figure 1.3.

1.2.1 Pulse Width Modulation

PWM pulse width modulation is the important part of the proposed work switching frequency is taken as 20 kilo hertz and control signal frequency is taken as 50 hertz for generating the gate pulse. Three inputs are considered that is showing in Figure 1.2.

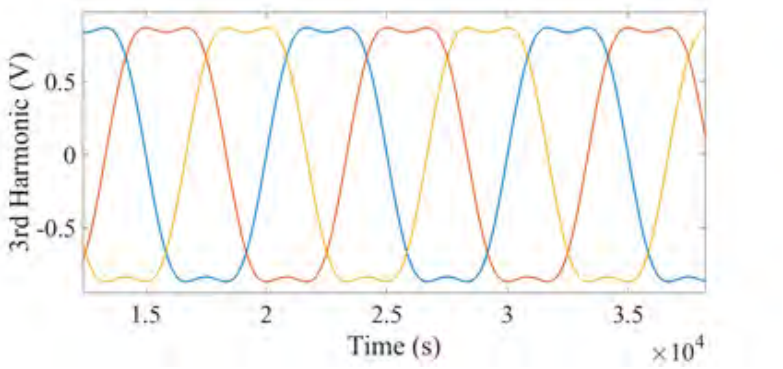

Figure 1.5 Distorted power supply with 3rd harmonics

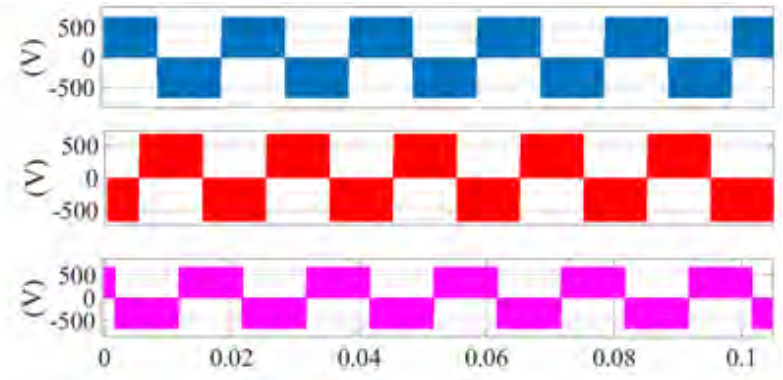

Figure 1.6 Inverter output voltage without filter.

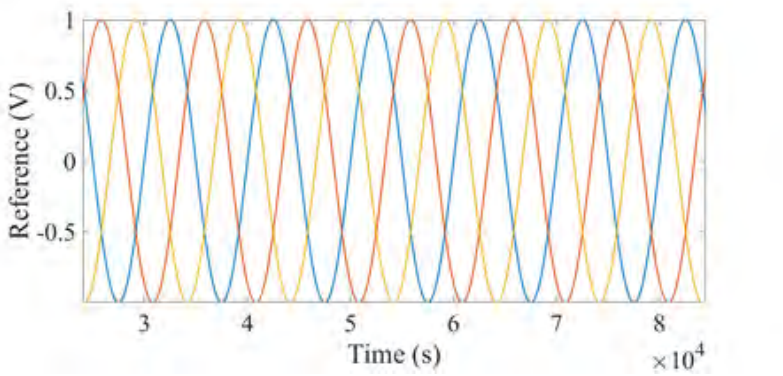

Figure 1.7 Results for reference voltage input to 3rd harmonics generation

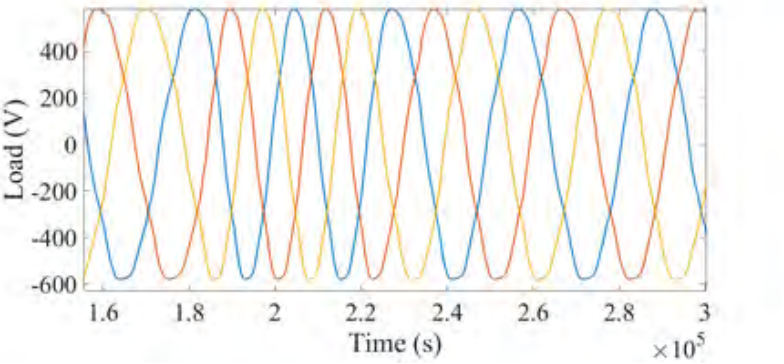

Figure 1.8 Load voltage for with pure sinusoidal condition.

- 3rd harmonic $sin(3\omega t)$
- Injection (constant value)
- Fundamental control $sin(\omega t)$

LC filter: The parameters values of the LC filter is taken as L= 10e-3 and C = 20micro farad. Three phase parallel RLC load has been applied for the purposed work. Nominal phase two phase voltage is 415 V and nominal frequency is considered as the 50 Hertz.

1.3 Results and Discussion

This paragraph representing the output obtained from the proposed work. Figure 1.5 showing that distorted power supply with third harmonics, Figure 1.6 represents the VSI output without Filter. Figure 1.7 is about the reference voltage is taken during the PWM generation. Load voltage is mentioned in Figure 1.8. Here load voltage is 415 volts with pure sinusoidal wave form. Total harmonics distortion is obtained minimum as per IEEE standard. The overall output of the proposed work is to maintain the load voltage. Novelty of the research is generating the PWM gate pulse with the distorted reference input.

1.4 Conclusion

This research intends to modeling of voltage source inverter by following the proposed PWM method. 3rd harmonics-based pulse width modulation investigated. All results obtained from this research is showing the good agreement with published results in same domain. The research has been carried out is based on the MATLAB and Simulink. The outcomes of the proposed work can be applied in inverter (DC to AC) based applications.

References

[1] J. Holtz and A. Khambadkone, "Low switching frequency and high dynamic pulsewidth modulation based on field-orientation for high-power inverter drive", IEEE Trans. Power Electron., vol. 7, pp. 627-632, Oct. 1992.

[2] T. A. Sakharuk, B. Lehman, A. M. Stanković (Stankovic) and G. Tadmor, "Effects of finite switching frequency and delay on PWM controlled systems", IEEE Trans. Circuits Syst., vol. 47, pp. 555-567, Apr. 2000.

[3] Hiti, S., Boroyevich, D., Cuadros, C. (1994, October). Small-signal modeling and control of three-phase PWM converters. In Proceedings of 1994 IEEE Industry Applications Society Annual Meeting (Vol. 2, pp. 1143-1150). IEEE.

[4] Weichmann, E. P., Ziogas, P. D., Stefanovic, V. R. (1987). Generalized functional model for three-phase PWM inverter/rectifier converters. IEEE transactions on industry applications, (2), 236-246.

[5] Mohamed, Y. A. R. I., El-Saadany, E. F. (2007). An improved deadbeat current control scheme with a novel adaptive self-tuning load model for a three-phase PWM voltage-source inverter. IEEE Transactions on Industrial Electronics, 54(2), 747-759.

[6] Hiti, S. (1995). Modeling and control of three-phase PWM converters. Virginia Polytechnic Institute and State University.

[7] Ravi, A., Manoharan, P. S., Anand, J. V. (2011). Modeling and simulation of three phase multilevel inverter for grid connected photovoltaic systems. Solar Energy, 85(11), 2811-2818.

[8] Shmilovitz, D. (2005). On the definition of total harmonic distortion and its effect on measurement interpretation. IEEE Transactions on Power delivery, 20(1), 526-528.

[9] Aiello, M., Cataliotti, A., Favuzza, S., Graditi, G. (2006). Theoretical and experimental comparison of total harmonic distortion factors for the evaluation of harmonic and interharmonic pollution of grid-connected photovoltaic systems. IEEE Transactions on Power Delivery, 21(3), 1390-1397.

[10] Loh, P. C., Vilathgamuwa, D. M., Gajanayake, C. J., Lim, Y. R., Teo, C. W. (2007). Transient modeling and analysis of pulse-width modulated Z-source inverter. IEEE Transactions on Power Electronics, 22(2), 498-507.

[11] Wasynczuk, O. (1989). Modeling and dynamic performance of a line-commutated photovoltaic inverter system. IEEE Power Engineering Review, 9(9), 35-36.

[12] Holmes, D. G., Lipo, T. A. (2003). Pulse width modulation for power converters: principles and practice (Vol. 18). John Wiley Sons.

[13] Holtz, J. (1994). Pulsewidth modulation for electronic power conversion. Proceedings of the IEEE, 82(8), 1194-1214.

[14] Chandorkar, M. C., Divan, D. M., Adapa, R. (1993). Control of parallel connected inverters in standalone AC supply systems. IEEE transactions on industry applications, 29(1), 136-143.

[15] Zhang, L., Watthanasarn, C., Shepherd, W. (2001, June). Control of AC-AC matrix converters for unbalanced and/or distorted supply voltage. In 2001 IEEE 32nd Annual Power Electronics Specialists Conference (IEEE Cat. No. 01CH37230) (Vol. 2, pp. 1108-1113). IEEE.

Z-Source Inverter for Electric Vehicle Applications- A Review

Manish Bharat
Research Scholar ,VTU
Assistant Professor
[1]*School of Electrical and Electronics Engineering*
REVA University, Bengaluru, INDIA

Dr. ASR Murty
Research Supervisor ,VTU
Retd. Professor , RRCE
[1]*School of Electrical and Electronics Engineering*
Bengaluru, INDIA

[a)] Corresponding author: manish.bharat@reva.edu.in

Abstract. - ***The transport industry is regarded as the futuristic and most powerful industry among all the industries. Since this industry is mostly driven by Electric Vehicle (EV)/Hybrid Electric Vehicles (HEV) powered by information and communication technologies (ICT) in future. These vehicles require advanced and efficient converters to drive. The paper presents the current Z-source converters applicability to drive EV/HEV to aid the transportation industry. The various topologies of Z-source converters have been discussed. The summary of the literature survey of the suitable Z-source topologies for EV/HEV application is also presented. The need for the new control technique along with new trans-Z source converter topology to drive EV/HEV is discussed. The paper also presents the authors proposal of dual power source trans-Z source converter for the EV/HEV applications.***

***Index Terms*—**Z-source, Inverter, Topologies, Drive, Electric Vehicle, Hybrid Electric Vehicle. Trans-Z source**.**

Introduction

The environmental and ecological issues are directly related to the transportation vehicles running on fossil fuels. Therefore, Electric Vehicles/Hybrid Electric Vehicles (EVs/HEVs) are being introduced into the market due to their environmentally friendly operations. In these vehicles the power electronic converter plays an important role in driving the motor reliably and efficiently. The traditional inverters like voltage source inverters (VSI), current source inverters (CSI) were used to drive these vehicles with limitations. The limitations of the CSI drives are high harmonics in the output current, requiring additional filters at the input & output, results in high components count. Whereas, VSI drives are not suitable for high power applications, but suitable for highly dynamic applications. These topologies have two stage structure and do not have buck & boost capabilities. In order to overcome the above drawbacks of these traditional VSI & CSI inverters, an improved topology known as Z-source (Impedance Source) inverter topology was introduced by F.Z. Peng in 2003 [1]. The paper covers the review of Z-source inverter and its derivatives and proposes a technically viable inverter for electric drive applications.

The rest of the paper is arranged in to various sections: section 2 discusses the traditional Z-source inverters, section 3 delas with other topologies of Z-source inverters, section 4 presents the control techniques

employed in the various inverters, section 5 deals with summary of the literature review, section 6 presents the authors proposal and section 7 presents the conclusion.

Z-SOURCE INVERTERS

The Z-source inverters (ZSIs) are the derivative of traditional VSI & CSI converters with an ability of buck-boost [2]-[3]. These converters are used as AC-DC, AC-AC, DC-DC and DC-AC converters in various applications [3]. The traditional Z-source inverter is depicted in figure 1.

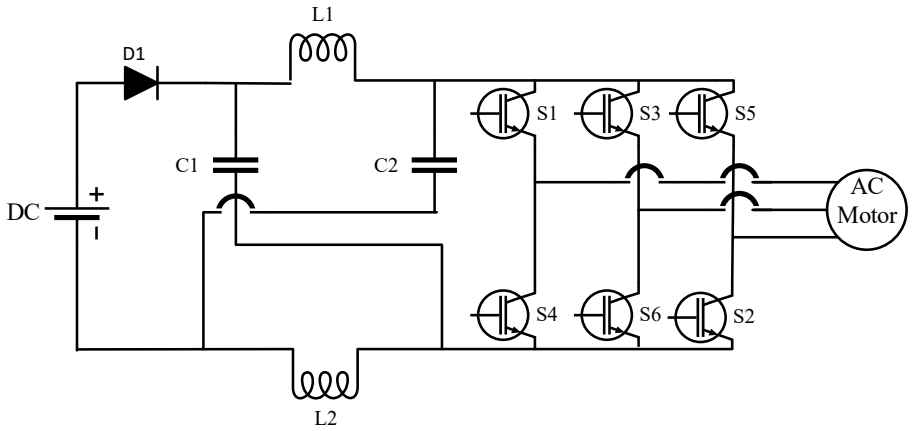

Fig.1: 3Ø Traditional Z-source inverter [3]

As seen from Fig.1 the Z-source inverter has a unique impedance network consisting of split inductance (L_1, L_2) and capacitance (C_1, C_2). The structure of this impedance network results in three operational states namely, initial/start-up state, active state and shoot-through state [3]. These three states of Z-source inverter are shown in figure 2(a), 2(b) and 2(c).

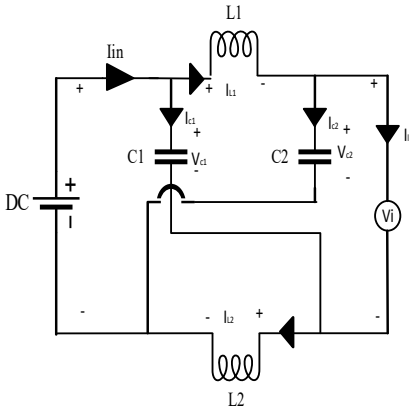

Fig.2 (a) Start-up state [3]

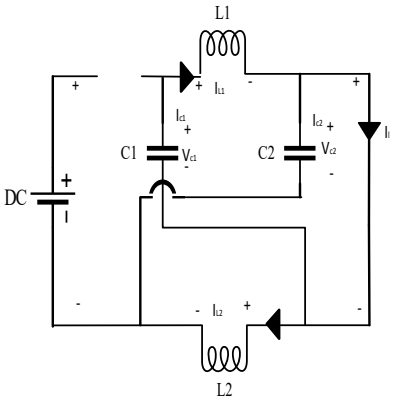

Fig.2 (b) Active state (Non-Shoot Through state) [3]

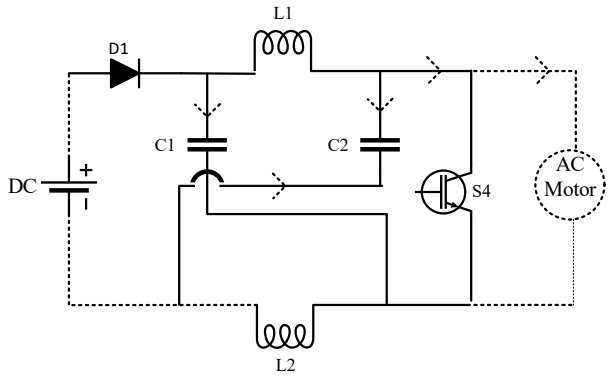

Fig.2 (c) Shoot-Through state.[3]

Since the Z-source inverter is symmetric, the parameters L_1=L_2 =L and C_1=C_2=C are equal. The converter operates in active and shoot-through state due to its symmetrical nature. The converter operates in active state (Non-Shoot Through Mode) for a period of T_1 of switching period T. The switching period is:

$$T = T_1 + T_0 \quad (1)$$

Referring to figure 2 (b), it can be observed that, the inductors are discharging and capacitors are charging during active mode. By applying KVL around a loop consisting of V_{in}, L, C and DC link voltage V_{dc}, the voltage relations are given by:

$$V_{dc} = V_{in} + V_C - V_L \quad (2a)$$

$$V_L = -V_C \quad (2b)$$

$$V_{dc} = V_{in} + 2V_C \quad (3)$$

Where V_{in} => Input dc voltage, V_{dc} => dc link voltage, V_L => voltage across inductor and V_C=>voltage across capacitor.

Next converter operates in shoot-through state for a period of T_0 of switching period T. During this state the dc link voltage is zero and voltage across inductor and capacitor are equal. Applying KVL around a loop consisting of V_{in}, L, C, the voltage relations are given by:

$$V_{in} - V_C - V_L = 0$$

$$V_L = V_{in} - V_C \quad (4)$$

$$V_{dc} = 0 \quad (5)$$

The voltage relations during active and shoot-through states are

$$\frac{1}{T}\int_0^T V_L(t)dt = \frac{T_{st}V_C + T_1(V_{in} - V_C)}{T} = 0 \quad (6)$$

Solving (6) for voltage across capacitor,

$$\frac{V_C}{V_{in}} = \frac{T_1}{T_1 - T_{st}} = \frac{1 - D_{st}}{1 - 2\,D_{st}} \tag{7}$$

From (7),

$$D_{st} = \frac{V_C - V_{in}}{2V_C - V_{in}} \tag{8}$$

Where $D_{st} = \frac{T_{st}}{T}$ is the shoor-through duty cycle.From equations (3) and (7), the dc link voltage is given by:

$$V_{dc} = \frac{T}{T_1 - T_{st}} V_{in} \tag{9}$$

Equation (9) can also be expressed as:

$$V_{dc} = \frac{1}{1 - 2D_{st}} V_{in} = BV_{in} \tag{10}$$

Where B is the boost factor depends upon shoot through duty cycle D_{st}.

The Z-source converters are preferred in various industrial applications like, traction, energy conversion systems as they can operate in both buck and boost modes. The basic types of Z-source inverter topologies have been discussed in proceeding sections.

Quasi Z-Source Inverter [1]

The impedance network elements of the traditional Z-source inverter have been rearranged to achieve a reliable power conversion along with a high conversion efficiency. The resultant topology is known as Quasi Z-source inverter topology. The re-structured impedance network has resulted in 4-operating modes as shown in figures 2,3,4 and 5.

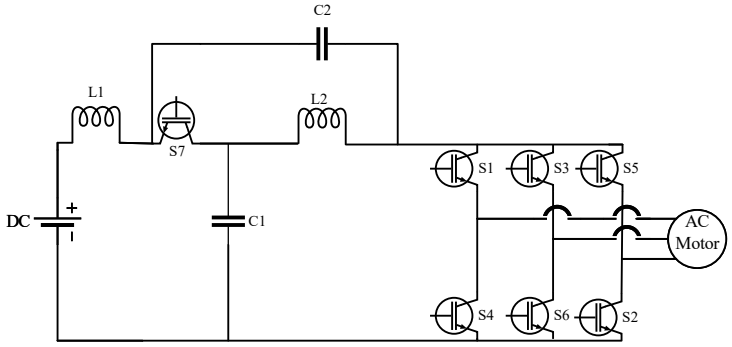

Fig.2: Voltage fed continuous current Z-source inverter [1]

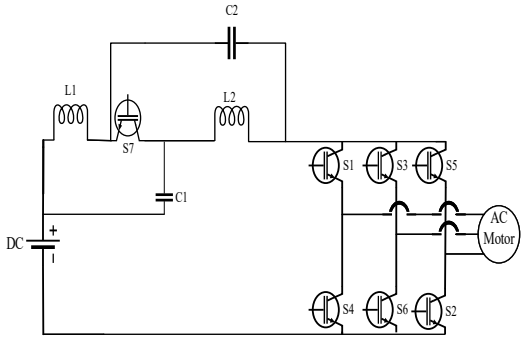

Fig.3: Voltage fed dis-continuous current Z-source inverter [1].

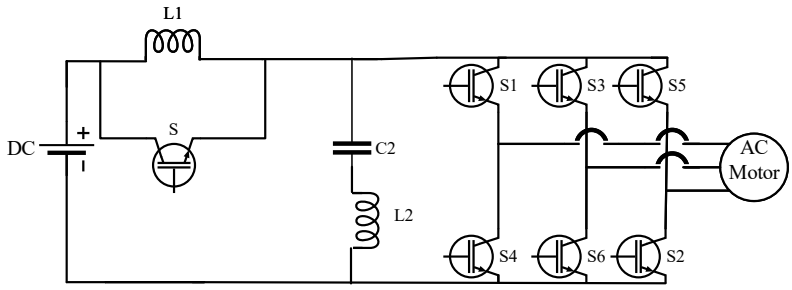

Fig.4: Current fed continuous current Z-source inverter [1]

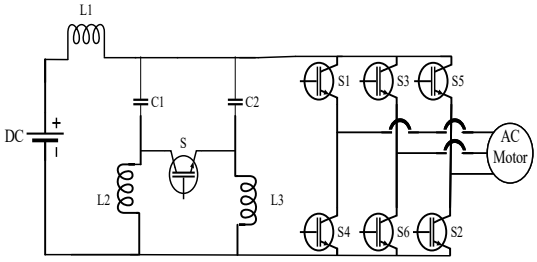

Fig.5: Current fed dis-continuous current Z-source inverter [1].

Embedded Z-Source Inverter [1] & [4]

The embedded impedance source inverter is realised to achieve a continuous input current with lower capacitor voltage rating. The embedded z-source inverter schematic is shown in figure 6.

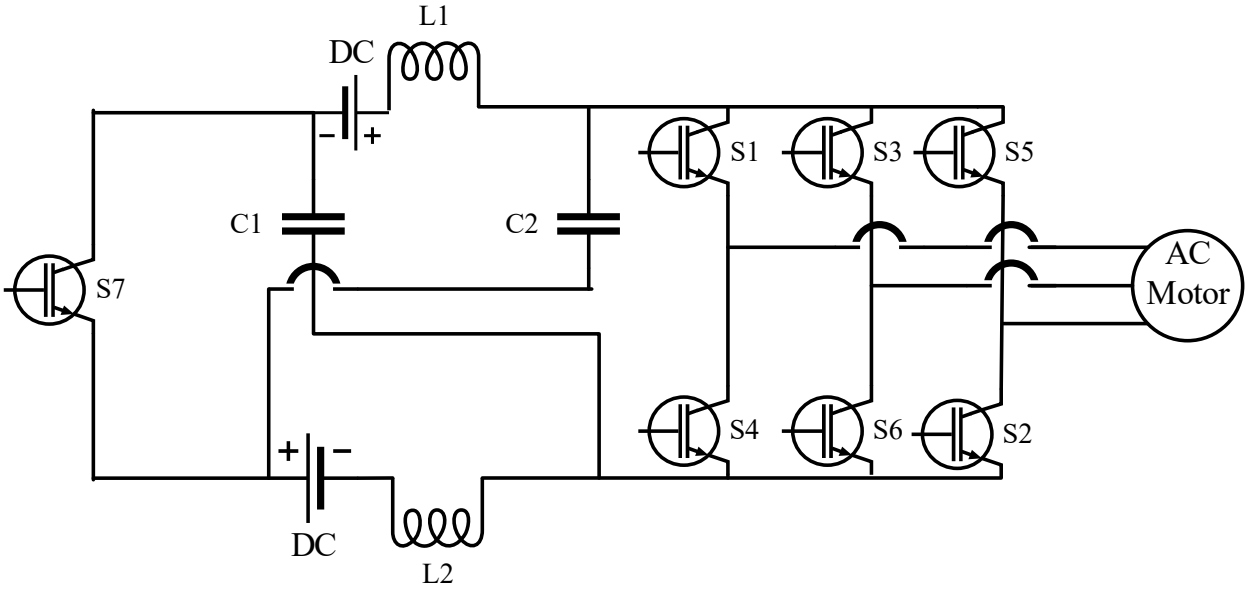

Fig.6: Embedded Z-source inverter [1]

The major advantage of this topology is that it reduces the voltage and current ripple. In this structure the dc sources are embedded with z-source elements.

Embedded Quasi Z-Source Inverter [1] & [5]

The basic features and operation of embedded quasi z-source inverter is exactly similar to embedded Z-source inverter [1] & [5]. The structure of this inverter is depicted in figure 7.

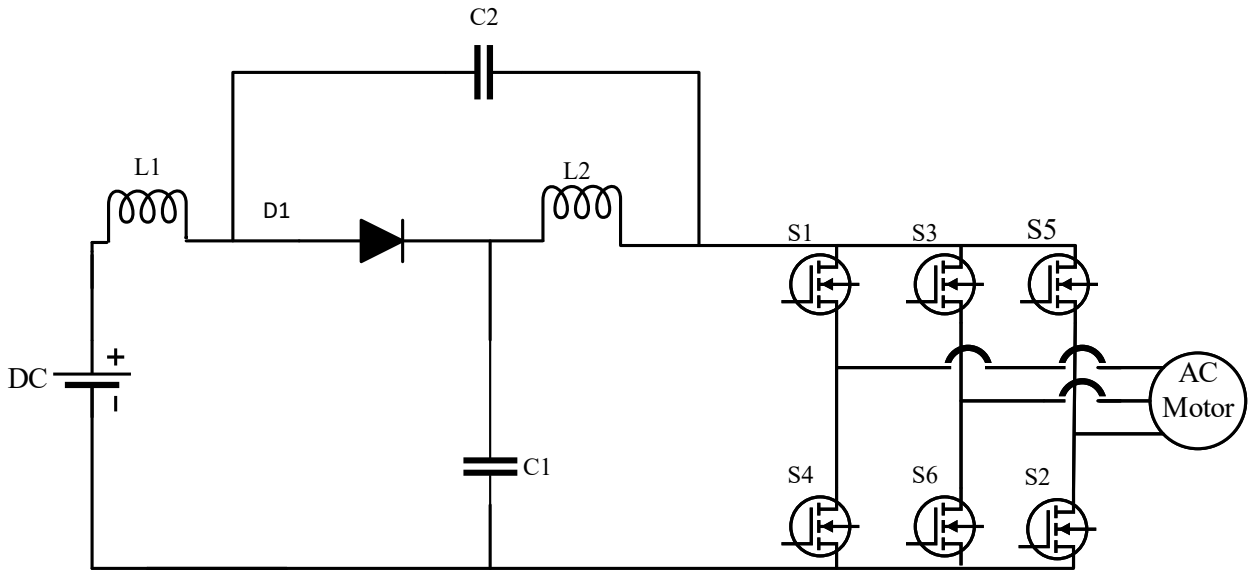

Fig.7: Embedded Quasi Z-Source Inverter [5]

This topology can operate with two sources without altering the voltage gain of traditional quasi z-source inverter [1].

Trans Z-Source Inverter [1] & [6]

The trans Z-source inverter is an improved version of traditional Z-source inverter with high voltage gain and less stress on the switches. The typical structure of the trans Z-source inverter is depicted in figure 8.

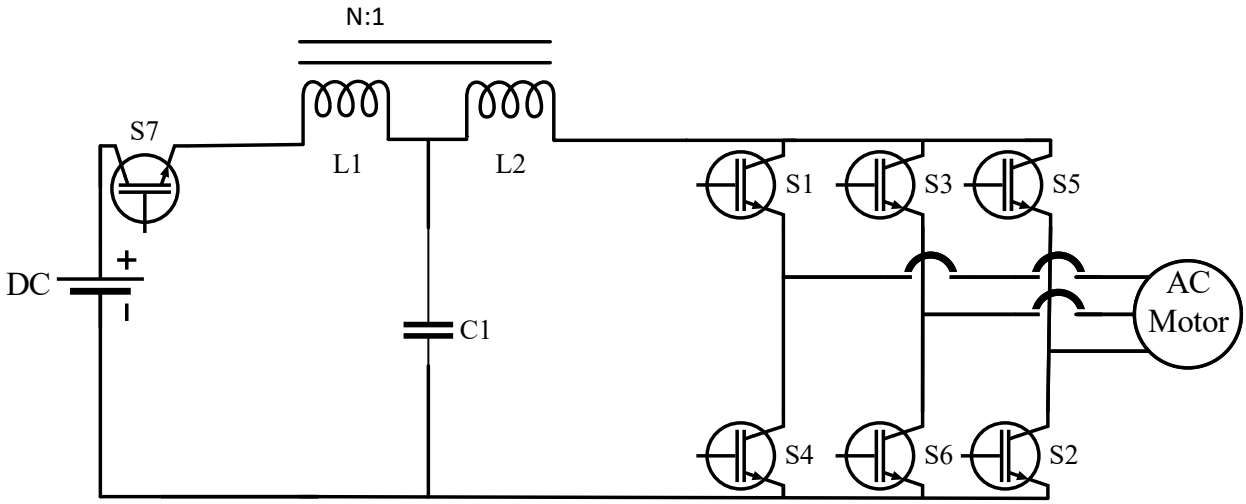

Fig.8: Trans Z-Source Inverter

Shoot through barriers have been eliminated in this inverter due to restructured impedance network. The cost of the circuit is high due to transformers and coupled inductors.

OTHER Z-SOURCE TOPOLOGIES

It is observed that various researchers have worked on z-source converters to improve their boost factor, current delivering capability by modifying the structure of the impedance, and dc input source location in the converter circuit. The Jing Yuan et al [7] have proposed an embedded enhanced-boost Z-source inverter. The converter design is such that the stress on the semiconductor switches has been reduced, the dc link voltage remains zero during shoot through state but the inductor currents increase. Since the dc sources are embedded in to the z-source network, the current becomes continuous. The circuit complexity is high due to the additional circuit elements in the modification of Z-network. This modified Z-source inverter is suitable for the applications which employs fuel cells as their energy source. The embedded switched capacitor Z-source inverter has been proposed in [8]. This converter performance is same as the converter proposed in [7]. The structure of the impedance network is different.

It is true that the performance of the converter can be improved by employing proper control mechanism of semiconductor switches. Malathi et al [9] have proposed a photovoltaic fed Z-source inverter with proportional integral (PI) and proportional, integral & derivative (PID) based control mechanism to improve the performance of the inverter. It is observed and claimed by the researchers that the performance of the inverter was better with PID rather than PI control mechanism. The gamma Z-source inverter is another variant of ZSI [10]. It has an impedance connected in a way that it resembles gamma letter and hence the name gamma Z-source (Γ-Z-source) inverter. The voltage gain of the inverter can be changed by varying the transformer ratio. This type of inverter is much suited for AC/DC microgrid.

The differential mode Γ-Z-source inverter is proposed in [11]. In this inverter the inductors are located in such a way that the ripple content in both voltage, currents of Z-network is less. The stress on the switches is also reduced but the total harmonic distortion (THD) is considerably high. Enhanced-Boost Z-Source Inverters with Switched Z-Impedance has been proposed by Fathi Kivi [12]. This inverter has two impedance networks to achieve high voltage gain with low shoot through state. The output wave form quality is high with high modulation index with short shoot through state.

The Z-Source Dual Active Bridge Bidirectional AC-DC Converter for Electric Vehicle Applications is proposed by Srijeeth et al [13]. The proposed inverter is mainly suitable for vehicle to home and grid to vehicle applications. ReddyPrasad Reddivari et al [14] have proposed a modified gamma z-source inverter for fuel cell -battery fed hybrid electric vehicle application. In this paper the proposed inverter performance was studied through simulation. The performance of the modified gamma z-source inverter is better than that of traditional gamma z-source inverter. The modified gamma z-source inverter study revealed that the battery size can be reduced in hybrid electric vehicles.

The traditional Z-source inverters have discontinuous input current, as a result the dc voltage becomes uncontrollable and hence the stability of the system. Thilak Senanayake et al [15] have introduced an improved impedance source consisting of input LC filter, a semiconductor switch in lieu of input diode and an impedance network. This structure helps the inverter to draw a continuous current from the dc source with less ripple as the LC filter present at the input of the inverter. The stress on the semiconductor devices also reduces. The presence of the input switch makes the inverter to function in both directions which is the necessary requirement of electric vehicles /hybrid electric vehicles. Also, dc link voltage can be controlled and there will be a continuous input current from the power source. Zeeshan Aleem et al [16] have proposed an improved gamma z-source inverter. An improvement is achieved by incorporating the diodes into the impedance network. The performance of the proposed inverter is same as that of its predecessors but for reduced leakage inductor currents.

The bidirectional quasi-Z-source inverter has been proposed in [17] for electric vehicle applications. The bidirectional operation of the inverter is achieved by connecting an active switch in antiparallel with the diode. An inner current control loop at the dc side, voltage control mechanism is used to achieve the better performance.

CONTROL STRATEGIES IN Z-SOURCE INVERTERS

The performance of any inverter completely depends upon efficient & reliable control strategy. It is understood that the Z-source inverters with modification can be employed in electric vehicle/hybrid electric vehicle drive applications. The review on the impedance network modification along with the control strategies employed in the Z-source inverters is carried out and the details are presented in the proceeding paragraphs.

M. Z.Zizoui et al [18] have proposed a 9 switch z-source power inverter driving double induction motors for electric vehicle application. The inverter uses a maximum constant boost control mechanism to operate the dual induction motors. Sertac Bayhan et al [19] have introduced a Z-Source (ZS) four-leg inverter fed with photovoltaic system along with a Model Predictive Control (MPC) strategy. The load employed in the experimental setup is unbalanced. In this inverter an LC filter is used in stead of boost converter and thus a single stage power converter is obtained. The control strategy and the structure of this modified z-source inverter can handle both balanced and unbalanced loads.

Siddhartha A.et al [20] presented a modified Z-source inverter connected to a grid integrated with charging mechanism for storage systems. The control mechanism used is pulse width modulation (PWM) technique. The input power source employed in this study was photovoltaic (PV) array. The performance of the presented inverter indicates that it can be employed commercially for standalone applications of power at malls, parking lots etc. It can also be utilized for charging EVs. In the next paper, the practical limitations of embedded Z-source dc-dc converters for PV applications have been studied and presented [21]. The modified Trans Z-source inverter is presented in [22] where in the input current is continuous and the high boost factor. The output voltage can be varied by varying transformer turns ratio and shoot through duty ratio. The control technique used in this converter is PWM.

Catherine Amala Priya. E et al [23] have presented a renewable energy source fed grid connected gamma z-source inverter with harmonics optimization technique. The converter employs both PWM and SVPWM as control mechanism. The performance study was conducted on Γ-Z-source inverter. The performance study reveals that the SVPWM controlled inverter has better performance due to reduced harmonics. A Single stage high boost Quasi-Z-Source inverter for off-grid photovoltaic application has been proposed in [24]. In this study a current fed control at AC side is used with second order filter. The result of the study was that there is a reduction output disturbance. In [25] & [26] the high voltage gain, reduced transformer and shoot through duty ratio z-source inverters are presented. An embedded z-source inverter with three dc sources of small magnitude is presented in [27]. The modified topology reduces the stress on the capacitors. The control techniques used to study the performance of the proposed modified embedded z-source inverter was PWM with a reduced ripple inductor current.

In [28] the performance analysis of Induction motor drives fed with traditional inverters such as VSI, CSI, Z-source has been presented. It is a simulation-based study and PWM technique was employed in the simulation study. In [29] a comparative study of Z-source inverter and dc-dc converter fed VSI has been presented. A simple boost control technique and sinusoidal PWM were employed in the study. The comparative analysis of various topologies of traditional z-source inverters have been studied and presented in [30]-[33]. The z-source inverter is more suitable for various traction applications as they have both buck -boost capability.

SUMMARY OF THE REVIEW STUDY

The review study conducted so far suggests that the advanced power electronic control systems and z-source inverters are the future trends in transportation industry. The simplicity and ease of modification in impedance network employed in the design of the inverter/converter are the major contributors to achieve high performance of the systems wherever these converters employed. The structure and the control

mechanisms must be carefully selected to achieve the required performance of the converter. The traditional z-source inverters comparative topologies are tabulated in table 1.

Table-1: Z-Source Topologies Comparison

Impedance network	**Boost Factor**	**Number of Capacitors**	**Number of Inductors**	**Voltage stress on the switches**
Z-Source	$\frac{1}{1-2D}$ where $0 \leq D \leq 0.5$D	2	2	$\frac{1}{1-2D} V_{in}$
Q-Z-Source	$\frac{1}{1-2D}$ where $0 \leq D \leq 0.5$D	2	2	$\frac{1}{1-2D} V_{in}$
Embedded Z-Source	$\frac{1}{1-2D}$ where $0 \leq D \leq 0.5$D	2	2	$\frac{1}{1-2D} V_{in}$
Embedded Q-Z-Source	$\frac{1}{1-2D}$ where $0 \leq D \leq 0.5$D	2	2	$\frac{1}{1-2D}$ X $(V_1 + V_2)$
Trans-Z-Source	$\frac{1}{1-(1+n)D}$ where $0 \leq D \leq (1+n)^{-1}$D	1	Integrated 2 windings	$\frac{1}{1-(1+n)D}$ X V_{in}

Further, the review study involves the other modified z-source inverter topologies proposed by various researchers. These topologies were derived from traditional Z-Source inverter topology. The modifications were done by considering the structure of the impedance, switching device change/connectivity, in order to achieve high boost factor, voltage gain, low THD, continuous input current, reduced ripple in inductor currents and so on. These z-source variant topologies were proposed with various input power sources such as DC source, PV source etc. Table-2 shows the other Z-source inverter topologies suitable for EV/HEV applications.

Table-2 Other topologies of Z-Source Inverter for EV/HEV

Impedance network	Type of vehicle
Modified Γ-Z-source Inverter	HEV
Improved Z-Source Inverters / Trans-Z-source inverter	EV/HEV
Modified Γ-Z-source Inverter	EV
Bidirectional Q-Z-Source	EV
9 Switch Z-Source	EV

The review of the literature on the z-source converters, their variants suggests that the z-source converters can be a suitable system for various EV/HEV future transportation vehicles. The various technicalities involved in the design, development and implementation of these z-source topologies are very challenging. The study has revealed that:

i. There is no particular topology of ZSI which can be utilized for drive application with high efficacy, reliability and low cost.
ii. Most of the proposed models have complex hardware requirements and control, techniques.
iii. Knowledge on the techniques of control employed for the ZSI variants have to be studied and assessed.
iv. Knowledge on the various parameters which contributes to the overall cost of the systems must be gathered and minimized.
v. The requirements of passive elements for Trans-ZSI for drive applications with multiple power input sources have to be clearly defined and used in the construction of ZSI for drive application.
vi. The critical parameters associated with converters for the drive application must be clearly spelt and defined, which is a missed link.
vii. The topologies studied have not specified about the quality of the power delivered to the load.
viii. Is the quality of the power delivered by the converter to drive EV/HEV acceptable?
ix. The minimum possible input DC voltage, boost factor, ripple in the inductor current, passive components cost, size, details have to be clearly specified before suggesting any of the converter for drive applications.
x. The converter cost, power quality, battery life extension technologies, low power devices utilization are the major consideration.

PROPOSED AUTHORS SOLUTION

The fundamental topologies of Z-source inverters discussed in preceding sections were employed in various applications such as traction, energy conversion due to their high voltage gain and input current handling capacity. Since Z-source topologies can be easily modified to suit the applications and especially for electrical drive application. Based on the literature review study, it is noted that the future transportation vehicles can be driven with the modified z-source topology converters. The transportation vehicles which can be driven by these converters are electric vehicles and hybrid electric vehicles.

Further, Electric Vehicles/Hybrid Electric Vehicles (EVs/HEVs) are means of the future transportation vehicles. These transportation vehicles do not contribute to pollution as they operate on clean energy. These vehicles bring in string of benefits to the public and transportation industries.

These vehicles need highly efficient and reliable power converters to yield better performance. The power converters those are employed in electric drive applications are mostly pulse width modulation (PWM) based. These are voltage source (VS) and current source (CS) inverters. But these inverters are limited by a range as VSI performs as buck converter whereas CSI performs as boost inverter. In order to extend the range of operation, these inverters are combined with additional dc-dc converter to operate in both buck-boost mode. This increases the cost and complexity of the inverter as it becomes the double stage converter instead of single stage. Therefore, to extend the range of operation a magnetically coupled inverter known as Trans-Z Inverter has been developed for electric drive and other applications. It should be noted here that the trans-Z inverter is not specifically developed for EV/HEV applications.

The Trans-Z inverter is a type of inverters in which energy flows in two ways with the help of single diode, performs as buck-boost converter, has wide range, single stage in nature. Since, the EVs/HEVs vehicles need still improved and advanced converters, the researchers are concentrating on Trans-Z inverters. The Trans-Z source inverters have less capacitor counts in the circuitry and hence the cost reduction. The control mechanisms play a very important role in the performance of the inverter and end applications. Most commonly employed control mechanism in Trans-Z source inverter is predictive control and has variants. The predictive control variants are:

a. Trajectory based predictive control,
b. Hysteresis based predictive control, and
c. Model based predictive control

Model based predictive control is also known as finite control set and is more popular due to its design simplicity i.e. No modulator is required. These control techniques need to be reviewed carefully to bring in certain changes such that the performance of the converter is high along with reliability.

The proposed research is to throw a light on the control techniques, structure of the trans-Z source inverter such that the range can be increased. In addition, use of two inputs helps the Trans-Z source inverter to be independent of the fuel shortage if correct capacity fuel sources are not employed. The advanced power electronic devices with high operating characteristics makes the inverter design simple, increases efficiency, reliability and performance due to low count of components in design. The proposed research work is to focus on the development of new control technique for trans-Z source inverter with two input power sources that results in wide range of operation and hence the reliability.

References

1. Daouda Mande, João Pedro Trovão and Minh Cao Ta, "Comprehensive Review on Main Topologies of Impedance Source Inverter Used in Electric Vehicle Applications", World Electric Vehicle Journal 2020, 11, 37; doi:10.3390/wevj11020037.
2. LI Bo, LI Yue, YIN Huayi, and Hu Mengjie, "An Improved Strategy for Z Source Inverter"13th IEEE International Conference on Control & Automation (ICCA) July 3-6, 2017. Ohrid, Macedonia, 978-1-5386-2679-5/17/$31.00 ©2017 IEEE pp904-908 2017.
3. Kancharana Vinod Kumar, Reddiprasad Reddivari & Debashisha Jena (2019): A Comparative Study of Different Capacitor Voltage Control Design Strategies for Z-Source Inverter, IETE Journal of Research, DOI: 10.1080/03772063.2019.1650669.
4. Yam P. Siwakoti, Fang Zheng Peng, Frede Blaabjerg, Poh Chiang Loh, and Graham E. Town, "Impedance-Source Networks for Electric Power Conversion Part I: A Topological Review" IEEE Transactions on Power Electronics, Vol. 30, No. 2, February 2015 pp: 699-716.
5. Anh-Vu Ho, Ji-Suk Hyun, Tae-Won Chun, Hong-Hee Lee, "Embedded Quasi-Z-Source Inverters Based on Active Switched-Capacitor Structure", 978-1-5090-3474-1/16/$31.00 ©2016 IEEE pp:3384-3389.
6. Wei Qian, Fang Zheng Peng, and Honnyong Cha," Trans-Z-Source Inverters", IEEE Transactions on Power Electronics, vol. 26, no. 12, December 2011 pp:3453-3463
7. Jing Yuan, Yongheng Yang, Ping Liu, Yanfeng Shen, Zhipeng Qiu, Frede Blaabjerg, "An Embedded Enhanced-Boost Z-Source Inverter", 978-1-5386-6054-6/18/$31.00 © 2018 IEEE.
8. Jing Yuan, Yongheng Yang, Ping Liu, Yanfeng Shen, and Frede Blaabjerg, "An Embedded Switched-Capacitor Z-Source Inverter with Continuous Input Currents", 978-1-5386-8330-9/19/$31.00 ©2019 IEEE, page 2366-2371.
9. R.Malathi, M.Rathinakumar," Comparison of PV based Embedded Z-Source Inverter fed Three Phase Induction Motor with PI Controller and PID Controller based closed loop systems", 3rd International Conference on Advances in Electrical, Electronics, Information, Communication and Bio-Informatics (AEEICB17), 978-1-5090-5434-3©2017 IEEE.
10. Hossein Torkaman, Ebrahim Afjei , Ali Keyhani , Mobina Poursmaeil, "Control and management of hybrid AC/DC microgrid based on Γ-Z-source converter", doi: 10.1049/iet-gtd.2018.6365. IET Gener. Transm. Distrib., 2020, Vol. 14 Iss. 14, pp. 2847-2856 © The Institution of Engineering and Technology 2019.
11. Reddiprasad Reddivari, Debashisha Jena, "Differential mode gamma source inverter with reduced switching stresses", 2017 IEEE PES Asea Pacific Power and Energy Engineering Conference (APPEEC), 978-1-5386-1379-5/17/$31.00 ©2017 IEEE.

12. H. Fathi Kivi, and H. Madadi Kojabadi," Enhanced-Boost Z-Source Inverters with Switched Z-Impedance", DOI 10.1109/TIE.2015.2477346, IEEE Transactions on Industrial Electronics.

13. J. Srijeeth, Vignesh Chenni Thiagarajan, S.R. Mohanrajan, "Z-Source Dual Active Bridge Bidirectional AC-DC Converter for Electric Vehicle Applications", 978-1-5386-9316-2/18/$31.00 ©2018 IEEE.

14. ReddyPrasad Reddivari, Pruthviraj B G, Manish Bharat, and Arjun Kumar G B, "Müdified Gamma Süurce Inverter für Fuel Cell -Battery Hybrid Electric Vehicles", 978-1-4673-6658-8116/$3l.00 ©20 16 IEEE.

15. Thilak Senanayake, Ryuji Iijima, Takanori Isobe, Hiroshi Tadano, "Improved Impedance Source Inverter for Hybrid/Electric Vehicle Application with Continuous Conduction Operation", 978-1-4673-9550-2/16/$31.00 ©2016 IEEE, page no:3722-3726.

16. Zeeshan Aleem, Moin Hanif, "Improved ī-Z-source Inverter", 978-1-5090-0737-0/16/$31.00 ©2016 IEEE.

17. Sang-hyup Han, Heung-Geun Kim, Bon-Gwan Gu, Honnyong Cha, Tae-won Chun, Eu-Chul Nho, "Induction Motor Control System Using Bidirectional Quasi-Z Source Inverter", 9th International Conference on Power Electronics-ECCE Asia June 1 - 5, 2015 / 63 Convention Center, Seoul, Korea, page no:588-593.

18. M. Z.Zizoui, B.Tabbache , F.Belkhiri and M.E.H.Benbouzid, "Maximum Constant Boost Control of 9-Switch zSource Power Inverter-Based Electric Vehicles", The 5th International Conference on Electrical Engineering – Boumerdes (ICEE-B) October 29-31, 2017, Boumerdes, Algeria.

19. Sertac Bayhan, Mohamed Trabelsi, and Haitham Abu-Rub, "Model Predictive Control of Z-Source Four-Leg Inverter for Standalone Photovoltaic System with Unbalanced Load", 978-1-4673-9550-2/16/$31.00 ©2016 IEEE page:3663-3668.

20. Siddhartha A. Singh, Giampaolo Carl, Najath A. Azeez, and Sheldon S. Williamson, "Modelling, Design, Control, and Implementation of a Modified Z-source Integrated PV/Grid/EV DC Charger/Inverter", DOI 10.1109/TIE.2017.2784396, IEEE Transactions on Industrial Electronics.

21. ReddiPrasad Reddivari, Debashisha Jena, "Practical Limitations of Embedded Z-Source DC-DC Converters in PV Applications", 978-1-5386-2462-3/18/$31.00 ©2018 IEEE.

22. Swathyprakash and Rani S, "Modified Trans-Z-Source Inverter with Continuous Input Current and Improved Boost Factor", International Conference on Electrical, Electronics, and Optimization Techniques (ICEEOT) – 2016, 978-1-4673-9939-5/16/$31.00 ©2016 IEEE.

23. Catherine Amala Priya. E and G. T. Sundar Rajan, "Renewable Energy Source based Γ- Z source inverter interlinked to grid with Harmonics optimization Techniques" 978-1-5386-1508-9/18/$31.00 ©2018 IEEE.

24. Arvind Yadav, Subhash Chandra, "Single stage high boost Quasi-Z-Source inverter for off-grid photovoltaic application", 2020 International Conference on Power Electronics & IoT Applications in Renewable Energy and its Control (PARC) GLA University, Mathura, UP, India. Feb 28-29, 2020.

25. Soroush Esmaeili and Abdolreza Sheikholeslami, "Transformer Types of Extended Z-Source Inverter with High Voltage Gain and Reduced Transformer Turns Ratio", The 6th International Power Electronics Drive Systems and Technologies Conference (PEDSTC2015) 3-4 February 2015, Shahid Beheshti University, Tehran, Iran. 978-1-4799-7653-9/15/$31.00 ©2015 IEEE page no:183-188.

26. Soroush Esmaeili, Shekouh Karimi, Pouya Tarassodi and Alireza Siadatan, "Two-Stage Asymmetrical -Z-Source Inverter with High Voltage Gain and Reduced Shoot-Through Duty Ratio", 2016 International Symposium on Power Electronics, Electrical Drives, Automation and Motion, 978-1-5090-2067-6/16/$31.00 ©2016 IEEE.

27. Milad Abbasi and Ebrahim Babaei, "A New Topology of Embedded Z-Source Inverter with Low Voltage Stress on Capacitors", 978-1-4673-9749-0/16/$31.00 ©2016 IEEE.

28. Md. Khurshedul Islam* , Md. Mustafa Zaved, Air Mohammad Siddiky, Khandakar Abdulla Al Mamun, "A Comparative Analysis among PWM Control Z-source Inverter with Conventional PWM Inverter for Induction Motor Drive", 978-1-5090-6122-8/16/$31.00 ©2016 IEEE.

29. Mrudul A. Mawlikar, Ms. Sreedevi S Nair, "A Comparative analysis of Z source inverter and DCDC converter fed VSI", 978-1-5090-2794-1/17/$31.00 ©2017 IEEE.

30. Reddiprasad Reddivari & Debashisha Jena (2018) "A critical analysis of Z-source converters considering the effects of internal resistances", International Journal of Electronics, 105:10, 1785-1803, DOI: 10.1080/00207217.2018.1482007

31. Reddiprasad Reddivari, Debashisha Jena," A Detailed Model of Z-Source Converter Considering Parasitic Parameters", 978-1-5386-2462-3/18/$31.00 ©2018 IEEE.

Closed loop control of Half Bridge Bidirectional DC – DC Converter for EV Application

Ragasudha C P[1] A. Nageswara Rao[2] Sophie Salins[3] Sonam Pal A[4]

[1, 3, 4] Presidency University, Bengaluru, India, [2] CMR Institute of Technology, Bengaluru

[1]ragasudha@presidencyuniversity.in

Abstract

This paper briefs about the performance of a Bidirectional DC – DC Converter in the domain of Electric Vehicles along with achieving the required speed of the motor while applying different loads. A Half Bridge Bidirectional Converter linked to a battery on Low Voltage(LV) side and a separately excited DC motor on the High Voltage(HV) side is employed in this paper along with the closed loop configuration of the motor drive by utilizing a PID Controller. The gains of the PID Controller are determined by the auto-tuning algorithm in MATLAB/SIMULINK. The converter's performance was analysed for the two modes.

Keywords: Electric Vehicle, Regenerative Braking Mode, Half Bridge Converter, Separately Excited DC Motor, PID Controller, Auto – Tuner.

List of Notations and Abbreviations

Electric Vehicle (EV), Hybrid Electric Vehicle (HEV), State Of Charge (SoC)

1. INTRODUCTION

Ever since the hike in gasoline prices and the harmful pollution caused by conventional vehicles, the demands for the Electric Vehicle (EV)/Hybrid Electric Vehicle (HEV) has increased. An EV depends on an Energy Storage System (ESS) for the traction power and, the HEV depends on both ICE and an ESS [1][2][7]. But the EV/HEV ESS have lot of limitations when it comes to pricing, storage capability and providing better mileage to the vehicle. These constraints in the ESS technology of the Electric Vehicle prevents them from advancing in the market. Since the primary concern, while EV/HEV drive design, is to boost the performance, many developments are made to achieve the same [3]. In our work we have demonstrated the performance of an EV drive comprising of a DC motor fed by a Bidirectional Converter. The utilization of the Bidirectional Converter in an EV drive increases the efficiency since it provides the provision of bidirectional power flow [8][9]. The closed loop control of speed of the DC motor by a PID Controller is also presented to achieve the required speed during varying loads.

1.1. Bidirectional DC – DC Converter

It was inferred that to improve the reliability of the ESS in the motor drive, the voltage level of the ESS must be greater. This can be accomplished by adding more cells to the battery pack of the ESS. But this method can increase the bulkiness of the drive which is not a desirable feature [1][2][7]. The solution for this problem is the utilization of a Bidirectional Converter which has the characteristic of flow of power in two directions. Bidirectional converters lower the current level to raise the level of voltage of an energy storage device to a greater level reducing the losses giving a rise to the performance of the motor drive. The Bidirectional DC – DC Converters are broadly divided into two general divisions i.e., Non – Isolated and Isolated Bidirectional Converter topologies. Since the Isolated Converters are to be provided with transformer and galvanic isolation, these converters are considered to be heavy for an EV drive train. Therefore, we have opted for the Non – Isolated Bidirectional Converters for the work.

The different Non – Isolated Bidirectional converters are basic Buck – Boost, Buck – Boost Cascaded, Cuk, Half Bridge, SEPIC/Zeta, Switched – Capacitor, and Interleaved Converters. In Buck – Boost Converters, the passive components and the power switches operates under high thermal and electrical stress resulting in high power loss. The Buck – Boost Cascaded converter requires a greater number of components [2][4][5]. The Half - Bridge converter has only one inductor and have greater performance due to the lower inductor current. The Switched – Capacitor converters suffer from high ripple current which causes Electro – Magnetic Interference (EMI) at the output due to the presence of a greater number of passive components. The Interleaved converters are extremely expensive and have a complex control strategy [2][6][7]. Out of all the converter topologies, the Half – Bridge topology was selected for our work since it was compact, efficient and easy to implement its control strategy [1].

2. BIDIRECTIONAL DC – DC CONVERTER WITH BATTERY AND DC MOTOR

Figure 2.1 shows the Bidirectional Converter fed Separately Excited DC Motor drive. MOSFET switch Q2 with the diode D1 is modulated to accomplish the boost converter operation. MOSFET switch Q1 with the diode D2 is modulated for the converter to work in buck mode which reverses the flow of power. It should be remembered that the inductor current directions in the two modes are opposite. To achieve motoring and regenerative braking of the engine along with the motor's speed control, a control model is provided using a PID controller. In this model, a Lead Acid battery model was used to validate the motor output in both the modes. This strategy produces the required results when various speed commands are applied

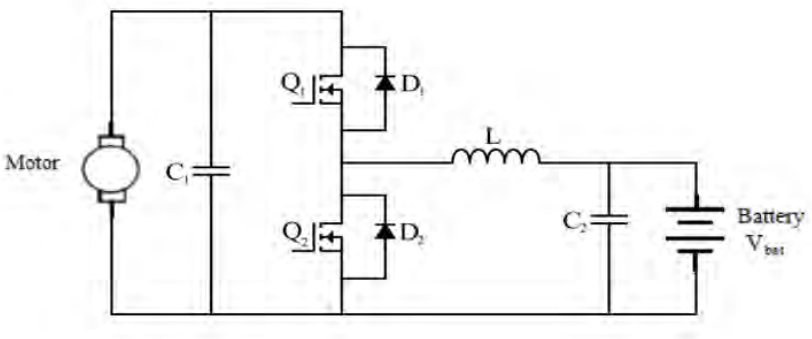

Figure 2.1. Bidirectional Converter fed DC motor

2.1 *Determining PID Controller's gain by PID Auto – Tuner in Simulink*

The PID Tuner uses the auto-tuning algorithm to identify a linear transfer function from the input and output data sets and tune the controller gains. The PID Controller's step response was tuned to have the following responses as shown in Table 2.1.1 and the Controller gains are determined as shown in Table 2.1.2.

Table 2.1.1: Step response parameters from auto – tuning of PID Controller

PID CONTROLLER STEP RESPONSE PARAMETERS		
Sl. No.	**Parameters**	**Values**
1	Rise Time (s)	0.5s
2	Settling time (s)	0.15s
3	Overshoot (%)	2.8%

Table 2.1.2: PID Controller gains from auto – tuning of PID Controller

PID CONTROLLER GAINS		
Sl. No.	**Parameters**	**Values**
1	K_P	0.015
2	K_I	0.1
3	K_D	0.0002

Table 2.2.1: Parameters and values used for modelling

Parameters	**Values**
Motor Ratings	5HP, 240V,1750rpm
Inductor (L)	50µH
Capacitor (C)	220µF
Capacitor (C)	220µF
Battery voltage	48V
Battery capacity	140AH

2.2 *Closed loop simulation of the drive*

The MATLAB Simulation of the drive is as shown in figure 2.2.1. The parameters used for the simulation is given in Table 2.2.1. The total simulation time was considered as 2 seconds out of which the converter works in boost mode for the initial 1 second and buck mode for the other 1 second. The required speed of 60 rad/s (3600 rpm) is to be achieved for both the modes.

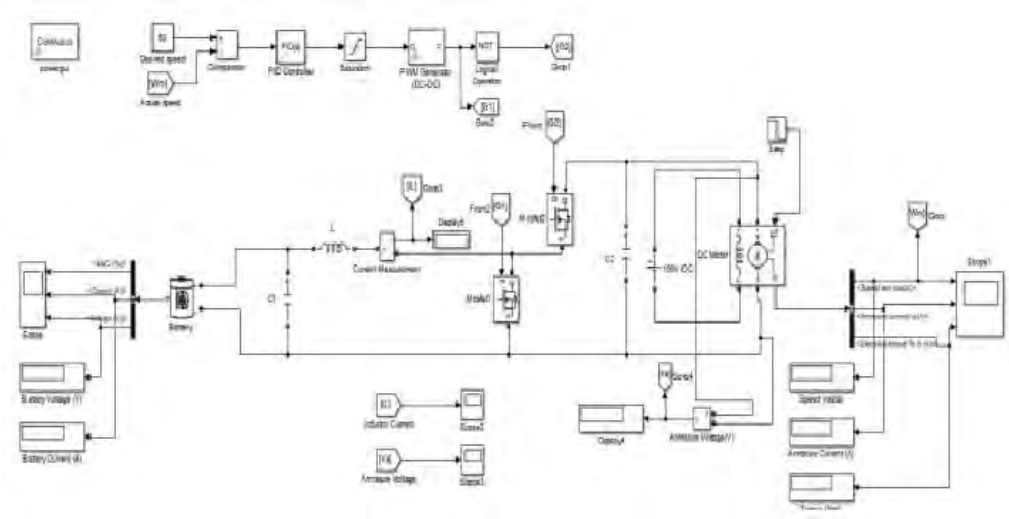

Figure. 2.2.1 Closed loop simulation of Bidirectional DC-DC Converter fed separately excited DC Motor.

2.3 Simulation results

Various system parameters obtained from the closed loop simulation of DC-DC converter fed separately excited DC motor are presented in this section along with the waveforms. Consolidated data is given in Table 2.3.1.

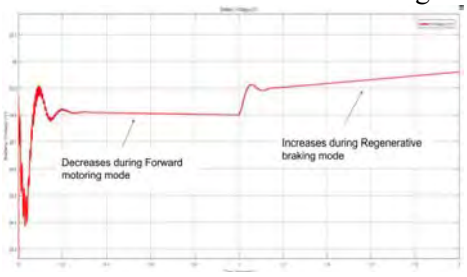

Figure 2.3.1 Battery Voltage in Volts

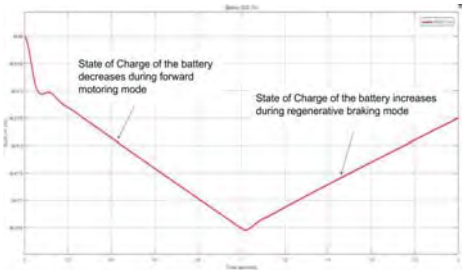

Figure 2.3.2 The SOC of battery in %

Battery Voltage and SoC of the Battery: The battery is discharged to run the motor during motoring mode and the battery gets charged during regenerative braking mode.Therefore the battery voltage decreases till 1s and increases till another 1s as shown in figure 2.3.1. As battery gets discharged during forward

motoring mode, its SoC is seen to decrease and when the battery gets charged during regenerative mode the SoC of the battery rises as in figure 2.3.2

Battery Current: The battery current increases since the current is drawn to power the motor during motoring mode and decreases during regenerative braking mode which is shown in figure 2.3.3.

Inductor Current: During forward motoring mode the inductor gets charged by the battery and the current rises and is discharged to charge the HV side capacitor to run the motor. During regenerative braking mode the HV side charges the inductor and the output capacitor and then gets discharged to charge the battery. Waveforms are given in figure 2.3.4

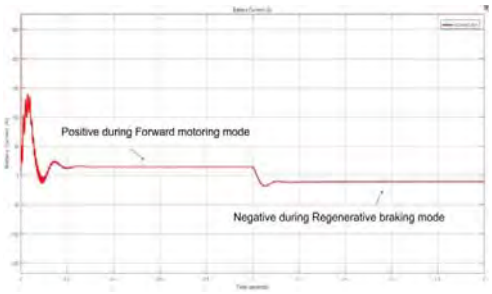

Figure 2.3.3 Battery Current in Amps

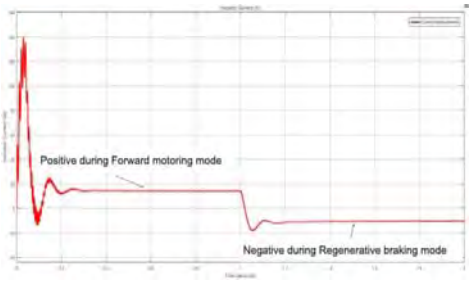

Figure 2.3.4 Inductor Current in Amps

Motor Torque: For the PID Controlled drive, during forward motoring mode a torque of 10Nm is applied to the motor up to 1 second and a torque of -10Nm is given for the next 1 second so that battery gets charged by the motor during regenerative braking mode since it acts as a generator as in figure 2.3.5.

Armature Current: Since the torque and armature current is directly proportional to each other it is positive during forward motoring mode and negative during regenerative braking mode and is around 9A.Waveforms are given in figure 2.3.6.

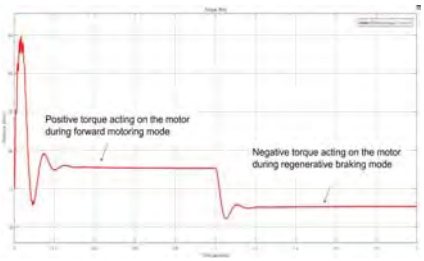

Figure 2.3.5 Motor Torque in Nm

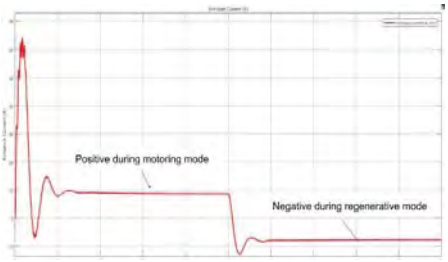

Figure 2.3.6 Motor Armature Current in Amps

Motor speed: The speed of the motor is to be maintained constant during both the modes. The required speed of 60 rad/s is reached and the desired speed is reached at a very fast rate during both the modes as shown in figure 2.3.7.

Armature Voltage: During motoring mode, the back emf is always less than the armature voltage as the duty ratio changes itself to run the motor at the required speed. Waveforms are given in figure 2.3.8. The back emf should be greater than the armature voltage to maintain the constant speed during regeneration.

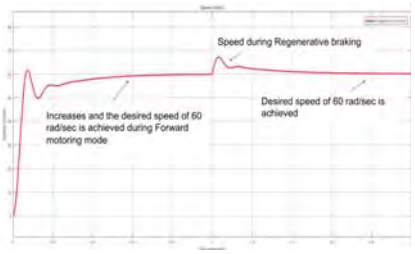

Figure 2.3.7 Motor speed in rad/s

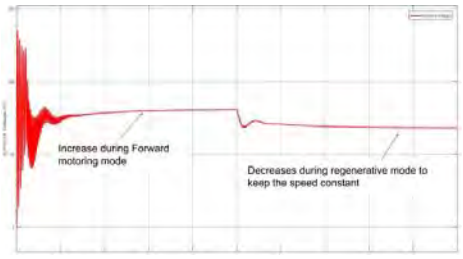

Figure 2.3.8 Motor Armature Voltage in Volts

Table 2.3.1: Observations from simulation results of PID controlled Drive

Sl. No.	Parameters	Motoring Mode	Regenerative Braking Mode
1	Battery Voltage (V)	Decreases from 48.84V to 48.81V	Increases from 48.81V to 48.96V
2	Battery SOC (%)	Decreases from 86.68% to 86.676%	Increases from 86.676% to 86.678%
3	Battery Current (A)	Range of 10A to 12A	Range of 10A to 12A
4	Inductor Current (A)	10A	-10A
5	Motor Torque (Nm)	10Nm	-10Nm
6	Armature Current (A)	9A	-9A
7	Motor speed (rad/s)	60 rad/s at 0.5s	60 rad/s at 1.5s
8	Armature Voltage (V)	Increases to 77V	Decreases to 68V

3. CONCLUSION

In this work, we have demonstrated the Motoring and Regenerative action along with the control of speed of the separately excited DC motor drive. The Half-Bridge Converter configuration was chosen for the work because it provides higher efficiency compared to other topologies of the Bidirectional Converter. The PID Controlled closed-loop system was efficient for the control of speed as the desired speed was reached at a faster rate at a time of 0.5s and hence the battery charge drawn to power the motor was less. The model was analysed in MATLAB/SIMULINK and the outcomes are supported by the waveforms.

4. FUTURE WORK

Despite its low cost, high reliability, and high dynamic efficiency, the PID Controlled drive is less efficient and fragile in the presence of disturbance and instability, as well as in avoiding large transients between directions. These issues can be addressed by using sophisticated control schemes like fuzzy logic which offers a fast solution as well as robustness due to adaptive characteristics relevant to non-linear and systems which are not accurate, instability, varying parameters, and load distortions.

5. REFERENCES

[1]. Joshi MC, Samanta S. 'Modeling and control of bidirectional DC-DC converter fed PMDC motor for electric vehicles' Annual IEEE India Conference (INDICON) 2013 Dec 13 (pp. 1-6). IEEE

[2]. Gorji SA, Sahebi HG, Ektesabi M, Rad AB. 'Topologies and control schemes of bidirectional DC–DC power converters: an Overview'. IEEE Access. 2019 Aug 23; 7:117997-8019.

[3]. Lai JS, Nelson DJ. 'Energy management power converters in hybrid electric and fuel cell vehicles'. Proceedings of the IEEE. 2007 Apr 30;95(4):766-77.

[4]. Shah JP, Soori PK, Chacko S. 'Energy management strategies for modern electric vehicles using MATLAB/Simulink. journal of electronic science and technology' 2015 Sep 25;13(3):282-8..

[5]. Du Y, Zhou X, Bai S, Lukic S, Huang 'A. Review of non-isolated bi-directional DC-DC converters for plug-in hybrid electric vehicle charge station application at municipal parking decks' Twenty-Fifth Annual IEEE Applied Power Electronics Conference and Exposition (APEC) 2010 Feb 21 (pp. 1145-1151). IEEE.

[6]. Caricchi F, Crescimbini F, Capponi FG, Solero L. 'Study of bi-directional buck-boost converter topologies for application in electrical vehicle motor drives', Thirteenth Annual Applied Power Electronics Conference and Exposition 1998 Feb 15 (Vol. 1, pp. 287-293).

[7]. Ravi D, Reddy BM, Shimi SL, Samuel P. 'Bidirectional DC to DC converters: an overview of various topologies, switching schemes and control techniques', International Journal of Engineering & Technology. 2018 Sep;7(4.5):360-5.

[8]. Hinov N, Dimitrov V, Vacheva G.' Mathematical Modelling and Control of Hybrid Sources for Application in Electric Vehicles' 24th International Conference Electronics 2020 Jun 15 (pp. 1-5). IEEE. Systems ELMA 2019, 6-8 June 2019, Varna, Bulgaria

[9]. Sharma A, Mishra R, Yadav AK, Phukan A. 'Bidirectional DC-DC Converter for Incorporating Regenerative Braking in E-bikes', International Conference on Electrical, Electronics, Communication, Computer, and Optimization Techniques (ICEECCOT) 2018 Dec 14 (pp. 1019-1024). IEEE.

Reverse Droop Control of Distributed Generation Inverters in Low Voltage Microgrid

Dr. Chethan Raj D
School of Electrical and Electronics Engineering
BMSE, Bengaluru, INDIA
chethanraj9@gmail.com

Dr. Vivekanandan Subburaj
School of Electrical and Electronics Engineering
REVA University, Bengaluru, INDIA
vivekanandan.subburaj@reva.edu.i

Dr. Santoshkumar Hampannavar
School of Electrical and Electronics Engineering
REVA University, Bengaluru, INDIA
vivekanandan.subburaj@reva.edu.in

Abstract: In the low-voltage microgrid system with multi-inverter running in parallel, due to the impedance difference of each inverter output line, it is difficult for the distributed power generation units in the system to allocate the active power of the public load according to the traditional anti-droop control strategy, which affects the stability of the system. In view of this problem, the output power distribution performance of low voltage microgrid system is analyzed theoretically, and the main factors affecting the power distribution performance are obtained. The introduction of virtual resistance into the double-closed-loop control of voltage current not only inhibits the effect of coupling between active and reactive power on the stability of the system, but also improves the output power quality of the system. Virtual resistance can track the change of active power difference between active power and reference output of each distributed power supply in real time and compensate for the bus voltage drop due to line impedance difference in time and effectively. The proposed strategy enables each distributed power supply to distribute the active power in the public load reasonably. Finally, the validity and correctness of the strategy are verified on the simulation platform.

Keywords

1. INTRODUCTION

With the emergence of the non-renewable energy crisis and the enhancement of the greenhouse gas effect, various new energy sources such as wind, solar and tidal energy have become the focus of more and more researchers. At present, the utilization of new energy in the power system is mainly distributed power supply system with microgrid as the carrier. The microgrid system consists of distributed power sources (Distributed Generator, DG), loads and controllers, etc., to provide users with electrical energy [1]. In recent years, the power distribution performance of microgrids has attracted the attention of domestic and foreign scholars [2-5].

In the microgrid system, when the peer-to-peer control mode is used to control each DG in the system, the dependence of each DG on the communication equipment is greatly reduced, and the control only depends on the local information of the system [6]. In this control mode, the selection of each DG control strategy in the microgrid system is very important, which has caused Droop control to be widely used [7].

Droop control is a common control method for parallel operation of multiple DGs in microgrid systems. It not only provides voltage and frequency support for the system, but also realizes reasonable power distribution according to their respective droop characteristic equations [8]. However, the droop control also has the following problems: (1) Due to the inherent characteristics of the microgrid system, it is difficult for the traditional droop control strategy to give full play to the energy supply efficiency of the DGs in the system, and even affect the stability of the system [9-11]; (2) The selection of the droop control method is related to the voltage level of the microgrid system. The low-voltage microgrid system uses traditional anti-sag control.Similar to traditional droop control, it also has the advantages of small fluctuations and plug and play [12-14].

In order to solve the problem that the power distribution accuracy of the microgrid system is reduced due to the traditional anti-sag control, domestic and foreign scholars have proposed a variety of improvement strategies. Literature [15-17] introduced virtual impedances on the basis of traditional anti-sag control strategies to mitigate the adverse effects of power coupling between inverters on the microgrid system, but they did not consider the impact of virtual impedance on the bus voltage Influence. Literature [18-20] used methods such as constructing adaptive virtual resistance or adaptive virtual impedance to compensate for the voltage drop generated by virtual impedance or virtual resistance while suppressing the system's circulating current.However, the above-mentioned adaptive virtual control strategy increases the line voltage drop and cannot take into account the power quality.

Literature [21-23] respectively proposed an adaptive droop coefficient to achieve the purpose of power sharing, but the adjustment of the adaptive droop coefficient is still poorly adjusted, resulting in poor dynamic performance. Although the above-mentioned improved droop control strategy improves the power distribution accuracy of the system to varying degrees, there is no experiment to prove the improvement effect of the power quality of the system. Aiming at the characteristics of R-X in low-voltage micro-grid systems, this paper proposes a low-voltage micro-grid power distribution strategy based on adaptive virtual impedance based on the P-V relationship [24].This method can improve the distribution accuracy of the output power of each DG in the microgrid system when the impedance of each DG output line is resistive.

Finally, simulation experiments verify the feasibility of the strategy proposed in this paper.

2. POWER FLOW CHARACTERISTICS BETWEEN DISTRIBUTED GENERATION INVERTERS

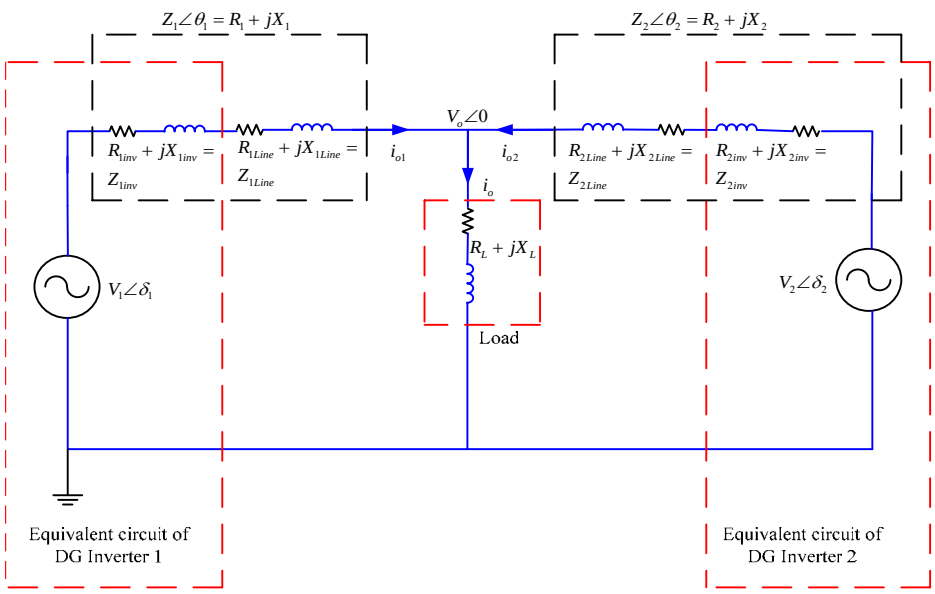

Figure 2.1 Equivalent circuit diagram of DG inverter parallel operation

The voltage source distributed generation inverter is an important way to connect the distributed power supply and the power grid in the microgrid. The regulation characteristics of the DG inverter are crucial for the power distribution between the distributed generation sources. The DG inverter with droop control can adjust its own frequency and power according to measured active and reactive power.

The following is an overview of the basics of droop control using Figure 1 to analyses the output power of two DG inverters operating in parallel. The sum of the line and output impedance of the DG inverter1 and DG inverter 2 is given by [3]:

The equivalent circuit impedance $Z_n (n = 1,2)$ is:

$$Z_n = R_n + jX_n \tag{1}$$

The DG inverters output current (n=1,2) is:

$$i_n = \frac{V_n\angle\delta_n - V_o\angle 0}{Z_n\angle\theta_n} \tag{2}$$

The output power of DG inverters (n=1,2) is:

$$S_n = P_n + jQ_n = V_n\angle\delta_n . i_n^* \tag{3}$$

P_n is the output active power of DG inverter n; Q_n is the output reactive power of DG inverter n; i_n^* is the output current conjugate.

$$P_n = \frac{1}{Z_n}[(V_n V_o \cos\delta_n - V_o^2)\cos\theta_n + V_n V_o \sin\delta_n \sin\theta_n)] \tag{4}$$

$$Q_n = \frac{1}{Z_n}[(V_n V_o \cos\delta_n - V_o^2)\sin\theta_n - V_n V_o \sin\delta_n \cos\theta_n)] \tag{5}$$

When the impedance of the DG inverter system is resistive $\theta = 0^o$, the active and reactive power of the DG inverter output respectively is:

$$P_n = \frac{V_o(V_n - V_o)}{R_n} \tag{6}$$

$$Q_n = -\frac{V_n V_o}{R_n}\delta_n \tag{7}$$

Droop control is actually controlled by the principle of linear relationship between the power of the inverter output and the amplitude of the system frequency and output voltage. The Droop control method is generally used in the control of distributed generation units in the Peer-to-peer control strategy [8].

Reverse droop control strategy can be derived [9,10]:

$$V_n - V_{ref} = -m_{PV}(P_n - P_{ref}) \tag{8}$$

$$f_n - f_{ref} = n_{Qf}(Q_n - Q_{ref}) \tag{9}$$

Where f_{ref} is the nominal frequency of the system and f is the actual frequency of the system; V_{ref} is the rated voltage of the system and V is the actual output voltage of the system. Q_{ref} is the system rated reactive power and Q is the actual output reactive power; m_{PV} is the reverse droop(P-V) coefficient and n_{Qf} is the reverse(Q-f) droop coefficient. Figure 2 shows the droop characteristics of reverse droop control[Chen (2014), Wang (2014)].

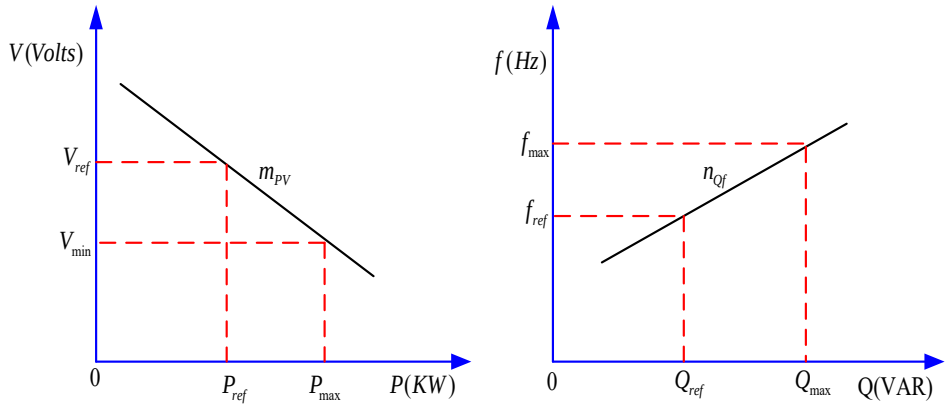

Figure 2.2 Reverse droop control curves

3. DIAGRAM OF REVERSE DROOP CONTROL

In a microgrid, a reverse droop control is used to adjust the voltage and frequency of the DG inverters output, so that the micro-grid can operate under different load requirements. As can be seen from Figure 3, where L_f is the filter inductor, C_f is the filter capacitor, r is the filter inductor equivalent resistance and Z_{Load} is the load impedance, the reverse droop control model of microgrid can be divided into two parts: voltage and current loop control model and power droop control model. First, the output voltage and current of the microgrid power supply are obtained by sampling the DG inverter module. The output power of the microgrid power supply is obtained by the power calculation unit and the low-pass filter and then calculated according to the active power droop controller and the reactive power droop controller respectively. The reference voltage values V_{dref} and V_{qref} is finally adjusted by the voltage PI control and i_{dref} and i_{qref} are adjusted by the current P control to obtain controllable sinusoidal modulation signal m to the DG inverter[10,11] .

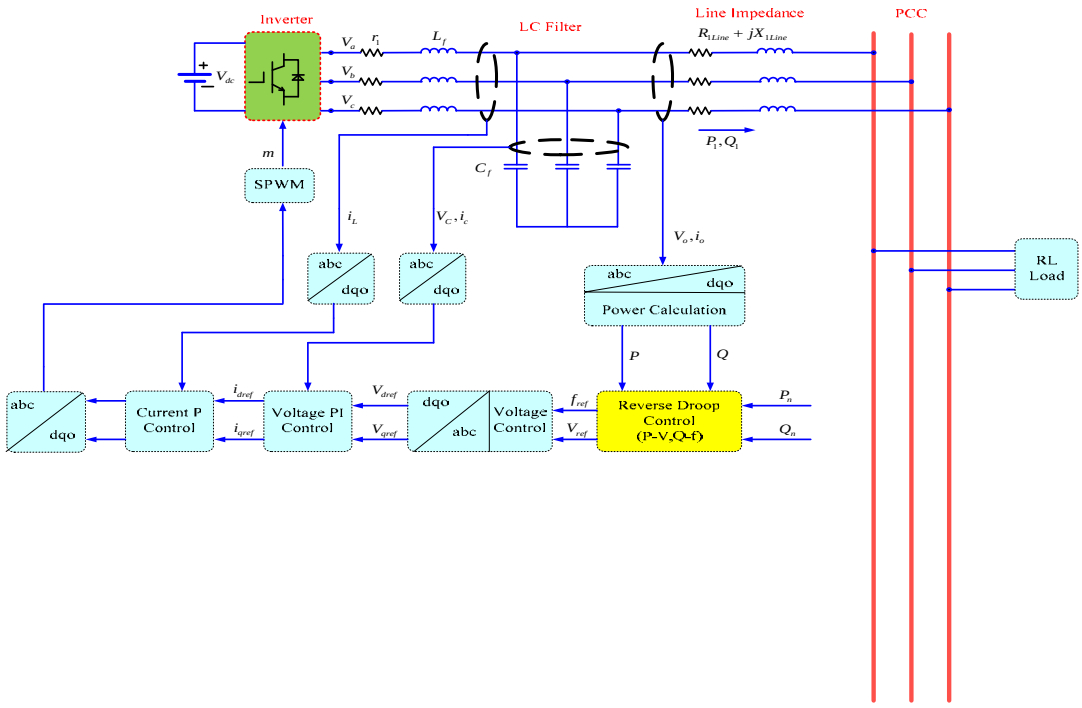

Figure 3.1 Control diagram of reverse droop control

From the above analysis, it can be seen that the output impedance of the inverter is complex and its nature is uncertain. In general, the output impedance of the inverter itself is small and the output impedance characteristic is determined by the line impedance. However, the impedance of the line at the output end of the inverter in the microgrid is flexible and it is not possible to use the reverse droop control directly [12-13].

3.1 Vitrual Resistance Method:

Decoupling the output power requires knowing exactly the information of the output impedance and requires real-time on-line impedance measurement. This technology is still under research and is not mature enough. Therefore, the output impedance of the DG inverter is altered using virtual resistance method as shown in the figure 4[14-15]:

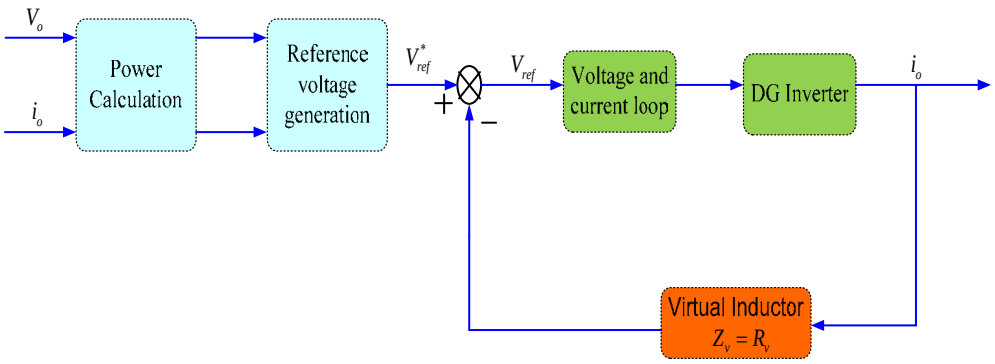

Figure 3.2 Virtual resistance block diagram.

When the load is suddenly changed, the voltage amplitude and frequency are adjusted to obtain a good power sharing effect. This method can achieve accurate power sharing, has better dynamic modification performance and is suitable for resistive line impedance conditions[15-16].

Virtual resistor is expressed as:

$$Z_{vir}(s) = R_v, Z_o(s) = \frac{C_1 s^2 + C_2 s + C_3}{C_4 s^3 + C_5 s^2 + C_6 s + C_7} \tag{10}$$

$$\begin{aligned} C_1 &= L, C_2 = r + K_{pi} K_{pwm} K_{pv} R_v, C_3 = R_v K_{pi} K_{pwm} K_{vi}, C_4 = LC \\ C_5 &= rC + K_{pi} K_{pwm} C, C_6 = 1 + K_{pi} K_{pwm} K_{vi}, C_7 = K_{pi} K_{pwm} K_{vi} \end{aligned} \tag{11}$$

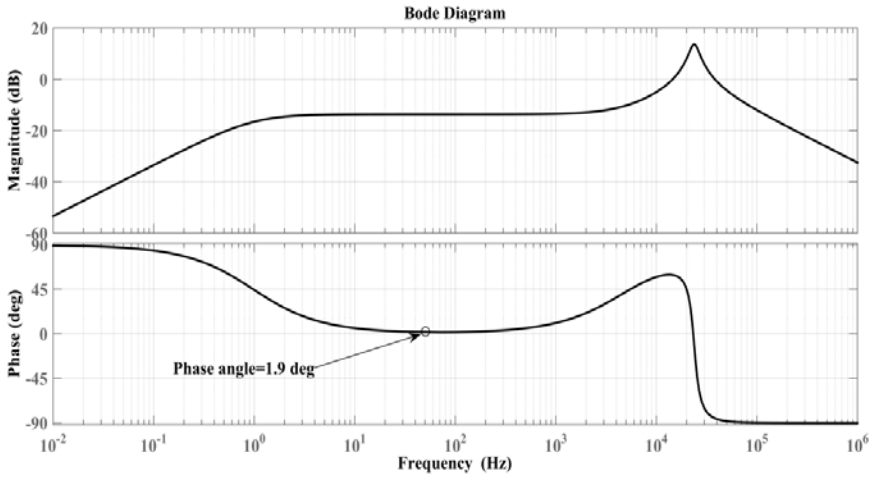

Figure 3.3 Bode diagram of inverter output impedance with virtual resistor.

If the line impedance is resistive, virtual resistor is added the control loop of reverse (*P-V/Q-f)* droop control to improve the power decoupling effect. Impedance angle at 50 Hz is 1.9° as shown in the Figure 5. The parallel inverter output impedance tends to be more resistive, which has a major role in improving the power sharing.

4. SIMULATION RESULTS

Power sharing analysis of reverse droop control with virtual resistors under resisive line impedance with frequent changes in load.

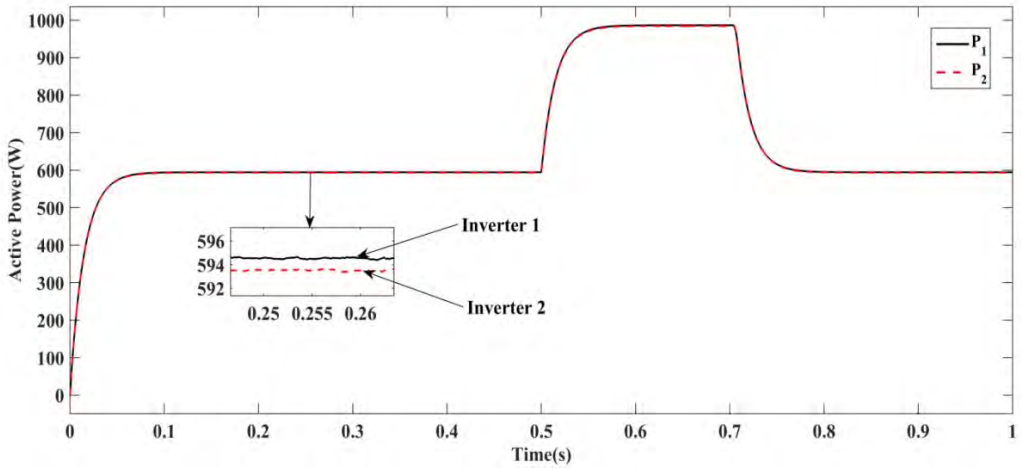

Figure 4.1 Active power sharing using reverse droop control with virtual resistors under resistive line impedance with frequent changes in load.

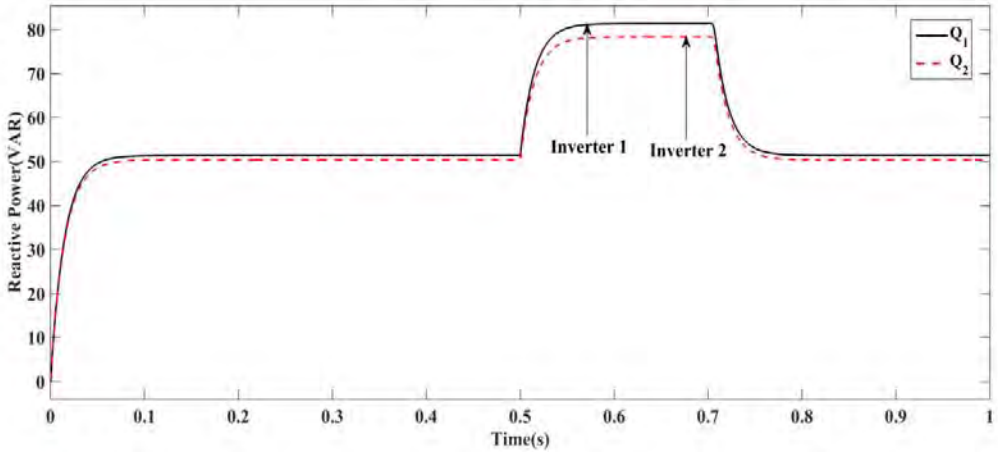

Figure 4.2 Reactive power sharing using reverse droop control with virtual resistors under resistive line impedance with frequent changes in load.

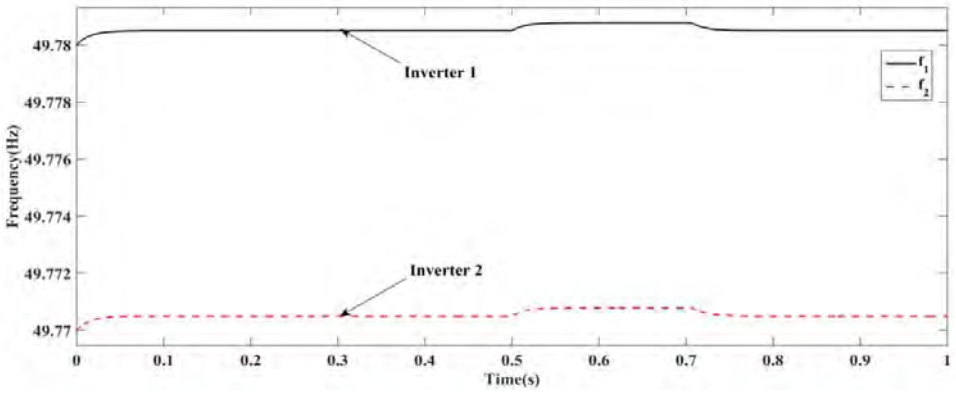

Figure 4.3 Parallel DG inverters output frequency using reverse droop control with virtual resistors under resistive line impedance with frequent changes in load.

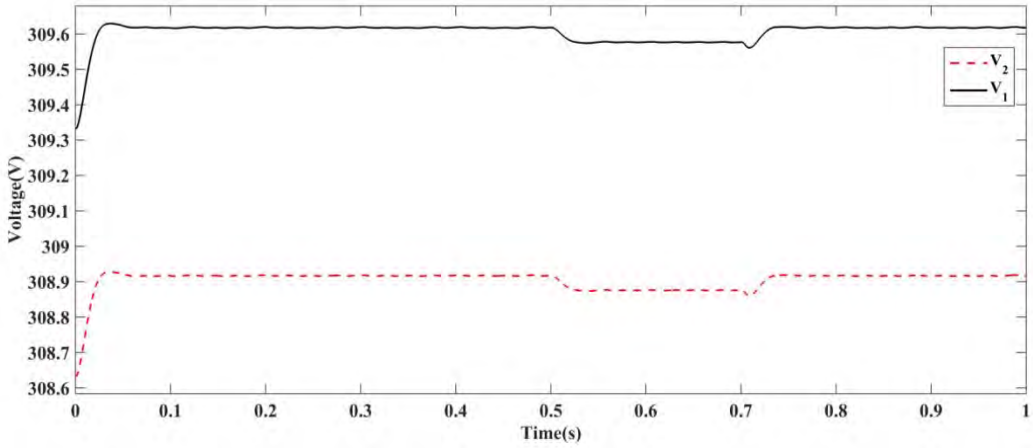

Figure 4.4 Parallel DG inverters output voltage amplitude using reverse droop control with virtual resistors under resistive line impedance with frequent changes in load.

Power sharing of parallel inverters is investigated with common load of P_{load} = 1201 W, Q_{load} = 121 VAR and at 0.5 s sudden local load value of P_{load} = 801 W, Q_{load} = 81 VAR is added and removed at 0.7s verify the dynamic response and line impedance of $R_{1Line} + jX_{1Line}$ =0.7+j0.002Ω, $R_{2Line} + jX_{2Line}$ =0.8+j0.003Ω. Reverse droop control based on virtual resistors can reduce the influence of the line impedance difference on the parallel inverters by setting the total output impedance of the DG inverters to be resistive, which improves decoupling of power and improves the proportional load sharing P_1=594 W, P_2=592 W, Q_1=53 VAR, Q_2=52 VAR and at load change at 0.5 s, P_1=935 W, P_2=932 W, Q_1=89 VAR, Q_2=86 VAR as shown in the Figure 6,7 and frequency variation of DG inverters is within the range of 49.77 Hz to 49.78 Hz, the maximum fluctuation of 0.004 Hz as shown in the Figure 4.32. Voltage variation of DG inverters is V_1=309.6 V, V_2=308.9 V as shown in the Figure 8,9. Thus, the reverse droop control with virtual resistors improves power sharing compared to reverse droop control.

5. CONCLUSION

This paper proposes an improved traditional reverse droop control strategy suitable for virtual resistance in low-voltage microgrid systems. Under the premise that the output impedance of the inverter is made resistive through design parameters in the literature, adaptive virtual resistance is introduced. The virtual resistance value varies with the difference between the actual output active power of the DG and the reference output active power. The design of the virtual resistance link aims to eliminate the adverse effect of the excessive voltage drop of each DG in the system caused by the introduction of the virtual resistance link and achieve the purpose of evenly distributing the output active power of each DG to the public load.

6. REFERENCES

[1] LASSETER B. Microgrids distributed power generation[C] // 2001 IEEE Power Engineering Society Winter Meeting, 2001, 1: 146-149.

[2] FANG Lei, NIU Yugang, WANG Siming, et al. Optimal capacity determination method based on day-ahead scheduling and real-time control[J]. Power System Protection and Control, 2018, 46(23): 102-110.

[3] WANG Chunmei, XIONG Binyu. Two-stage method for unbalanced power smoothing in microgrid based on energy storage dispatch mode[J]. Smart Power, 2019, 47(2): 22-29.

[4] ROCABERT J. Control of power converters in AC microgrids[J]. IEEE Transactions on Power Electronics, 2012, 27(11): 4734-4749.

[5] VANDOOM T L, KOONING J D, MEERSMAN B, et al.Automatic power sharing modification of P/V droop controllers in low voltage resistive microgrid[J]. IEEE Transactions on Power Delivery, 2012, 27(4): 2318-2325.

[6]GUO Wenming, MU Longhua. Control principles ofmicro-source inventers used in microgrid[J]. Protection and Control of Modern Power Systems, 2016, 1(1).

[7] WANG Chengshan, XIAO Chaoxia, WANG Shouxiang. Integrated control and analysis of micro-power grid[J]. Automation of Electric Power Systems, 2008, 32(7): 98-103.

[8] GUO Qian, LIN Liaoyuan, WU Hongyan, et al. Distributed power control strategy for microgrids considering adaptive virtual impedance[J]. Automation of Electric Power Systems, 2016, 40(19): 23-29.

[9]LI Y W, KAO C N. An accurate power control strategy for inverter based distributed generation units operating in a low voltage microgrid[J]. IEEE Transactions on Power Electronics, 2009, 24(12): 2977-2988.

[10] LOPES J A P, MOREIR C L, MADUREIARA A C.Defining control strategy for microgrids islanded operation[J]. IEEE Transactions on Power Systems, 2006, 21(2): 916-924.

[11] IYER S V, BELUR M N, CHANDORKAR M C. Analysis and mitigation of voltage offsets in multi-inverter microgrids[J]. IEEE Transactions on Energy conversion, 2011, 26(1): 254-63.

[12] LAAKSONEN H, KOMULAINEN R. Voltage and frequency in inverters based weak LV network microgrid[C] // 2005 International Conference on Future Power Systems, November 18-18, 2005, Amsterdam, Netherlands.

[13] Research on control strategy of low-voltage microgrid parallel inverter[J]. Smart Power, 2019, 46(7): 34-39.

[14] WANG Chengshan, XIAO Chaoxia, WANG Shouxiang. Multiple feedback loop control scheme for inverters of the micro-source in microgrids[J]. Transactions of China Electrotechnical Society, 2009, 24(2): 100-107.

[15] YUAN Chang, CONG Shixue, XU Yanhui. Overview on grid-connected inverter virtual impedance technology for microgrid[J]. Power System Protection and Control, 2017, 45(9): 144-154.

[16] ZHAO Qiao'e, ZHANG Lele, WU Xiaodong, et al. Control strategy for multi-inverters based on parallel virtual resistance[J]. Power System Protection and Control, 2017, 45(15): 30-39.

[17] HE Jinwei. An islanding microgrid power sharing approach using enhanced virtual impedance control scheme[J]. IEEE Transactions on Power Electronics, 2013, 28(11): 5272-5282.

[18] KANG Yingwei, WANG Duhong, ZHANG Jingwei, et al. Droop control strategy for multi-resistive inverters of low voltage microgrid based on adaptive virtual impedance[J]. Science Technology and Engineering, 2017, 17(10):40-45.
[19] MAHMOOD H. Accurate reactive power sharing in an islanded microgrid using adaptive virtual impedances[J].IEEE Transactions on Power Electronics, 2015, 30(3): 1605-1617.
[20] ZHANG Huaguang. Distributed adaptive virtual impedance control for accurate reactive power sharing based on consensus control in microgrids[J]. IEEE Transactions on Smart Grid, 2017, 8(4): 1749-1761.
[21] XU Jiqiang, LU Wenzhou, WU Lei. Self-regulation sag coefficient control strategy for low voltage microgrid inverter[J]. Motor and Control Application, 2017, 44(6): 13-18.
[22] SUN Xiaofeng, YANG Yalin, ZHAO Wei, et al. Adaptive droop control strategy for microgrid inverter[J]. Power System Technology, 2014, 38(9): 2386-2391.
[23] GUO Tong, LI Yanqing, TONG Nian, et al. Control strategy of microgrid based on self-adjusting droop coefficient[J]. Journal of Electric Power Science and Technology, 2017, 32(2): 77-83.
[24] LAAKSONEN H, SAARI P, KOMULAINEN R. Voltage and frequency control of inverter based weak LV network microgrid[C] // 2005 International Conference on Future Power Systems, November 18-18, 2005, Amsterdam, Netherlands.
[25] YAO W, CHEN M, MATAS J, et al. Design and analysis of the droop control method for parallel inverters considering the impact of the complex impedance on the power sharing[J]. IEEE Transactions on Industrial Electronics, 2011, 58(2): 576-588.
[26] LAAKSONEN H, SAARI P, KOMULAINEN R. Control of voltage and frequency in inverter and synchronous generator based urban LV microgrid[C] // Proceedings the Sixth IASTED International Conference on European Power and Energy Systems, 2006: 26-28.

1

Evolution of Integrated Battery Charging Technology in e-mobility applications

Gopinath A, B P Divakar
gopinath.a@reva.edu.in

School of Electrical and Electronics Engineering, REVA University,Bangalore, India,

Abstract

This paper presents an initiative, progress, and development of battery charging techniques in electric driven vehicles extensively, with respect to the demanding needs for addressing the issues of exhaustible fuel resources, environmental hazards due to carbon emission etc. Alerted by the haunting issues of conventional IC engine vehicles, manufacturers are making significant attempts to reduce the dependency on IC engines by converting the vehicles to Hybrid Electric, Plug-in Hybrid Electric and Electric Vehicles. Battery is a prime source for driving the traction circuit in Electric Vehicles (EVs), due to rapid change in standard of living, it is required to adopt an adequate technology to charge the battery of Hybrid Electric Vehicles (HEVs), Plug-in Hybrid Electric Vehicles (PHEVs) and Electric Vehicles (EVs). Basically, charger can be a standalone or onboard. The merits of the standalone (external) chargers are potentially feasible for higher power rating, no limitation of size and weight. The limitations of onboard charger are size, space and weight. To overcome the limitations of onboard charger, the existing power electronic traction circuit of the vehicle is used as a charging circuit and motor winding as an input inductor, when the vehicle is at halt. The evolution of battery charging technology is presented by comparing different integrated

An Edited Volume, 9–18.

battery chargers based on their topologies and their additional potential to support the grid is explored based on various factors.

Keywords: Integrated Charger, Plug-in Hybrid Electric Vehicles, standalone charger, onboard charger..

1.1 Introduction

Depletion of fossil fuels, environmental hazards due to carbon emission, etc. compelling the user to switchover to (fossil- fuel free) electric driven vehicles. Which in turn open a way to replace IC (Internal Combustion) engine driven vehicles gradually by Hybrid Electric Vehicles (HEVs), Plug-in Hybrid Electric Vehicles (PHEVs) and Electric Vehicles (EVs). Due to inadequate charging facilities, idea of integrating the charger to Plug-in Hybrid Electric Vehicles (PHEVs) and Electric Vehicles (EVs) is initiated. This integration led to increased weight, space, and cost. Most of these issues are resolved by effective use of existing traction circuitry as a battery charging circuit. Since this drive train is idle when the vehicle is at halt. This idea was initiated more than three decades ago [1]. This paper presents the evolution of integrated charger extensively in electric driven vehicles also explores the potential of integrated chargers in V2G (Vehicle to Grid) integration to support the grid capability. Basically, EV battery chargers are presumed to be unidirectional, which accounts for less component count, reduced risk of inter connection and ease of control.

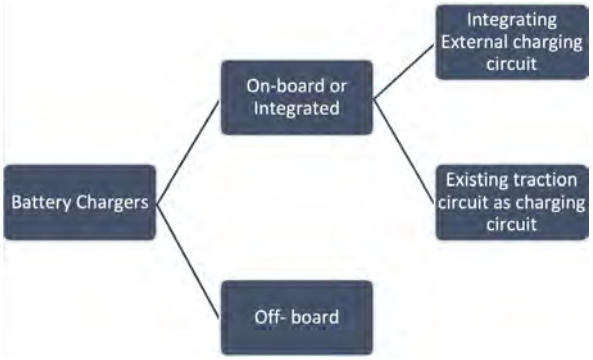

Figure 1.1 Classification of Battery Chargers

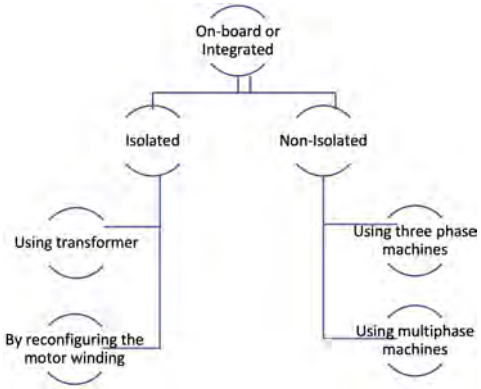

Figure 1.2 Classification of Integrated Battery Chargers

1.2 CLASSIFICATION OF BATTERY CHARGERS

Basically, EV-battery chargers are classified as on-board and off-board chargers. In onboard charging, external charging circuit can be integrated with the vehicle, in recent developments, to overcome the burden of external integration, the existing traction circuitry is used as a charging circuit, the block diagram of the basic classification of battery chargers is as shown in the Fig. 1.1

1.3 ON-BOARD OR INTEGRATED CHARGERS

The integrated chargers can be classified based on the isolation of input and output ports to ensure the safe operation as isolated and non-isolated is shown in Fig 1.2. In the existing power electronic drive circuit, the motor is connected to the traction circuit, the motor winding can be utilized to provide isolation between input and output. In doing so, there would be a chance of torque production which is addressed by reconfiguring the motor winding [7-8]

As per the literature [4] the integrated chargers can be listed separately based on the isolation between input and output as shown in the Fig 2. The galvanic isolation was achieved by using a transformer on the AC input side [5] or by using reconfigured machine winding. The major obstacle in the machine winding during charging is generation of torque, to nullify the torque developed, the machine winding is reconfigured suitably [16].

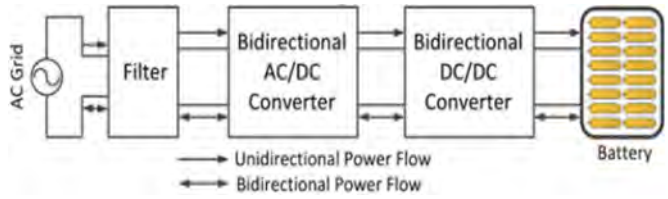

Figure 1.3 Typical two stage Battery Charger

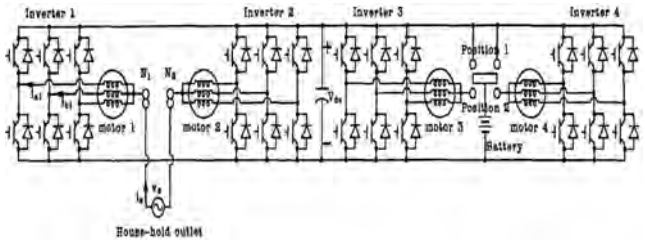

Figure 1.4 Integrated Battery Charger for four-wheel drive EV as in [2]

1.4 TOPOLOGICAL DEVELOPMENTS

The conventional battery charger for EVs generally consists of ac-dc converter, dc-dc converter to facilitate the transfer of power from source to load (battery) based on the nature (unidirectional or bidirectional). There would be two power stages. First stage takes care of unity power factor operation by sinusoidally shaping grid current, and second stage plays a role of regulating the battery charging current or voltage.

A battery charger plays a crucial role in the development of PHEV'S EV's. An integral battery charger, which uses traction circuit of four-wheel drive, is proposed with no additional components except a transfer switch [2] A battery charger plays a crucial role in the development of PHEV'S EV's. An integral battery charger, which uses traction circuit of four-wheel drive, is proposed with no additional components except a transfer switch [2].

Here equivalent power circuit is comprised of ac-dc boost converter and a dc chopper (Fig 3), in the charging mode, the utility source is connected between the neutral points of two motors, ac source voltage can be converted to desired dc link voltage and dc link supplies constant current or voltage to the battery through two phase shifted choppers. At each inverter the upper three IGBT's and lower three IGBT's are on and off simultaneously as a single power switch to make the current in each phase identical without any phase displacement to avoid the generation of torque in the motor. The idea

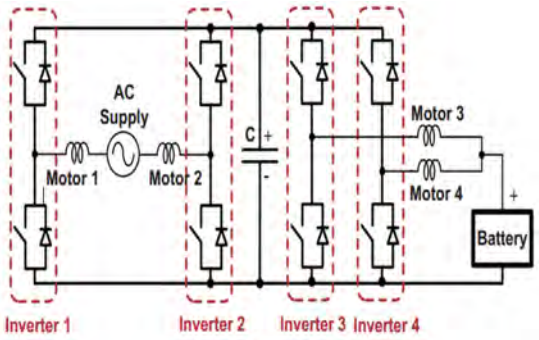

Figure 1.5 Fig 5. Equivalent circuit during charging

was validated by presenting experimental results. Since idea of two-wheel drive dominates over the four-wheel drive-in terms of cost and other factors. By utilizing the available power electronic components and motors a low-cost integrated charger is proposed which uses a digital controller to regulate the converter

Fig 6. Integrated charger with two motors – two inverters configuration as in [4], [9] and [10]

Here existing two inverters are used as ac/dc converters and two motors as inductors of converters. The control signals for two inverters are set to generate similar zero sequence currents in the windings of the motors. The equivalent circuit of the charger is as shown in Fig 7. Two neutral points of three phase motors are connected to ac source to charge the battery, as per the control scheme adopted only bottom switches are used to regulate the input current, top switches are kept off to minimize the switching loss. Gradually the number of converters and motors used in the integrated charger circuit is reduced, which accounts for less weight, space, cost, and ease of control. An integrated charger with one motor and two converters is proposed in [4] as it involves two converters, control complexity increases, required contact switches are an additional hardware. One motor with one power converter is proposed in [5] here the motor used is special type called switched reluctance motor its special winding configuration helps to provide isolation as these motor windings can be used as an isolated transformer during charging mode. But some of the limitations of this topology are under utilization of copper per phase and increased per phase mmf losses. Since isolation between input and output is an essential feature for the safe operation of the charger, the prioritized isolation was provided by reconfiguring the machine winding,

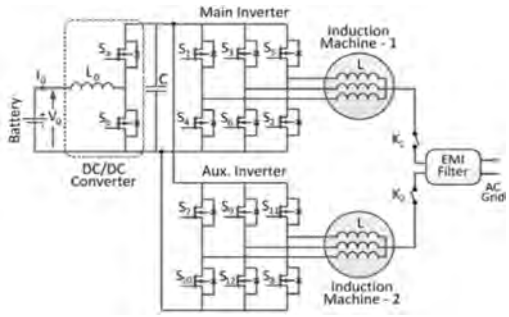

Figure 1.6 Integrated charger with two motors – two inverters configuration as in [4], [9] and [10]

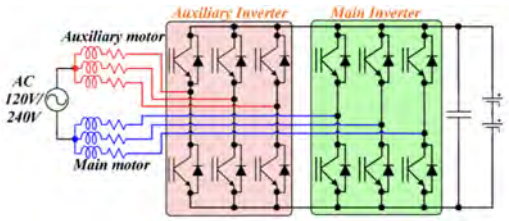

Figure 1.7 Low-cost charger circuit diagram: utilizing the available power electronics systems to charge the batteries of PHEV/EV as in [3]

which led to increased number of motor phases [14], [16]. In the literature attempts were made to increase i. The charging efficiency, ii. Input-power factor, iii. User safety

To reduce i. Number of components ii. Power loss iii. Cost iv. Extra hardware requirement

By looking at various factors which help the most economic and efficient operation of the integrated charger, different available topologies are reviewed extensively and some of the performance parameters of various integrated topologies are tabulated in the Table-I

1.5 BIDIRECTIONAL TOPOLOGY

Most of the integrated charger topologies uses bi-directional switches, which facilitates the flow of power in either direction, this feature will enhance the ability of the charger to feed power back to grid if needed. This really helps in strengthening the grid capability to cater to loads locally. In this direction

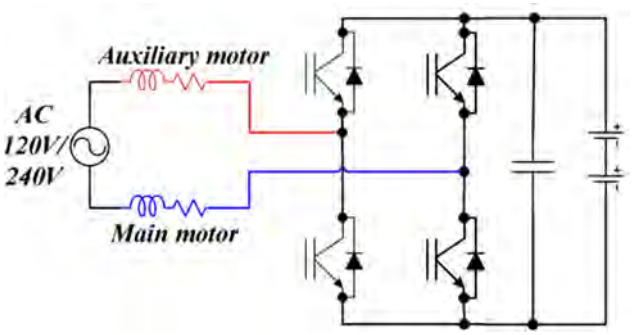

Figure 1.8 Equivalent circuit low-cost charger a PHEV/EV as in [3]

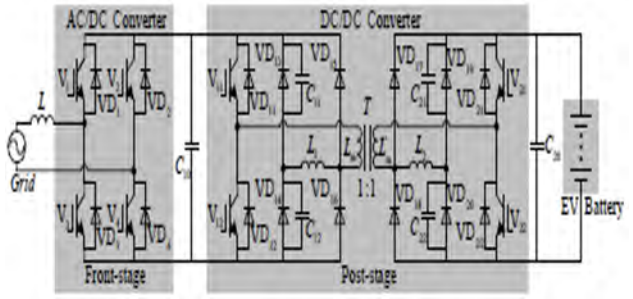

Figure 1.9 Two stage charger topology for V2G as in [22]

a two-stage bidirectional converter topology is proposed for Vehicle to Grid (V2G) system [22]

Table 1.1 Performance comparation of different integrated charger topologies

Integrated charger topology	**References**	**Bidirectional or unidirectional**	**Power stages**	**Type of motor**	**Isolated or Non- isolated**	**Extra hardware required**	**Charging efficiency**	**Discharging efficiency**	**Advantages**	**Limitations**	Applications
Four motors with four converters	[2]	Bidirectional	2	Induction motors	Non- isolated	Control circuits for 24 power switches, and contact switches	Not reported	Not reported	1. Can be operated almost at unity power factor 2. No extra filter inductor	1. Complexity of control. 2. Comparatively high cost.	Plug-in Electric Vehicles
Two motors with two converters	[20]	Bidirectional	2	Induction motors	Non- isolated	Control circuits for 24 power switches, and contact switches	Not reported	Not reported	1. Can be operated almost at unity power factor 2. No extra filter inductors	1. Complexity of control 2. Comparatively high cost	Plug-in Hybrid Electric Vehicles
	[4]	Bidirectional	2	Not reported	Non- isolated	Contact switches	Not reported	Not reported	1. Can be operated almost at unity power factor	1. Complexity of control 2. Comparatively higher cost	Plug-in Hybrid Electric Vehicles
	[21]	Bidirectional	1	Induction motors	Non- isolated	Contact switches	93.60%	Not reported	1. Can be operated almost at unity power factor 2. No extra filter inductors	1. Cannot be applied for delta connected motors 2. Fixed value of motor leakage reactance	Plug-in Hybrid Electric Vehicles
	[17]	Bidirectional	2	Not specified	Isolated	1. More number of switches 2. Requirement of HF transformer	Not reported	Not reported	1.Can be operated almost at unity power factor 2. No extra filter inductors	1. Cost is more compared to one motor, one converter topology 2. Complexity of control	Plug-in Hybrid Electric Vehicles
	[18]	Bidirectional	2	Not specified	Isolated	Requirement of HF transformer	Improved efficiency due to low switching losses	Not reported	1. Can be operated almost at unity power factor 2. No extra filter inductors 3. Absence of DC-link capacitor	1. Modified circuit configuration 2. Cost is more compared to one motor, one converter topology	Plug-in Hybrid Electric Vehicles
One motor with two converters	[9]	Bidirectional	2	Induction motors	Non- isolated	Two dedicated converters	Not reported	Not reported	1. Comparitively less cost, less space and weight	1. Complexity of control. 2. Cost is more compared to one motor, one converter topology.	Plug-in Hybrid Electric Vehicles
	[11]	Unidirectional	1	Induction motors	Non- isolated	Control circuits for 12 power switches	86%	Not reported	1. Close to unity power factor operation 2. No independent ac/dc converter	1. Complexity of control. 2. Cost is more compared to one motor, one converter topology	Plug-in Hybrid Electric Vehicles
	[14]	Bidirectional	2	Induction motors	Non- isolated	Two set of stator windings, control circuits for 12 power switches	Not reported	Not reported	1. Close to unity power factor operation. 2. No independent ac/dc converter	1. Complexity of control. 2. Cost is more compared to one motor, one converter topology	Plug-in Hybrid Electric Vehicles
One motor with one converter	[13]	Bidirectional	2	Induction motors	Non- isolated	Extra Contact switches	Not reported	Not reported	1. Reduced complexity of control. 2. Reduced size and weight.	1. Increased magnetizing currents. 2. Expensive wound rotor induction motor	Electric Vehicles
	[20]	Bidirectional	2	Induction motors	Non- isolated	Extra Contact switches	Not reported	Not reported	1. Reduced complexity of control. 2. Reduced size and weight.	1. Increased magnetizing currents. 2. Expensive wound rotor induction motor	Plug-in Hybrid Electric Vehicles
	[15]	Unidirectional	2	Permanent magnet motor	Isolated	Need of extra capacitor	Not reported	Not reported	1. Reduced complexity of control 2. No need of extra filtering	1. Increased magnetizing currents. 2. Need of center tapped stator winding	Electric Vehicles

Many attempts are being made to utilise the stored vehicle battery energy to increase the grid capability by means of V2G power transaction [23-25]

1.6 Conclusion

This article is mainly focused on intensive analysis of some of the EV Battery charging topologies and comparing them to explore their potential in charging the Electric Vehicle battery with most efficient and economical way without much extra cost at the same time to expose the potential of EV chargers in V2G operation to strengthen the grid in supplying the local load.

References

[1] D. Thimmesch, "An SCR Inverter with an Integral Battery Charger for EVs," IEEE Trans. Ind. Appl., vol. 21, no. 4, pp. 1023-1029, August 1985.
[2] S.-K. Sul and S.J. Lee, "An integral battery charger for four-wheel drive electric vehicle", IEEE Tran. on Industry Applications, Vol. 31, No 5, September/October 1995.
[3] Lixin Tang and Gui-Jia Su "Low cost digitally controlled charger for plug in hybrid electric vehicles" IEEE Energy Conversion Congress and Exposition pp. 3923-3929, Sep. 2009.
[4] L. Shi, A. Meintz, and M. Ferdowsi, "Single-Phase Bidirectional AC-DC Converters for Plug-in Hybrid Electric Vehicle Applications," in Proc.IEEE VPPC, 2008.
[5] M. Barnes and C. Pollock, "Forward converters for dual voltage switched reluctance motor drives," IEEE Trans. Power Electronics., vol.16, no.1,pp.83–91, Jan. 2001
[6] Subotic et al., "Isolated chargers for evs incorporating six-phase machines," 653–664 63 IEEE Trans. Ind. Electron., 2015.
[7] S. Haghbin et al., "An isolated high-power integrated charger in electrified-vehicle applications," 4115–4126 60 IEEE Trans. Veh. Technol., 2011.
[8] A. S. Abdel-Khalik et al., "Interior permanent magnet motor-based isolated on-board integrated battery charger for electric vehicles," 124–134 12 IET Electr. Power Appl., 2017.
[9] G. Pellegrino et al., "An integral battery charger with power factor correction for electric scooter," 751–759 25 IEEE transactions on power electronics, 2009.
[10] C. Shi et al., "A three-phase integrated onboard charger for plug-in electric vehicles," 4716–4725 33 IEEE Trans. Power Electron., 2017.
[11] S. Loudot et al., "Fast charging device for an electric vehicle," Sep. 30 2014, uS Patent 8,847,555.
[12] I. Subotic et al., "An ev drive-train with integrated fast charging capability," 1461–1471 31 IEEE Trans. Power Electron., 2015.
[13] I. Subotic et al., "Integration of six-phase ev drivetrains into battery charging process with direct grid connection," 1012–1022 32 IEEE Trans. Energy Convers., 2017.

[14] M. S. Diab et al., "A nine-switch-converter-based integrated motor drive and battery charger system for evs using symmetrical six-phase machines," 5326–5335 63 IEEE Trans. Ind. Electron., 2016.

[15] L. De Sousa et al., "Method and electric combined device for powering and charging with compensation means," Oct. 6 2015, uS Patent 9,153,996.

[16] I. Subotic et al., "Onboard integrated battery charger for evs using an asymmetrical nine-phase machine," 3285–3295 62 IEEE Transactions on industrial electronics, 2014.

[17] T. Na et al., "A review of on-board integrated electric vehicles charger and a new single-phase integrated charger," 288–298 4 CPSS Transactions on Power Electronics and Applications, 2019.

[18] I. Subotic et al., "Isolated chargers for evs incorporating six-phase machines," 653–664 63 IEEE Trans. Ind. Electron., 2015. 34 12 IET Electr. Power Appl., 2017.

[19] N. Bodo et al., "Efficiency evaluation of fully integrated on-board ev battery chargers with nine-phase machines," 257-266 32 IEEE Trans. Energy Convers., March 2017.

[20] D. G. Woo, G. Y. Choe, J. Kim, B. Lee, J. Hur, G. Kang, "Comparison of Integrated Battery Chargers for plug-in electric vehicles: Topology and Control," in Proc. IEMDC, 2011, pp. 1294-1299.

[21] L. Tang, G. J. Su, "A Low-Cost, Digitally-Controlled Charger for Plug-in Hybrid electric Vehicles," in Proc. IEEE ECCE, 2009, pp. 3923-3929.

[22] Yan, Xiangwu, Bo Zhang, Xiang Ning Xiao, Huichao Zhao, and Liming Yang. "A bidirectional power converter for electric vehicles in V2G systems." In 2013 International Electric Machines Drives Conference, pp. 254-259. IEEE, 2013.

[23] Foti, S., Testa, A., Scelba, G., De Caro, S., Tornello, L. D. (2020). A V2G Integrated Battery Charger Based on an Open End Winding Multilevel Configuration. IEEE Open Journal of Industry Applications, 1, 216-226.

[24] Quispe, B. B., e Melo, G. D. A., Cardim, R., Ribeiro, J. M. D. S. (2021, March). Single-Phase Bidirectional PEV Charger for V2G Operation with Coupled-Inductor Cuk Converter. In 2021 22nd IEEE International Conference on Industrial Technology (ICIT) (Vol. 1, pp. 637-642). IEEE.

[25] Luh, M., Blank, T. (2021, September). Auxiliary Resonant Commutated Pole Inverter (ARCPI) with SiC MOSFETs for efficient Vehicle-to-Grid (V2G) charging. In 2021 23rd European Conference on Power Electronics and Applications (EPE'21 ECCE Europe) (pp. P-1). IEEE.

1

A Literature Review on PV Inverter Topologies Connected to Grid

Arpita Banik, Bansilal Bairwa, Mamatha N
arpita.b@reva.edu.in

School of EEE, REVA University, Bangalore, India 560064

Abstract

The global power sector is witnessing a gradual transition from typical thermal power-generating sources toward clean energy technologies. Non-conventional sources of energy are the most appropriate solution to give clean and inexhaustible energy to conquer the worldwide energy emergency. The renewables share was 8.6 percentage within the world energy combine in 2010 and is predicted to extend to 22.5 percentage in 2020 as per a recent thematic analysis report renewable energy by the data collected globally. With the advancement in power electronics technology, photo-voltaic system (PV) is getting more popularity in generation of electricity. Inverters connected to grid have developed significantly with high decent variety. Efficiency, estimate, weight, dependable execution have all improved significantly with evolvement of technically advanced and innovative electrical converter configurations and these factors have diminished the expenses of inverters. This study incorporates a short dialog on network associated PV inverter, overall development of PV system, classification of inverter topologies, expected properties of PV inverters to perform better, selection of PV inverters and a comparative study on different inverter topologies in terms of their pros, cons, cost and rating.

Keywords: MLI , SCC, Boost converter, Pulse Width Modulation.

An Edited Volume, 9–16.

1.1 Introduction

Sustainable power source is particularly fundamental for gathering present and future energy necessities[1]. Photo-voltaic (PV) control, in light of the fact that it is perfect and boundless supply of energy, is maybe the best innovation among all sustainable power sources and in this way a generous amount of investigation and research is being led towards improving photo-voltaic system effectiveness and to use the PV control, network interconnection of PV system is required. Being a clean contamination free and inexhaustible source of energy, photo-voltaic system has got extraordinary enthusiasm as an alternative source of energy. Major confinement to the utilization of PV power was the surprising expense of the PV modules [2]. But with advancement of technology and decrease in price for PV modules, in past few decades, PV inverters connected to the grid have advanced significantly and have turned out to be a standout amongst the best and quickest creating innovations in power electronics and power system field. In total global installed capacity of renewable energy sources PV system had a share of 8.7% in 2010, which got increased up to 32.4% in 2017 and is expected to get increased up to 39.6% by 2020[3]. PV systems are mainly divided into 2 classes as, the standalone (off-grid) system and the the grid-connected (on-grid) system [4]. The standalone (off-grid) system works free of the utility grid while, the grid-connected applications use PV system related to the grid network. As of now, contrasted with the standalone system, the usage of grid-connected system is wide embraced in pragmatic applications[5, 6]. A normal structure grid connected PV system is shown in Figure 1.1.

1.2 Worldwide growth of photo voltaic (PV)

Overall development of photo-voltaic has been near exponential somewhere in the range of 1992 and 2018. During this time frame, photo-voltaic (PV), otherwise called sunlight based PV, created from a claim to fame market of little scale applications to a standard power source. At the point when sunlight based PV technology was first perceived as a promising sustainable power source innovation, endowment programs, for example, feed-in taxes, were actualized by various governments so as to give financial motivating forces to ventures. The worldwide exponential development of photo-voltaic up to 2018 is presented in Figure 1.2 [7].

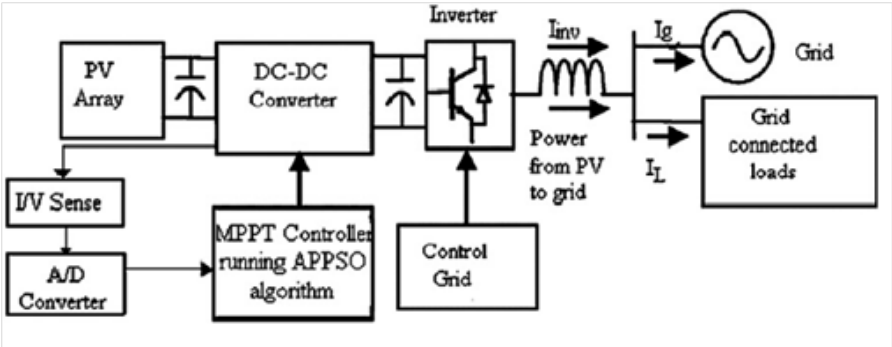

Figure 1.1 structure of grid connected PV system.

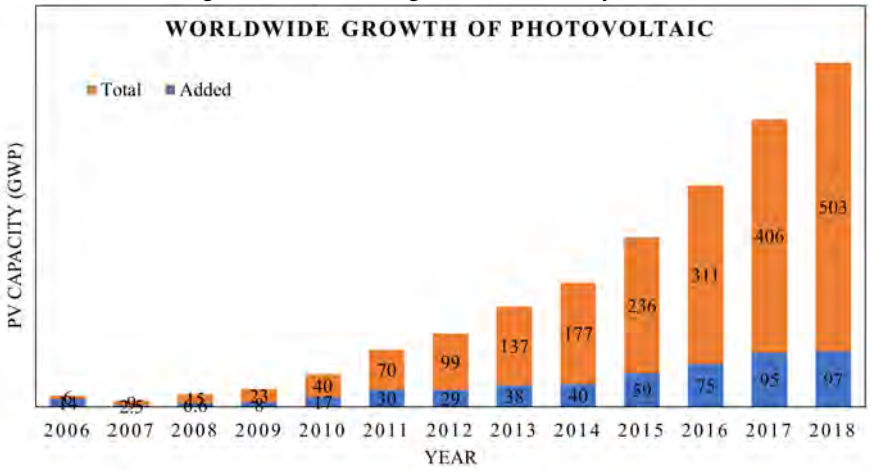

Figure 1.2 Worldwide growth of photo voltaic.

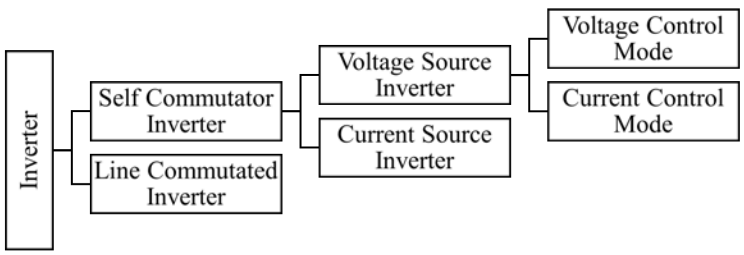

Figure 1.3 classification of inverters.

1.3 Classification of power electronic inverters

Phase, frequency, and voltage extent of the three-phase AC happening to the PV system is required in a PV system associated with the grid for the suitable synchronization with the grid. The transformation from DC to AC is finished by power electronic inverter which is the core of network associated PV system [7, 8, 9]. These inverters are primarily of two classes named as self commutated inverters and line commutated inverters. Self commutated inverters can control turn-ON and turn-OFF procedure of switching devices splendidly. Whereas, line commutated inverters performance is dependent upon circuit parameters and switching performance is controlled by the direction of current flow. Classification of grid connected inverters is shown in Figure 1.3.

1.3.1 Line-commutated inverter

In case of line-commutated Inverter commutation of the switching devices is performed by reversing the polarity of Alternating voltage and in this manner the flow of negative current (or zero current) starts the turn-OFF method. Line commutated inverters uses mainly semi controller devices like thyristors where turn-on process is controlled through gate terminal and turn-off is controlled by line current or grid voltage. In case of force commutation, external commutation circuit can also be included in such semi controlled devices[10, 11, 12, 13].

1.3.2 Self-commutated inverter

In Self-Commutated Inverter gate terminal controls turn-on and turn-off procedure of the power semiconductor device (switch). Shifting of current among various devices is performed in a systematic way. Power semiconductor devices I.e., MOSFETs and IGBTs are mainly used as switching devices in self-commutated inverters. For applications beyond 100kW and 20 kHz, IGBTs are used. Whereas, for a high frequency and low power application of 20– 800 kHz, 20kW, MOSFETs are generally used[14, 15].

1.4 Different Inverter topologies

Inverters can be categorized into various types depending upon the types of components used and the configuration. These various types of topologies are discussed as follows:

1.4.1 In view of stages to process power

As per the no. of power processing stages, inverters can be categorized as single-stage and multiple-stage inverter. Both are discussed with diagram below:

1.4.1.1 single-stage inverter

A single-stage inverter with line frequency transformer contributes in control of currents injected to the grid, the amplification of voltage and maximum power point tracking process [16]. The inverter is designed so as to deal with a peak power twice of the ostensible power which can be expressed by the below equation (1).

$$P_{grid} = 2P_{grid}sin^2(\omega_{grid}t) \tag{1.1}$$

In single-stage inverter the line frequency transformer increases the weight of the inverter and also causes peak efficiency loss of about 2% . These drawbacks of line frequency transformers can be overcome by using high frequency transformers or transformer less inverters.

1.4.1.2 Multiple-stage inverter

In this type of inverters, DC is first collected from the PV module and then it is controlled through the buck-boost converter[**?**]. Finally DC-DC converter output is given to DC-AC converter (Inverter) and finally the output from this inverter is given to the grid. The input voltage to the converter here is very low as no transformer used is here.

1.4.1.3 Single-stage and multiple-stage inverters with de-coupling capacitor

Single-stage and multiple-stage inverters require decoupling capacitors to filter out the voltage spikes present in PV module output[**?**]. Highly capacitive bulky electrolytic capacitors are used here for this purpose.

1.4.2 Cascade Inverter

In cascaded inverter used in PV system output of two full bridge inverter gets associated in arrangement to raise the quantity of voltage levels. Single inverters with three dissimilar to voltage levels can deliver AC output voltage of five levels with the assistance of cascaded topology. Historical overview of grid connected PV inverter gives clear idea on past and present technology of grid connected PV inverter[**?**].

1.5 Selection of inverters for grid connection and their control methods

1.5.1 Lawful necessities

- **Galvanic isolation:** Galvanic isolation is one of the most important factors to provide safety. Mainly to interrupt the flow of leakage current it is done through isolation transformer or isolation switch in case of transformer less inverters.
- **Detection of anti-islanding:** In this process PV system supplies power to the nearby load even if the connection of power grid is removed. This factor must be taken serious care because it may damage the equipment's and cause harm to the workers as well.

1.5.2 Properties expected from standalone inverters

Standalone inverters are expected to have following properties [20]:

- Output voltage should be sinusoidal
- System disconnection when the DC-link voltage goes low
- Output voltage and frequency must be maintained within permissible values
- Cables capable of withstanding large fluctuations in the input voltage
- Regulation of output voltage
- System must be highly efficient in light loads
- Capacity to handle surges must be there
- THD generated by the inverter must be low
- Must be capable of handling frequency variations, under and over voltage fluctuations

1.5.3 Properties expected from grid-connected inverters

Grid-connected inverters are expected to have following properties[20]:

- Dynamic response must be faster
- Unity power factor is expected
- Proper frequency control
- Output with low harmonics
- Synchronization with grid must be Accurate
- Fault current tolerance
- Under or over frequency and voltage protection

1.6 Conclusion and future work

PV inverter connected to the grid is one of the most developing technologies to support electricity generation using renewable source of energy and to satisfy the increased load requirement in an effective manner. PV system has got more focus as it is environment friendly and inexhaustible. With enormous support given by government and continuous improvements done by researchers have made this system highly efficient and cost effective. In this review paper, various types and topologies of PV inverters connected to grid are examined along with their pros and cons. The performance parameters of inverters and how they are expected of performing is also discussed here in this paper. Overall global growth of PV system is discussed and shown in Figure 1.2. It is expected that, in coming future improved design and updated technology will make this grid connected inverters perform with highest efficiency and reliability. Selection of proper controller for this grid connected inverters is not discussed here. In future a review can be done on selection of controller part to make this inverter more efficient and cost effective.

References

[1] Ishikawa T Grid-connected photovoltaic power systems: survey ofinverter and related protection equipments. Report IEA (International Energy Agency) PVPS T505; 2002. ⟨http:www.iea-pvps.org⟩

[2] Rahim NA, Saidur R, Solangi KH, Othman M,Amin N, Survey of Grid-connected photovoltaic inverters and related systems.

[3] https://www.power-technology.com

[4] El Nozahya MS, Salama MMA. Technical impacts of grid-connected photo- voltaic systems on electrical networks—areview. JRenew Sustain Energy 2013;5:032702.

[5] Akorede MF, Hizam H, ArisI, Ab Kadir MZA. A critical review of strategies for optimal allocation of distributed generation units in electric power systems. IREE 2010;5(2):593–600.

[6] Nema P, Nema R, Rangnekar S. A current and future state of art development of hybrid energy system using wind and PV-solar: a review. Renew Sustain Energy Rev 2009;13(8):2096–103.

[7] ”China’s solar capacity overtakes Germany in 2015, industry data show”. Reuters. 21 January 2016.

[8] Lai, Chun Sing; Jia, Youwei; Lai, Loi Lei; Xu, Zhao; McCulloch, Malcolm D.; Wong, Kit Po (October 2017). ”A comprehensive review on large-scale photovoltaic system with applications of electrical energy storage”. Renewable and Sustainable Energy Reviews. 78: 439–451. doi:10.1016/j.rser.2017.04.078.

[9] ”China Targets 70 Gigawatts of Solar Power to Cut Coal Reliance”. Bloomberg News. 16 May 2014. Retrieved 16 May2014.

[10] ”China’s National Energy Administration: 17.8 GW Of New Solar PV In 2015 (20% Increase)”. CleanTechnica. 19 March 2015.

[11] ”Snapshot of Global Photovoltaic Markets 2017” (PDF). report. International Energy Agency. 19 April 2017. Retrieved 11 July2017.

[12] ”2018 Snapshot of Global Photovoltaic Markets” (PDF). International Energy Agency. 2018. Report IEA PVPS T1-33:2018.

[13] MyrzikJMA,CalaisM.Stringandmoduleintegratedinvertersforsingle-phasegrid connected photovoltaic systems—a review. In: Proceedings of the IEEE Bologna PowerTech conference. vol. 2; 2003. p. 430–7.

[14] Kjaer SB, Pedersen JK, Blaabjerg F. Power inverter topologies for photovoltaic modules—a review. In: Proceedings of conference rec IEEE-IAS annual meeting. vol. 2; 2002. p. 782–8.

[15] Haeberlin HEvolution ofinverters forgrid connected PV-systemsfrom to2000.In: Proceedings of the 17th European photovoltaic solar energy conference. 2001. p. 426–430; 1989.

[16] A review of PV. Inverter technology cost and performance projections, NREL/SR620-38771; January 2006.

[17] IEA International Energy Agency. Grid-Connected photovoltaic power system: surveyof inverterandrelated protectionequipments, TaskV,Report IEA-PVPST5T05; 2002.

[18] Ishikawa T. Grid-connected photovoltaic power systems: survey of inverter and related protection equipments. Report IEA (International Energy Agency) PVPS T5- T05 ⟨http:www.iea-pvps.org⟩; 2002.

[19] Calais M, Agelidis VG. Multilevel converters for single-phase grid connected photovoltaic systems—an overview. In: Proceedings of the IEEE ISIE’98. vol. 1; 1998. p. 224–9.

[20] Azmi SA; Dept. of Electron. Electr. Eng., Univ. of Strathclyde, Glasgow, UK; K. H. Ahmed; S. J. Finney; B. W. Williams, Comparative analysis between voltage and current source inverters in grid-connected application. In: Proceedings of IET Conference on Renewable Power Generation (RPG 2011); 6-8 Sept. 2011. P. 1–6.

EFFICIENCY IMPROVEMENT OF SYNCHRONOUS BUCK CONVERTER BY NEW PASSIVE AUXILIARY CIRCUIT

Sudharani Potturi[1] **K. Jyotheeswara Reddy[2]** **Aruna J R[3]**

[1,2] REVA University, Bangalore [3] RLabs Enterprise Services Ltd

chekuri.rani@gmail.com

Abstract

This paper presents a novel Synchronous buck converter for portable systems. A zero voltage transition is incorporated and designed to operate at high efficiency and lower voltage. The conventional PWM synchronous buck converter is modified by connecting a new passive auxiliary circuit. This auxiliary circuit offers ZVS (zero-voltage switching) for the main switch. Hence this auxiliary circuit enables the circuit with less switching losses and high overall efficiency. Comparative analysis of Synchronous and basic Buck converter is presented using MATLAB/Simulink software and the superiority of auxiliary circuit is proven by the simulation results.

Keywords. Buck Converter, Efficiency, Auxiliary circuit, Synchronous

1. INTRODUCTION

Nowadays, low voltage supplies are gaining their importance in consumer electronics. Due to low conduction losses, synchronous rectifiers are used in most of the LVDC power supplies. A synchronous rectifier [1,11] is an electronic switch that improves power conversion efficiency by offering low conduction losses in a SMPS [6]. Even then, the conversion efficiencies are being decreased due to high input and low output voltages [1,4]. To increase efficiency of the synchronous buck converter, soft-switching techniques [2,10] are adopted, which in turn reduces switching losses. Implementing ZVS [3] offers low conduction losses as its operation is closer to the PWM converters [12]. Just before the instant of turning on of main switch, the auxiliary circuit of the converter [5,16] is activated. It is ceased once the main switch is tuned on [2].

The ratings of the auxiliary circuit components have lower ratings than the other switches, as the auxiliary circuit is made active during a snippet of the switching

cycle. This feature offers less amount of switching losses[14,15] than the main switch [4].

SYNCHRONOUS BUCK CONVERTER

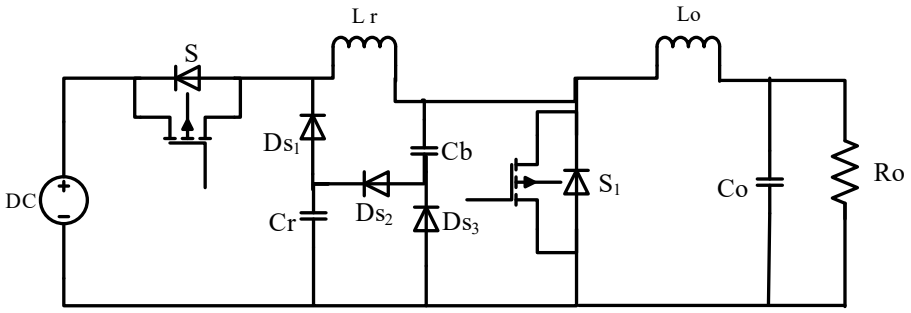

Fig.1. Synchronous Buck Converter with auxiliary circuit

Circuit diagram of a proposed converter with auxiliary [5-6] circuit is shown in Fig. 1. S is considered as main switch and S1 is taken as synchronous switch. The components of auxiliary circuit are resonant capacitor-(C_r), buffer capacitor-(C_b) and resonant inductor-(Lr). D_{S1} D_{S3} and D_{S2} are auxiliary Schottky diodes [12]. The circuit operations over a switching cycle is analysed in eight stages [7,9]. The waveforms of various parameters in all these stages are shown in Fig.2. and the respective equivalent circuits are presented in Fig.3.

Mode 1 (t_0-t_1): When switch S is off and the body diode of Synchronous switch is on, $V_{Cb} = 0$, $i_{D1} = Io$, $V_{Cr} = 0$ Is=0, iLr = 0. At the instant t_0, main switch is on (with zero-current turn-on) [7]. Then the current through resonant inductor rises and current i_{D1} falls simultaneously. The rising and falling of these currents takes place at same rate. This mode ends at $t = t_1$ as shown in fig.2. The body diode D_1 gets turned off due to the presence of resonant and buffer capacitors. In this state,

$$i_s = i_{Lr} = \frac{V_i}{L_r} K\,(t - t_0) \quad \text{.....(1)}$$

$$i_{D1} = I_0 - I_{Lr} = -\frac{V_i}{L_r}(t - t_1) + I_0 \text{.....(2) and } t_{01} = \frac{L_r}{V_i} I_0 \quad \text{.....(3)}$$

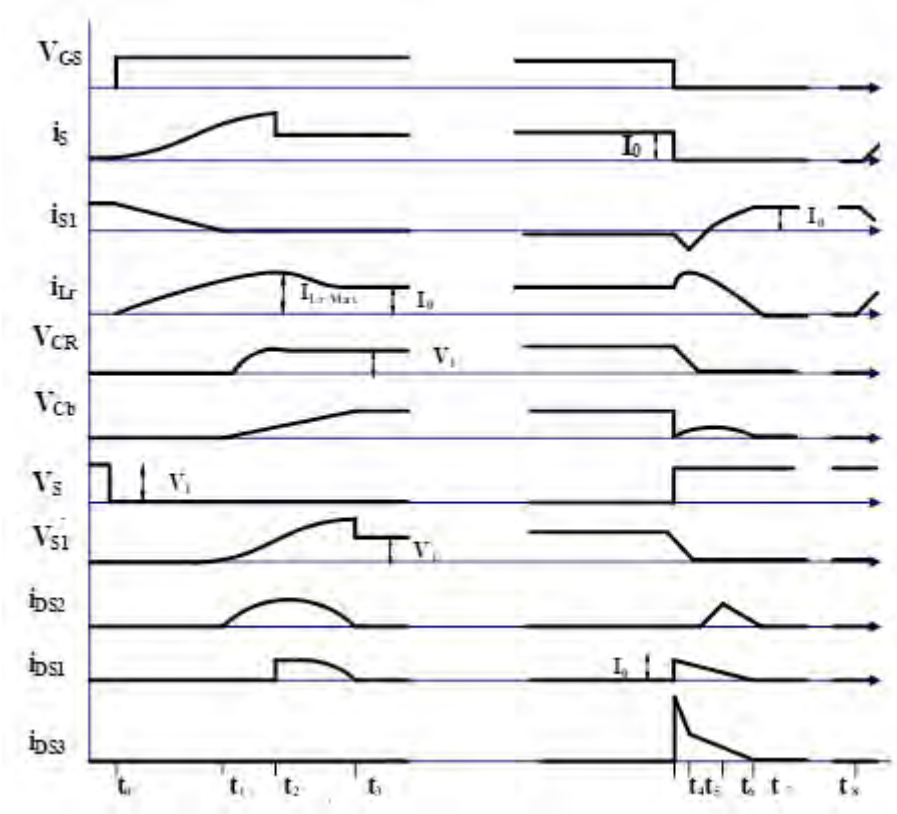

Fig.2. Waveforms of the proposed converter

Mode 2 (t_1-t_2): Diode D_{S2} starts conducting at the instant t_1. Here Voltage across resonant and buffer capacitors is zero. The resonant capacitor and resonant inductor along with buffer capacitor are responsible for the occurrence of resonance. At the end of this stage, the capacitor Cr charges to the supply voltage V_i and makes the diode D_{s1} to conduct

$$i_{Lr}(t-t_1)=\frac{V_i}{Z_1}[Sin\omega_1(t-t_1)+I_0] \quad \text{.....(4)}$$

$$v_{cr}(t-t_1)=\frac{C_0}{C_r}\left[-V_i\cos w1(t-t_1)+V_i\right] \quad \text{.....(5)}$$

$$v_{cb}(t-t_1)=\frac{C_0}{C_b}\left[-V_i\cos w_1(t-t_1)+V_i\right] \quad \text{.....(6)}$$

$$C_0=\frac{C_rC_b}{C_r+C_b} \text{ , ... (7)} \quad \omega_1=\frac{1}{\sqrt{L_rC_0}} \text{.....(8)} \quad Z_1=\sqrt{\frac{L_r}{C_0}} \text{.....(9)}$$

$$t_{12}=\frac{1}{w_1}sin^{-1}\left(\frac{C_0}{C_b}-1\right) \text{.....(10)}$$

Mode 3 (t_2-t_3): When $t = t_2$, $v_{cr} = V_{Cr\max} = V_i$, $v_{cb} = V_{Cb1}$, $i_s = I_0$, $i_{Lr} = i_{Lr\max}$.

When D_{S1} turns is turned on, resonance is initiated by buffer capacitor and resonance inductor. This mode ends when $i_{Lr} = I_0$ and $VC_b = V_{cbm}$. Both diodes D_{S1} and D_{S2} are turned off under ZCS due to resonance inductor.

$$i_{Lr}(t-t_2) = (i_{Lr\max} - I_0)\cos w_2(t-t_2) - \frac{V_{Cb1}}{Z_2}\sin w_2(t-t_2) + I_0 \ldots\ldots (11)$$

$$v_{cb}(t-t_2) = (I_{Lr\max} - I_0) Z_2 \sin w_2(t-t_2) + V_{Cb1}\cos w_2(t-t_2) \ldots\ldots (12)$$

The time interval of this stage can be found as follows:

$$t_{23} = \frac{1}{w_2}\tan^{-1}\left(\frac{I_{Lr\max} - I_0}{V_{Cb1}}\right) \quad \ldots\ldots (13)$$

Where

$$w_2 = \frac{1}{\sqrt{L_r.C_b}} \quad Z_2 = \sqrt{\frac{L_r}{C_b}}$$

Mode 4 (t_3-t_4): In this mode, the load current is carried by S and L_r. Now the circuit operates like PWM buck converter[8,12].

Hence $i_s = I_0 = i_{Lr}$.....(14)

Mode5 (t_4-t_5): in this mode, switch S is turned off under ZVS, and the synchronous switch is turned on under ZCS. As S1 is conducting, the voltage across buffer capacitor becomes zero. Resonance inductor and capacitor initiates resonance [13]. The equations are given below,

$$V_{Cb}(t-t_4) = 0 \quad \ldots (15)$$

$$i_{Lr}(t-t_4) = I_0 \cos w_3(t-t_4) - \frac{V_i}{Z_3}\sin w_3(t-t_4) \ldots\ldots (16)$$

$$v_{cr}(t-t_4) = I_0 Z_3 \sin w_3(t-t_4) - V_i \cos w_3(t-t_4) \ldots\ldots (17)$$

Where, $w_3 = \frac{1}{\sqrt{L_r.C_r}}$ $Z_3 = \sqrt{\frac{L_r}{C_r}}$ and interval of this period is given as

$$t_{45} = \frac{1}{w_3}\tan^{-1}\left(\frac{V_i}{I_0 Z_3}\right)$$

At the end of this stage, $V_{Cr} = 0$ and D_{S2} turn is turned on under ZVS.

Mode 6 (t_5-t_6): L_r and C_b are responsible for new resonance at this stage

$$v_{cb}(t-t_5) = I_{Lr2} Z_2 \sin w_2(t-t_5) \quad \ldots\ldots (18)$$

$$i_{Lr}(t-t_5) = I_{Lr2}\cos w_2(t-t_5) \quad \ldots\ldots (19)$$

This mode ends when $i_{Lr} = I_0$, therefore

$$t_{56} = \frac{1}{w_2}\tan^{-1}\left(\frac{I_0}{i_{Lr2}}\right),\ w_2 = \frac{1}{\sqrt{L_r C_b}}\ Z_2 = \sqrt{\frac{L_r}{C_b}}$$

Mode 7 (t_6-t_7): At $t = t_6$, i_{Lr} becomes I_0 and S_1 is turned off with Zero current switching. L_r and C_b transfer their stored energy to load. The corresponding equations are,

$$v_{cb}(t - t_6) = \frac{I_0}{C_b}(t - t_6) + V_{Cb2} \text{ …….. (20)}$$

$$i_{Lr}(t - t_6) = -\frac{V_0}{L_r}(t - t_6) + I_0 \text{ …….(21)}$$

At the ned of this stage, $i_{Lr} = 0$. The total time period with respect to this stage is expressed as

$$t_{67} = \left(\frac{I_0 L_r}{V_0}\right) \text{ ……. (22)}$$

Mode 8 (t_7-t_8): Now body diode of switch S_1 provides path for load current. As long as the switch S is not turned on, the converter operates as a basic PWM buck converter[13] until the switch S is turned on in the next switching cycle. In this mode,

$$i_{sL} = I_0$$

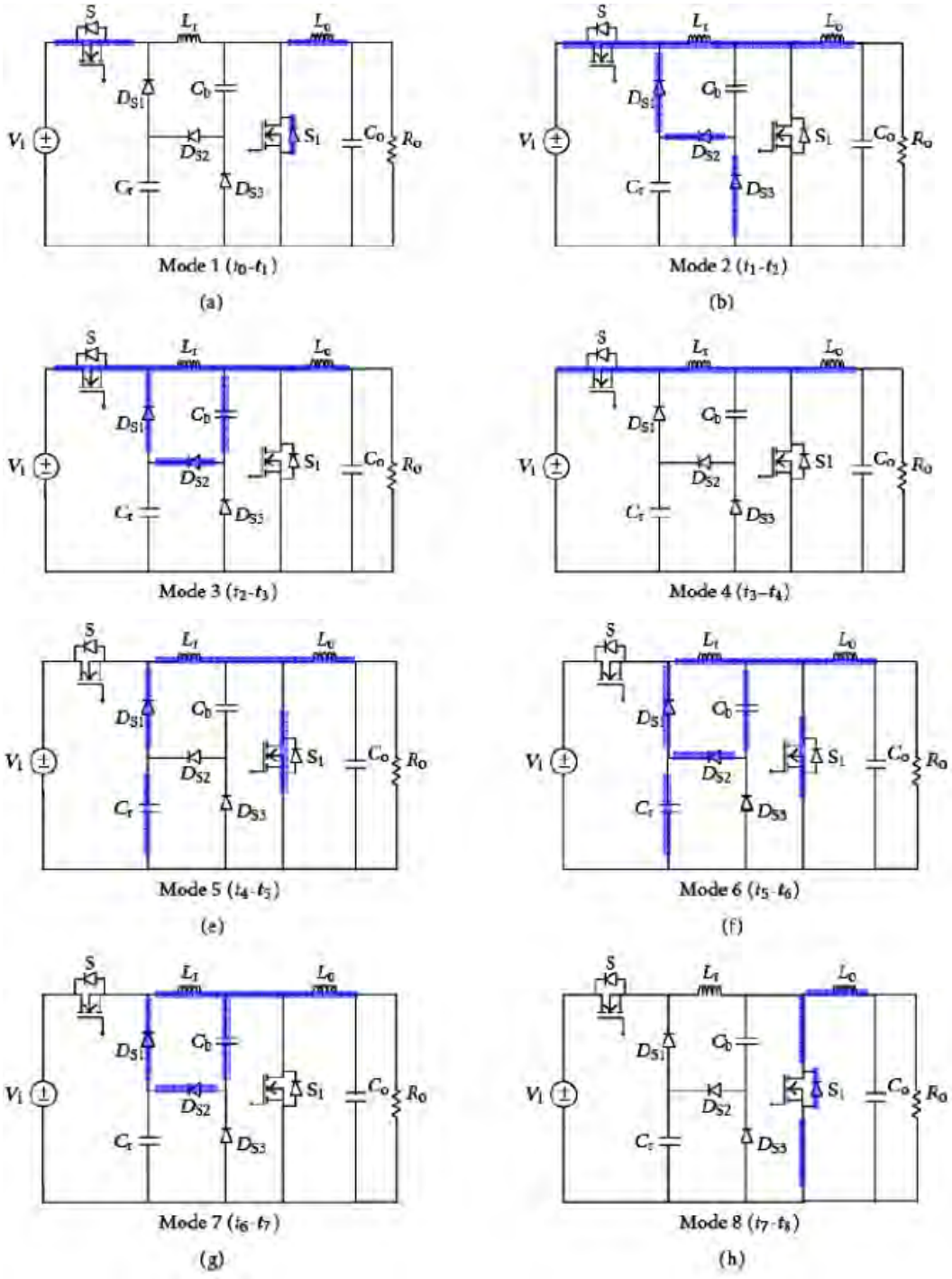

Fig. 3. Modes of Operation

2. SIMULATION RESULTS

Simulink models of simple Buck converter and modified Synchronous buck converter are developed and simulation results are presented. And comparison table is also given , which shows that the synchronous buck converter has 13.1% more efficiency than basic converter. In both the cases Input voltage of 12 V is taken with resistive load.

2.1. Simulated circuit of basic buck converter

The simulated circuit of buck converter with resistive load is shown in fig.4. The output current and voltage of the basic converter are shown in fig. 5a) and b) respectively. For an input voltage of 12V, load current of 0.4A and output voltage of 4.3 V is obtained. The duty ratio is 0.358 in this case.

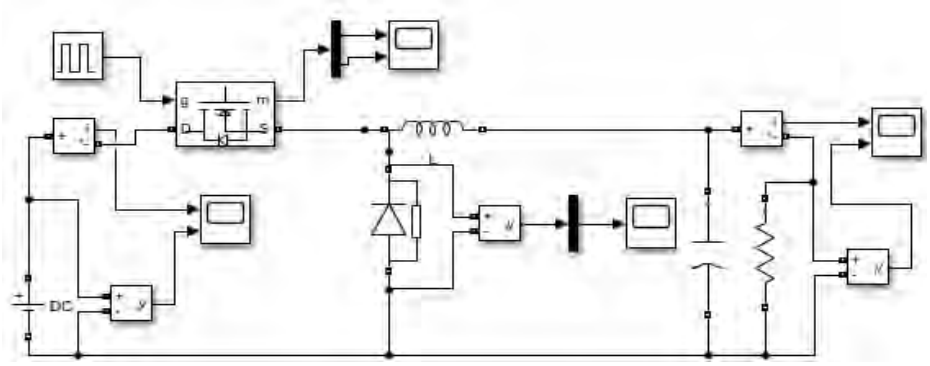

Fig.4. Simulated circuit of basic buck converter

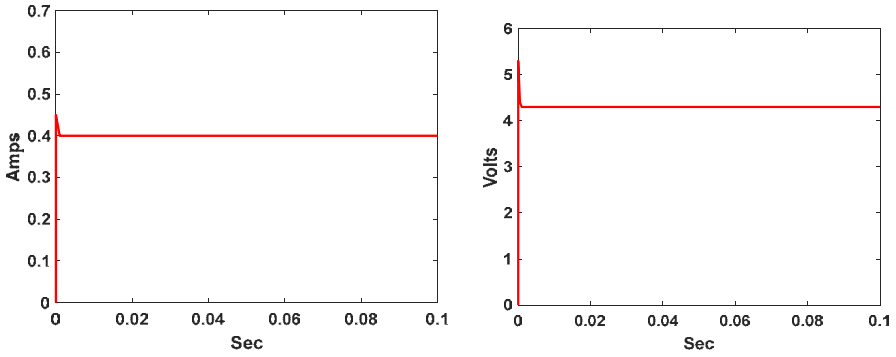

Fig. 5. a) Basic buck converter output current b) Basic buck converter output voltage

2.2. Simulation Results of proposed Converter

SIMULINK Model of the Synchronous buck converter shown in fig.1. is developed and the results are presented. Fig.6. a) and b) gives the output voltage

and currents of the converter for an input voltage of 12V and 1A. A current of 11 A and voltage of 3.3V is obtained. The steady state values are achieved at 0.1 sec.

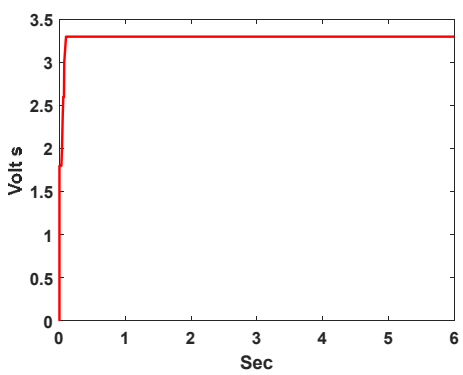

Fig. 6. a) Output Voltage

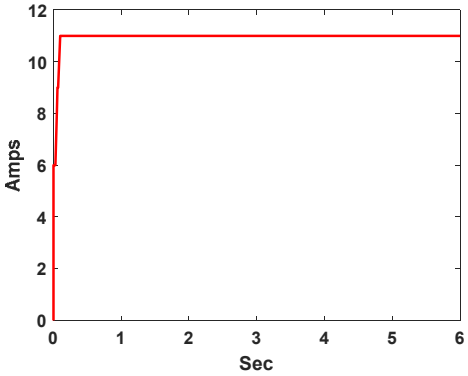

b) Output Current

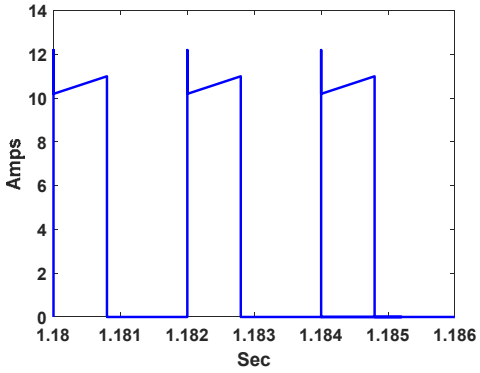

Fig. 7. a) Current though main switch

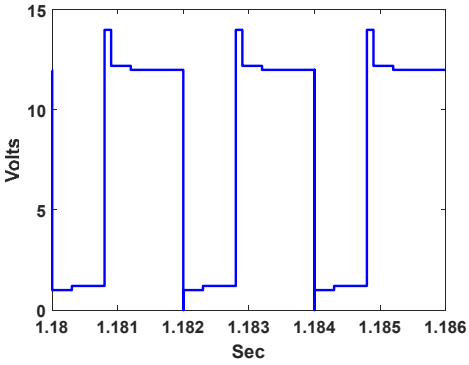

b) Voltage across main switch

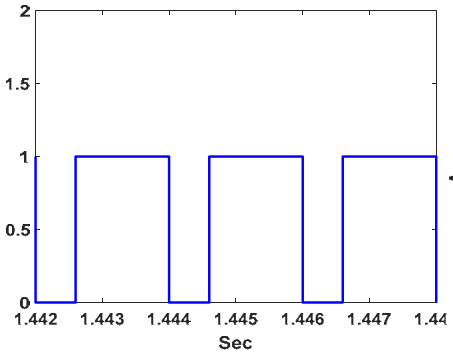

Fig. 8. a) Triggering Pulses for MOSFET Switch

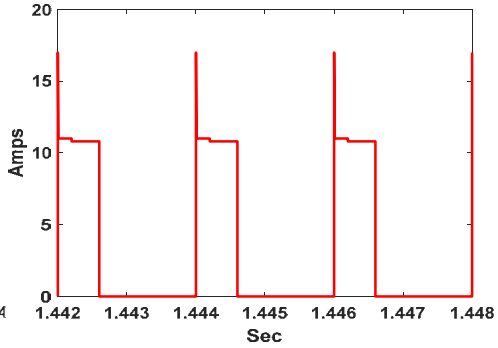

b) Current through synchronous switch

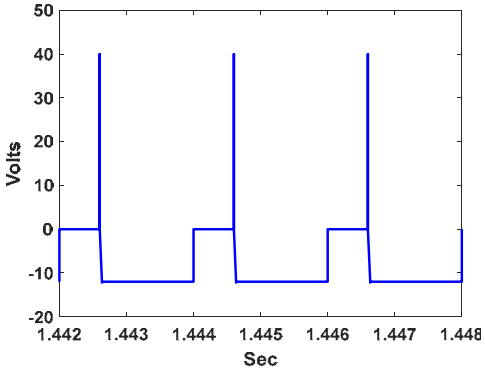

c) Voltage across synchronous switch

In fig.8a), the triggering pulses for the MOSFET are shown. Currents and Voltages across the main switch S are shown in fig.7a) and b) respectively. When the switch S is turned on at a time of 1.18sec, current passing through it is 10 A and reaches a maximum value of 11A. When switch S is tuned off, current suddenly falls to "0" and a voltage spikes to a value of 14 and later reaches constant value of 12. Similarly, the current and the voltage of synchronous switch are shown in fig.8.b) and c) respectively. The voltage across the synchronous switch is -12V and during transition the voltage spikes to 40V and the current is 11A.

2.3. Comparative Analysis

TABLE I

Type of Converter	**Input Voltage and Currents**		**Output Voltages and Currents**		**Main Switch Voltages and Currents**		**Synchronous switch Voltages and Currents**	
	Volts	**Amps**	**Volts**	**Amps**	**Volts**	**Amps**	**Volts**	**Amps**
Basic Buck Converter	12	1	4.3	0.4	12	1	-	-
Synchronous Buck Converter	12	11	3.3	11	12	10.5	12	10.5

The above comparison table shows that the proposed converter has better efficiency compared to the Basic Buck converter[8], which is 13.1% more.

3. CONCLUSION

This paper proposed a synchronous buck converter, which has an auxiliary circuit which is befitted for low voltage systems. As both ZCS and ZVS are implemented for switching of main and synchronous switches, switching losses are decreased considerably. The proposed converter is proven efficient when compared to conventional converter. And also stresses on the devices are avoided due to the soft switching implementation.

4. REFERENCES

[1] Wu, Haifu, Jianzhong Zhang, Jin Zhao, Yaqian Zhang, and Lucai Hu, “A New Soft-switching Synchronous Buck Converter without Auxiliary Switch,” 10th International Symposium on Power Electronics for Distributed Generation Systems (PEDG), pp. 537-541, 2019International Telecommunication Union (ITU), report on Climate Change, Oct. 2008.

[2] K. Pal and M. Pattnaik, "Performance of a Synchronous Buck Converter for a Standalone PV System: an Experimental Study," 2019 IEEE 1st International Conference on Energy, Systems and Information Processing (ICESIP), 2019, pp. 1-6, doi: 10.1109/ICESIP46348.2019.8938345.

[3] Q. Tong, N. Zhong, M. Yang and D. Zhang, "A ZVS DC-DC Converter Based on Buck Topology," 2019 IEEE International Conference of Intelligent Applied Systems on Engineering (ICIASE), 2019, pp. 324-327, doi: 10.1109/ICIASE45644.2019.9074092

[4] S. Kaewarsa, C. Prapanavarat, U. Yangyuen, “An improved zero voltage-transition technique in a single-phase power factor correction circuit,” International conference on power system technology – POERCON 2004, 21-24 Nov. 2004, vol.1, pp.678 –683.

[5] C.M.Wang, “Zero-voltage-transition PWM dc-dc converters using a new zero-voltage switch cell,” in Proc. IEEE INTELEC Conf.,2003, pp.784-789.

[6] M.L. Martins, J.L. Russi, H. Pinheiro, H.A. Grundling, H.L. Hey, “Unified design for ZVT PWM converters with resonant auxiliary circuit,” Electric power applications, IEE proceedings, vol.151,issue 3, 8 May 2004, pp. 303-312.

[7] P. A. Tabbat, A. Khoshkbar-Sadigh, I. Talebian, V. Marzang and E. Babaei, "Analysis and Investigation of a Soft-Switched Synchronous Buck Converter," 2021 12th Power Electronics, Drive Systems, and Technologies Conference (PEDSTC), 2021, pp. 1-5, doi: 10.1109/PEDSTC52094.2021.9405843.

[8] K.M.Smith and K.M.Smedly, “A comparison of voltage-mode soft switching methods for PWM converters,” IEEE Trans. Power Electron., vol.12, no.2, pp.376-386, Mar.1997

[9] C.J.Tseng and C.L.Chen, “Novel ZVT-PWM converter with active snubbers,” IEEE Trans. Power Electron., vol.13, no.5, pp.861-869,Sept.1998

[10] A. K. Panda and K. Aroul, "A Novel Technique to Reduce the Switching Losses in a Synchronous Buck Converter," 2006 International Conference on Power Electronic, Drives and Energy Systems, 2006, pp. 1-5, doi: 10.1109/PEDES.2006.344408.

[11] W.Huang and G. Moschopoulos, “A new family of zero-voltagetransition PWM converters with dual active auxiliary circuits,”IEEE Trans. Power Electron., vol.21, no.2, pp.370-379, March 2006

[12] M.L.Martins, J.L.Russi, H.L.Hey, “Zero-voltage transition PWM converters: a classification methodology,”IEEE proceedings on electric power applications, 4th March 2005, vol.152, no.2, pp.323 – 334

[13] N.P.Filho, V.J.Farias, and L.C.deFreitas, “A novel family of DCDC PWM converters uses the self resonance principle,” in Proc.IEEE PESC Conf., 1994, pp.1385-1391.

[14] M.D.Mulligan, B.Broach, and Thomas H.Lee,” A constant frequency Method for Improving light-load efficiency in synchronous buck converters,” IEEE Power Electronics letters,vol.3, no.1, pp.24-29, March 2005.

[15] H. Do, "Zero-Voltage-Switching Synchronous Buck Converter With a Coupled Inductor," in IEEE Transactions on Industrial Electronics, vol. 58, no. 8, pp. 3440-3447, Aug. 2011, doi: 10.1109/TIE.2010.2084973.

[16] Anil kumar HV and Sudharani P. "A Single Phase Integrated Converter with ZVS for High Power Factor Correction (PFC)." International Journal for Scientific Research and Development 4.3 (2016): 683-687.G. Koutitas, P. Demestichas, ‘A review of energy efficiency in telecommunication networks’, Proc. In Telecomm. Forum (TELFOR), pp. 1-4, Serbia, Nov., 2009.

1

Regenerative Braking System Using a DC/DC Buck-Boost Converter

Sudhakar Rao, Bansilal Bairwa, Daamiyan Ahmed, Sam Staines
sudhakar.rao@reva.edu.in

School of EEE, REVA University, Bangalore, India 560064

Abstract

In a battery-powered electric vehicle, regenerative braking is the conversion of the vehicle's kinetic energy into chemical energy stored in the battery, where it can be used later to drive the vehicle. It is braking because it also serves to slow the vehicle. It is regenerative because the energy is recaptured in the battery where it can be used again. The conservation of this energy is very important, as it allows us to drive further distances in electric-powered vehicles, and be more efficient overall. In this project, we wish to use a DC/DC buck-boost converter, connected to a wheel. This wheel will produce kinetic energy that is sent to the DC/DC converter, which is then sent to a battery that supplies it back to the vehicle in question. The most common power processing converter used for the battery converter in hybrid/electric vehicles is a buck and boost converter. When recovering the kinetic energy from the vehicle, the device operates in buck mode, where the voltage level is decreased to a level that is within the safe voltage range of the battery. When propelling the vehicle, the device operates in boost mode, and the DC voltage is regulated to output a higher voltage level for the electric motor drive and motor. In this case, when regenerative braking is activated, we allow the motor to stop completely, and the dynamo takes over in this case. The momentum of the wheel when it's braked is sent over to the dynamo. It will generate a voltage which is boosted by the buck-boost converter to

An Edited Volume, 9–15.

supply energy to the battery, rather than allowing it to go to waste. This is a more practical demonstration as a solitary motor acting as both a motor and generator would be overly pricy.

Keywords: regenerative braking, conservation of energy, buck-boost converter, dynamo, motor, generator.

1.1 Introduction

The invention of the Electrical Vehicle is nothing short of a miracle. Electrical and Hybrid vehicles are shown to be emission free, which is extremely necessary in this heavy pollution ridden climate. Fuel based modes of transport dependent on petrol cause major harm to the environment, as well as diminishes at a rate that is impossible to replenish, therefore the slow shift of dependency onto Electrical and Hybrid vehicles over the conventional sort, is a needed change. Every year, the government is pushing for more and more electrical vehicles to be built in an attempt to stop the damage being done to the ozone layer, and to reduce the usage of fossil fuels overall. In India, automobiles are one of the key forms of economic growth, and they are a booming source of revenue, only growing year by year. This however does mean that they are one of the largest sources of pollution. Due to this, the Indian government is in a frenzy to switch to a complete focus on electrical vehicles by 2030. Electrical cars are hardly a new invention, rather the roots were found all the way back in the 1900s. However the electrical vehicular mania did not last long, as electrical cars in that time were restricted by their top speed and mileage. There were a number of issues other than that, which made it difficult to adopt the technology in the past. The first attempts of regenerative braking were found back then, as even primitive regenerative braking could improve a car's range by 10-25%. Traditional braking systems use up and waste quite a lot of energy in the form of heat. They use mechanical braking to dissipate the kinetic energy gathered, into wasteful heat energy using a frictional method to bring the car to a stop. Studies show, that about a third to a half of the energy used for the operation of a car, is consumed during breaking, especially within urban areas where braking constantly is necessary. The energy we waste away as heat can be converted into something far more useful. In this case, Regenerative Braking. Regenerative Braking is present only in electrical and hybrid vehicles and is implemented to recapture the wasted heat energy. This heat energy can be converted into electrical and stored in batteries, as to improve the overall health of the car, and the driv-

ing range of said vehicle.Some of the main benefits of regenerative braking include:

- Reduces wastage of fuel
- Extends the charge of the battery by recharging it with the converted heat energy the strain upon the breaks and keeps it healthier and working longer energy

1.2 Regenerative Braking System

The block diagram Figure 1.2 shows the general schematic of the proposed circuit. This regenerative braking system focuses on feasibility, by using a dynamo alongside a DC/DC buck-boost converter and a 12V battery, forthe main operation of the circuit. The battery is also connected to a 5V output which is sent to make the Arduino ESP32 function, producing results onto the devices connected via Bluetooth [1, 2, 3]. During forward movement, the 12V battery supplies energy to the motor, giving it enough electricity to propel itself forward. This is motoring mode, and works in a rather straightforward fashion. The battery sends this voltage to the motor through the DC/DC converter, allowing it to supply the motor with the needed amount of voltage to function. This is done in boost mode. During regenerative braking, the momentum of the wheel is taken up by the dynamo, allowing the motor to be stopped. The dynamo acts as a generator and supplies energy to the battery. If the generated voltage by the dynamo is higher than the battery voltage, the converter operates in buck mode, otherwise it operates in boost mode to reach 12V. The battery being charged can be supplied to the relevant vehicle to save both fuel and energy[4, 5, 6]. The Arduino ESP32 is necessary for Bluetooth support, requiring 5V to function which it is supplied by from the 12V battery. The 5V can be gained using a zener diode, to convert the 12V into a usable 5V. The Arduino ESP32 is only used for the Bluetooth functionality, programmed to function and produce results to external Bluetooth devices. It uses hotspot functionality, by using the Network name and Password, so when the hotspot is active, the user can gain clear voltage readings of the circuit, whenever it is used, alongside a history of previous usage. The LED shows the voltage reading of the generated voltage and the battery voltage[10]. The DC/DC Buck-Boost converter is the proposed converter for this system. A buck-boost converter is necessary to raise or lower the voltage when being sent towards the battery or the motor. This circuit is made up of a DC source (Motor), MOSFET, 2 capacitors, 2 inductors, 1 load, and a PI controller that is fed the

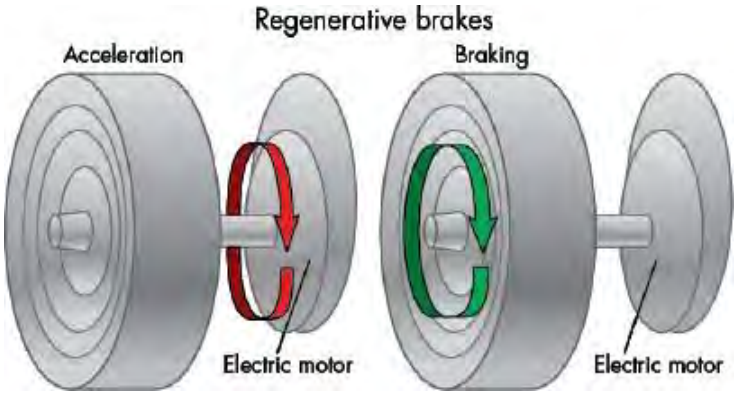

Figure 1.1 Basic diagram representing Regenerative braking.

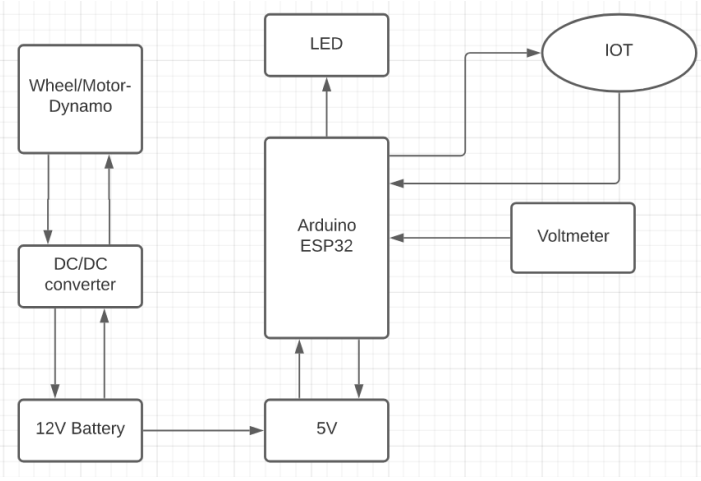

Figure 1.2 Block diagram of Proposed Regenerative braking system.

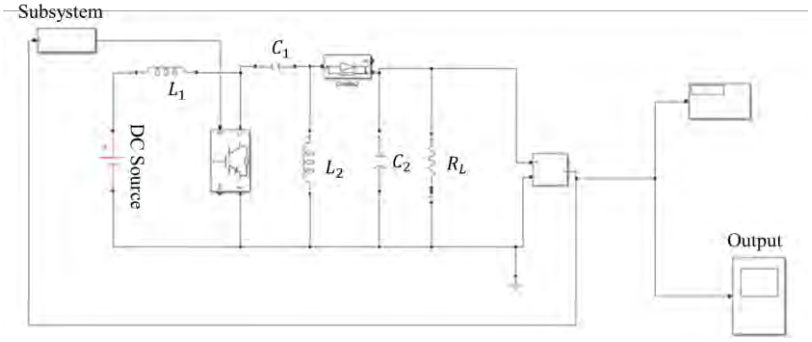

Figure 1.3 Simulink Circuit diagram of proposed converter.

Table 1.1 Caption

S.No	Components	Values
1.	DC source	10V
2.	L1	100H
3.	L2	100H
4.	C1	100F
5.	C2	100F
6.	Load1	204
7.	Gain in subsystem	1/12

Output, which is essentially fed back to the MOSFET. The values of each circuit element are:

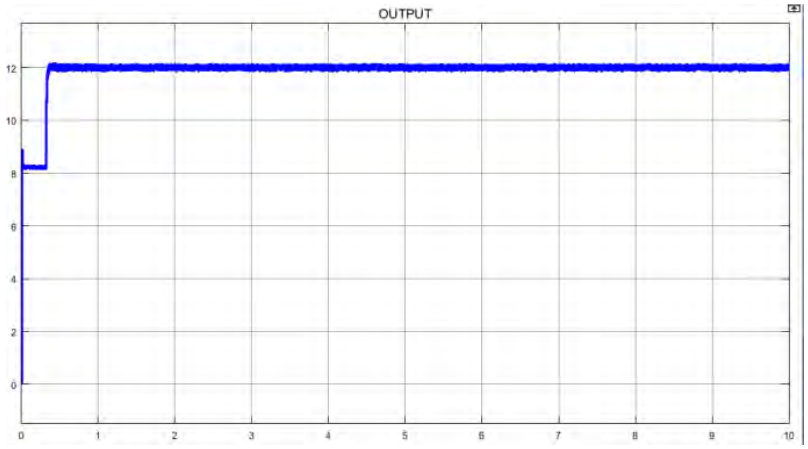

Figure 1.4 Regenerative braking Output from simulation.

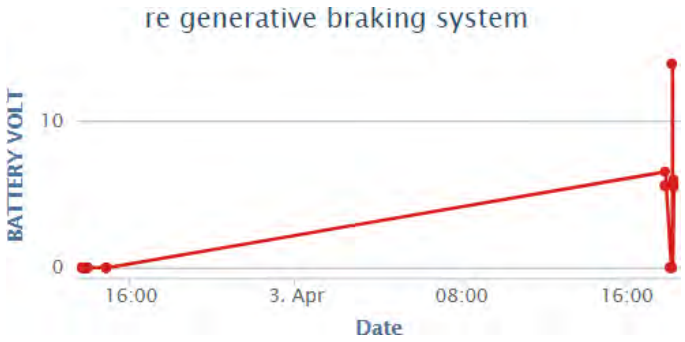

Figure 1.5 Graphical representation of Output of IOT.

The PI controller receives constant feedback from the o/p, which it feeds to the gain channel in the MOSFET. In the actual circuit, the PI controller subsystem is replaced with the Arduino ESP32. It acts in the same manner, as the same way the PI controller operates in the simulation circuit[7, 8, 9]. When we run this circuit, our goal is to produce a 12V at the output, for the battery as to charge it in regenerative braking mode. As our motor in this specification runs at 10V, the boost mode of this converter is used to bring it to 12V. The diode in this circuit is to keep the signal DC, converting any stray AC signals into pure DC, as the battery can only use DC. The following graph Figure 1.4, is the operation of the converter for a time period of 10s, giving it enough sample time to show that it can maintain 12V with some margin of error in the simulation.

1.3 IoT Simulations

The simulation consists of the DC/DC buck-boost converter mainly, the DC source input acting as a stand in for the motor, the output being 12V meaning to be fed to the battery. The feedback of said output is sent to the PI controller, which sends it to the MOSFET appropriately, rather than the Arduino for the simulation. The IOT can show the graphical results of testing the generated voltage that was to be sent to the battery, shown in Figure 1.5 The final produced voltage in the IOT device, is 12V as it should be (other values were produced while testing the output)

1.4 Conclusion and future work

While working on this project, we found ourselves understanding the importance of energy conservation in general, and with that the importance of Regenerative braking. The percentage of energy saved using this method may seem underwhelming, but in the age of electrical cars, and eco friendly methods of transport, we can see that every bit of energy that we can retain, can be essential in the future. Regenerative braking, and other similar methods of energy conservation, have only improved over the years. Initially the downsides to such heavy emphasis on conservation were considerable, such as lowering the life of the vehicle considerably, reducing the range, and taxing the speed greatly, but technological advances, alongside the boom of electrical and hybrid vehicles, we are entering the age where regenerative braking will soon be common place in most cars, rather than an experimental luxury.

The Buck-Boost method of Regenerative braking is relatively simple, and not as complex or expensive as other methods, such as using ultra capacitors for storage, however using a dynamo during regenerative breaking, allows us to simulate and conceptualize how exactly basic regenerative braking can function. As Electrical vehicles become more commercial, as regenerative braking works with it, hand in hand, it is only a matter of time, before regenerative braking is implemented just about everywhere having another benefit of IOT being implemented and becoming more commonly used in both daily life appliances, and more complex tasks. Being implemented to show a basic rundown of the energy being spent in our own vehicles can give us some much needed perspective and understanding of our own usage, which will only become more relevant the further ahead we move with our technology.

References

[1] Electronic Braking System of EV And HEV-Integration of Regenerative Braking, Automatic Braking Force Control And ABS - Yimin Gao and Mehrdad Ehsani

[2] Development of a Predictive Model for Regenerative Braking System - Andrea Caratti, Gabriele Catacchio, Carlo Gambino and Narayan C. Kar

[3] Studies of Regenerative Braking in Electric Vehicle - M.K Yoong*, Y.H Gan, G.D Gan, C.K Leong, Z.Y Phuan, B.K Cheah. K.W Chew, Member, IEEE

[4] Advanced Integrated Bidirectional AC/DC and DC/DC Converter for Plug-In Hybrid Electric Vehicles - Young-Joo Lee, Student Member, IEEE, Alireza Khaligh, Member, IEEE, and Ali Emadi, Senior Member, IEEE

[5] A Dual Control Regenerative Braking Strategy for Two-Wheeler Application – Siddharth Metha, S.Hemamalina

[6] Yoong, M. K., Gan, Y. H., Gan, G. D., Leong, C. K., Phuan, Z. Y., Cheah, B. K., Chew, K. W. (2010, November). Studies of regenerative braking in electric vehicle. In 2010 IEEE Conference on Sustainable Utilization and Development in Engineering and Technology (pp. 40-45). IEEE.

[7] Onar, Omer C., et al. "A bidirectional high-power-quality grid interface with a novel bidirectional noninverted buck–boost converter for PHEVs." IEEE transactions on vehicular technology 61.5 (2012): 2018-2032.

[8] Prince, Agna, Peter K. Abraham, and B. Aryanandiny. "Design and implementation of ultra capacitor based regenerative braking system for a dc motor." 2018 International Conference on Emerging Trends and Innovations In Engineering And Technological Research (ICETIETR). IEEE, 2018.

[9] Mehta, Siddharth, and S. Hemamalini. "A dual control regenerative braking strategy for two-wheeler application." Energy Procedia 117 (2017): 299-305.

[10] Karthikeyan, P., and V. Siva Chidambaranathan. "Bidirectional buck–boost converter-fed DC drive." Artificial Intelligence and Evolutionary Computations in Engineering Systems. Springer, New Delhi, 2016. 1195-1203.

Energy Efficiency Enhancement of Wind Power Plant by using P&O MPPT

[1]K. Ramamohan Reddy, [2]K. KalyanKumar, [3]N. Siddhik
K.S.R. College of Engineering (Autonomous), Kadapa, AP

Abstract

Globally, Renewable Energy Resources (RER) are playing vital role for generating electrical energy due to conventional fossil fuel based power plant are harms environment. Also, availability of fossil fuels is going to run out. The primary resources for RER are sun, wind, hydro and tidal. Among energy harnessing rate has been rapidly increased in solar PV and wind power plants. Since sun and wind energy are abundant in nature. Nevertheless, natural resources are seasonable which are varying with respect to the climatic condition. Therefore, sun and wind power generator are produced fluctuating electrical energy which causes stability issue.It can be compensated by MPP tracking technique. At present, MPPT technique is incorporated with RER for generating maximum electrical energy based on available resources. In this manuscript a wind power plant withPerturb and Observer based MPPT model has been developed by using MATLAB/Simulink for analyze the significance of MPPT. From the simulation results show that, wind power plants are capable of generating constant power with the help of Perturb and Observer MPPT. Furthermore, the wind power out is significantly enhanced with the accurate designed boost converter.

Keywords. Photovoltaic, Rural, MPPT

1 INTRODUCTION

Due to rapid growth of urbanization and industrialization, the requirement of electrical energy has been increased. Accordingly, power industries are enhancing the electrical energy generating capacity by capacity addition program. During capacity addition, fuels are playing key role. Because of conventional thermal based power plants are fossil fuels are used as primary resource for generating thermal energy. It is used to generate required steam. The fossil fuels are namely coal, diesel, and petrol. Among, over 60% power plants using coal as a primary fuel for generating required thermal energy. The fossil fuel-based power plants faced two challenges such as availability of fossil fuels are going to run out in near further. In addition, the fossil-based power plants are harming the environment. The coal-based power plants are releasing the carbon dioxide, carbon mono oxide and NO etc. These are harming the environment as well as living organism. Therefore, power sectors are concentrating ecologically friendly resources for generating electrical energy. In addition, availability also consider for generating electrical energy [1],[2].

Globally, renewable energy resources are playing a key role for extracting electrical energy. The renewable energy resources (RER) are solar, wind, tidal, and hydro etc. Among them electrical energy generation has been increased from solar and wind power plants. By using suitable energy conversion device, it is possible to convert available RER into electrical energy. For an example, solar PV system, solar PV array are used to convert available irradiations into electrical energy. The photovoltaic cells are connected in series which forms the solar module. Then number of solar cell modules is connected to form a solar PV array. The basic principle behind the solar PV system is photovoltaic effect. The PV cells are received, irradiations form sun. The solar cell made upon two different layers of silicon. Such as P and N type semiconductor materials. By nature, N type semiconductor materials release the electron when sun irradiation is hit on the materials. While P type materials are received the extra electrons. It is a simplest principle behind the solar PV arrays. The output of solar PV array is strongly depending on the environmental conditions such as available irradiations, irradiation received by the solar PV array, cell temperature. The received irradiations by the solar PV cell are high generating electricity also high whereas low number of irradiations are hit in the solar PV which yields the less energy. Therefore, solar PV array yield potential has been varied with respect to the irradiations [2]-[4].

The sun continuously moving therefore received irradiation by the solar PV array has been varied with respect to time. So, electrical energy harnessing rate is varied with respect to time. For an example mid of the solar PV generate high energy, while morning and evening yield potential has been low that of mid of the day. Therefore, extracting maximum energy is challenge task which is achieved by keeping solar PV working on MPP. It is made by the MPPT technique. The role of MPPT is track the maximum power from available irradiations. Traditional MPPT such as Incremental Conductance, Perturb and observation, Hill

climbing is able to track the maximum power steady under climatic condition. Whenever, rapid climatic change occurs at instant soft computing based MPPT technique are capable of tracking maximum power from solar PV system such as ANN, Fuzzy etc [5],[6].

Furthermore, electrical energy extraction rate is significantly increased from wind power plant. The wind power plants are tracking electrical energy from wind. The wind is referring to the movement of air due to uneven heating of earth surface by sun. From wind electrical energy has been extracted by blades. Globally total install capacity of wind power plant is 300 GW which is rapidly increased every hour. According to the International Energy Agency Report, wind power has been contributing 18% of power sharing by 2050. However, wind power plants are doesn't produced constant electrical energy since wind output energy is depends on the available wind speed. Suppose wind speed is high which produced high energy yield otherwise vise-versa. In addition, wind power yield potential has been varied with respect to temperature, pressure and humidity, respectively. Therefore, extracting maximum power from wind power plants is challenge task [7]-[9].

In this paper, wind power plant with MPPT is modelled and analysed with the help of MATLAB Simulink block set. Also, an accurate design has been developed for enhancing voltage form generation to desired level. The manuscript has following section such as in section 2 dealt with proposed model block diagram description followed by section 3 discussion about P&O MPPT and section 4 is simulation results and analysis, and section 5 is concluding the main findings.

2 PROPOSED WIND MODEL

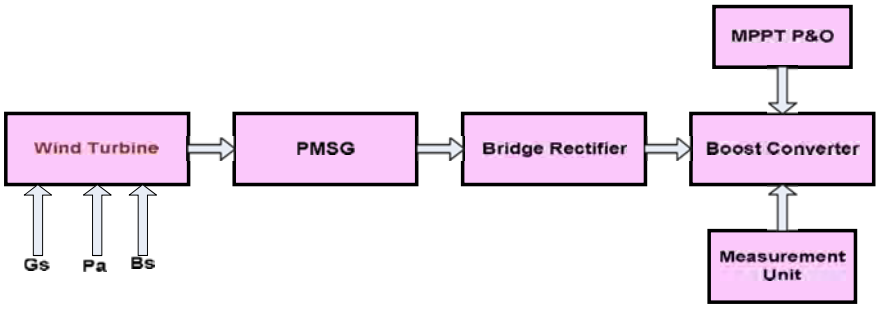

Figure 2.1. Proposed Wind Model

As shown the above figure, it shows the entire unit of proposed model. The first block represents the wind turbine. It received three input such as generator speed (Gs), Pitch Angle (Pa) and Generator Base Speed (Bs), respectively. The turbine is generating required kinetic energy for permanent magnet synchronous generator. Here salient pole synchronous generator has been used. Due to it seed torque characteristics is comparable to the non- salient pole synchronous generator. The PMSG is generating electrical energy depends on the received mechanical energy from wind turbine. Subsequently, the generated electrical energy is fed to thebridge rectifier. It is used to rectifier the given input power from AC to DC. It is fed to the input of boost converter. The boost converter boosts the voltage at desired level according to the L and C and Switching sequence. The voltage level increases, or a decrease depends on the duty cycle of switch. The duty cycle generation is depending on the generator output voltage and rectifier voltage and power [10], [11].

3 WIND ENERGY CONVERSION SYSTEMS

Traditionally, squirrel cage induction motor is used to generate electrical energy which working based on the Danish concept, respectively. It is directly connected to the grid. The speed of such a motor is content such as fixed speed. Perhaps, at the instant of heavy wind hitting on the wind blades subsequently generating electrical energy is also high. Later on adjustable speed control technique has been incorporated with existing squirrel cage induction motor. This is restricting high wind pressure on wind tower. In wind power plants, Double Filed Induction Generator (DFIG) are popularly used which coupled to the turbine with help of gear box. Due to aging phenomena the gear gets damaged. Therefore, it is required frequent maintenance for smooth mechanical coupling between generator and turbine. However, the rotor of PMSG is directly coupled to the wind turbine, so there is no need for gear system. So, cost wise PMSG is lower that of DFIG. The significance of PMSG is low excitation loss, reasonable efficiency, power density is high and so low maintenance cost [2-3]. However, wind power plants are introduced power quality issue

on the transmission and distribution system. To compensate the power quality issue at present dynamic voltage resistor(DVR), a thyristor switched series capacitor (TSSC) has been incorporated with the existing system for enhancing the power quality. In addition with, to reduced voltage sag and swell issues by using DVR. Moreover, wind power plants are causes following impacts on the power systems such as short and long duration effects. The first effect time duration is marginally is very low that is milliseconds to hours which is responsible for system unbalancing. Whenever, generated powers is transferred to the grid which causes the power quality problem, voltage sag and swell and so reactive power problems, respectively. Suppose, required compensating devices are we are not included which continue until wind power get off. Since, wind power plants never run at constant speed. The main classification of voltage variations are voltage sag and swell, short and long voltage irruptions, respectively. It can be rectified by suitable compensator such as STATCOM. It is synchronous condenser which is connected parallel to the AC system, respectively. Now a day's, STATCOM is incorporated with harmonics filter to attain effective control. Other hand, power has been enhanced by SVS. The primary role of SVS is automatically matches the impedance with the required system. For an example, power system load is capacitive that of other, by using reactor SVS consumes the VAR from the power systems. Nevertheless, capacitor bank of SVS get enable when power system is more inductive. Due to absence of excitation, PMSG is popularly used in the wind power plants, so machine cost is low as well maintenance cost is low. Perhaps, it has low speed characteristics. Therefore, DVR system has been incorporated to the wind energy system for maintaining the system consistency and reliability, respectively. The DVR has switching devices such as thyristor, MOSFET or IGBT and voltage source inverter with a low pass filter. The Pulse Width Modulation Technique has been used for triggering VSI. The role of low pass filter is suppressing the harmonics content which is developed during voltage conversion from DC to AC, respectively. Modern power system has separate control unit for match the voltage phase angle and frequency [12]-[14].

4 PERTURB AND OBSERVE MPPT

The wind power plant are cant able to generate constant power since the out electrical energy obtained from wind power plant is strongly depends on the available wind speed. The wind speed on depends on the atmosphere conduction. Therefore wind speed is continuously varying therefore extracts maximum power from crucial task. Due to fluctuation output, these power generation units are interconnected with the utility grid is difficult issue. To rectifying such a problem, the wind power plants incorporated with MPPT. Traditionally, MPPT techniques are enhancing energy yield potential of solar PV system. The same MPPT technique has been incorporated with the wind power system for enhancing energy yield potential [15].

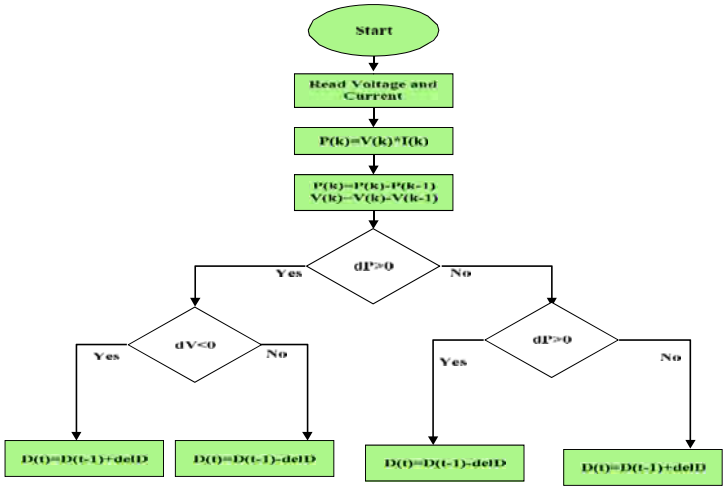

Figure 4.1 Flow Chart for P & O MPPT

Figure 4.1 shows the flow chart for P&O MPPT. At first the voltage and current has been measured by suing suitable sensor. It is used to estimate the power. Next, instantaneous voltage and current has been measured. This is used to estimate instantaneous power. Then, change in power is grater then zero or not has been checked. If yes change in voltage is zero or not has been checked. At this moment, condition is true then duty cycle is increased while duty cycle is get reduced. Nevertheless, change in power is greater than zero then duty cycle of the switching device is reduced. Otherwise, duty cycle is increased.

5 SIMUATION RESULTS AND ANALYSIS

The proposed wind model has been developed in the MATLAB Simulink for analyse the significance of proposed P & O MPPT.

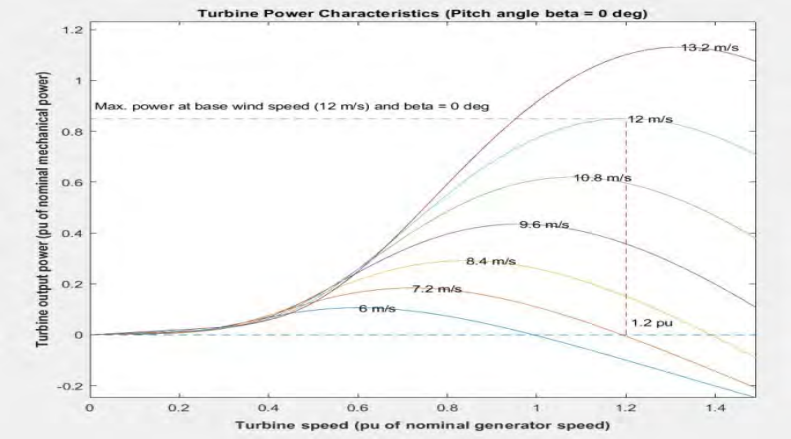

Figure 5.1. Turbine speed Vs Turbine output power

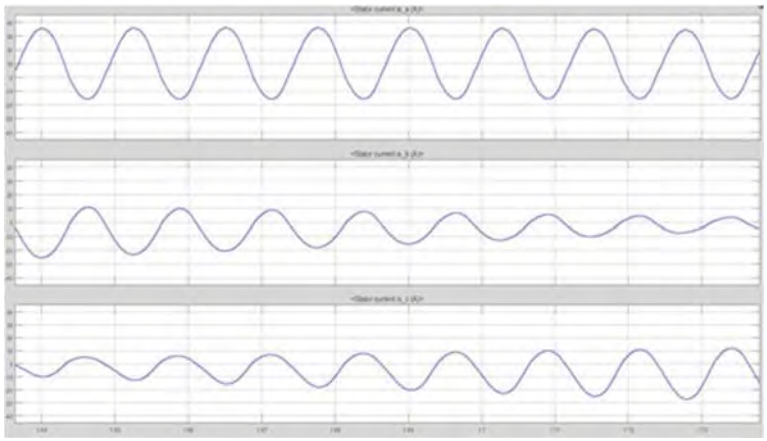

Figure 5.2. Three phase stator current Vs time

As shown the figure its shows the relationship of three phase current of PMSG. From the figure observe thateach phase current has 90-degree phase shit each other.

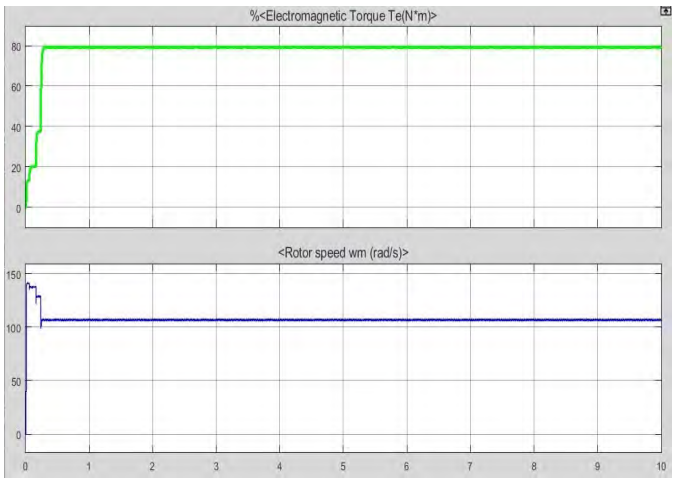

Figure 5.3. Mechanical Characteristics Vs Time

As shown the figure 5.3 It showed the relation between mechanical characteristics of PMSG, such as rotor speed and electromagnetic torque. Initially, electromagnetic torque and rotor speed fluctuation however it will reach a stable value within fraction of seconds. Which infers that motor attain smooth speed very soon.

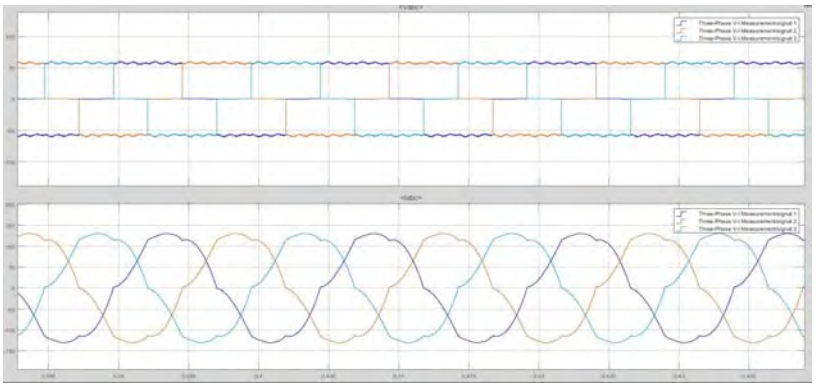

Figure 5.4. Three phase and Three Phase Relationship

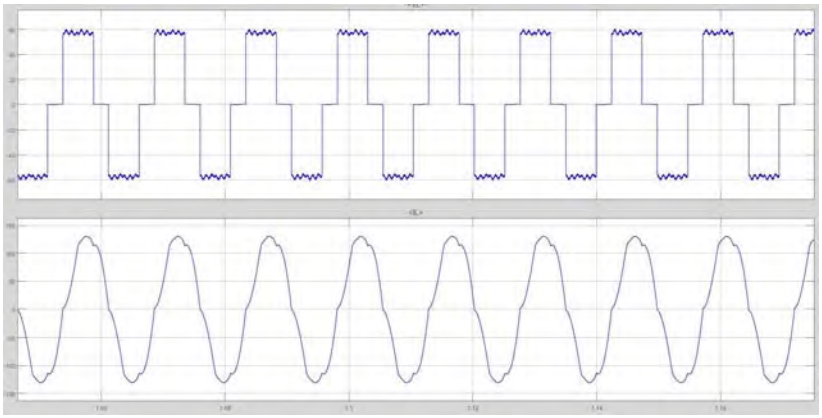

Figure 5.5. Line Voltage and Line Current Relation

Figure 5.4 shows the output of three phase voltage and three phase current respectively. It is the output ofPMSG. The output of PMSG is almost perfect three phase voltage and current, respectively. From figure 5.5 observed that line voltage and current are in phase and so peak of line voltage a small fluctuation is presents. This generated voltage is fed to the input of universal bridge rectifier. The bridge rectifier made by non-gate device such as diode.

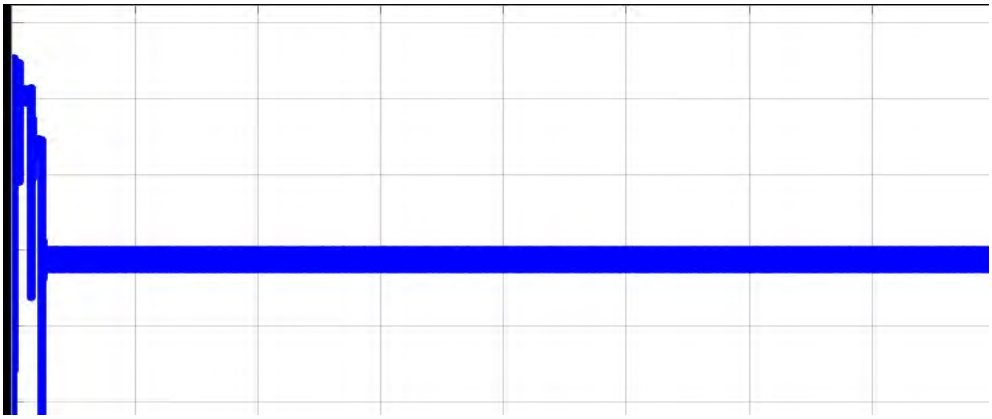

Figure 5.6. Universal bridge Rectifier output

Figure 5.6 Shows the universal bridge rectifier output, from the figure observed that the output of universal bridge rectifier is initially vary but very short time it will reach to 60V for entire duration. The output of universal bridge rectifier is lower than that of input supply which is due to loss.

Figure 5.7 Relation between boost converter output

Above figure 5.7 shows the relation between output quantities such as boost voltage (Vboost), boost current (I boost) and boost power (Pboost). It is observed that boost converter output is higher than the input voltage. In addition, observe that, due to perturb and observe the load voltage remains constant, it is maintain by the adjusting duty cycle by P&O. Basically wind power plants are installed far away from the city Centre. Therefore, generated alternating electrical energy has been converted into direct current and transmits to the city Centre. Furthermore, the role of boost converter is step up the voltage level with the help of low ratting L and C so cost wise cheaper than the transformer. Since, step-up transformer is used to step-up the voltage from lowlevel to higher level. The role of P&O MPPT is maintaining constant electrical energy by adjusting duty cycle ofswitching devices. The duty cycle adjustment depends on the generated electrical quantities and previous measured quantities.

6 CONCLUSION

From the literature found that, wind power plant not produced continuous and constant output**.** Therefore, it causes power quality issues on the power system. It rectified by the suitable compensating devices. On compared to all other compensating technique, hybrid compensating technique is costly but it suppress all types of harmonics issues as well as maintains the system voltage at desirable level. The wind power plant with MPPT is modelled and analysed by using MATLAB simulink. From the simulation found that, with P&O MPPT, the developed model has produced constant power for entire duration. Furthermore, with the help of boost converter, step-up the voltage which is suppress the transmission loss since wind farms are installed far away from the city centre. In future, the proposed MPPT technique compared with other MPPT technique to finding effective MPPT for Wind power plants.

7 REFERENCE

[1]. T. Mariprasath1, V. Kirubakaran2, “Feasibility Analysis of Karanja as Alternate Liquid Dielectrics for Distribution Transformers”, John Wiley & Sons Ltd, International Transactions on Electrical Energy Systems, Vol. 27, pp.1-8, DOI:10.1002/etep.2345, 2017. Impact Factor= 1.692.

[2]. T. Mariprasath1, V. Kirubakaran2, “Thermal Degradation Analysis of Pongamia Pinnata Oil as Alternative Liquid Dielectric for Distribution Transformer”, Springer, Sadhana-Academy Proceedings in Engineering Sciences, Vol. 41(9), pp.933-938, 2016. DOI: 10.1007/s12046-016-0529-0. Impact Factor=0.849.

[3]. T.Mariprasath1, V.Kirubakaran2, Sreedhar Madichetty3, K Amaresh4, "An Experimental Study on Spectroscopic Analysis of Alternating Liquid Dielectrics for Transformer", Springer, Electrical Engineering, Impact Factor = 1.180, 2020. Available at: https://doi.org/10.1007/s00202-020-01136-x

[4]. Govindugrai Venkata Suresh Babu1, T. Mariprasath2, S. Khadarvali3, C.Harshavardhan Reddy4 & Karnam Amaresh5, "Autonomous load sharing technique in solar photovoltaic system-based DC microgrid" International Journal of Ambient Energy,pp.1-8,2020. DOI:10.1080/01430750.2019.1710251

[5]. T. Mariprasath1, V. Kirubakaran2, “Power Transformer Faults Identification using SFRA”, International Journal of Scientific & Engineering Research, Vol. 5 (5), pp.81-87, 2014.

[6]. Parimitamohanty, G.Bhuvaneswari, R.Balasubramanian, Navdeep KaurDhaliwal, "MATLAB based modeling to study the performance of different MPPT techniques used for solar PV system under various operating conditions",Renewable and Sustainable Energy Reviews,Volume 38, October 2014, Pages 581-593

[7]. JinghuaLi,JiashengZhou,BoChen, "Review of wind power scenario generation methods for optimal operation of renewable energy systems",Applied Energy, Volume 280, 15 December 2020, 115992

[8]. S. Marisargunam, L. Kalaivani, T. Mariprasath, "Performance analysis of wind generator using SVM",International Conference on IoT and Application (ICIOT),19-20 May 2017

[9]. Soraida AguilarVargas,Gheisa Roberta TellesEsteves,Paula MedinaMaçaira, "Wind power generation: A review and a research agenda", Journal of Cleaner Production, Volume 218, Pages 850-870,1 May 2019,

[10]. Martin P. Ćalasan, Vladan P. Vujičić, " A robust continuous conduction mode control strategy of switched reluctance generator for wind power plant applications",Electrical Engineering volume 99, pages943–958 (2017)

[11]. Khairy Sayed, Mazen Abdel-Salam, "Dynamic performance of wind turbine conversion system using PMSG-based wind simulator", Electrical Engineering volume 99, pages431–439 (2017)

[12]. T.Mariprasath, V.Kirubakaran, M.Ravindaran, “Modern Trends in Renewable Energy Technology”, Cambridge Scholars Publishing,2019

[13]. Anil Bharadwaj, Suman Maiti, Nirmalya Dhal & S. Chakraborty, "Control and sizing of modular multilevel converter-based STATCOM with hybrid energy storage system for large-scale integration ofwind farms with the grid",Electrical Engineering volume 101, pages743–757 (2019)

[14]. Bangjun Lei, Tao Zhang & Shumin Fei, "An improved nonlinear robust control design for grid-side converter of VSC-HVDC connected to wind power generation system",Electrical Engineering volume 100, pages2309–2318 (2018)

[15]. Abdelhakim Belkaid, Ilhami Colak, Korhan Kayisli, "Implementation of a modified P&O-MPPT algorithm adapted for varying solar radiation conditions",Electrical Engineering volume 99, pages 839–846 (2017)

A novel method for application of non-conventional sources of energy with power quality improvement for local non-linear load using MLMS

T Kishore Kumar, Dr. P. Balachennaiah, P. Durga Prasad, Dr. C. Kumar Reddy

Address: Department of Electrical and Electronics Engineering, KSRM College of Engineering, kadapa, AP, India.,
Dept of Electrical and Electronics Engineering, AITS, Rajampet, AP, India.

Email:

Abstract

In an Energy Micro-Grid, a collection of energy networks is used to meet all of the local area's energy needs. The use of energy storage systems (e.g., electrochemical storage) appears to be a promising solution, taking into account costs, supply security, technological maturity, and ease of installation. It uses a micro-grid to integrate wind and solar photovoltaic electricity (PV) sources with energy storage batteries to feed the non-linear load (BES). The switching controls and the adjustment of the grids all address power quality (PQ), power reliability, non-linear load correction and economical resource usage. In order to adjust for nonlinear load and improve the PQ system a modified version for Adaptive Filtering Technology is employed, including the "momentum-based least mean square (MLMS)" technology, giving GVSC control signals. As a result, the convergence rate is improved, and the limitations of conventional control of the same family are removed. Back electromotive force control technique is used to obtain switching signals from conventional vector control scheme and encoder less estimation of speed and Wind turbine-powered SG rotor position. Using perturb and observe (P&O) maximum power point estimation for wind and adaptive P&O with variable perturbation step size for solar MPP estimation, the external environmental unrest can be overcome. Under steady state and dynamic conditions, including changing wind speeds, intermittent solar isolation, and variable load conditions, MATLAB/SIMULINK simulation results are obtained.

Keywords: Power quality, MLMS, Power generation, Solar PV, Wind energy, Maximum power point and perturb and observe.

1. INTRODUCTION

Natural sources of energy that have virtually no pollution or renewable energy sources must be taken into consideration. Wind energy is one of the renewable energy sources that ensures clean energy since wind energy generators for conversion of electricity may be efficiently gathered and used. Clean energy solution is photovoltaic control. Furthermore, it can be used without the usage of a rotary generator. The more wind power managed by PV, which goes hand in hand, should contribute to some extent, because strong winds generally occur at night and on cloudy days [1].

As a result of an efficiently and cost-effective use of renewable energy sources [2], some energy sources, such as wind turbines and solar panels, are incorporated. As the performance of these systems depends on wind speed and solar irradiation, its reliability is under all conditions reduced in meeting load needs. Some researchers have suggested combining diesel generators with wind/solar energy system [3][4]. Micro-grids commonly integrate these energy sources as power generators for distribution via appropriate power conversion stages. For example, DC-DC-AC converters are used by solar photovoltaic generators, and AC-DC-AC converters with local control are used by generators of wind [5].

When the wind speed falls below the cut-in speed, the wind generator is turned on. The wind generator starts to generate with unregulated frequency when wind speeds resume, until it is linked to the micro-grid and operates through a loop control. The absence of the wind generator means that the battery power generation can maintain crucial charges dependent on the battery charge. In those queries about grid connection and insulation a wind/PV house power system powered by the EV battery will be provided. A bidirectional converter is primarily controlled by a concurrent inverter [6] to operate a wind generator, interfacing with the back-to-back AC-DC-AC and the Battery interface.

It is currently actively supported to create the public LV network-connected PV system. These systems are usually from several to ten kWP in size, and on the top of dwellings or public buildings are solar panels installed. The efficient photovoltaic system operation varies, including sun intensity, cell temperature and cloud shading. The time unpredictability of production of electrical energy leads to expected power quality issues such as voltage imbalances, flushes, and downsizing [7].

The PV system is connected to the grid by a power converter and an inverter for modulation of pulses width. These interface converters provide a range of functions, including PV output adjustments to meet inverter voltage and maximum power point tracking, to operate the PV system as efficiently as feasible. There is a risk that converters will introduce harmonic distortions at both lower and higher frequency rates which result in parallel and series resonances, condenser bank and transformer overheating and the misuse of protective devices that could create problems of power quality [8]. When electricity prizes and demand are at their highest level, they try to feed the most power they can. The system thus succeeded

in recovering its excess revenues. When the SECS and the WEGS (Windows Systems) combine, the system's efficiency and reliability will be improved [9][10]. The voltage and frequency of electric WEGS compliance generated to meet grid code can be controlled and controlled [11], VSCs are adapted as an interface between the machine and the utility grid as the full voltage converter. [12]. For example, 10 voltage stresses caused by harmonic current have been shown to increase the operating temperature of a power bank by 7 and can reduce the expected lifetime of the bank by 30. [13]. Because of its inherent simplicity and strength, the least mean square (LMS) algorithm [14],[15] has become one of the most popular adaptive filter algorithms. But LMS is often slowly converging. Several LMS changes have been proposed over the year to remedy this situation. One of those changes is Proaki's first proposed LMS (MLMS) adaptive algorithm [16]. Roy and Shynk [17] have shown that the MLMS approximates the conjugate algorithm of gradients. MLMS is helpful when error bursting is problematic in applications. The MLMS recursion is WK+1= WK+μ(DK-WTK) XK+α(WK-WK-1) the parameter estimate at the kth iteration, DK is a real valued desired response XK = [x1k , x2k , ……, xdk]T Ɛ Rd is the input response, α Ɛ (-1.1) is the momentum factor, and μ >0 is the input size.

The approximations of the conjugate gradient algorithm (MLMS) are being used for the improvement of the energy quality of the gird-connected wind-based solar system [18]. It overcomes the slow convergences restricts of the convectional LMS and provides advantages when error bursting is the problem in applications. Compared to LMS, MLMS eliminates weight convergence dependence on step size, while it provides higher performance with high-noise signal. The improved dynamic performance comes from inclusion of feed terms for changes in wind and solar insolation. Identification if it is possible to achieve maximum output by using maximum output (MPP) systems for extracting both resources. A literature listing specifically from convection schemes (p &o), incremental conductance (InC), computer soft logic, artificial network neural, and optimization-based schemes [19–21] offers a variety of techniques. In this literature there is a special listing. The non-linear charge presence leads to additional problems in the power quality, including waveform voltage and current distortion. Finally, an important issue to be investigated may be the interaction between the harmonic currents and loads of the inverters; a harmonic distortion which can be multiplied by the resonant behaviour of the grid [21].

2. SYSTEM CONFIGURATION

Figure.2.1 depicts the AC micro-grid system with wind and solar panels in which two VSCs, MVSC and GVSC, back-to-back, provide decoupling power control. The DC connection via the BES and bidirectional DC-DC converters is connected to a solar PV array (one-stage). The combined wind turbine-driven SG and solar photovoltaic generation meet the demand for load. At a point of common linkage, the nonlinear load is connected (PCI). The grid includes the excess PV array and

wind power generation. The harmonics are filtered via a PCI connected ripple filter. The interface inductors are linked with GVSC in series to reduce the current harmonics. The DC engine simulates the wind emulator. With solar insolation change, the variable wind speeds, sudden charge disconnect, the promising system performance is achieved.

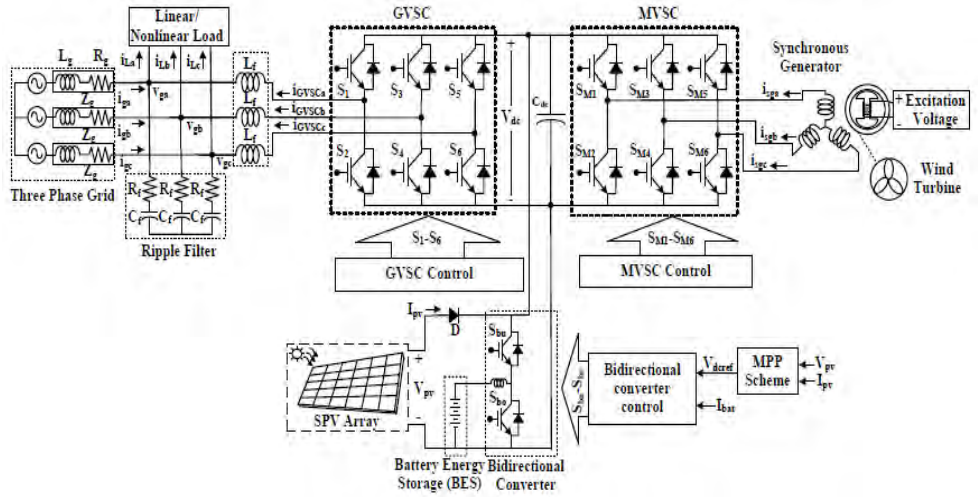

Figure 2.1. System configuration.

The proposed system control algorithms comprise three sub-sections. The GVSC switching controller is based on MLMS, Vector Control (VC) and Bidirectional Conversion Control is based on Vector Control (VC). The GVSC switching control is based upon MLMS (VC). Together with MPP approaches, these control algorithms for wind and solar assess the efficiency of the system.

A. MPP Extraction Scheme

Inherently, solar insolation and wind speed vary with time and place. On the other hand, the system using those 2 renewables requires the best energy extraction approach to be applied individually. The P&O control system follows the wind MPP effectively while adaptive P&Os are used to estimate solar MPP with variable disturbance step size.

Wind-P&O Control Scheme

The P&O scheme is the most common and easily controlled way to identify the MPP from non-linear wind characteristics. This algorithm controls the speed of the wind turbine generator (gene set.) to achieve the MPP; (Pwind). The SG speed is disturbed in the given direction while observing the force drawn from the SG. When the SG's power increases, it signifies that the SG gets stronger. The velocity of the SG must therefore be disrupted in the same way that the optimum operating point has gone toward the MPP. On the other hand, if the SG power decreases, the

optimal operating point will be moved away from the MPP, and the disruptive SG speed will need to be reversed now.

Solar-Adaptive P&O MPP Control

MPP approaches with a fixed disturbance are likely to oscillate. The control calculates the MPP operating point with a short circuit current product with an ideal constant proportionality. The perturbation step size tuning procedure is carried out based on irradiance level and operating point oscillations. This led to the naming of rough and fine tuning. The solar photovoltaic array controls the level of insolation of coarse tuning and its oscillation around the MPP determines fine tuning.
The widespread equation as,
$V=V(n)+sign\{V(n)-V(n-1)\}*sign(\Delta P)*\Delta V(n)$
In this case, the sign (•) sets +1 or -1 according to the value within the function. This control effectively traces the MPP under sudden changes in the level of insolation and reduces oscillations around the MPP by disturbing the step size.

B. GVSC Switching Control

The control system for the GVSC is presented in Figure.2.2. Use of MLMS-based adaptive control enables power-quality improvement and load-current distortion compensation in a time-invariant system with stochastic inputs like variable wind and solar conditions. This device is supplied with the GVSC switching pulses. This is the case when the least square algorithm progresses. MLMS can be easily managed for system conditions and parameter uncertainty. Adding "momentum" enables quicker convergence. It updates the weight according to the previous gradient without affecting the complexity of the system. This accelerates the convergence process and effectively compensates the load harmonics with noise-polluted inputs.

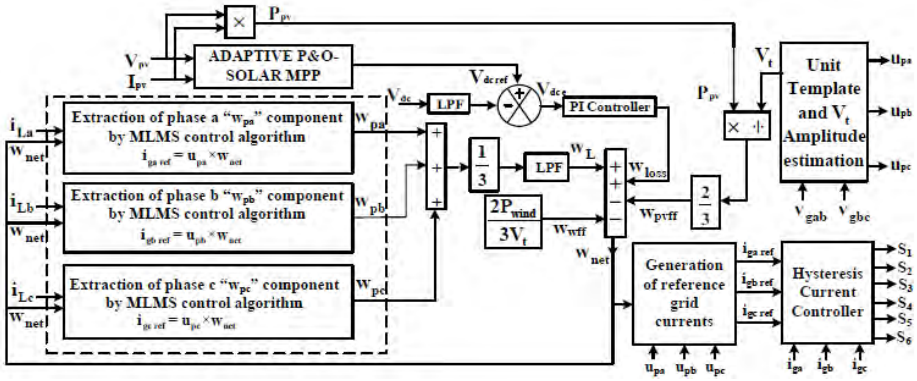

Figure 2.2. Control structure for GVSC.

MLMS Algorithm

The scheme of the MLMS algorithm is shown in Figure.2.3. LMS with previous weight vectors is updated to achieve the next weight vector. MLMS's second order update weight equation is as follows,

$$w(n+1) = w(n) + 2\xi e(n)x(n) + \alpha[w(n) - w(n-1)]$$

where, ξ is the step size controlling the convergence rate, α is the momentum factor that scales the gradient descent, and the working ranges are ξ>0 and α<0.

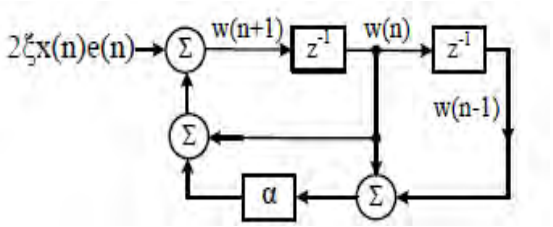

Figure 2.3. MLMS algorithm.

The derivation of the second order weight update equation of MLMS, is given as follows. The variables used are given as,

w(n) is the weight vector $= [w_0(n), w_1(n), \ldots, w_{M-1}(n)]^T$

e(n) is the output error $= d(n) - w^T(n)x(n)$

x(n) is the input signal $= [x(n), \ldots, x(n-M+1)]^T$

d(n) is the desired response and y(n) is the analogous estimate of d(n) and is given as,

$$y(n) = w^T(n)x(n)$$

The MLMS is the recursion of the weight increments and can be derived from the simplified implementation of conjugate gradient algorithm.

C. MVSC Switching Control

Figure 2.4 illustrates how to implement the MVSC control. The control system controls both the current direct reference axis (Id ref) generator and the quadrature-axis (Iq ref). The torque-producing component comprises two components: the square axis and torque-products. The wind-P&O MPP Scheme employs the benchmark generator speed to compare the SG speed (gen est) calculated by the benchmark BEMF Technology (gene ref) of the wind-P&O MPP scheme (gen ref).

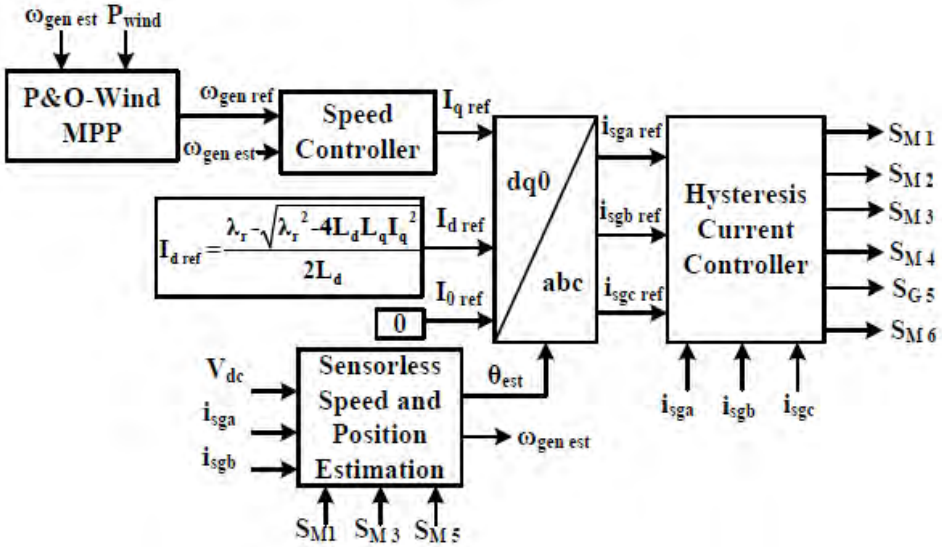

Figure 2.4. Control structure for MVSC control.

D. Bidirectional Converter Controller

Figure.5 shows how to control the bidirectional converter depending on a battery charge status (SOC). The battery reference current is generated using two methods (Ibat ref). Mode 1 is activated when the grid is connected. In Ibat ref, the maximum charging current is used, if the SOC is less than 100 percent. Ibat ref will be null if the SOC is 100% or higher. The battery is stopped charging. Mode 2 is enabled as soon as a grid breakdown occurs. Ibat ref is generated by feeding the DC link voltage mistake to the PI controller. The controller compares the reference battery to the sensed battery current (Ibat). Controller PI compared the reference battery to the sensed current battery (Ibat). Pulse width modulation (PWM) block gets the PI controller Output and generates buck (Sbu)-boot (SB) switching pulses.

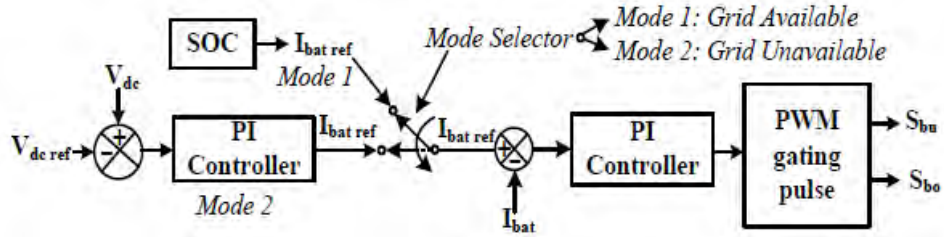

Figure.2.5 Control structure for bidirectional converter.

3. RESULTS

A. Steady State Behaviour of the Micro-grid:

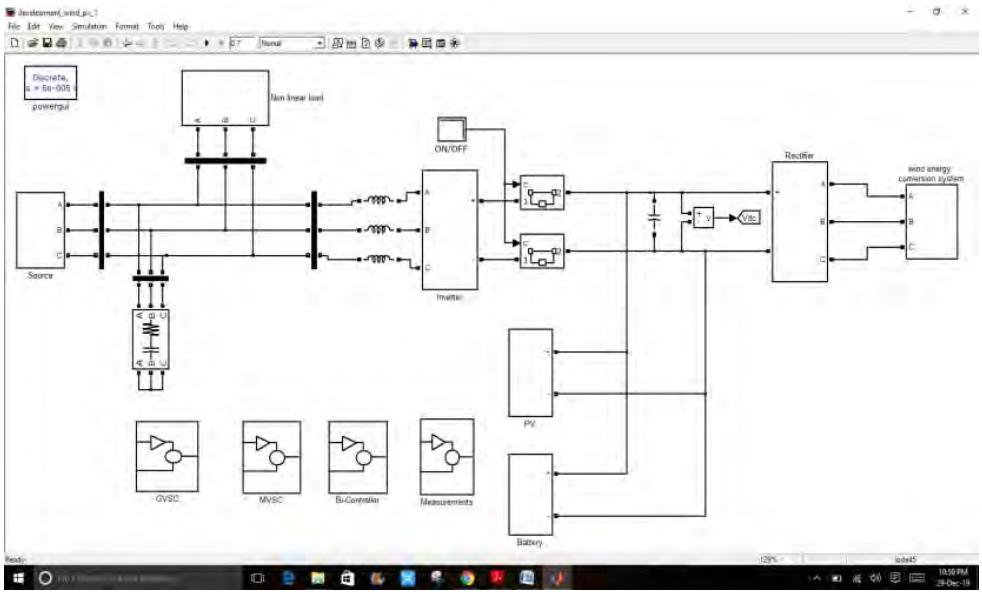

Figure.3.1- Simulation diagram of the micro-grid at steady state condition

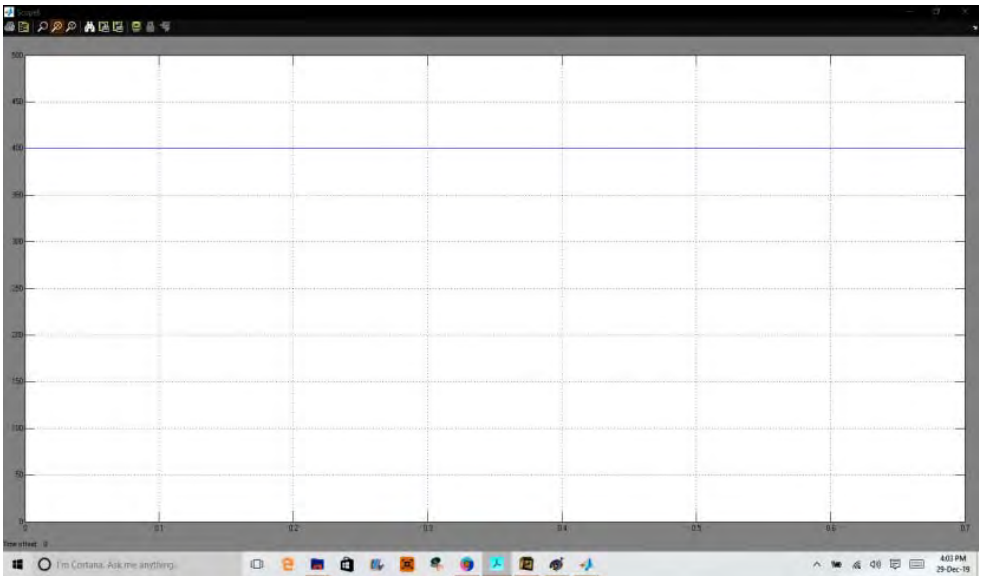

Figure.a- Vdc

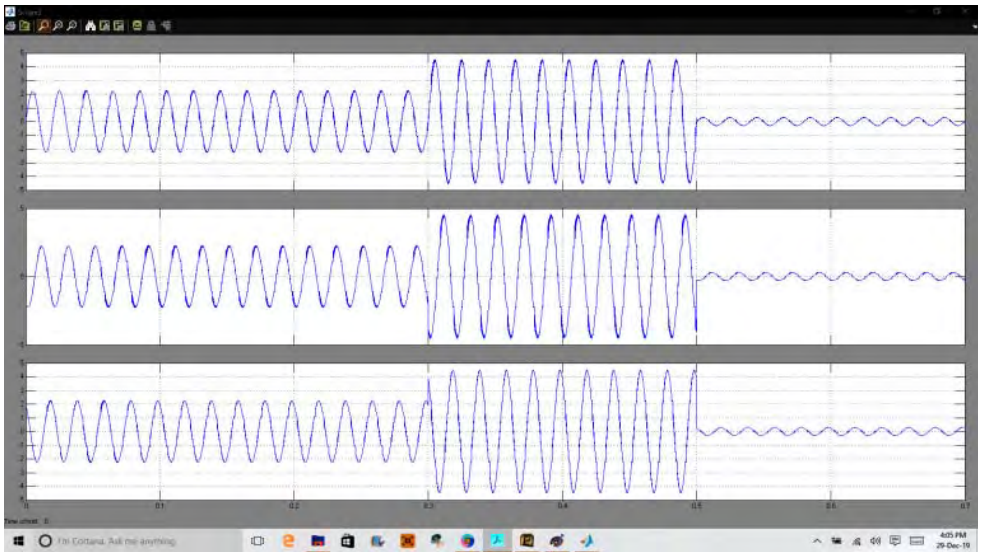

Figure.b- synchronous generator currents(isga, isgb, isgc).

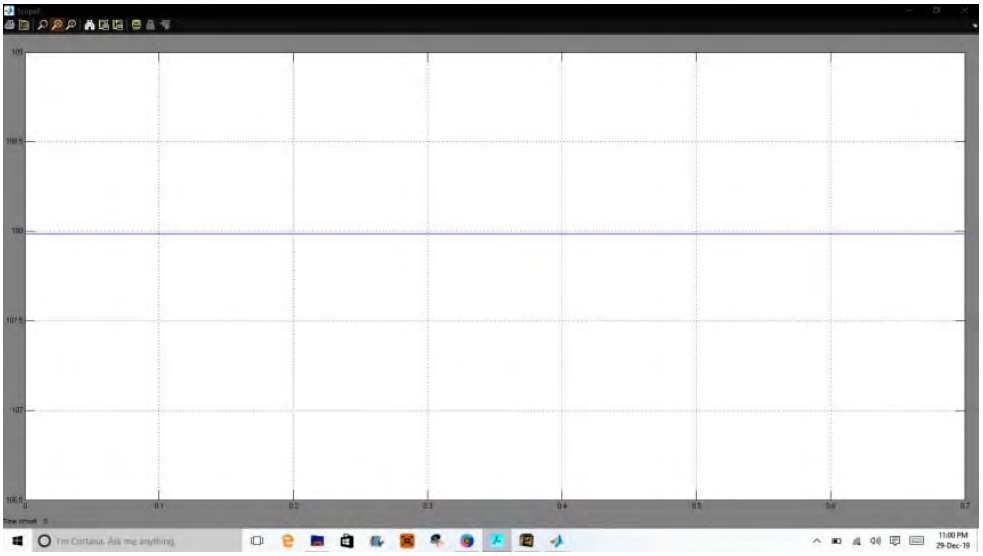

Figure.c- estimated speed (ωgen_est) of SG.

Figure.d- rotor position (θest)

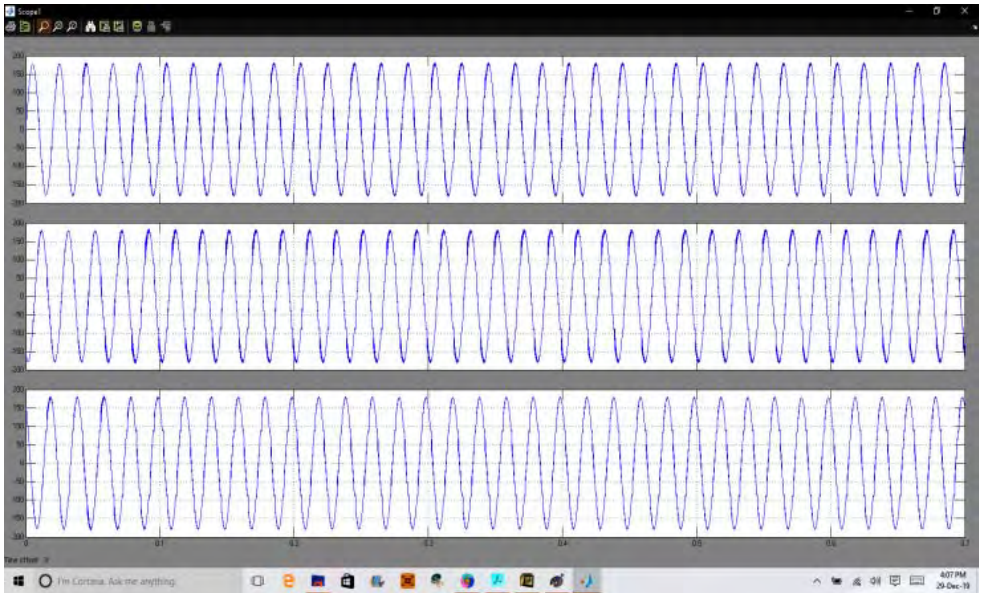

Figure.e- grid voltages

Figure.f- load currents

Figure.g- GVSC currents

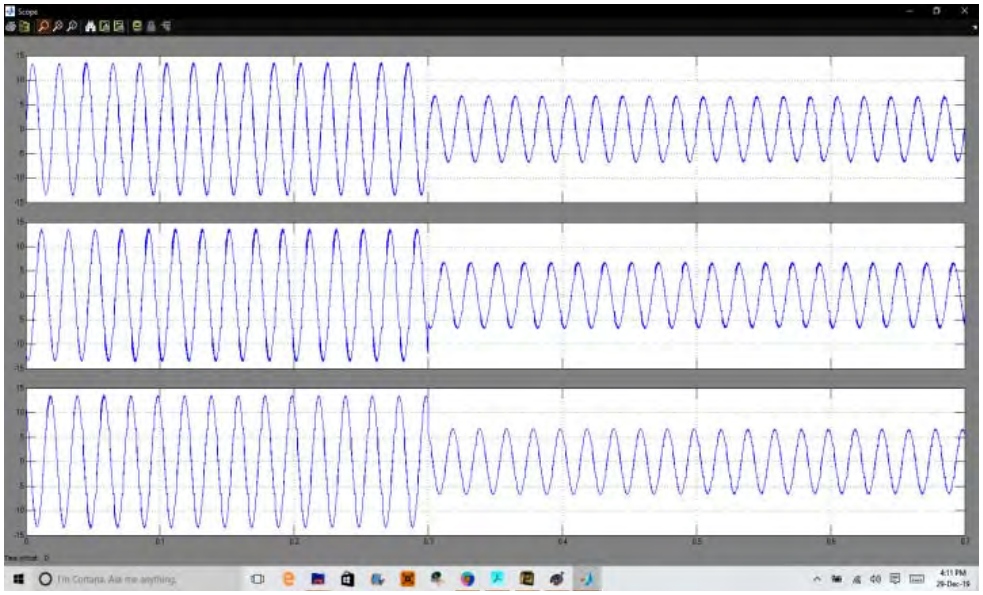

Figure.h- grid currents

The micro-grid performance is shown in Figure.6 in stable condition. The solar and wind power is considered to be in its rated condition and the bidirectional converter maintains the DC connection voltage. The generation from the wind powered SG is low with a low wind speed of 7.2 m/s and 12 m/s, and so the generated currents in magnetic dimensions are. The maximum SG generation is reached when the wind speed reaches cutting speed and can be observed in Figures (a-b). In the conditions mentioned above, the estimated speed (alongside SG), which changes according to the speed of SG and is depicted in Figures, is observed for deceleration and accelerating along with the period of rotor position (alongside) variety (c-d). There are harmonics in the load currents, while the grid currents are balance and sine. The GVSC currents, load currents and phase 'a' grid currents are shown in Figure (e,f,g). The system operates under DSTATCOM mode, when the SG powered by the solar and the wind turbines has nil, and the battery is off. The GVSC provides compensatory currents. The grids current is sinusoidal and undergoes phase reversal and are presented in Figure. (h).

B. Response of Micro-grid under Wind Speed Change:

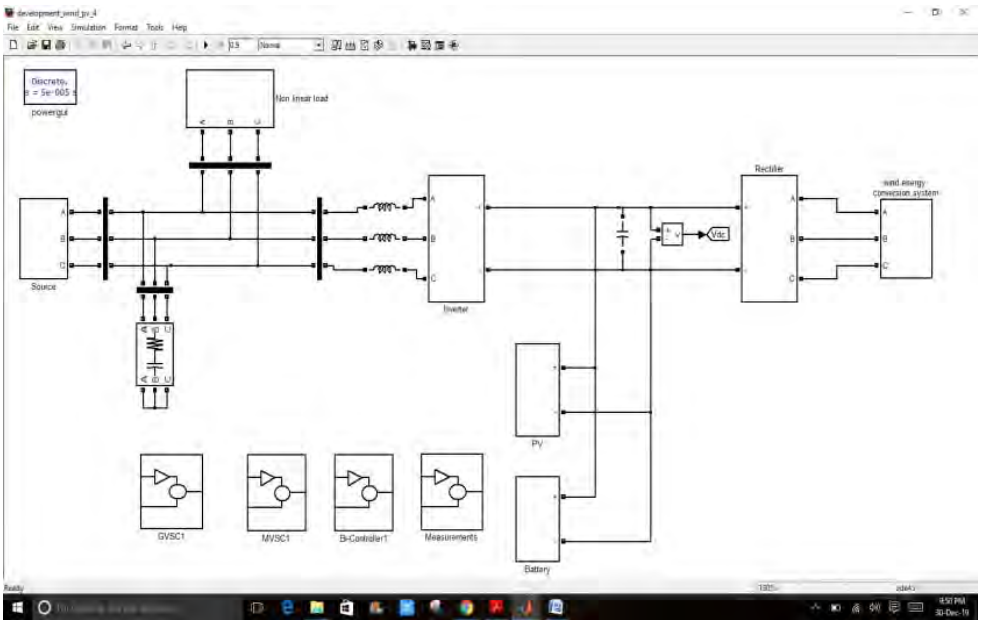

Figure.3.2- Simulation diagram of the micro-grid under wind speed change.

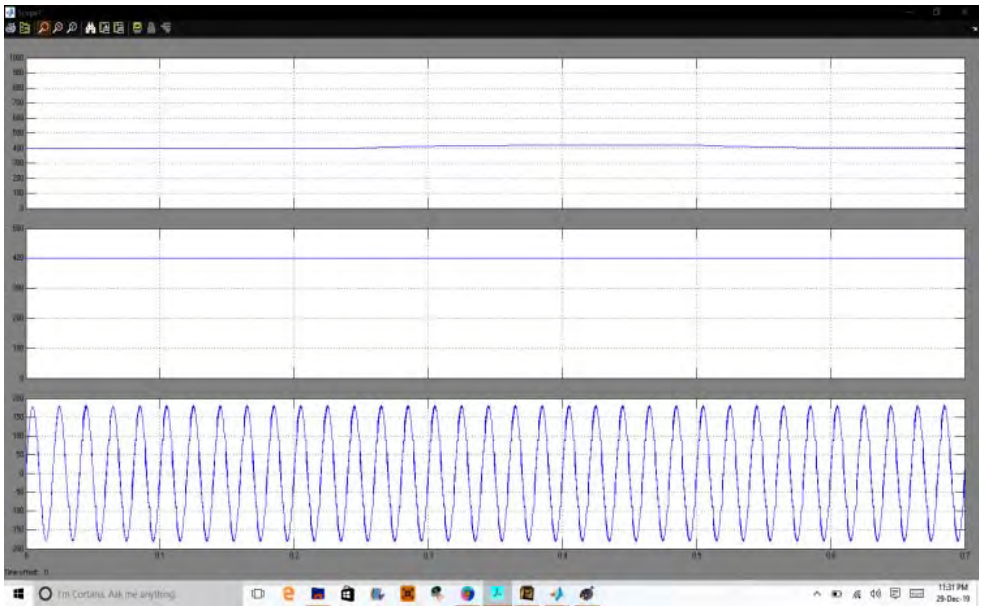

Figure.i- DC link voltage and the AC grid terminal voltage along with the grid voltage of one phase under wind speed rise and fall.

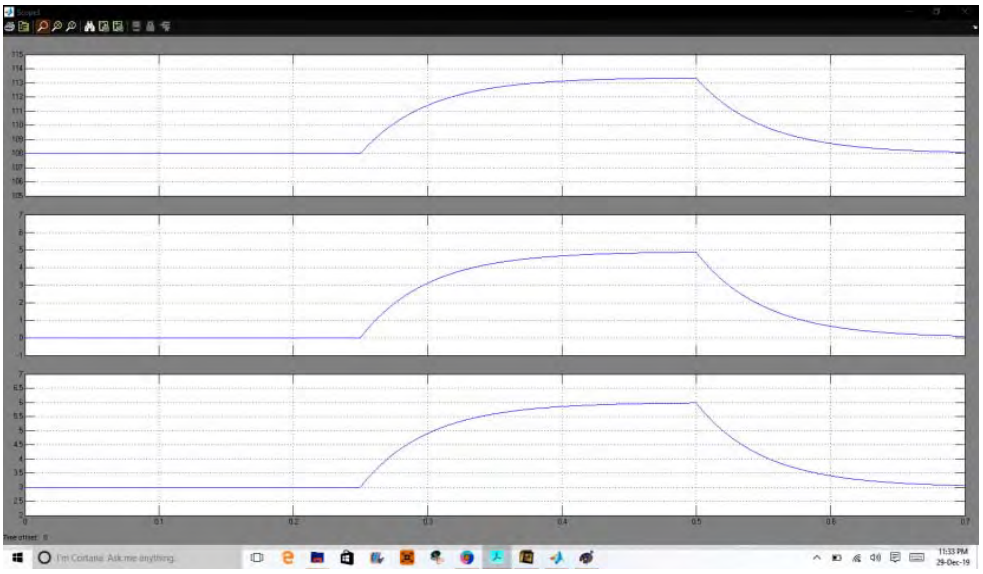

Figure.j- SG estimated speed, direct axis (Id) and quadrature axis (Iq) current.

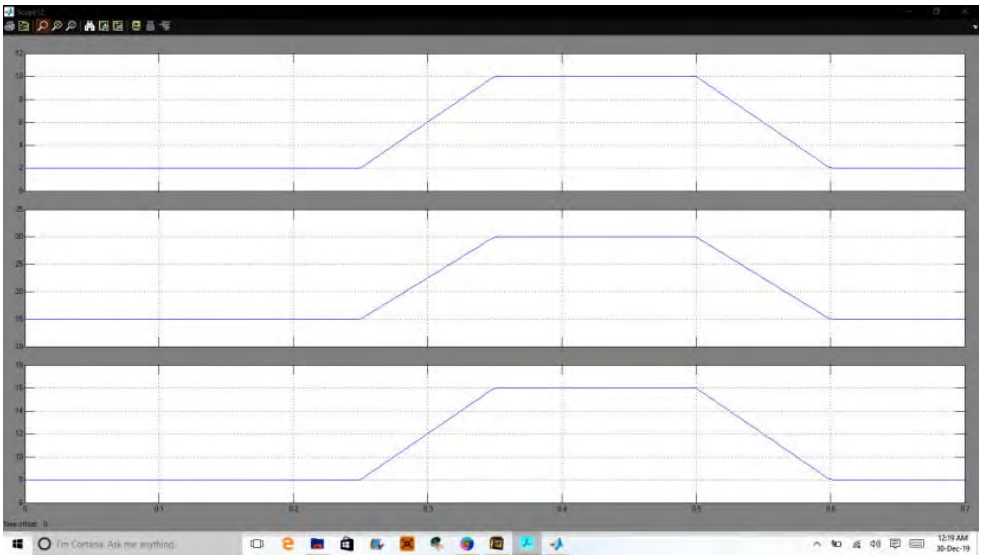

Figure.k- wind feed-forward component (wwff), DC loss component (wloss) and the total weight component (wnet).

The effects of the wind speed must be studied in order to ensure the correct operation of the micro-grid. In Figure. I, when wind speed rises and falls within a wind tunnel, the DC connection tension and a one-stage grid voltage are shown. The bidirectional converter control overcomes the transient voltage of the DC connection and keeps the DC connecting voltage constant. Figure (j) shows SG's estimated speed, direct axis (Id), and quadrature axis currents to show the effect of changes in wind speed (Iq). In Figurers Figure. (k), internal signal changes and the

variation in wind speed and no wind conditions are shown (k). Its size increases with the increase in wind speed as the generation of wind-powered SG increases. The DC loss part (wloss) and the weight component are simultaneously modified (wnet).

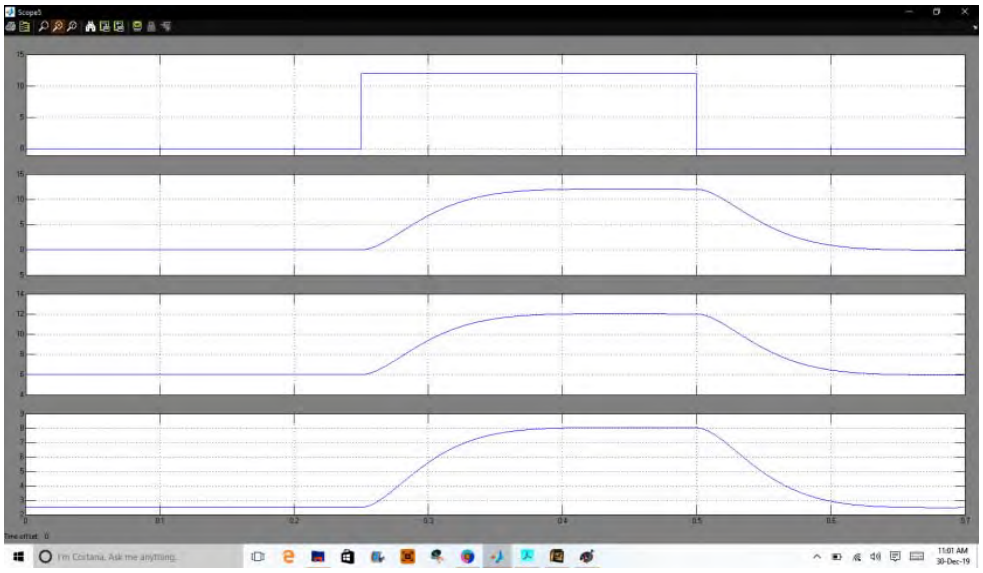

Figure.l- wind feed-forward component (wwff), DC loss component (wloss) and the total weight component (wnet).

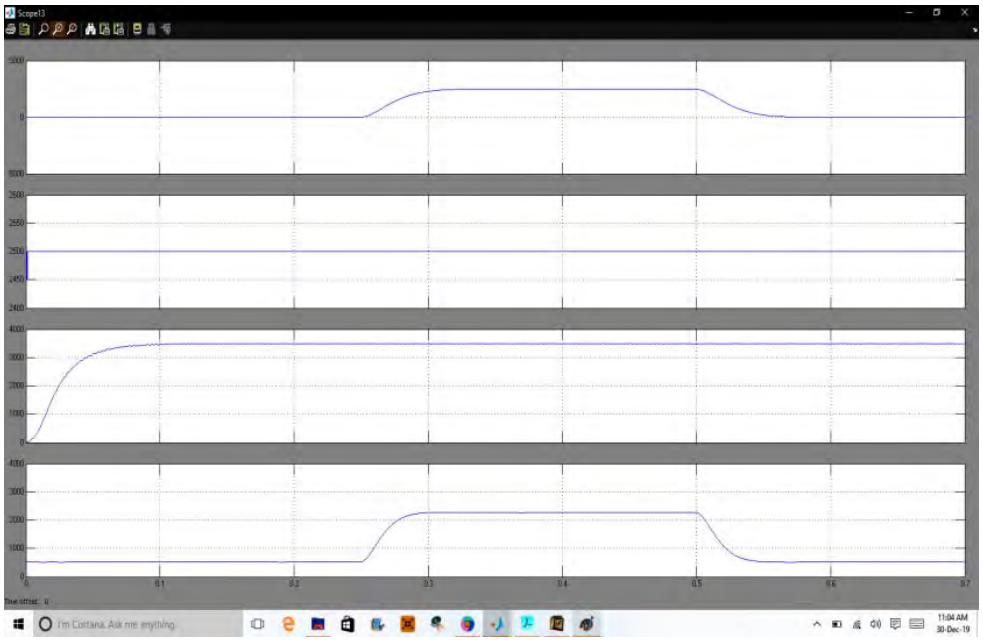

Figure.m- power variations of solar, wind, load and grid

The SG rate increases as the wind speed from 7.2m/s to 12m/s and the Id and Iq components of the SG current increase at the same time. The internal signal changes with

the change of wind speed and no wind conditions are present in Figures. (l). The wind power supply component (wwff) increases in magnitude as wind powered SG generation increases the wind velocity w.r.t. The DC loss (wloss) component and the overall weight component are changed simultaneously (wnet). If the wind velocity is 0, or wind velocity is 0 wwff. If the wind speed is less than that. Figures. (e) show the changes in power of the wind speed system.

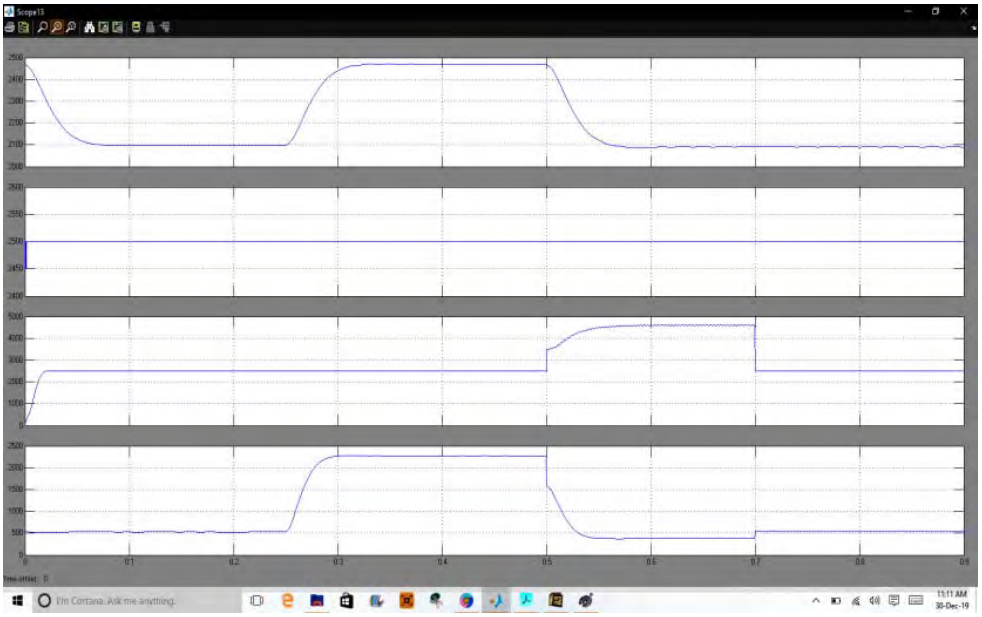

Figure.n- power variations when the load demand is increased and decreased.

In Figure n, you can see how power fluctuates as the load demand increases and decreases. There is a decrease in excess power fed into the grid when renewable energy generation reaches its rated value, and vice versa when the load demand rises.

C. Response of Micro-grid under Solar Insolation Change:

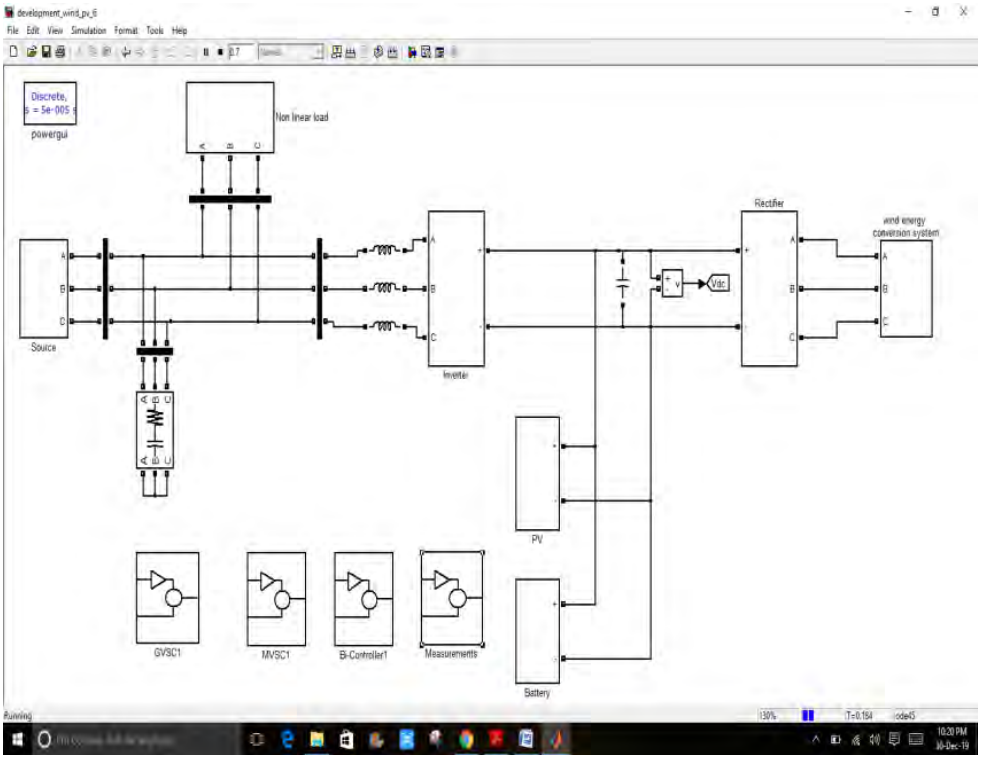

Figure.8- Simulation diagram of the micro-grid under solar insolation variation.

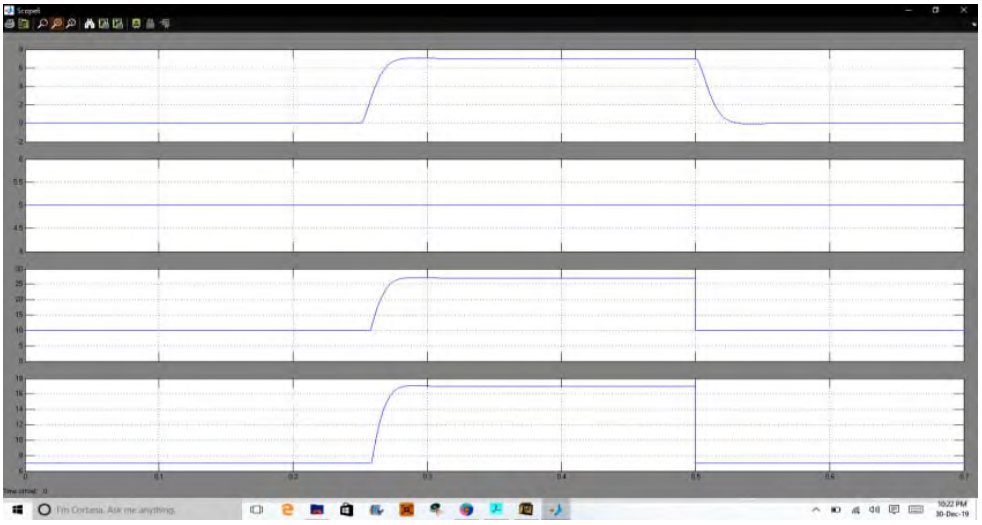

Figure.(o) internal signal variation.

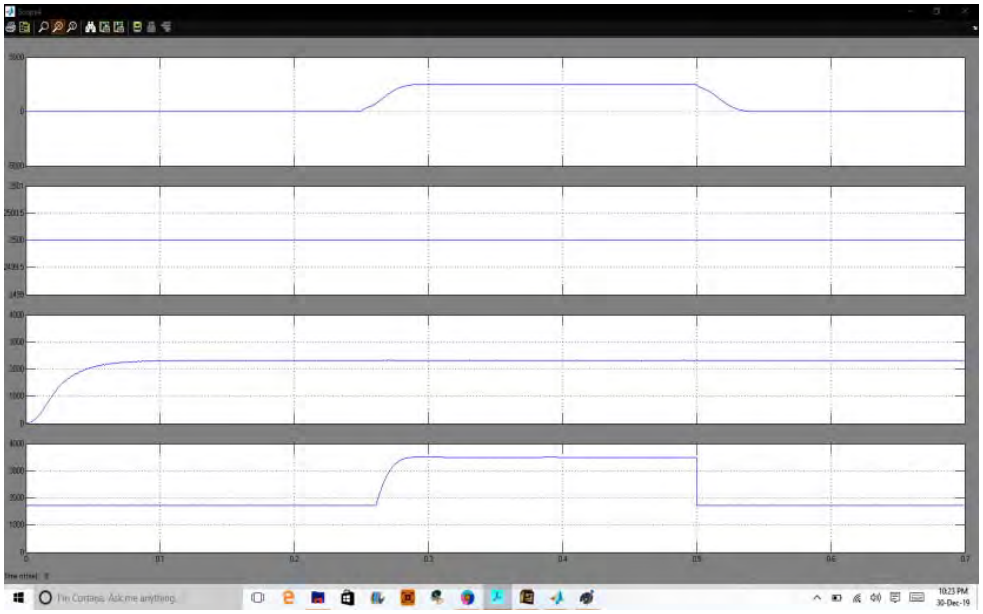

Figure.(p) Power variations.

The intensity of sunlight varies with time and is missing during the night. The performance of the micro-grid as solar insolation changes is shown in Figure 5. In line with changes to solar insolation, PV array current increases and decreases. The two-way converter control eliminates the transient voltage of the DC connector. The AC voltage of the grid is maintained sine quenched. As the Figure shows (o). If the solar insolation increases, the photovoltaic power supply (wpvff) is increased and at zero insolation. The load weight component does not change until wind, BES and grid generation meet the demand for load. Increases in wloss and wnet values can be observed at the same time. Figure (p) Shows how solar, wind, load and grid power vary with changes in the solar insolation. The micro-grid generates enough power to meet the load demand.

4. CONCLUSION

MLMS adaptive control is being used in wind-solar AC micro-grids to improve the power quality. A reduction in harmonics is necessary in the weight of the component and system, as well as in general system performance. The result was achieved by successfully removing the basic load current component with low static mistakes and fast convergence rates. In MATLAB Simulink, the prototype has been tested with wind speed and solar insolation from morning to night and variations in load from the domestic and medium-sized systems.

5. REFERENCES

[1] Y.-M. Cheng, Y.-C. Liu, S.-C. Hung, and C.-S. Cheng, "Multi-input inverter for grid-connected hybrid PV/wind power system," IEEE Trans. Power Electron., vol. 22, no. 3, pp. 1070–1076, May 2007.

[2] S. Yu, L. Zhang, H. H. C. Iu, T. Fernando, and K. P. Wong, "A DSE-based power system frequency restoration strategy for PV-Integrated power systems considering solar irradiance variations," *IEEE Trans. Ind.Informat.*, vol. 13, no. 5, pp. 2511–2518, Oct. 2017.

[3] M. A. Elhadidy "Performance evaluation of hybrid (wind/solar/diesel) power system. Renew Energy" 2002:401–13.

[4] P. Mochi, "Primary Review on MPPT Method and Size of Grid Connected Solar Photovoltaic Inverter," *2018 8thIEEE India International Conference on Power Electronics (IICPE)*, JAIPUR, India, 2018, pp. 1-6.

[5] S. Dasgupta, *et al.*, "A plug and play operational approach for implementation of an autonomous-micro-grid system," in *IEEE Trans. Ind. Informatics*, vol. 8, no. 3, pp. 615-629, Aug. 2012.

[6] K. Sarita *et al.*, "Power Enhancement with Grid Stabilization of Renewable Energy-Based Generation System Using UPQC-FLC-EVA Technique," in *IEEE Access*, vol. 8, pp. 207443-207464, 2020, doi: 10.1109/ACCESS.2020.3038313

[7] D. Gallo, R. Langella, A. Testa, J. C. Hernandez, I. Papic, B. Blazic, and J. Meyer, "Case studies on large PV plants: Harmonic distortion, unbalance and their effects," *IEEE Power & Energy Society General Meeting*, 2013.

[8] M. Farhoodnea, A. Mohamed, H. Shareef, and H. Zayandehroodi, "An enhanced method for contribution assessment of utility and customer harmonic distortions in radial and weakly meshed distribution systems," *International Journal of Electrical Power and Energy Systems*, vol. 43, pp. 222-229, 2012.

[9] X. Hou, Y. Sun, J. Lu, X. Zhnag, L. H. Koh, M. Su and J.M.Guerrero, "Distributed hierarchical control of AC micro-grid operating in grid-connected, islanded and their transition modes," IEEE Access, vol. 6, pp. 77388-77401, 2018.

[10] S. Boudoudouh and M. Maaroufi, "Renewable energy sources integration and control in railway micro-grid," IEEE Trans. Ind. Appl., Early Access, 2019.

[11] A. R. Millner, C. Smith, R. Jaddivada and M. Ilic, "Component standards for stable micro-grids," IEEE Trans. Pow. Sys., Early Access, 2018.

[12] A. Radwan and Y. Mohamed, "Grid-connected wind-solar cogeneration using back-to-back voltage source converters," IEEE Trans. Sustain. Energy, Early Access, 2019.

[13] S. Chattopadhyay, M. Mitra, and S. Sengupta, *Electric power quality*. West Bengal, India: Springer, 2011.

[14] S. Haykin, *Adaptive Filter Theory.* Englewood Cliffs, NJ: Prentice- Hall, 1986.

[15] B. Widrow and S. D. Stearns, *Adaptive Signal Processing.* Englewood Cliffs, NJ: Prentice-Hall, 1985.

[16] J. G. Proakis, "Channel identification for high speed digital communications," *IEEE Trans. Automat. Contr.,* vol. AC-19, pp. 916–922, Dec. 1974.

[17] S. Roy and J. J. Shynk, "Analysis of the momentum LMS algorithm," *IEEE Trans. Acoust., Speech, Signal Processing,* vol. 38, Dec. 1990.

[18] R. Sharma, W. A. Sethares and J. A. Bucklew, "Analysis of momentum adaptive filtering algorithms," *IEEE Trans. Signal Proces.*, vol. 46, no. 5, pp. 1430-1434, May 1998.

[19] B. Subudhi and R. Pradhan, "A comparative study on maximum power point tracking techniques for photovoltaic power systems," *IEEE Trans. Sustain. Energy*, vol. 4, no. 1, pp. 89–98, Jan. 2013.

[20] N. Femia, G. Petrone, G. Spagnuolo and M. Vitelli, "Optimization of perturb and observe maximum power point tracking method," *IEEE Trans. Pow. Elect.*, vol. 20, no. 4, pp. 963-973, July 2005.

[21] S. K. Kollimalla and M. K. Mishra, "Variable perturbation size adaptive P&O MPPT algorithm for sudden changes in irradiance," *IEEE Trans. Sustain. Energy*, vol. 5, no. 3, pp. 718-728, July 2014.

[22] J. F. G. Cobben, W. L. Kling and J. M. A. Myrzik, "Power quality aspects of a future micro grid," in *IEEEInternational Conference on Future Power Systems*, 2005

1

Investigation on Inverter Arc Welding Circuit

Nethra K, Bansilal Bairwa, Christina Sundari V Himabindu
k.nethra@reva.edu.in

School of EEE, REVA University,Bangalore, India 560064

Abstract

Arc welding is a type of welding process using an electric arc to generate heat to melt and join metals. A power supply produces an electric arc between a consumable or non-consumable electrode and the base material using either direct (DC) or alternating (AC) currents. Orthodox welding machines use grid frequency transformers to reduce the arc voltage to a lower voltage, then chopper circuit is used to adjust welding current. But grid frequency transformers are bigger and heavier than high frequency transformers. Thus, portability poses as a disadvantage in conventional welding machines. To solve the problem of weight and size of conventional arc welding machine, an inverter circuit was also developed. The inverter provided much higher frequency than 50Hz or 60Hz for transformers used in welding circuits. In this paper, we have proposed to develop an entire inverter section for an arc welding machine along with the necessary high frequency step-up transformer. The aim of developing the inverter circuit for an arc welding machine is to serve the foundation for developing weld machines based on the other available methods like Tig, CO2 etc. variables such as operating frequency, output voltage and current are the only factors in design.
Keywords: Arc welding, frequency transformers.

An Edited Volume, 1–6.

1.1 Introduction

Welding equipment has become one of the most important tools that a producer can possess hence the need to design and construct an inverter welding machine[1, 2, 3]. By introducing a PWM generator into the circuit control over the frequency of inverted output from the inverter section is achieved. The inverted output is stepped up to the arc required voltage using an appropriate step-up transformer[4, 5, 6]. In this paper, new onsite small scale inverter welding machines are designed and be used.

1.2 Methodology

The first objective is to calculate and design the entire circuit according to the flow of the block diagram and simulate the circuit on the Simulink program in MATLAB, followed by implementing the designed circuit on hardware and proceed further to obtain the arc parameters at the output.High Power MOSFETs (IRF9540) can switch over 60A and 30V and are TO-220 package. In this, the MOSFETs acts as switches in the inverter section to produce an alternating current controlled by a PWM generator. The SG3525A pulse width modulator control circuit offers improved performance and lower external parts count when implemented for controlling all types of switching power supplies. The output stage of the SG3525A features NOR logic resulting in a low output for an off-state.

- 8.0V to 35V operation
- 5.1 $V_{trimmed}$ reference
- 100Hz to 400kHz Oscillator range
- Separate Oscillator Sync Pin
- Adjustable Dead-time Control
- Input Under Voltage Lockout
- Latching PWM to prevent Multiple pulses
- Pulse-by-pulse shutdown
- Dual source/Sink outputs: -400mA peak
- Pb-free packages are available

A high frequency step-up transformer s used to step-up the voltage to an arc sufficient voltage from the outputs of the inverter section. Given that arcs in smaller scale welding takes place between voltages of 30 to 50V, a suitable transformer s selected based on the iput and output requirement. DC-DC boost converter is used to step up to higher voltage. PIC is a fam-

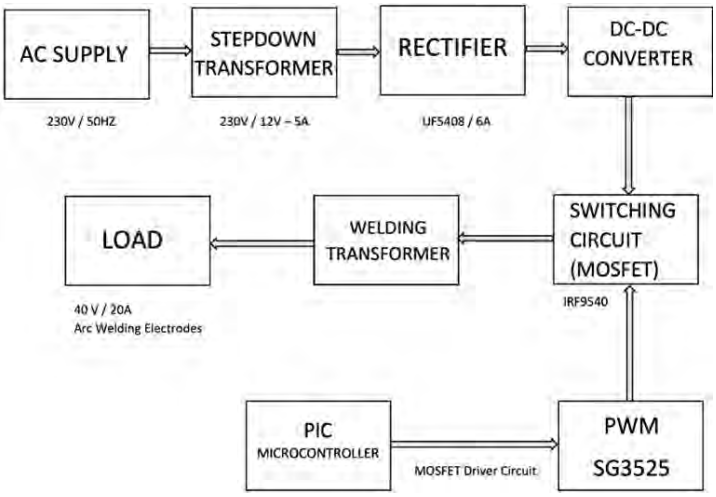

Figure 1.1 Block Diagram of Inverter Arc Welding Circuit [1]

.

ily of modified Harward architecture micro-controllers made by Microchip technology, derived from the PIC1650 originally developed by General Instrument's Microelectronics Division. The initially referred to **Peripheral Interface Controller**. This PIC micro-controller having a feature of high performance RISC CPU. Capacitors are used as filters in the power supply unit. The action of the system depends upon the fact, that the capacitors stores energy during the conduction period and delivers this energy to the load during the inverse or non-conducting period. In this way, time during which the current passes through the load is prolonged and ripple is considerably reduced [7, 8, 9, 10].

$$Switching\ frequency = \frac{1}{C_t * (0.7R_t + 3R_d)} \tag{1.1}$$

$$D = 1 - \frac{V_s}{V_o} * \eta \tag{1.2}$$

$$L = \frac{Vs_{min} * D}{F_s * \Delta I_L} \tag{1.3}$$

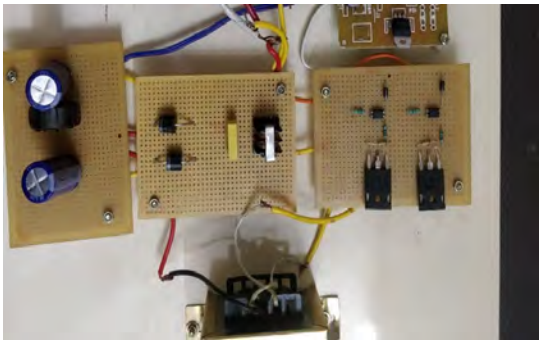

Figure 1.2 Hardware implementation of the filter circuit and Snubber circuit .

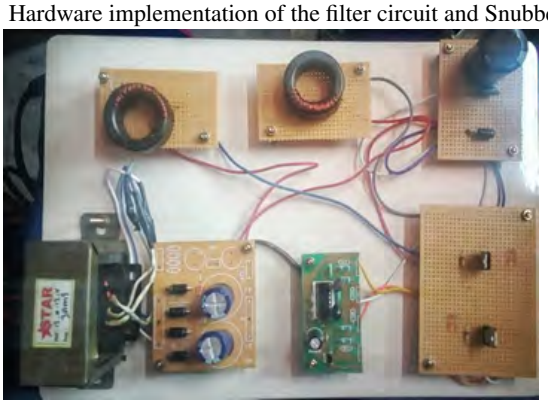

Figure 1.3 Hardware implementation of the inverter section along with the SG3525 IC .

Table 1.1 Parameters values adopted for this research

S.No	Parameters	Remarks
1.	Switching frequency	200 x 103 Hz
2.	C_t	0.1nF
3.	R_d	100 Ω
4.	F_s	200khz
5.	D	0.35
6.	C	10.93 μF
7.	L	9.85 μH
8.	I_0	2.5 A
9.	Load Resistance	16 Ω
9.	V_{in}	13 V

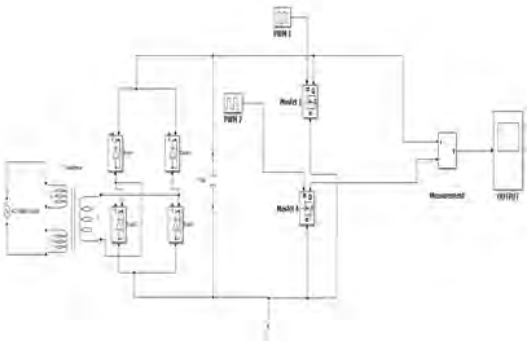

Figure 1.4 Block Diagram of Inverter Arc Welding Circuit.

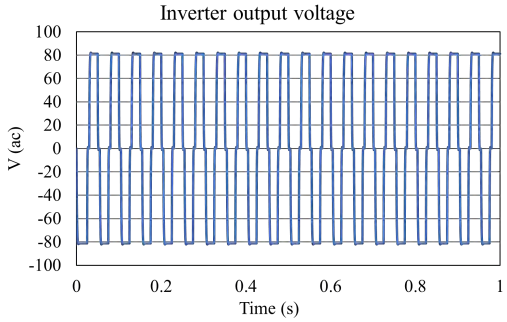

Figure 1.5 Simulation output for inverter.

1.3 Results and Discussion

We developed a MATLAB Simulink modelfor the welding inverter, along with a separate simulation of the DC-DC Boost converter section with parameters set almost equal to practical desired values. This work carried out simulation of an inverter along with full bridge rectifier circuit shown in Figure 1.4 Hardware implementation of the filter circuit and Snubber circuit as shown in Figure 1.2. Hardware implementation of the inverter section along with the SG3525 IC have been used in this work. Table 1.1 represents the parameters and their values adopted for this research.

1.4 Conclusion

By developing this inverter circuit we aim to implement it into an end user portable welding machine and also frame a cost effective product delivering the required job work to the user irrespective of availability of a power source

and place. However, since the circuit is a DC operated one, there comes into picture a frequent maintenance of the said battery. One of the proposed dc source that can be used for the machine is a 48v 100Ah battery, capable of sustaining welds for considerate amount of time. This however is subject to availability. In conclusion the proposed inverter circuit for use in application of an arc welding machine will prove to be propitious and constructive to its user. An introduction of an isolator circuit such as an optocoupler can be done for the protection of power components within the circuit. LCD displays can be used with the machines for ease of use and also detecting and monitoring faults in the system.

References

[1] Chae, Y-M., et al. "PWM converter-inverter arc welding machine using new type NCT." PESC 98 Record. 29th Annual IEEE Power Electronics Specialists Conference (Cat. No. 98CH36196). Vol. 2. IEEE, 1998.

[2] Navarro-Crespin, Alejandro, et al. "Digital control for an arc welding machine based on resonant converters and synchronous rectification." IEEE Transactions on Industrial Informatics 9.2 (2012): 839-847.

[3] Chae, Y-M., et al. "A new instantaneous output current control method for inverter arc welding machine." 30th Annual IEEE Power Electronics Specialists Conference. Record.(Cat. No. 99CH36321). Vol. 1. IEEE, 1999.

[4] Tschirner, Petra, Bernd Hillers, and Axel Graser. "A concept for the application of augmented reality in manual gas metal arc welding." Proceedings. International Symposium on Mixed and Augmented Reality. IEEE, 2002.

[5] Wu, Mingfei, and David Flynn. "An advanced gas metal arc welding machine design for low spatter welding." 2018 IEEE 27th International Symposium on Industrial Electronics (ISIE). IEEE, 2018.

[6] Wang, Jian-Min, and Sen-Tung Wu. "A novel inverter for arc welding machines." IEEE Transactions on Industrial Electronics 62.3 (2014): 1431-1439.

[7] Saraev, Yu N., et al. "Investigation of the stability of melting and electrode metal transfer in consumable electrode arc welding using power sources with different dynamic characteristics." Welding international 31.10 (2017): 784-790.

[8] Weglowski, M. S. "Investigation on the arc light spectrum in GTA welding." Journal of Achievements in Materials and Manufacturing Engineering 20.1-2 (2007): 519-522.

[9] Yudov, Dimitar D., Daniela J. Mareva, and Vencislav C. Valchev. "Investigation of Two-Stage Inverter Supply for Pulse Arc Welding." 2018 20th International Symposium on Electrical Apparatus and Technologies (SIELA). IEEE, 2018.

[10] Zhu, Jinhong, et al. "Investigation on control strategies for pulse gas metal arc welding process." 2008 3rd IEEE Conference on Industrial Electronics and Applications. IEEE, 2008.

ANFIS-BASED GRID-CONNECTED INVERTERCONTROL TECHNIQUE AIMED AT IMPROVING DYNAMIC PERFORMANCE IN MICROGRID SYSTEMS

Sudhakiran Ponnuru[1], Dr. Ashok Kumar.R [2], Dr. N.M.Jothi Swaroopan [3].
Research Scholar,[2]Professor,Department of Electrical Engineering, Annamalai University, Chidambaram, Tamilnadu, India
[3] professor ,Department of Electronics and Instrumentation Engineering, RMK Engineering College, Chennai, Tamilnadu, India

Email:sudhakiranannamalaiphd17@gmail.com,ashokraj_7098@rediffmail.com, jothi.eee@rmkec.ac.in

Abstract

A micro-grid interfacing converter with multi-control is proposed here. It offers a multi-objective control technique for grid interlinked converters using an ANFIS controller. The controller under consideration uses the combined characteristics of controllers based on fuzzy logic and the structure of Neural network to substantially enhance reaction of the grid-connected converter under system disturbances. In the proposed method, the ANFIS controller's control settings are dynamically modified depending on the Sugeno control system's operational circumstances. As a consequence, it responds quickly to disruptions with slight error and settling duration. The GCI is utilized to offer many additional functions related to the proposed multi-objective control system. The suggested controller's predictive response is shown through MATLAB simulations is efficient than an AFPI controller during interruptions. The case studies and results of the suggested system are also compared to literature to verify the controller's effectiveness

Keywords Micro grid Grid Interconnected Converter ANFIS controller Power Quality Fuzzy-logic Controller

1. INTRODUCTION

Today's electricity is transitioning to a new era, with a high renewable generation incorporated into the distribution network through distributed energy resources [1], [2]. Grid-Connected Inverters (GCI) are often used to connect generating units to the utility grid. One of its main responsibilities is to deliver all active energy into the system. However, because to the scarcity and environment of renewable sources and market price concerns, It is possible that generating units will be unable to provide the rated actual power to the grid. As a result, the grade of converters is often underutilized. The GCI's unused apparent power rating may therefore be utilized for several additional functions. [3],[4]. However, the growing use of converter-based generating units and non-linear loads in the distribution network affects power quality (PQ). Renewable energy source units, critical and valuable local loads affect the power quality. Poor PQ will affect the on-grid energy price in PQ-sensitive markets [5],[6]. Various control methods for renewable generating sources connected to the electric grid have been suggested [7,8]. The electric grid's power quality is guaranteed via controlling equipment or a GCI with multipurpose capabilities. [9],[10]. Adding controlling equipment to

solve the PQ issue raises system costs, perhaps unfeasible for low-voltages. A GCI with multifunctional capabilities has recently been suggested to solve this issue[11],[12].A current regulated voltage-source inverter (VSI) is used to link generating sources to the grid side place of point of coupling connection (PCC)[13],14]. The most often used current controllers for GCIs are PR, PI, and hysteresis controllers [15]. Every existing control method has benefits and drawbacks. In [16], [17], with the help of an optimization method based on grey wolf, the switches of the high-speed step-up converter are activated. The performance of the new controller is compared to that of a standard Controller based on particle swarm optimization. [18]. The use of fixed gain linear controllers Literature also describes PI/PID controllers with synchronous rotation (dq0) for regulating GCI.The literature mentions several PI controller versions to solve operating point issues (as well as the inclusion of a grid voltage feed forward link, control with many states of feedback)It increases the bandwidth of the PI controller. But it will test the system's stability. Because PI, PID, and PR controllers are neither intelligent nor adaptable, researchers have turned to intelligent methods like Neuronal networks, fuzzy logic, and evolutionary algorithms to regulate GCIs. The fuzzy logic-based supervisory control system continuously modifies the PI controller's gains depending on the operating conditions described in ref [19]. The APFI controller cannot effectively minimize disturbances during rapid load changes, and enhance settling time and overshoot.[20] controls a bidirectional converter with a battery storage depending on the microgrid's voltage to address generation and load issues. A proportional-integral controller is utilized with a selector-based control method. In [21], a control method for renewable source with hybrid storage units is used. A second harmonic phased locked- loop (PLL) is used to synchronize/resynchronize the micro-grid system in emergencies. An adaptive power management algorithm efficiently operates and manages the micro-grid system in both modes. [22] Implements consensus-based control for storage units in a DC micro-grid using a serially connected multi-input converter. The serially connected multi-input converter contains two phases, one for super-capacitors and the other for batteries. [23] Developed an adaptive droop control technique that adjusts the droop settings based on mathematical computations. The adaptive droop controller was designed to enhance the low-voltage DC microgrid's performance by balancing load sharing and voltage regulation. [24] Uses adaptive control methods for a single-stage PV based battery management system. It is linked to a micro-grid that uses maximum electricity. Two batteries and Superconducting Magnetic Energy storage (SMES) systems combined PV - Wind DC-bus micro-grid is evaluated in [25], [26].

This work proposes an ANFIS controller to regulate the GCI. A Sugeno type fuzzy model is implemented for the ANFIS controller. The Sugeno type fuzzy model is the combination of fuzzy and neural network. As a consequence, it is easier to calculate and adjust than the Mamdani type fuzzy model.The ANFIS quickly detects changes in system circumstances and dynamically adjusts the

output control signal. Because of this, the control mechanism mandates to operate in a linear zone under all operating circumstances, minimizing overshoot, oscillations, and settling time. In addition to its fundamental duty of adding active electricity into the grid at power factor equal to 1, the GCI is regulated to offer various auxiliary services. Correcting reactive load demand, disturbed load and neutral current. All are accomplished with fewer membership functions and rules than mamdani-type models, resulting in reduced computation costs. The system is modeled in Matlab. The suggested controller's efficiency is validated by comparing the results to the existing literature.

2. SYSTEM DESCRIPTION

Figure 1 shows the DG linked to a three phase four conductor generating system through a various operational GCI. A tri-phased tri-limbed, two-level inverter is implemented. The renewable generating source is powered by the dc-link (PCU). Decoupling renewable generating sources from the power grid is achieved using dc-link capacitors ($C_{dc1}$and C_{dc2}) [4]. The GCI's output connects to the utility grid via an LCL filtering circuit. To attenuate resonances, $R_d$is linked in series withC_f. Loads are linked to the PCC with both balanced and unbalanced

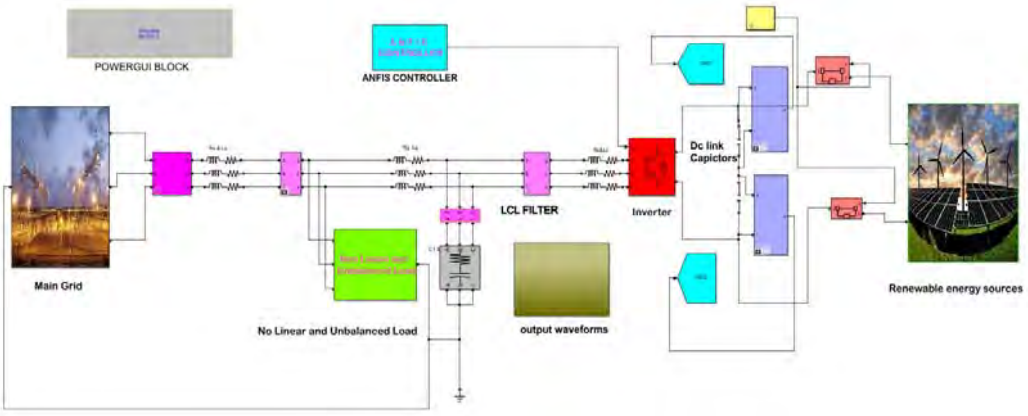

Figure 1. Schematic Diagram of Proposed System.

3. CONTROL SCHEME

The proposed multi-objective controls approach seeks to introduce DG active energy into the utility grid. Controlling load reactive energy requirement, current harmonics, neutral current, and unbalanced currents, are all regulated concurrently by the GCI to guarantee grid current is controlled in all operating circumstances with minimal THD, with IEEE standards. Operating like an active power filtering device, the GCI only provides additional services if zero DG's output. To accomplish the aforementioned objectives, appropriate reference current must be retrieved.

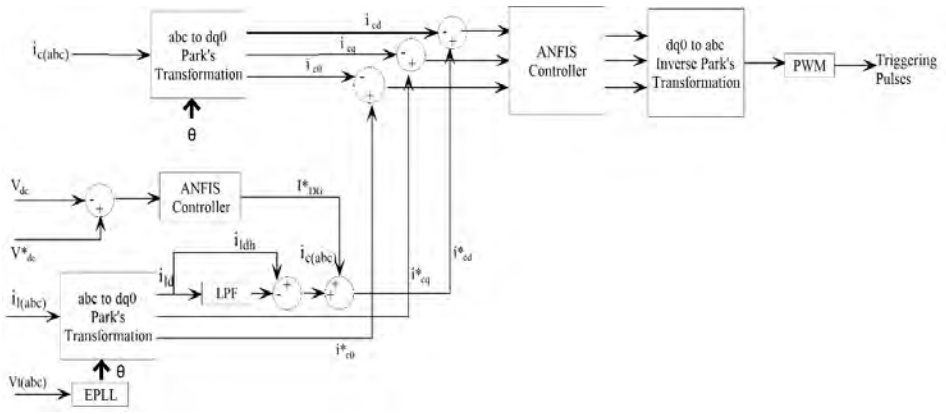

Figure 2. Control Scheme of the System

On the other hand, dc-link voltage and GCI output current are used to compute reference current. All control methods are implemented in the dq0 frame [12]. The enhanced phase locked loop (EPLL) supplies the reference angle (θ) for the dq0 transformation. to regulate the DG units produce active current i^*_{DG}, the difference between i^*_{cd} and i_{ldh} is done

$$i^*_{cd} = i^*_{DG} + i_{ldh} \tag{3.1}$$

To modify the full load side reactive power requirement, the load current's q-axis component (i_{lq}) shows the load's reactive power requirement. Thus, the GCI's q-axis reference current is represented by Eq (2). The 0-axis component additionally compensates for imbalanced load current. Equation (2) therefore sets the GCI's 0-axis reference current. Finally, the current controller produces switching signals for the GCI based on the change in the required current (i^*_{cdq0})) and the actual current (i_{cdq0}).

$$i^*_{cq} = i_{lq}; i^*_{c0} = i_{l0} \tag{3.2}$$

3.1 Implementation of standard AFPI controller

AFPI controller has a nonlinear adaptive control method that provides stable control performance in the face of unknown system characteristics [27–28]. Mamdani type Fuzzy controller is used to track the PI controller gain values.

4. PROPOSED ANFIS STRUCTURE.

The performance of an ANFIS controller is compared to that of a conventional AFPI controller. It explains how to create an effective transient performance for the proposed system with minimum overrun and clearing time.

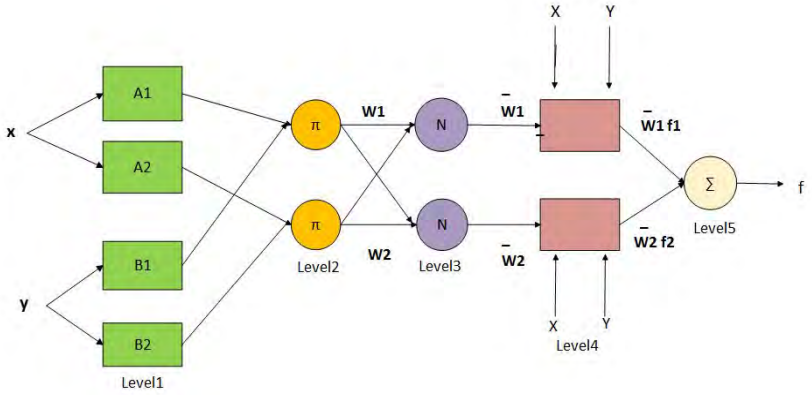

Figure 3. Type-3 ANFIS Structure

The exterior and interior current loops, which are hierarchical control loops, govern GCI. Inner control loops respond faster than outward loops for smooth system operation. As a result, the bandwidth of the inner control loop is enhanced.

Takagi and Sugeno's type-3 fuzzy inference technique is utilized here. Each rule's output is a linear combination of the input variables plus a constant term. In the final output, each rule's output is weighted. Fig. shows the comparable ANFIS structure..

The following sections explain the different levels of this ANFIS structure:

Level1: In this level, every hub I is versatile and has a hub work..

$$O_i^1 = \mu_{Ai}(x) \tag{4.1}$$

x is the hub I input, Ai is the arbitrary worth connected with this hub capacity, and Ai will be Ai's enrollment work. Commonly, Ai(x) is chosen as

$$\mu_{Ai}(x) = \frac{1}{1+\left[\left(\frac{x-c_i}{a_i}\right)^2\right]^{b_i}} \tag{4.2}$$

x is the information and ai, bi, ci signifies the reason boundary set

Level2: Each hub in this level is a decent hub that figures the terminating strength dependent on a standard.

Every hub's yield is the result of every approaching sign and is given by,,

$$O_i^2 = \omega_i = \mu_{Ai}(x) \times \mu_{Bi}(y), \quad i = 1,2 \tag{4.3}$$

Level 3: In this level, each hub is a decent hub. Each ith hub processes the proportion of the ith rule's terminating solidarity to the all out of every one of the standards' terminating qualities. The ith hub's yield is the standardized terminating strength given by

$$O_i^3 = \overline{\omega_i} = \frac{\omega_i}{\omega_1 + \omega_2}, \quad i = 1,2 \tag{4.4}$$

Level 4: In this level, every hub is a versatile hub with a hub work characterized by

$$O_i^4 = \overline{w}_i f_i = \overline{w}_i (p_i x + q_i y + r_i), \; i = 1,2 \tag{4.5}$$

wi is the Level 3 result and pi, qi, ri is the subsequent ensuing variable data

Level 5: This level has just single steady hub that produces the all out yield as the all out of all signs got, for example.

$$O_i^5 = \text{overall output} \sum_i \overline{w_i} f_i = \frac{\sum_i w_i f_i}{\sum_i w_i} \tag{4.6}$$

5. SIMULATION RESULTS AND DISCUSSION.

Here are the case studies in this simulation research. The DG unit's output power is set zero till t = 0.1 s. From t = 0.1 to 0.7 Sec, the DG can only produce 18 kW. The DG output increases from 0.7 to 1.25 sec to 27.5 kW. The load demand is 8.5 kW from t = 0 to 0.4 Sec. In this range, the load demand rises to 23.5 kW. 1 to 1.25 sec reduces the load demand to 18 kW.

5.1. Case: 1when load is constant

Its Simulink architecture is shown in Fig 1 and its specifications are listed in Table 1. Fig. 4compares converter and grid active powers with PI, AFPI, and ANFIS controllers. Fig. 5 shows the waveforms of Grid Current, and converter current at t=0.1. As shown in fig.8, ANFIS controller eliminates harmonics better than PI and AFPI controller. Data on GCI Active Power Dynamic Response are in Table 2.

Table 1. Simulation system parameters

S.No	Simulation Parameters	Values
1	Voltage at Grid, Frequency	400V (L-L), 50 Hertz
2	Input DC Bus Voltage, Capacitance	700 Volts, 15 milli farad
3	LCLfilter	R_C= 0.05 Ohms; R_G = 0.15 Ohms; R_D = 1 Ohm Lc = 0.214 mh; C_F= 100 micro farad; L_G= 0.145 mH
4	Non Linear Load Parameters	3 Phase: R = 50 Ohms,L = 50 mH; 1 Phase: (A-n): R = 50 Ohms, L = 50 mH; (B -n): R = 50 Ohms, L = 50 mH;
5	RES Input power Capacity	21KW

Table 2. Dynamic responses of GCI Active power with various controllers

GCI Active Power	PI Controller	AFPI Controller	ANFIS Controller
Peak Overshoot	20000	19000	18900
Settling Time	0.24	0.2	0.18
Rise Time	0.109	0.1055	0.102

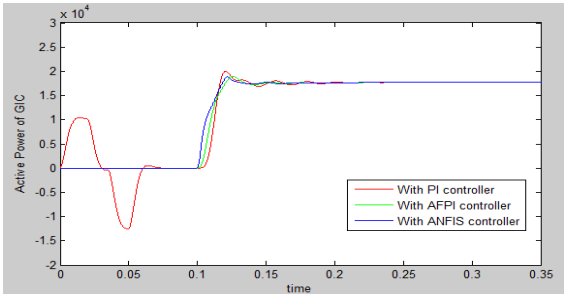

(a)

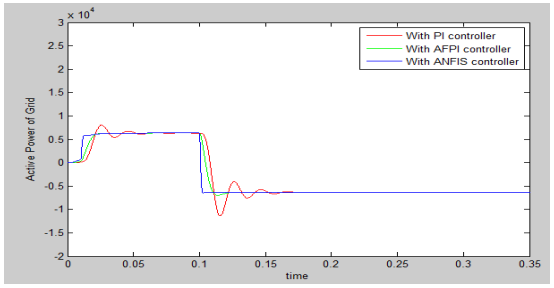

(b)

Figure 4. (a) Converter active Power (b) Grid Active Power

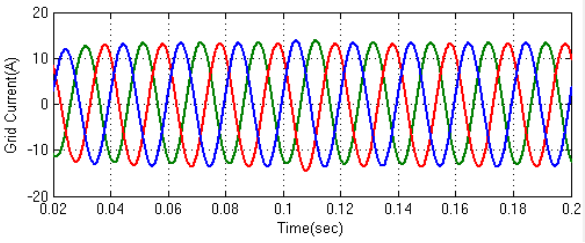

(a)

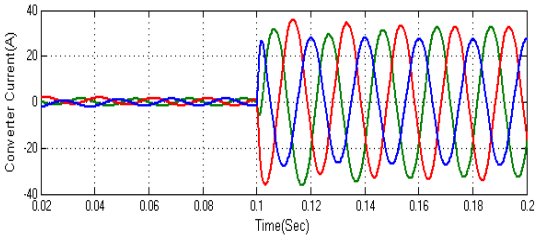

(b)

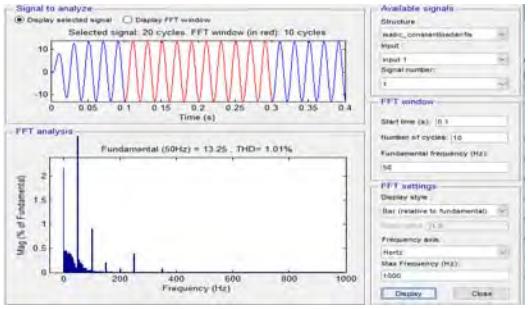

(c)

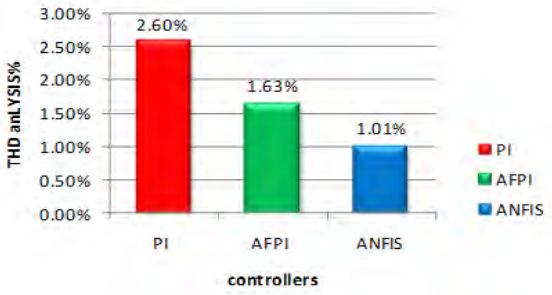

(d)

Figure 5. During constant Load (a) Grid Current (b) converter current (c) ANFIS THD Analysis (d) Comparison Graph

5.2. Case2: Load changing Conditions

In this instance, the starting load is 8.5 kilowatts, which is raised to 23.5 kilowatts between time= 0.4 and 1 sec. Later, the load is reduced to 18 kilowatts. Fig. 6 compares converter and grid active powers as well as DC link voltage for all controllers (PI, AFPI and ANFIS). Fig. 7 shows the proposed ANFIS controller's system responses such, Grid current, and converter current. The suggested controller shows improved dynamic responsiveness to unexpected load fluctuations. Table 3 shows the THD values for grid current under constant and changing load circumstances. Table 4 shows the DC link voltage dynamic response under various load conditions.

Table 3. Grid current THD values with various controllers.

Grid Current THD	**PI Controller**	**AFPI Controller**	**ANFIS Controller**
During Constant Load	2.60%	1.63%	1.01%
During Load Changing Condition	3.43%	2.04%	1.20%

Table 4. Dynamic responses of DC link voltage with various controllers.

DC link Voltage	**PI Controller**	**AFPI Controller**	**ANFIS Controller**
Peak Overshoot	710	703	700.012
Ripple %	2.57%	0.71%	0.0031%

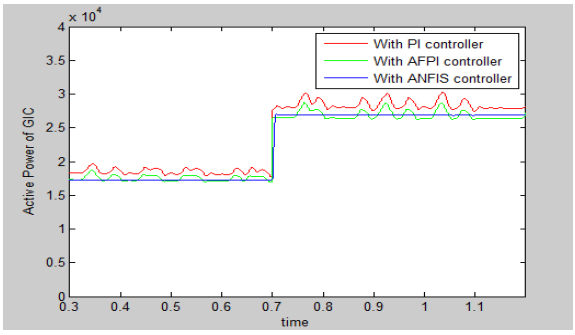

(a)

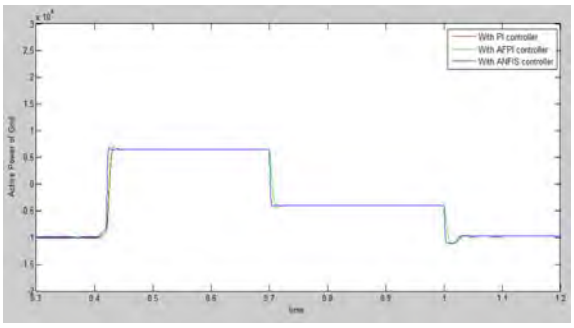

(b)

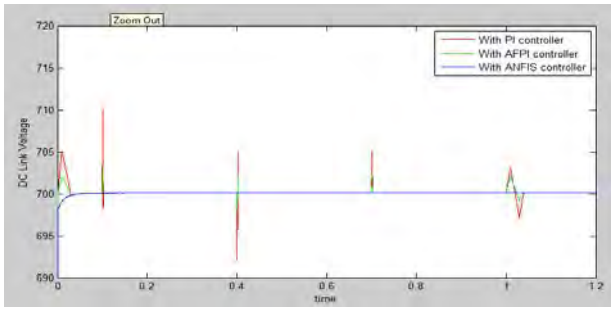

(c)

Figure 6. (a) Converter active Power of Grid (b) Active Power of Grid (c) DCLink voltage

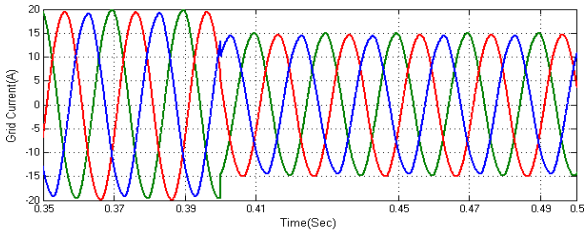

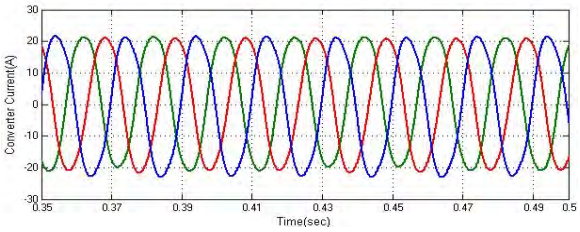

(a) (b)

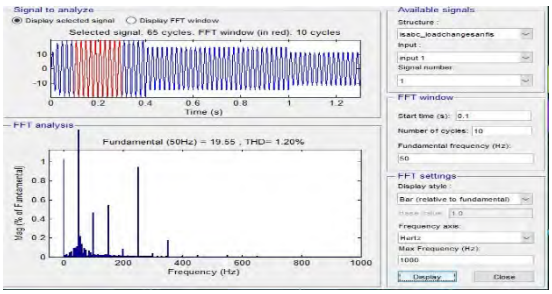

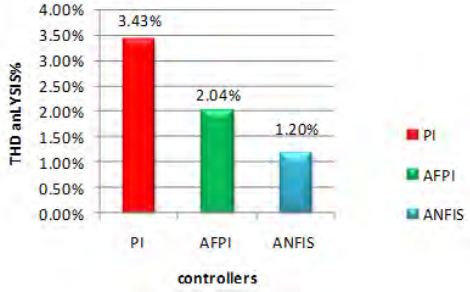

(c) (d)

Figure 7. During Variable Load (a) Grid Current (d) Converter Current(c) ANFIS THD Analysis (d) Comparison Graph

6. CONCLUSION

The above research proposed a multi-target GCI control using an ANFIS controller. The proposed control method successfully enhanced the AFPI controller's basic structure and the FLC's resilience to a range of uncertainties. The suggested multi-target control method utilized GCI to inject active electricity from generating units into the utility grid. At the same time, reduction of harmonics in load current, reactive power control, unequal and neutral control of currents were measured. The grid current was, therefore, nearly balanced in all operating situations. The ANFIS models are also faster than AFPI designs. Matlab/Simulink simulation tests were used to assess the effectiveness of the suggested controller. The controller's performance is evaluated in a number of scenarios, and its accomplishments are as follows: 1) The Grid current THD is reduced to 1.2% during the dynamic condition. 2) GCI active power settling time is minimized to 0.18 sec compared to AFPI's 0.24 sec. 3) The DC link voltage

ripple is reduced with less overshoot. The recommended controller outperformed the AFPI Controller in all circumstances, with lower overhead and faster adjustment times. The IEEE standards were met while reducing THD of current at grid side.

ACKNOWLEGDEMENTS

The author thanks Annamalai University for providing support and necessary infrastructure for completing this research

REFERENCES

[1] G. Pepermans, J. Driesen, D. Haeseldonckx, R. Belmans, W. D'haeseleer,"Distributed generation: definition," benefits and issues, Energy Policy 33 (6)(2005) 787–798.

[2] Q.N. Trinh, H.H. Lee, "An enhanced grid current compensator for grid-connected distributed generation under nonlinear loads and grid voltage distortions," IEEE Trans. Ind. Electron. 61 (12) (2014) 6528–6537.

[3] J. He, Y.W. Li, M.S. Munir, "A flexible harmonic control approach through voltage-controlled DG–grid interfacing converters," IEEE Trans. Ind. Electron.59 (1) (2012) 444–455.

[4] M. Singh, V. Khadkikar, "A. Chandra, R.K. Varma, Grid interconnection ofrenewable energy sources at the distribution level with power-quality improvement features," IEEE Trans. Power Deliv. 26 (1) (2011) 307–315.

[5] P. Li, X. Yu, J. Zhang, Z. Yin, "The control method of grid-tied photovoltaic generation," IEEE Trans. Smart Grid 6 (4) (2015) 1670–1677

[6] IEEE Application Guide for IEEE Std 1547, "IEEE Standard for Interconnecting Distributed Resources with Electric Power Systems" IEEE Std 1547. 2-2008.

[7] M. Mehrasa, E. Pouresmaeil, B.N. Jorgensen, J.P.S. Catalao, "A control plan forthe stable operation of microgrids during grid-connected and islanded modes"Electr. Power Syst. Res. 129 (2015) 10–22.

[8]M.V. Manoj Kumar, M.K. Mishra, C. Kumar," A grid-connected dual voltagesource inverter with power quality improvement features" IEEE Trans.Sustain. Energy 6 (2) (2015) 482–490.

[9] N. Hamrouni, M. Jraidi, A. Dhouib," A. Cherif, Design of a command scheme forgrid connected P.V. systems using classical controllers,"Electr. Power Syst. Res.143 (2017) 503–512.

[10] Z. Zeng, H. Yang, R. Zhao, C. Cheng, "Topologies and control strategies ofmulti-functional grid-connected inverters for power quality enhancement

acomprehensive review," Renew. Sustain. Energy Rev. 24 (2013) 223–270.

[11] J. Liu, L. Zhou, X. Yu, B. Li, C. Zheng, "Design and analysis of an LCL circuit-basedthree-phase grid-connected inverter", IET Power Electron. 10 (2) (2017)232–239

[12] E. Pouresmaeil, C. Miguel-Espinar, M. Massot-Campos, D. Montesinos-Miracle,O. Gomis-Bellmunt, "A control technique for integration of D.G. units to theelectrical networks", IEEE Trans. Ind. Electron. 60 (7) (2013) 2881–2893

[13] R.R. Chilipi, N. Al Sayari, A.R. Beig, K. Al Hosani, "A multitasking control algorithm for grid-connected inverters in distributed generation applicationsusing adaptive noise cancellation filters", IEEE Trans. Energy Convers. 31 (2)(2016) 714–727.

[14] E. Pouresmaeil, D. Montesinos-Miracle, O. Gomis-Bellmunt, "Control scheme ofthree-level NPC inverter for integration of renewable energy resources intoAC grid", IEEE Syst. J. 6 (2) (2012) 242–253.

[15] Z. Zeng, H. Li, S. Tang, H. Yang, , "Multi-objective control ofmulti-functional grid-connected inverter for renewable energy integration and power quality service", IET Power Electron. 9 (4) (2016) 761–770.

[16] Costa, A. F. S.; Nescient, V. R.; Amorim, J. D. P.; Gomes, E. A. S.; Araujo, L. M.; Sarubbo, L. A. ,"Residue from the production of sugar cane: an alternative nutrient used in biocellulose production by Gluconacetobacter hansenii." Chemical Engineering Transactions, v. 64, p. 7-12, 2018. DOI: 10.3303/CET1864002

[17] Hamerski, F.,"Study of variables in the process of carbonation of the broth of sugar cane. p. 148. Dissertation. Graduate degree in food technology." Federal University the Paraná, Curitiba, 2009.

[18]Sudhakiran Ponnuru1, R. Ashok Kumar2,,"GWO-based MPPT controller for grid connected Solid oxide

fuel cell with high step up DC-DC converter,"Indonesian Journal of Electrical Engineering and Computer Science,Vol. 23, No. 3, September 2021

[19] Vigneysh T., N. Kumarappan*, "Grid interconnection of renewable energy sources using multifunctional grid-interactive converters: A fuzzy logic based approach" Electric Power Systems Research 151 (2017) 359–368

[20] Bharath K R, Harsha Choutapalli, "Control of Bidirectional DC-DC Converter in Renewable based D.C. Microgrid with Improved Voltage INTERNATIONAL JOURNAL of RENEWABLE ENERGY RESEARCHBharath K R et al., Vol.8, No.2, June, 2018

[21] Narsa ReddyTummuru,Ujjal Manandhar, Abhisek Ukil ,"Control strategy for AC-DC micro grid with hybrid energy storage under different operating modes," International Journal of Electrical Power & Energy Systems Volume 104, January 2019, Pages 807-816

[22] Benfei Wang, Yu Wang, Yan Xu, "Consensus-based Control of Hybrid Energy Storage System with a Cascaded Multiport Converter in D.C. Microgrids" IEEE Transactions on Sustainable Energy (Volume: 11, Issue: 4, Oct. 2020)

[23] Prudhvi Kumar, Gorijeevaram Reddy, "Investigation of Adaptive Droop Control Applied to Low-Voltage DC Microgrid," Energies 2021, 14(17), 5356.

[24] Sudhakiran Ponnuru, Ashok Kumar R,"Switching Strategies of Single Stage Battery based Microgrid, "PRZEGLĄD ELEKTROTECHNICZNY ISSN 0033-2097, R. 97 NR 9/2021

[25] Kotb M. Kotb, Mahmoud F, "Performance Assessment of Integrating SMES and Battery Storage Systems with Renewable DC-bus Microgrids,"A Comparison Period. Polytech. Elec. Eng. Comp. Sci September 2021,https://doi.org/10.3311/PPee.17676

[26] Iqbal A, Waqar A, Madurai Elavarasan R, et al. "Stability assessment and performance analysis of new controller for power quality conditioning in microgrids"Int Trans Electr Energ Syst. 2021;e12891.https://doi.org/10.1002/2050-7038.12891

[27] W. Al-Saedi, S.W. Lachowicz, D. Habibi, O. Bass, "Power flow control ingrid-connected microgrid operation using particle swarm optimization undervariable load conditions, "Int. J. Electr. Power Energy Syst. 49 (2013) 76–85.

[28] I. Sefa, N. Altin, S. Ozdemir, O. Kaplan, "Fuzzy P.I. controlled inverter for gridinteractive renewable energy systems, "IET Renew. Power Gener. 9 (7) (2015)729–738

IMPROVING GRID TRANSIENT STABILITY THROUGH STATCOM WITH EV BATTERY AS ENERGY STORAGE SYSTEM

K Rajalakshmi, Dr. M Arunachalam, Rajini H, Meghana Singh M, Mpanga Mukekwa Landry, Rohit Suryakant Sharma

School of EEE

Rajini.h@reva.edu.in

Abstract—The increase in electricity cost and unavailability of electricity to EV users will be a major problem in the future scenario where number of EVs will increase on road. Intelligent charging technologies can facilitate hassle-free integration of EVs to the grid. Integration of STATCOM with energy storage devices (EV battery) can play an important role in improving the voltage stability at the bus where EVs are connected. This paper proposes a system that demonstrates how the integration through STATCOM with the supply utility can significantly improve the exchange of both active and reactive power with the utility through the bus to which EVs are connected.

Keywords—STATCOM, Transient stability, Electric vehicles, Battery, Energy Storage System

I. INTRODUCTION

STATCOMs are capable of providing both inductance and capacitance used in voltage support and provide active and reactive power independently. The STATCOM can provide both active and reactive power to the grid. It is connected through a transformer to the grid.

The STATCOM can quickly draw excess energy available in the grid and transfer it to the battery of the EV or transfer energy from the battery to the grid to improve transient stability. The STATCOM can quickly draw excess energy available in the grid and transfer it to the battery of the EV or transfer energy from the battery to the grid to improve transient stability. Voltage control can be accomplished by the use of battery as energy storage system. [1]

This paper presents a study on improving transient stability through the STATCOM model in MATLAB/SIMULINK. Depending upon the short-circuit impedance at the bus where EVs are connected, the maximum power that can be drawn will get limited. In conventional AC systems, the ability to transfer power is limited by many factors such as thermal limits, voltage limits, transient stability limit, short circuit limit etc. These limits

defined the maximum power that can be efficiently transmitted through transmission lines without causing any damage to the electrical equipment and transmission lines. The solution proposed to solve these problems consists of connecting a STATCOM to the point of common connection i.e., the power system to where the load is connected. [3] It is proposed that by introducing a STATCOM between the EVs and the load bus, the voltage stability and the maximum power that can be drawn from the utility can be improved. To achieve this, analysis is done using N-R load flow method and it is shown how the voltage stability is improved resulting in the maximum power that can be drawn from the utility. The results show that integration of EV through STATCOM with the supply utility can significantly improve the exchange of both active and reactive power with the utility through the bus to which EVs are connected and the voltage stability of the system to which EV is connected.

II. METHODOLOGY

In conventional AC systems, the ability to transfer power is limited by many factors such as thermal limits, voltage limit, transient stability limit, short circuit limit, etc. These limits define the maximum power that can be efficiently transmitted through transmission line without causing any damage to the electrical equipment and transmission lines.

The system provided with STATCOM can enhance the controllability and stability of the transmission system with an increase in power transfer capability of the system. The basic operating principle of STATCOM is reactive power generation by a voltage sourced converter which is similar to conventional rotating synchronous machine is shown schematically, in the form of a single-line diagram in the figure below

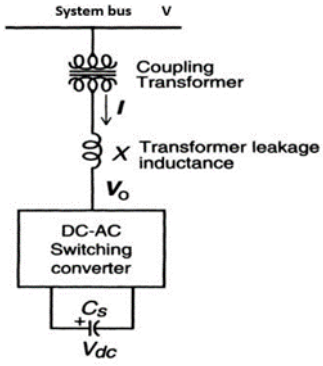

Fig1.Single line diagram of STATCOM

From a DC input voltage source, provided by the charged capacitor Cs, the converter produces a set of controllable three-phase output voltages with the frequency of the ac power system. Each output voltage is in phase with, and coupled to the corresponding ac system voltage via a relatively small (0.1-0.15 P.U.) tie reactance (which in practice is provided by the per phase leakage inductance of the coupling transformer). By varying the amplitude of the output voltages produced, the reactive power exchange between the converter and the ac system can be controlled in a manner similar to that of the rotating synchronous machine. That is, if the amplitude of the output voltage is increased abov that of the ac system voltage, then the current flows through the transformer inductance from

the converter to the ac system, and the converter generates reactive (capacitive mode) power for the ac system. If the amplitude of the output voltage is decreased below that of the ac system, then the reactive current flows from the ac system to the converter, and the converter absorbs reactive (inductive mode) power. If the amplitude of the output voltage is equal to that of the ac system voltage, the reactive power exchange is zero.

The figure below shows the three phase six pulse bridge converter. The three-phase output voltage is generated by a voltage-sourced dc to ac converter operated from an energy storage capacitor. The converter establishes a circulating current flow among the phases with zero net instantaneous power exchange for which the dc storage capacitor is needed. In a practical converter, the semiconductor switches are not lossless, and therefore the energy stored in the dc capacitor would be used up by the internal losses. By equipping the converter with a dc source like a battery, the switching losses can be accounted for and the converter can control both reactive and real power exchange with the ac system, and thus it can function as a static synchronous generator.

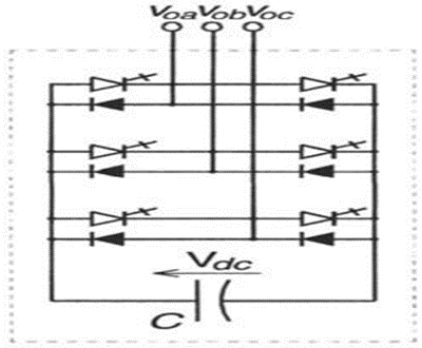

Fig.2. Three phase 6-pulse bridge converter

Control schemes- 1. Internal control

The figure 3 shows the internal control of the STATCOM which is an integral part of the converter. Its main function is to operate the converter power switches to generate a fundamental output voltage waveform with the demanded magnitude and phase angle in synchronism with the ac system.

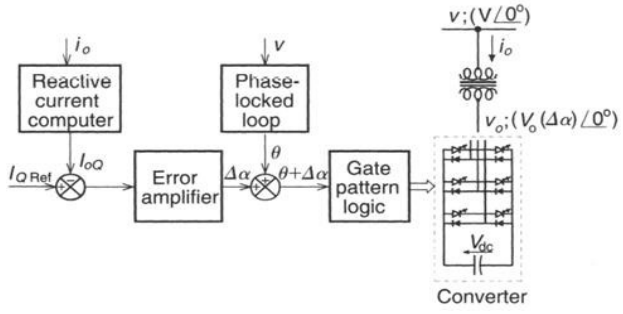

Fig.3.Internal control of STATCOM

The inputs to the internal control are: the ac system bus voltage, v, the output current of the converter, io and the reactive current reference, IQRef Voltage v operates a phase- locked loop that provides the basic synchronizing signal, angle θ. The output current, I0 is decomposed "into its reactive and real components, and the magnitude of the reactive current component, IQ , is compared to the reactive current reference, IQRef The error thus obtained provides, after suitable amplification, angle α, which defines the necessary phase shift between the output voltage of the converter and the ac system voltage needed for charging (or discharging) the storage capacitor to the de voltage level required. Accordingly, angle a is summed to (α) to provide angle (θ+ α), which represents the desired synchronizing signal for the converter to satisfy the reactive current reference. Angle (θ+ α), operates the gate pattern logic (which may be a digital look-up table) that provides the individual gate drive logic signals to operate the converter power switches. [4]

2. External control

In order to meet the general compensation requirements of the power system, the output of the static var generator is to be controlled to maintain or vary the voltage at the point of connection to the transmission system shown in the figure below.

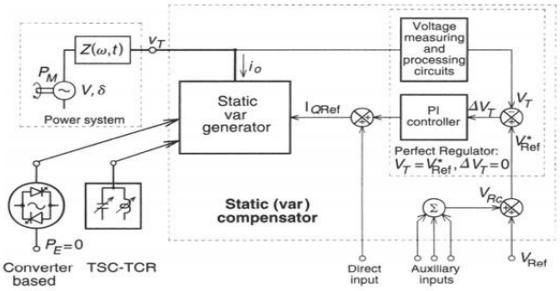

Fig.4.External control of STATCOM

The output of the static var generator is controlled so that the amplitude I0 of the reactive current i0 drawn from the power system follows the current reference IQRef With the basic static compensator control, the var generator is operated as a perfect terminal voltage regulator: the amplitude VT of the terminal voltage VT is measured and compared with the voltage reference VRef, the error ΔVT is processed and amplified by a PI (Proportional Integral) controller to provide the current reference IQRef for the var generator. In other words, IO is closed-loop controlled via IQRef so that VT is maintained precisely at the level of the reference voltage VRef in case of power system and load changes. [4]

A. Two bus system study model

The model assumed in this paper is shown in Fig.5, a two-bus system simulated in MATLAB Simulink.

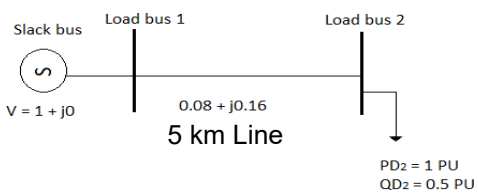

Fig. 5. Two bus system model

The STATCOM is introduced in the following two bus system as shown in Fig. 6. The introduction of STATCOM is expected to improve voltage stability.

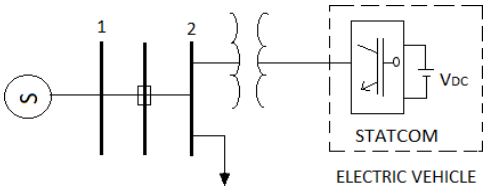

Fig. 6. Two bus with STATCOM model

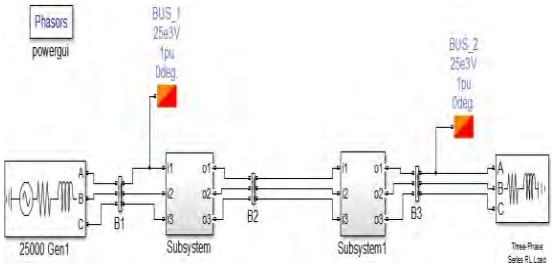

Fig.7. Simulink block diagram of system without STATCOM

Load flow of the system was conducted and different values of PD2 and QD2 were obtained keeping the power factor constant and the results were obtained by following the graph

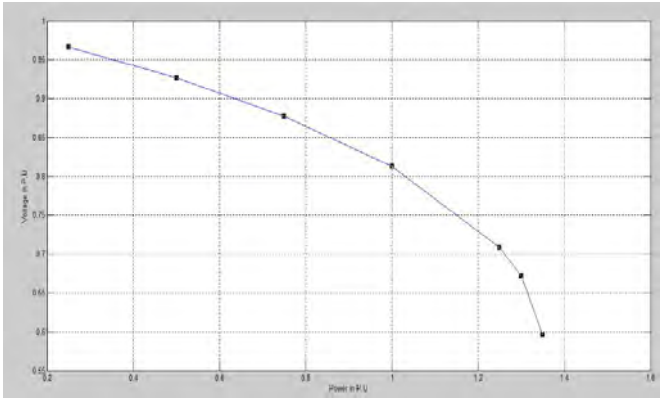

Fig. 8. Two buses without STATCOM graph

B. Simulation with STATCOM

A STATCOM is introduced in the 2-bus system and it is expected to improve the voltage stability. The voltage at load bus is obtained for three different values, when STATCOM is injecting no reactive power to the load bus, is injecting reactive power which is 50% of the

reactive power of load, and when STATCOM is injecting reactive power which is 100% of the reactive power of load and following graph was obtained after the load flow study.

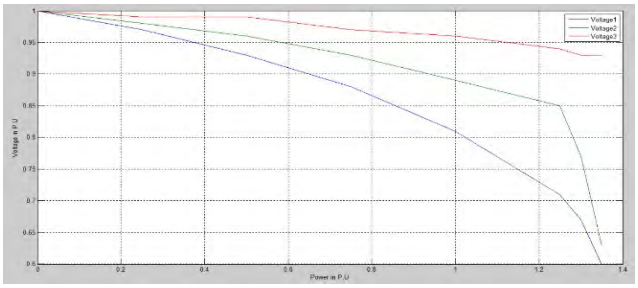

Fig. 9. Two buses with STATCOM model graph

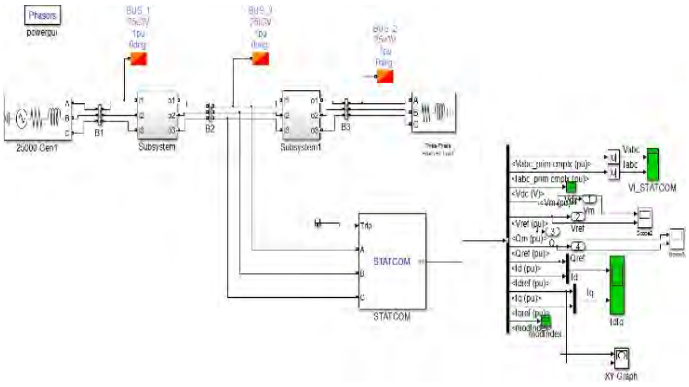

Fig 10. Simulink block diagram with STATCOM

Bus 3 is created at the output of STATCOM. Bus 3 is considered as a PV bus whose magnitude is specified as V = 1.0 p u. and the active power is specified as 0.0 p u. and load flow is performed.

1. SIMULINK BLOCK DIAGRAM WITH STATCOM AND 3 PHASE FAULT

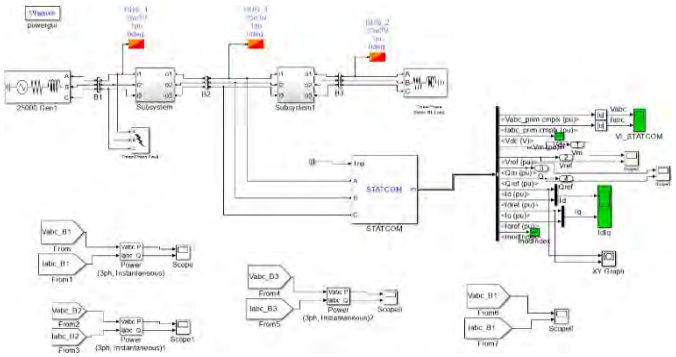

Fig. 11. Simulation block diagram with STATCOM and fault

The above simulation was carried out and fault and load flow studies were done. The following graphs were obtained.

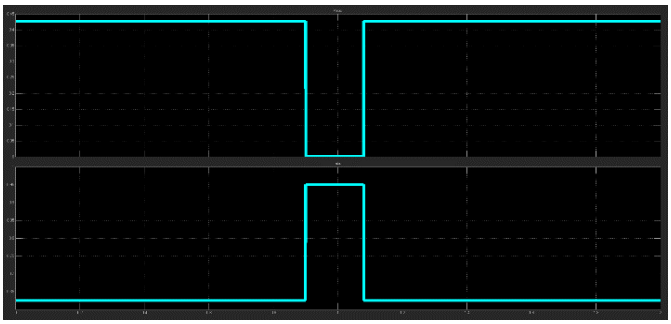

Fig.12.V, I Graph of system with STATCOM during fault

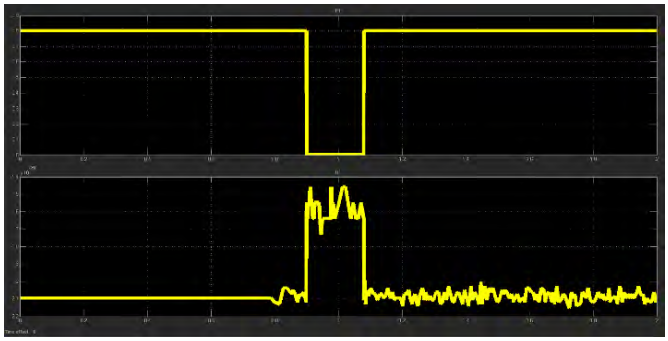

Fig.13. Active and Reactive power during fault period

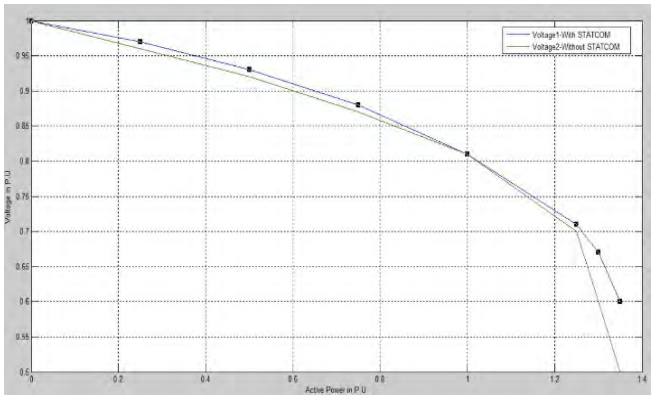

Fig.14. Comparison of P Vs. V Graph of system with STATCOM and without STATCOM

III. SIMULATION RESULTS

The results for the system connected to the load without STATCOM in fig.7 shows that with the increase in active power drawn by the load, the Voltage at bus 2 decreases. By increasing PD2 in small steps it was found out that 1.35+j0.67 P.U is the maximum power that can be transmitted.

The results for the system connected to the load with STATCOM in the system in fig.8 shows that with the increase in active power drawn by the load, the Voltage at bus 2 decreases in very small steps. With the increase in reactive power supplied by the STATCOM, the Voltage stability increases significantly.

The results for the system connected with a 3-Phase unsymmetrical fault and STATCOM in fig.13 shows that the voltage stability of the system improves and that STATCOM can provide reactive power support even during fault period.

IV. CONCLUSION

From the simulation it is inferred that the introduction of STATCOM in the system improves the voltage stability and the maximum power that can be drawn from the utility is improved significantly. The STATCOM has little active power providing capability. This can be improved by adding EV as Energy Storage System.

REFERENCES

[1] Tachibana, M., Palmer, M. D., Matayoshi, H., Senjyu, T., & Funabashi, T. (2015). Improvement of power system voltage stability using battery energy storage systems. 2015 International Conference on Industrial Instrumentation and Control (ICIC)

[2] Chandak et al. Protection and Control of Modern Power Systems (2019) 4:22, https://doi.org/10.1186/s41601-019-0138-0

[3] IEEE TRANSACTIONS ON INDUSTRY APPLICATIONS, VOL. 56, NO. 3, MAY/JUNE 2020, Enhancement of Power Quality in an Actual Hot Rolling Mill Plant Through a STATCOM,Gonzalo Arturo Alonso Orcajo , Member, IEEE, Josué Rodríguez Diez , José M. Cano , Member, IEEE,Joaquín G. Norniella, Joaquín Francisco Pedrayes González,

Carlos H. Rojas, Pablo Ardura G, and Diego Cifrián R

[4] Understanding FACTS: Concepts and Technology of Flexible AC Transmission Systems https://ieeexplore.ieee.org/book/5264253

DATA CENTER INFRASTRUCTURE AND POWER CONSUMPTION

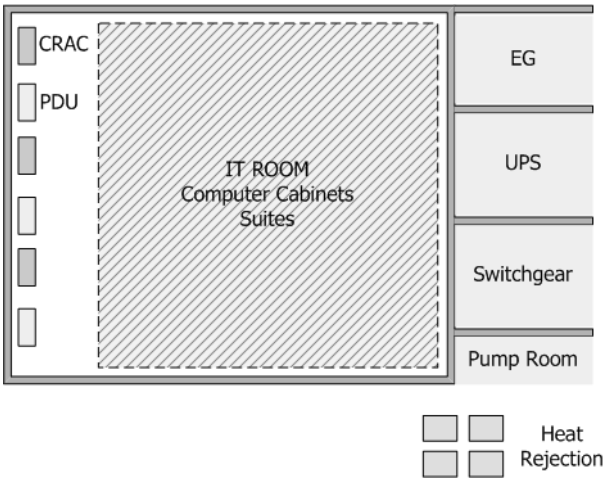

Figure 2.1. Typical Data Center Infrastructure [18, 19]

The overall design of a data center can be classified in 4 categories Tier I-IV each one presenting advantages and disadvantages related to power consumption and availability [18, 19]. In most cases availability and safety issues yield to redundant N+1, N+2 or 2N data center designs and this has a serious effect on power consumption. According to Figure 2.1, a data center has the following main units

1.1. Power Consumption in Data Centers

The equation should be submitted in the equation editor and should be keyed in as below in editable text:

$$R^n = \sqrt{(z_2 - z_j)^2 + (r^n)^2}, \tag{2.1}$$

The optimal description of this value depends on the system's characteristics and the type of equipment. As an example, for modulation and coding techniques in wireless communications the spectral efficiency is a common measure. For

electronic components the ratio of joule per bit best describes performance. In telecommunication networks and datacenters the ratio of watts consumed over the Gbps of data processed is preferred. In [22] an absolute energy efficiency metric is introduced, named as dBε.

2. CONCLUSION

A concise summary of the findings and a clear identification of the advance/contribution that this work provides to the field.

3. ACKNOWLEGDEMENTS

4. FIGURES AND TABLES CAPTION LIST

5. REFERENCES

[1] International Telecommunication Union (ITU), report on Climate Change, Oct. 2008.

[2] G. Koutitas, P. Demestichas, 'A review of energy efficiency in telecommunication networks', Proc. In Telecomm. Forum (TELFOR), pp. 1-4, Serbia, Nov., 2009.

[3] Gartner Report, Financial Times, 2007.

[4] I. Cerutti, L. Valcarenghi, P. Castoldi, 'Designing power-efficient WDM ring networks', ICST Int. Conf. on Networks for Grid Applic., Athens, 2009.

[5] W. Vereecken, et. al., 'Energy Efficiency in thin client solutions', ICST Int. Conf. on Networks for Grid Applic., Athens, 2009.

[6] J. Haas, T. Pierce, E. Schutter, 'Datacenter design guide', whitepaper, the greengrid, 2009.

[7] Intel, 'Turning challenges into opportunities in the data center', White Paper,

1

Assessment of 50 kW Grid Connected Solar Power Plant with Experimental Validation

Bansilal Bairwa, Sanjeeva Kumar, Vishal Kaushik S
bansilal.bairwa@reva.edu.in

School of Electrical and Electronics Engineering,REVA University,Bangalore, India 560064

Abstract

The global power sector is witnessing a gradual transition from typical thermal power-generating sources toward clean energy technologies. Non conventional sources of energy are the most appropriate solution to give clean and inexhaustible energy to conquer the worldwide energy emergency. The renewable share was 8.6 percentage within the world energy combine in 2010 and is predicted to extend to 22.5 percentage in 2020 as per a recent thematic analysis report renewable energy by the data collected globally. With the advancement in power electronics technology, photo voltaic system (PV) is getting more popularity in generation of electricity. Inverters connected to grid have developed significantly with high decent variety. Efficiency, estimate, weight, dependable execution have all improved significantly with involvement of technically advanced and innovative electrical converter configurations and these factors have diminished the expenses of inverters. This study deal with investigating the 50 kW with various aspectes.
Keywords: MPPT, Photo-voltaic, Solar, Energy, P& O.

An Edited Volume, 1–8.

1.1 Introduction

It is mandatory to observe geographical condition of the locations where we are going to install a solar PV system. And then analyze of climatic conditions. It is must to analyze the climatic condition and the different radiation levels. Primarily it includes selection of components like modules inverters cables combiner box, and others. And the PV array inverter matching is crucial part for design of the grid connected PV system. It is also mandatory to find out the appropriate number of modules, appropriate numbers of inverter support for a particular capacity. Designing a PV system based on the energy balance phenomena. The Energy yield at the DC side is given by the below equation[1, 2, 3].

$$\epsilon_{DC}^{y} = A_{tot} \int G_M \eta(t) dt \tag{1.1}$$

Here A_{tot} is total module area, that is equal to the total area of the cells, mention in below equation.

$$A_{tot} = N_T.A_M \tag{1.2}$$

Where N_T is the total number of cells and A_M is the area of the cell. The energy generated by the PV is equal to the consumed energy for one year. So, these phenomena have been applied for designing a grid connected PV system. This normally global radiation integration for the entire year.

$$N_T = \left[\frac{(\epsilon_L^y \ .SF}{(A_{tot} \ \int G_M(t)\eta(t)dt)} \right] \tag{1.3}$$

The required number of modules is calculated by the given equation Solar module can be connected in series and parallel configuration.

$$N_T = N_S.N_P \tag{1.4}$$

The power of the DC side at standard test condition is given in below equation,

$$\rho_{DC}^{STC} = N_T.\rho_{DC}^{mpp} \tag{1.5}$$

Installing a solar PV plant, the ratings of the inverter need to be calculated, for finding out the nominal DC power of the inverter. As the demand for world energy grows because of modern industrialization and population growth, renewable energy technologies are being further developed to improve energy production and energy quality. Since there is many countries with a

direct solar density of 1000W/m in tropical and temperate zones, the primary resource is photo-voltaic power. The need for integration of photo-voltaic systems with other energy sources such as battery storage and diesel generators is consequent in major power disruptions due to changing environmental conditions[**?**]. For estimating the size of solar photo-voltaic cells, the PGF (Panel Generation Factor) play a key role. The maximum watt peak required to meet the electricity demand from solar panels is referred to as the Panel Generation Factor[5]. PGF is dependent on location and climate, hence various locations may have varying PGFs based on the quality of solar insolation and irradiation falling on that location. The PGF is based on empirical relationships. The Panel Generation Factor is an important factor to consider when planning a solar PV plant since it tells us that for every Wp power in the panel, we should expect to get an average of Wh/day, and it varies by location, for Jaipur city considering 5.30 $\frac{W}{m^2}$. Storage of batteries cannot tolerate any variation in load and diesel generators can only provide short periods of backup. As the demand for world energy grows because of modern industrialization and population growth, renewable energy technologies are being further developed to improve energy production and energy quality. Since there is many countries with a direct solar density of 1000W/m in tropical and temperate zones, the primary resource is photo-voltaic power. The need for integration of photo-voltaic systems with other energy sources such as battery storage and diesel generators is consequent in major power disruptions due to changing environmental conditions. Storage of batteries cannot tolerate any variation in load and diesel generators can only provide short periods of backup[6].

1.2 Methodology

In these systems, mono-crystalline silicon cell-based modules were chosen. The cell's efficiency and temperature coefficients were carefully monitored. The typical module capacity of 250Wp was chosen to ensure that the modules are not too small or too large to be affected by wind forces. mono-crystalline silicon modules have been connected in series and parallel configuration. In this work, 15 modules are connected in series to form a string of the plant for every 52.5 kWp power. 14 strings are connected in parallel, and this series-parallel combination is connected to a Junction Box, from which wires are connected to an inverter for DC to AC conversion. The total installed module capacity is calculated up 52.5 kWp, which was achieved to compensate for losses and module rating. Experimental data were collected from

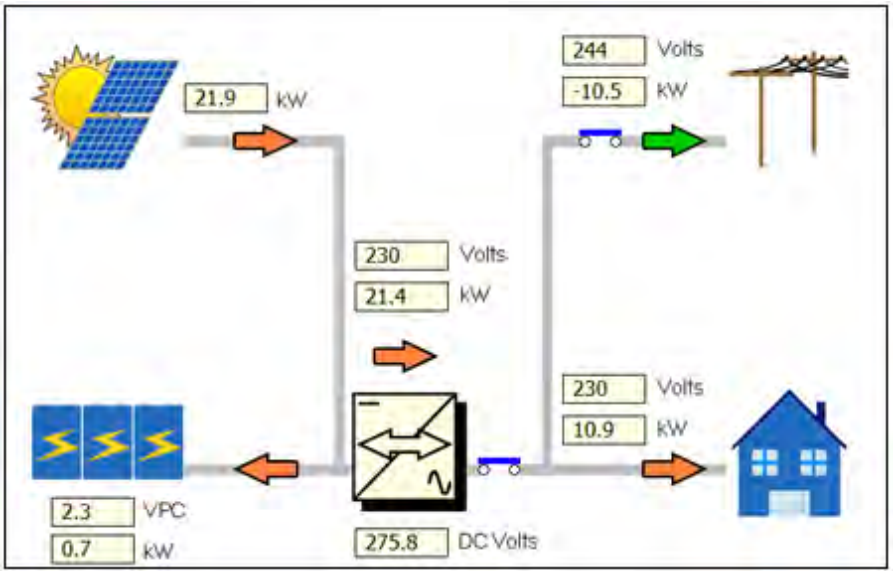

Figure 1.1 Overview of solar power plant with SCADA

grid-connected solar power installed at MNIT Jaipur. The controls of grid-connected solar power plants are mounted with a computerized monitoring system. Figure 1.3 shows the Solar PV control panel desktop view. The 52.5 kW photo-voltaic array is composed of 250 REIL modules. The array is composed of 14 strings of 15 parallel-connected modules (15*14*250 W= 52.5 kW). The PV array block menu enables you to visualize the I-V and P-V characteristics of individual modules or the entire array. The photo-voltaic array block features two inputs for varying sun irradiance $(W/m^2)$and temperature. A Signal Builder block connected to the PV array inputs defines the irradiance and temperature. Inverter Capacity = 50kVA/inverter; efficiency 93% at full load profiles. Figure 1.1 represents the schematic diagram of solar photo voltaic power plant of 52.5 kW full installed capacity. This configuration included 240V, 1000Ah battery bank 50 kVA power conditioning unit, Junction box , AC distribution board , load panel connected to SCADA. The Installed Capacity 52.5 kWp, Number of PV module is taken as 210, Number of Inverters 1 with 50 kVA rating, Efficiency 93% at full load, Number of modules in a string 15 and Number of strings in parallel is taken 14.

Table 1.1 Simulation parameters for solar panel

S.No.	Parameters	Specifications
1.	Parallel strings	15
2.	Series- connected modules per strings	14
3.	Max output current per MPPT (A)	8.3 A
4.	Maximum output power	250 Watt
5.	Maximum output Voltage (V)	30.28 V
6.	Short circuit current I_{sc}	8.8 A
7.	Open circuit voltage V_{ocv}	37 V
8.	Series resistance R_s	0.18
9.	Parallel resistance R_p	360
10.	No. of cells	60
11	Cell technology	Mono-crystalline

1.3 Results and Discussion

Table I. describe the components of the solar power plants have been used in this work.Components, such as PV cells or panel are combining them into arrays with the power electronic converters and inverters.Figure 1.2(a) show the experimental results for the month of January to December for solar power generation,inverter output average load and transferred power to grid, .Figure 1.2(b) shows the imported and exported energy for the month of January to December. The describe the designing control algorithms for solar power plant. In this work maximum power point tracking observed by two MPPT techniques such as perturb and observation and incremental conductance with the help of MATLAB and simulink. Solar irradiance based solar power output has been tracked by the given MPPT techniques at the room temperature. Thermal condition have been included in this work, some heating for voltaic panels photo-voltaic panels convert the sunlight into electricity.DC power has to be converted into AC power through some kind of power inverter, this AC power can be distributed with the load connected to commercial load. This systems include battery storage so this DC power is actually fed into a battery charger, and then the greatest power from the battery. DC DC converter, receiving the power from the array, DC, AC inverter, which is converting the DC power into three phase AC power. It is being connected to a model of the utility grid on the site. The the power obtained from the grid connected solar power plant and the simulink model is limited with the calculation 50kW.The module has been installed by the Rajasthan Electronics Instruments Ltd at the MNIT with the 250 kW rating as

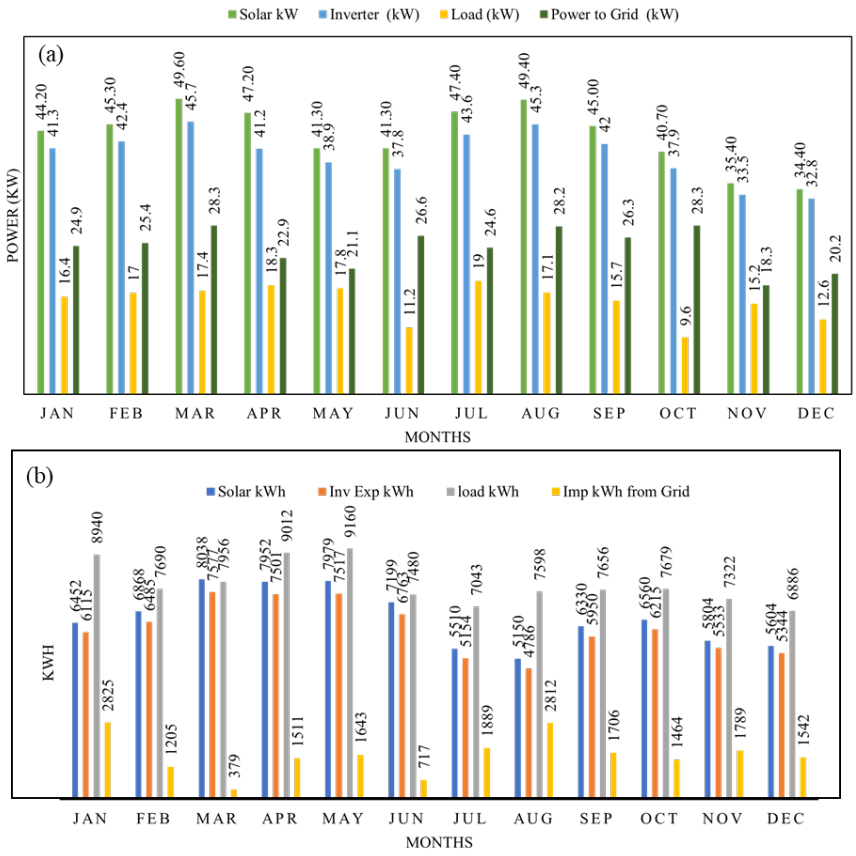

Figure 1.2 experimental results for the month of January to December.

mentioned in the Table 1.1. Figure 1.4 describe the modeling and simulation results for the purturb and observation and incremental conductance MPPT techniques. Simulation results validated with experimental results of the solar power plant at the given instant time.it shows a comparison of the MPPT techniques adopted in this work with experiment output of the solar power plant as represented as bar graph. yellow line represent the solar irradiance from 9:00 AM to 4:00 PM. This work deal with assessment of grid connected PV power plant installed in Malaviya National Institute of Technology Jaipur. Experiments results compared with simulation results. Incremental OCV and P&O maximum power plant tracking have been adapted in this work. Simu-

lation results have good agreement with experimental results extracted from solar optimal power solution installed at prabha bhawan at MNIT Jaipur.

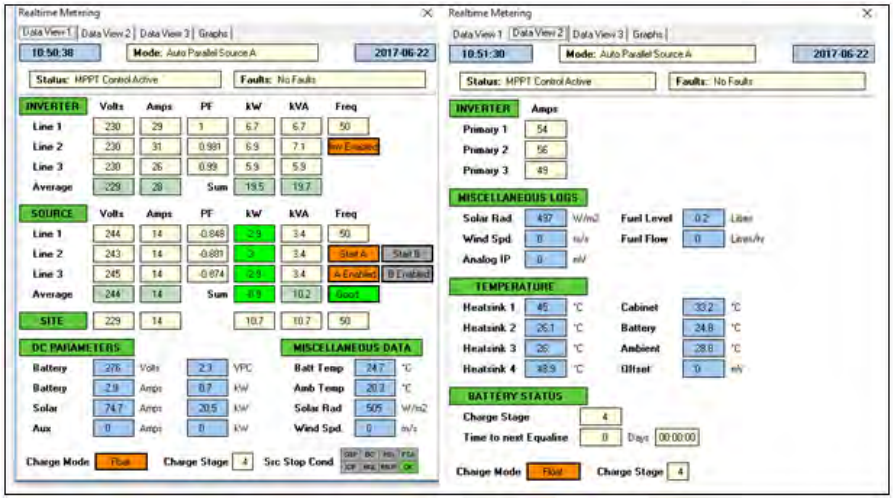

Figure 1.3 Solar PV control panel desktop view

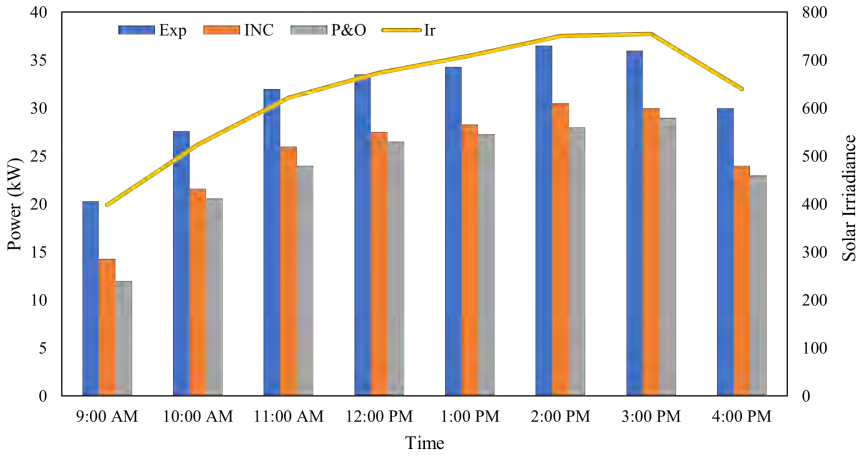

Figure 1.4 Simulated and experimental PV power for 50 kW solar power plant with PO and INC MPPT techniques.

1.4 Conclusion

As the demand for world energy grows because of modern industrialization and population growth, renewable energy technologies are being further developed to improve energy production and energy quality. Since there is many countries with a direct solar density of 1000W/m in tropical and temperate zones, the primary resource is photo-voltaic power. The need for integration of photo-voltaic systems with other energy sources such as battery storage and diesel generators is consequent in major power disruptions due to changing environmental conditions. Storage of batteries cannot tolerate any variation in load and diesel generators can only provide short periods of backup. This research aims to develop a behavioral model of a grid-connected PV system that accurately represents the actual PV system while also addressing the concerns. All photo-voltaic systems provide data loggers that record and store information about operating conditions and performance production. Despite the market's rapid expansion, very few of the numerous monitoring techniques available projected power and energy productions. Forecasting success is critical for all potential future solar energy developers, as it will support their investment decisions.

References

[1] M. H. B. Khairudin, R. H. G. Tan and J. Y. Wong, "Modelling of Grid Connected PV System for Performance Assessment," 2018 IEEE 7th International Conference on Power and Energy (PECon), 2018, pp. 144-149, doi: 10.1109/PECON.2018.8684079.

[2] S. I. Rasel, R. N. Ali, M. S. U. Chowdhury and M. M. Hasan, "Design simulation of grid connected Photovoltaic system using Simulink," 2015 International Conference on Advances in Electrical Engineering (ICAEE), 2015, pp. 238-242, doi: 10.1109/ICAEE.2015.7506840.

[3] H. Kanchev, N. Hinov, D. Amaudov and R. Stanev, "Modelling and control of a grid-connected PV system for smart grid integration," 2017 40th International Spring Seminar on Electronics Technology (ISSE), 2017, pp. 1-6, doi: 10.1109/ISSE.2017.8000956.

[4] M. Mathew and J. Hossain, "Analysis of a grid connected solar photovoltaic system with different PV technologies," 2017 IEEE International Conference on Circuits and Systems (ICCS), 2017, pp. 264-269, doi: 10.1109/ICCS1.2017.8326002.

[5] S. Ioannou, M. C. Argyrou, C. C. Marouchos and M. Darwish, "Efficiency Investigation of a Grid Connected PV System with Power Smoothing," 2019 54th International Universities Power Engineering Conference (UPEC), 2019, pp. 1-6, doi: 10.1109/UPEC.2019.8893628.

[6] Bairwa, Bansi L., Kapil Pareek, and Santosh kumar Hampannavar. "Investigation on lithium ion battery equivalent circuit models for dynamic load profiles". Energy Storage 3, no. 2 (2021): e231.

1

Application of Solar Energy for Wieless Power Transfer

Arpita Banik, Bansilal Bairwa, Saahithi S, Rajini H
arpita.b@reva.edu.in

School of EEE, REVA University,Bangalore, India 560064

Abstract

Solar panels are used here to generate power and store it in batteries as solar energy is renewable, inexhaustible and environmental pollution free. A proper storage technology can ensure continuous and reliable power supply. Wireless power transfer can be done without using any wire or physical connection. Inductive coupling is used for power transfer for short ranges, resonant inductive coupling for mid range and microwave power transmission for long range. During power plant generation and till it reaches consumers most of the energy is wasted. So, wireless power transfer is eco-friendly for the transfer of power. Wireless power transfer can be used for solving problems like energy crisis. This project will be carried out on implementing application of solar energy for wireless power transfer. Solar panels will be used to generate power for charging mobile phone wirelessly through electromagnetic waves.

Keywords: Wireless, Power, Transform, Solar, Energy.

1.1 Introduction

Wireless power transfer was first invented by Nikola Tesla. He invented this technique to eliminate losses during transmission of electric power. The loss during transmission of is 26% approximately. The main reason for power

An Edited Volume, 9–15.

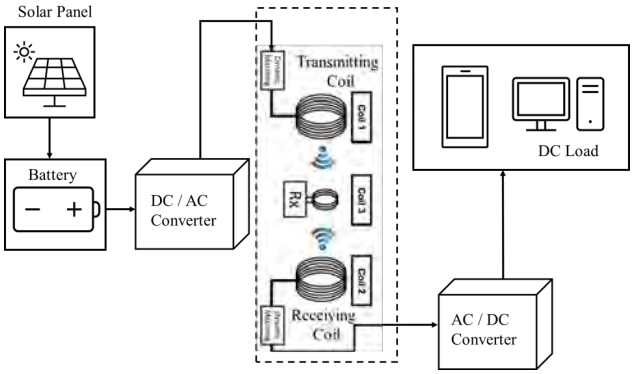

Figure 1.1 Block diagram of wireless power transfer.

losses is resistance of wires used in the grid. WPT is a system where electric power can be transferred from a power source to an electrical load without connecting any wires in between. Power transmission can be done using electromagnetic waves through air for short range, resonant inductive coupling for mid-range and microwave power transmission for long range. Wireless power transfer can be used for solving problems like energy crisis. This project will be carried out on implementing application of solar energy for wireless power transfer. Solar panels will be used to generate power for charging mobile phone wireless through electromagnetic waves. To transfer electric power from one point to another WPT is an efficient way through electromagnetic waves[1, 2, 3, 4]. Solar energy is used to generate power as it is renewable, inexhaustible and pollution free. Solar energy generated is stored in batteries. The voltage sources to the transceiver were providing by solar cells. The inductive coupling is used as the antenna to wireless power delivered from the transmitting to the input of a receiver. Receiver unit, the bridge rectifier is used convert AC voltage to produces DC voltage and produce DC output. A capacitor is included in the circuit to act as a filter to reduce ripple voltage. A battery will be included to store the power[5, 6, 7].

1.2 Methodology

1.2.1 Simulation

A 5V input will be given to the circuit. An oscillator circuit contains MOSFETS it will create high oscillating current, resistors are used to adjust signal levels and capacitor filter will be used to avoid ripples. The transmitter and

receiver coil is prepared by SWG copper wire for 4.5 cm diameter with 20 turns. In the receiver side bridge rectifier is shown to convert AC into DC along with capacitor to filter ripples.

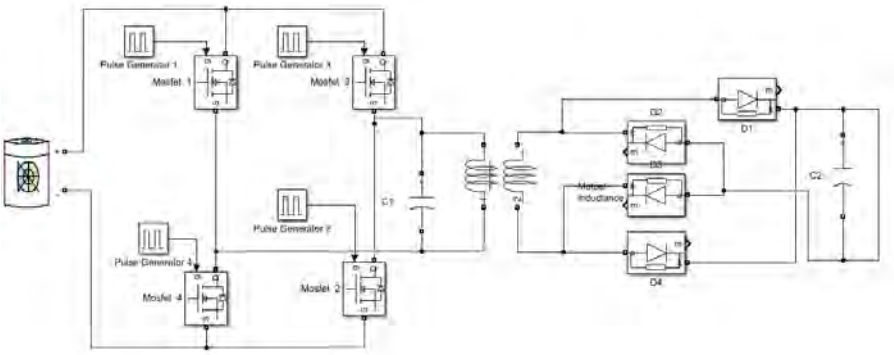

Figure 1.2 Simulink model for wireless power transform.

1.2.2 Hardware

[h] Here the battery voltage is applied to the MOSFET which is working as a switching the dc voltage. IC 4047 is generating triggering pulse at 2 KHZ. The output of the MOSFET is ac 12 volt is coupled with the transmitting coil. The transmitting coil transfers the power in air. The receiver coil receives the ac volt and it is given to the rectifier which is converting into ac to dc using rectifier and then transferred to the load[8, 9, 10, 11].

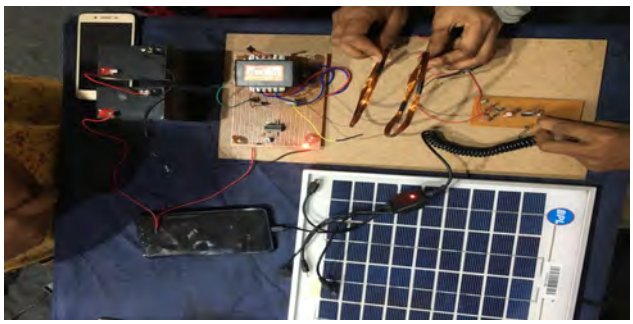

Figure 1.3 Experimental setup of the project

1.3 Results

Figure 1.6 represents the power is transferred from transmitting coil to receiving coil. The LED 1 indicated that the power is been transferred from 12v battery to the inverter circuit. The transmitted from transmitting coil to receiving coil is identified by LED2[12, 13, 14]. As shown in the Figure 1.5, a

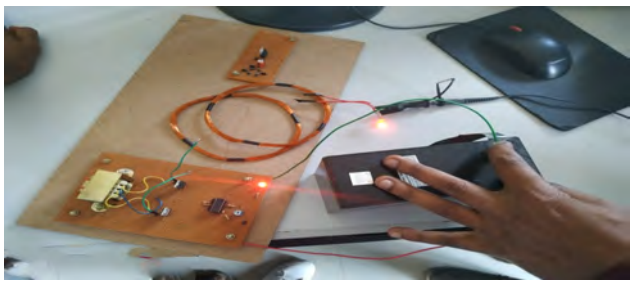

Figure 1.4 Power is transferred from transmitting coil to receiving coil.

book is placed in between transmitting coil and receiving coil to test if power can be transferred through it. LED 2 indicates that power is received through receiving coil even when the book is in between two coil and obstruction output achieved. Fig 6: shows the waveform of triggering pulse to the MOSFET to Checking the waveform of triggering pulse given to the MOSFET. IC 4047 is generating triggering pulse at 2 KHZ. The waveform of triggering pulse to the MOSFET is indicated in the CRO as shown in Figure 1.4. Figure 1.6 shows waveform of voltage V/S time for output and input. A constant input of 5V is given in transmitter coil and the output voltage up to 1.7V is got. It indicates that the input voltage has to increase. The future scope of the

Figure 1.5 Obstruction output of the proposed work

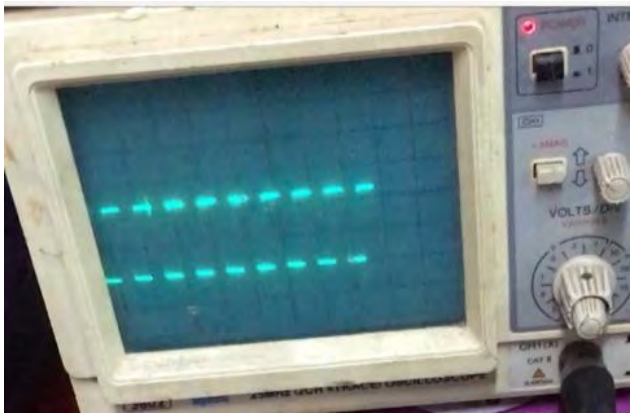

Figure 1.6 Block diagram of wireless power transfer.

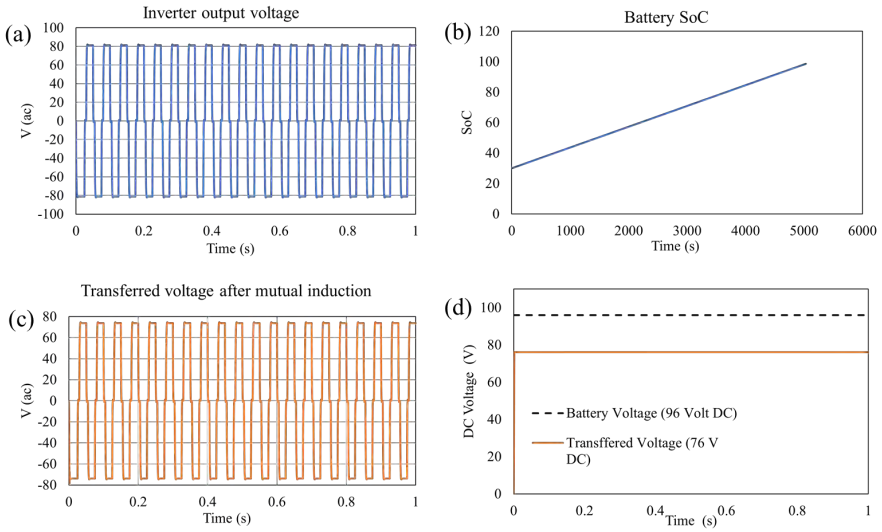

Figure 1.7 Simulation output for proposed work.(a) Inverter output voltage; (b) Battery SoC; (c) Transferred output after mutual induction (d) Battery voltage Vs total transferred voltage.

project is to find the way to charge any sought electrical gadgets wireless with higher efficiency. The distance between the battery and electrical gadget can be extended up to 1m. Boost converter can be used to get desired regulated DC voltage. Suitable structure of inductor coil can be used to get maximum energy transfer efficiency. This project is very useful for minimizing the use of many cables for power transfer. In future their will be no need to use of

cables to transfer power and to charge devices like laptop, electric car etc. and devices can alos be charged while moving. The threats generated due to wired power transfer such as electric shocks, shorting of wires, power theft etc. Can be avoided successfully by this project. This system can easily setup in colleges, home, hospital, industries, etc. The solar energy which is left un used can be connected to the main grid. As energy is used pollution caused during construction transmission poles and cables can be avoided. This project provides great way of saving power and unnecessary wastage of electricity as well as related extra electricity billing charges by means of automatic power control system[15, 16, 17].

1.4 Conclusion

From the overall experiment conducted from the project entitled " Application of solar energy for wireless power" we conclude that the study on wireless power transfer using electromagnetic waves has much aspect in terms of distance, range of frequency and results shows the nearer the distance, the voltage transferred is higher. This project has tried to create energy from renewable energy sources like solar source due to which pollution can be avoided. Electric power generated from the solar panel can be connected to main grid. The energy generated from the solar panel can then be used as power source for all the electrical appliances. To energy can be saved by avoiding unnecessary power wastage, automatic power management and control system plays an important role. Thus there is no need to take care of power saving. Advancements in electrical and electronics world is taking place, now it is required to design efficient user friendly products using the recent technologies. The project not only focuses on effective power transfer and power management but also mainly aims to transfer power wireless to charge electronic devices in efficient way. Lot of research is still in process for wireless power transfer, we tried to provide a wireless power transfer system for charging electric device like mobile phone effectively. Now the user can charge mobile phone by wireless power transfer system. The project gives solution for certain power issues effectively and this system can be implemented in home, hospital, college, library, industry etc.

References

[1] G. A. Covic and J. T. Boys,"Modern trends in inductive power transfer for transportation applications", IEEE Journal of Emerging and SelectedTopics in Power Electronics1, 28–41 (2013).

[2] Z. Wang and X. Wei,"Design considerations for wireless charging systems with an analysis of batteries", Energies8, 10664–10683 (2015).

[3] S. Li and C. C. Mi,"Wireless power transfer for electric vehicle applications", IEEE Journal of Emerging and Selected Topics in PowerElectronics3, 4–17 (2015).

[4] S. Moon and G.-W. Moon,"Wireless power transfer system with an asymmetric four-coil resonator for electric vehicle battery chargers", IEEETransactions on Power Electronics31, 6844–6854 (2016)

[5] Bairwa, Bansi L., Kapil Pareek, and Santosh kumar Hampannavar. "Investigation on lithium ion battery equivalent circuit models for dynamic load profiles". Energy Storage 3, no. 2 (2021): e231.

[6] Bairwa, Bansi Lal, Amit Soni, and Kapil Pareek. "Higher order equivalent circuit model analysis of lithium ion battery for electric vehicle." In AIP Conference Proceedings, vol. 2294, no. 1, p. 040011. AIP Publishing LLC, 2020.

[7] Bairwa, Bansilal, Santoshkumar Hampannavar, Kaushik S. Vishal, and K. M. Bhargavi. "Modeling and Simulation for Capacity Fade Prediction of Lithium-Ion Battery". In IEEE EUROCON 2021-19th International Conference on Smart Technologies, pp. 537-541. IEEE, 2021.

[8] C.A. Balanis, Antenna Theory: Analysis and Design, third ed.,John Wiley Sons, Inc., Hoboken, NJ, 2005.

[9] H.P. Kimmich, Bio-telemetry, based on optical transmission, Biotelem Patient Monit. 9 (1982) 129–143.

[10] S. Jarvis, J. Mukherjee, M. Perren, J.S. Sweeney, On the fundamental efficiency limits of photovoltaic converters for optical power transfer applications, in: 39th IEEE Photovoltaic Spec. Conf. (PVSC), 2013 pp. 1031–1035.

[11] T. Tsuji, T. Fujimoto, T. Izuto, T. Togawa, Telemetry of organ temperature with quartz crystal resonator using ultrasonic detection for preoperative patient monitoring, in: Proc. 12th Int. Symp. Biotel, 1993, pp. 378–380.

[12] J. Charthad, M.J. Weber, T.C. Chang, A. Arbabian, A mm-sized implantable medical device (IMD) with ultrasonic power transfer and a hybrid bi-directional data link, IEEE J. Solid State Circuits 50 (2015) 1741–1753.

[13] N.G. Holmer, K. Lindstrom, Highly isolated power supply energized by ultrasound, Med. Biol. Eng. 11 (2) (1973) 233–235.

[14] M.P. Theodoridis, Effective capacitive power transfer, IEEE Trans. Power Electron. 27 (2012) 4906–4913.

[15] A.K. RamRakhyani, G. Lazzi, On the design of efficient multi-coil telemetry system for biomedical implants, IEEE Trans. Biomed. Circuits Syst. 7 (2013) 11–23.

[16] T. Campi, S. Cruciani, F. Palandrani, V.D. Santis, A. Hirata, M. Feliziani, Wireless power transfer charging system for AIMDs and Pacemakers, IEEE Trans. Microw. Theory Tech. 64 (2016) 633–642.

[17] J. Huh, S.W. Lee, W.Y. Lee, G.H. Cho, C.T. Rim, Narrow-width inductive power transfer system for online electrical vehicles, IEEE Trans. Power Electron. 26 (2011) 3666–3679.

Flood Rescue Operation using Intelligent Drone for Supporting Disaster Management

Mahesh Kumar, Bharath Rao, Bhargav S, Hemanth L.

Address: School Electrical and Electronics Engineering, REVA University Bengaluru, India

Email: email2maheshkumar@gmail.com

Abstract

This project is primarily about the improvement of flood relief operations using UAV (Unmanned Aerial Vehicle) technology. This work provides a system to communicate with the victims in real time and to acquire the required statistics and data to plan the relief operations in a faster and efficient manner. The model will have a UAV, communication system and live video streaming system. The first responders will move to the location and to assess the situation like number of people stranded, boat routes planning and to do routine checks, they can use the UAV and its accessories to plan their action in an efficient way. It will have an on-board communication system to have half-duplex communication with the survivors and first responders. To make the disaster management easier and rescue planning faster, we have used a computer vision library tool which detects people and sends their location back to the Control Centre.

Keywords: Flood Relief, UAV, Communication, Disaster Management, Rescue Planning, Video Streaming

1. INTRODUCTION

We have taken inspiration from the enormous possibility of an Unmanned Aerial Vehicle (UAV) in diverse terrains, its ability to manoeuvre quickly in the air and its low-cost flight which helps in looking at the problem from a different perspective. Natural Disasters are always prone to invaluable data collection or sometimes there will be much data to be processed during the post disaster management. Having the right data at the right time will be helpful in quick

assessment of the situation we are in. NDRF (National Disaster Response Force) of India uses their elite team of volunteers and military men to quickly assess the situation and rescue people. During Bihar floods in India there was a case where the first responders got a call to rescue a pregnant woman from a village, but the name of the village was not heard clearly and due to this fail in communication the exact location of the woman was not acquired. Therefore, we need to have proper data to rescue the people on priority basis.

In this project, we have discussed the possible solutions for improving the disaster management during floods. UAVs in floods are valuable because of the immobility of vehicles on the land and the waterways restrict the amount of data to be collected in an area, thereby having a UAV which can fly over the area can be of great help.

2. PROPOSED WORK

The flood affected area will be located and the first responders will setup the control station at a suitable place. Fig. 2.2. demonstrates the working of the flood relief operations, but is not limited to, using UAV Once the control station is setup, they can deploy the UAV initially for knowing boat routes aerially and the route data will be sent back to the control station. Simultaneously another UAV can be deployed to begin the search operations looking out for people. This is done by OpenCV (open computer vision, it's an open-source computer vision documentation which helps in detecting

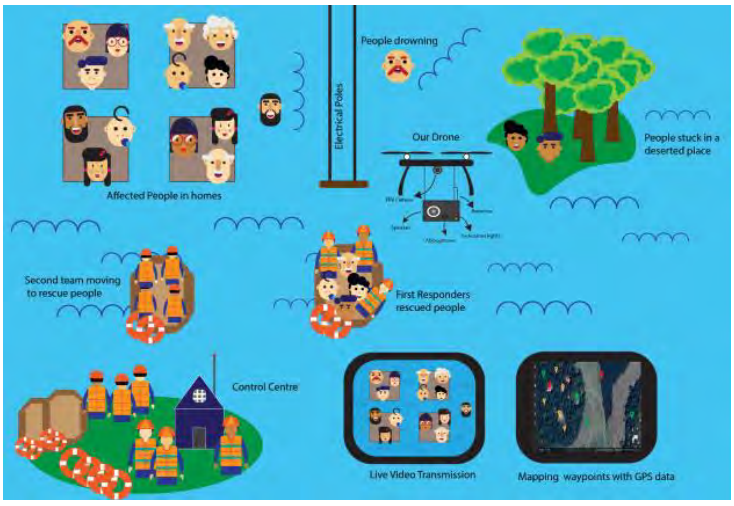

Figure 2.1. Illustrated idea.

people, water, trees, obstacles etc., using python programming and Machine Learning Techniques to train the cameras to better recognize the event and send valuable data. Once the people are detected, the GPS location of the people is sent to the control station where they mark the waypoints using the GPS data and plan the action accordingly. This system also helps in talking to the stranded people there and giving them valuable instructions and information on a timely basis.

Figure 2.2.

3. SYSTEM DESIGN AND CHALLENGES

A. Design of UAV:

The connections are made according to the block diagram shown in Fig. 3. Initially we have to setup the configurations for the transmitter. This is done using the screen provided in the transmitter as shown in figure 3.7. Here we key-in the quadcopter model and the transmitter is all set to operate for the quadcopter flight. Next, we set up the 'Fail Safe' option. This option helps us keep the drone in the initial stick position for different channels so that when the communication fails the drone gets the initial channel PPM so that it won't fly away from the area.

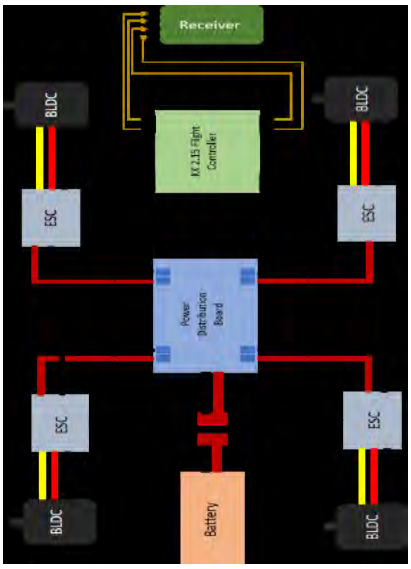

Figure 2.3. Block Diagram of Quadcopter

After setting up the transmitter for the quadcopter model we need to bind the receiver and the transmitter. This is done by placing the binding key in the receiver and power the receiver from the esc to the channel 1 of the receiver. Connect the Lithium Polymer Battery to the ESC and the Receiver will turn ON. Now hold the binding key in the transmitter and turn ON the transmitter. After few seconds the transmitter will indicate that the receiver has been bound.

We need to ARM the flight controller by holding the Channel 4 to the right and the quadcopter is ready to fly!

B. OpenCV people detection:

OpenCV is an open-source computer vision library, tools and hardware support which is used in Machine Learning (ML) and Artificial Intelligence (AI). It currently consists of various types of computer algorithms to detect faces, track objects, track camera movements and many more. This provides a vast range of applications to be explored. This project uses OpenCV with Python programming language to detect people stranded in the flood affected area.

C. Communication System:

Audio communication helps in good maintaining of communication with the other person in the flood hit areas, hence we use nRF24l01 transceiver module which we are using it like walkie talkie. Arduino Nano is a microcontroller

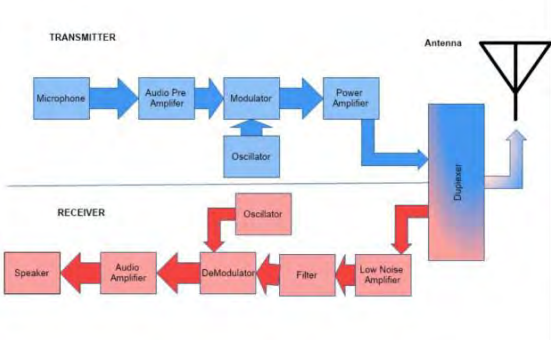

Figure 2.4. Communication block diagram.

board we will use to transmit and receive the audio. nRF24l01 is a 2.4GHz wireless transceiver module which is used to send the data and receive using radio waves. It uses SPI protocol for transmitting the data and its data rate is up to 2Mbps. We have flexibility of using channels up to 125 channels ranging from 2400 – 2525 MHz, this will give us 800 meter of range in line of sight and a good module to test the communication initially as it uses frequency within the ISM (Industrial Scientific and Medical) Band, later we can test the same audio communication with the operating frequencies of the first responders.

4. RESULTS AND DISCUSSION

The interpretation drawn after completion of some parts of the project is that the UAV is equipped with Pi Camera which gave us the bird's eye view of the area which it flew in. Later the video was sourced to the code and run to detect the people in the surroundings. In addition to this we had to run the code from the drone visuals taken from different sources. The code has been tested and it is proved to be effective in recognizing people who are standing and visible in the video. In the future scope of the project the code can send the location request to GPS Module and thereby send the same information to the control station. We developed the UAV which can do or can perform the tasks in fetching the required data and helping the first responders to better analyse the area and plan their actions accordingly.

Figure 2.5. UAV

As seen in Figure 2.4. the UAV has been tested for the flight and gives us good altitude range to hover over the disastrous area and to quickly manoeuvre over the area to give us valuable data. The quadcopter is developed using FlySky FSi6 transmitter and receiver and the KK 2.15 Flight Controller board which controls the path of the flight according to the input given by the pilot. Currently the drone can fly a small distance without any obstruction, and it is almost stable during the flight.

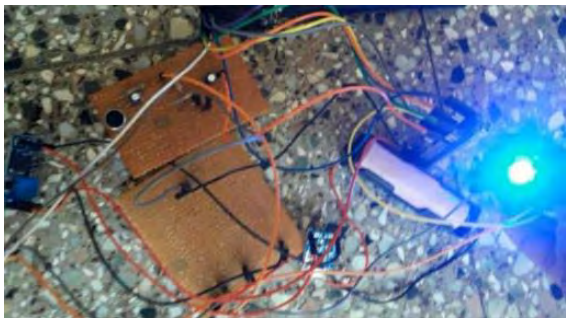

Figure 2.6. Communication working LED

Fig. 5 shows the output of the audio communication setup is received through the speaker when the input is given to the microphone. Here we used an electrate based microphone to capture the audio, this electrate microphone has a 2V of working voltage when biased with the amplifier circuit and connecting it to a pre-amplifier as constructed above amplifies the signal to around 5V which is analogous in nature.

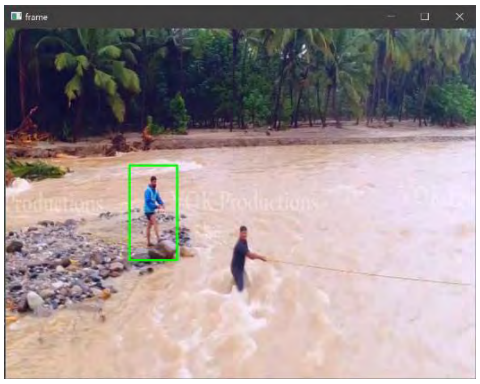

Figure 2.7. Propel detection output.

As seen in Figure 2.6, the OpenCV library code which we have used is being able to detect people stranded in the flood affected area. The above visual was outsourced, during the floods in Charmadi, India. The above picture is part of the outsourced video which we have fed to the code. Once the code detected people and marked a rectangle over them, we captured the same output as seen above.

This is the primary goal of the project which detects people in the flood affected area.

5. CONCLUSION

This UAV system for flood relief operation can fetch the data of human existence in a particular area using OpenCV code and the communication module helps in providing valuable information to the people stranded so that they take the necessary safety precautions and thereby help in proper conduct of flood relief operations. However due to the constraints in the computational power required to use advanced computer algorithms for people detection and the constraints in reducing the noise generated by the audio communication circuit we will need to enrich the features in the project before actual implementation and testing in the flood affected area.

6. REFERENCES

[1] Kirtan Gopal Panda, Shrayan Das, Debarati Sen, And Wasim Arif, Design and "Deployment of UAV-Aided Post-Disaster Emergency Network", Indian Institute of Technology Kharagpur, Kharagpur 721302, India, National Institute of Technology Silchar, Silchar 788010, India. This work was supported by the Ministry of Electronics and Information Technology, Government of India, through the program "Development of National Disaster Spectrum (NDS) and Disaster Communication Backbone Architecture (DiCoBA) with Prototype Development" under Grant 21(1)2015-CC & BT Dated 30-09-2015.

[2] https://bangaloremirror.indiatimes.com/bangalore/others/ham-radio-to-the-rescue/articleshow/70650174.cms

[3] https://thedatafrog.com/en/articles/human-detection-video/

Two-Quadrant Bidirectional DC to DC Converter: Simulation and Analysis for EV Application

Mahesh Kumar, Sujo Oommen, Burri Ankaiah, Lavanya Gowda Y S, Priyanka S L, Kavana H Y, Kavayashree N S.

Address: School Electrical and Electronics Engineering, REVA University Bengaluru, India

Email: email2maheshkumar@gmail.com

Abstract

The aim of this paper is to design and simulate a non-isolated bidirectional DC/DC converter which is used to charge the Electric Vehicles battery. A bi-directional DC-DC converter provides the required bidirectional power flow for battery charging and discharging based on the SoC of the battery and direction of the current flow. In this paper initially the basic behaviour of the charging and discharging module of the battery is designed to realize the behaviour of the battery as in how much constant voltage and the current is required. Analysing this data, a basic two quadrant non-isolated bidirectional DC/DC converter is simulated with constant PWM and SPWM Control techniques. The simulated non-isolated power converter topology is transformer-less, simple, low cost, light weight and has better efficiency and high reliability than isolated BDC. These converters are preferred in the high-power applications. The simulation is done using MATLAB/Simulink

Keywords: Bidirectional DC/DC Converter, Battery Charging, SPWM Techniques

1. INTRODUCTION

In the present scenario of hefty requirement of generation of electricity from renewable energy sources, and the energy storage with interfacing with the grid meant batteries has become a major challenge.[1] Energy storage meant batteries is most suitable for the renewable energy sources like solar, wind etc. A bi-directional DC-DC converter provides the required bidirectional power flow for battery charging and discharging. The duty cycle of the converter controls charging & discharging based on the state of charge of the battery and direction of

the current. [2] BDCs are gaining interest because of high demand of renewable energy sources and battery-operated electric vehicles. They provide power interchange between the dc bus and energy storage system.[3]

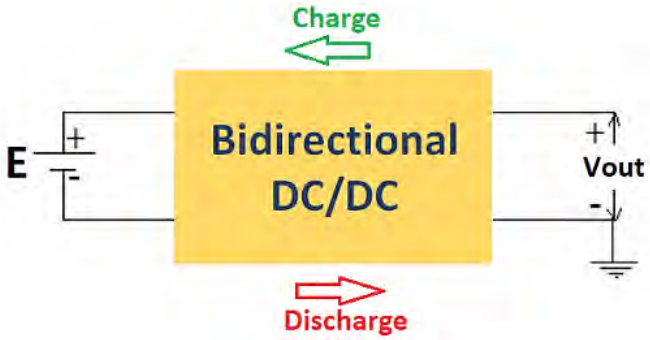

Figure 1.1. Concept of Bi-directional DC/DC converters

Bidirectional dc–dc converters allow transfer of power between two dc sources, in either direction. Due to their ability to reverse the direction of flow of current, and thereby power, while maintaining the voltage polarity at either end unchanged, they are being increasingly used in applications like dc uninterruptible power supplies, battery charger circuits, telecom power supplies and computer power systems.[4]

2. BATTERY CHARGING BEHAVIOUR

To realize the behaviour of the battery simple battery charging module is considered and shown in the Figure.2.1 for 24 V,10 Ah, Lithium-Ion Battery, thus this parameter will be helpful enough to realize the total constant voltage and current required for charging the battery also the replica of the same on the SOC of the battery. The initial and nominal SOC is kept 50%, during the initial battery charging the graph shown in Figure.2.1 is the rising slope w.r.t the charging time.

Figure 2.2. 24 V,10 Ah, Lithium-Ion Battery Charging Behavior

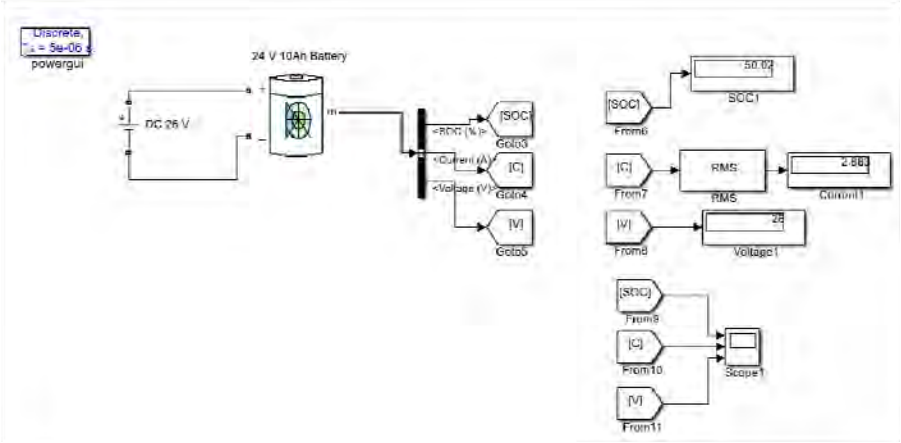

Figure 2.3. Simulation of 24 V,10 Ah, Lithium-Ion Battery Charging Behavior.

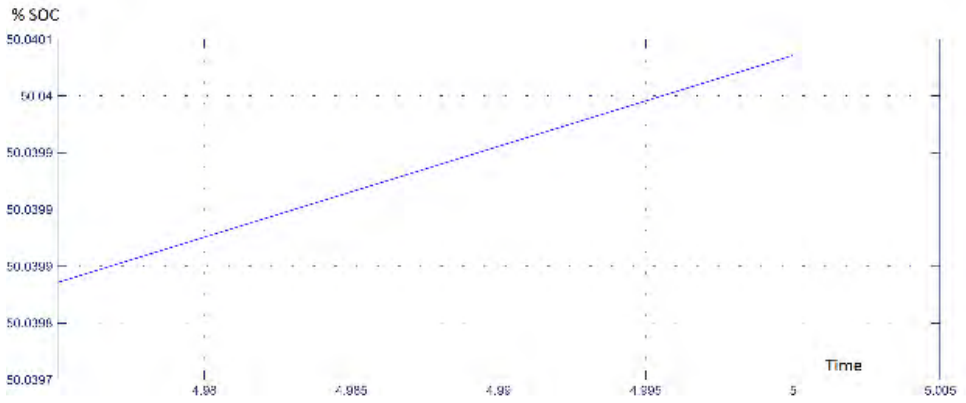

Figure 2.4 %SOC vs Time- Charging

Input Voltage	SOC (in %)	Current (in amp)	Time (in sec)
26	50.8	2.88	10
26	53.12	2.87	405
26	55.16	2.68	727
26	57.79	2.54	1047
26	60.54	2.25	1614

Table 2.1 CHARGING CHARACTERSTICS COMPARISOINS

Thus, this module gives the clarity that when the constant volage at-least 10% higher than the nominal voltage of the battery and the constant current the battery will then be able to charge at a stimulated duration. Hence to charge for 10% this module takes 26.9 mins.

3. BATTERY DISCHARGING BEHAVIOUR

The module shown in Figure.3.1 is the Battery discharging module. The initial and nominal SOC is kept 50%, during the initial battery charging the graph shown in Figure.2.1 is the rising slope w.r.t the charging time.

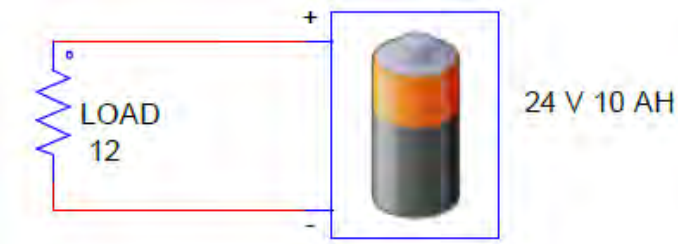

Figure 3.1 24 V,10 Ah, Lithium-Ion Battery Discharging Behaviour

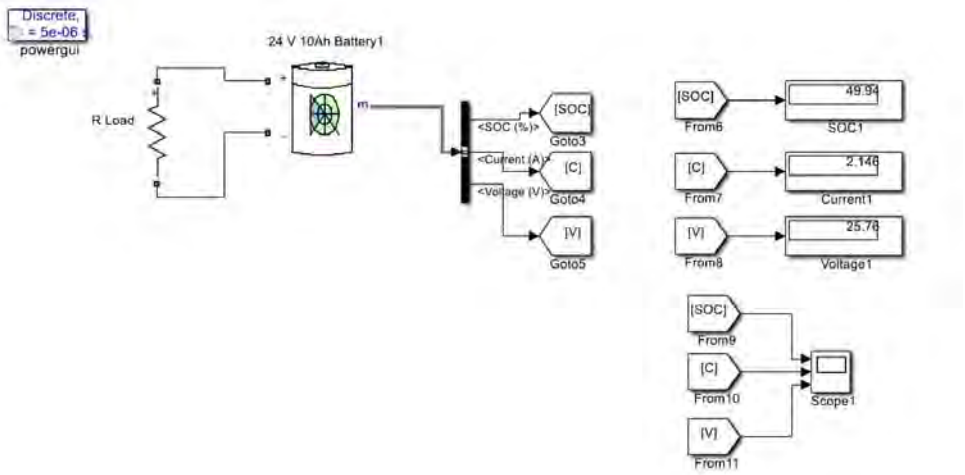

Figure 3.2 Simulation of 24 V,10 Ah, Lithium-Ion Battery Discharging Behaviour.

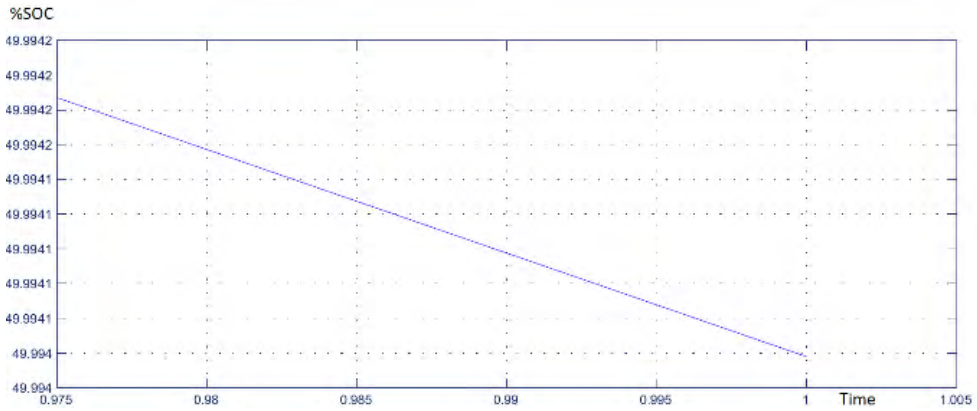

Figure 3.3. %SOC vs Time- Discharging

R Load	SOC (in %)	Current (in amp)	Time (in sec)
12 Ω	49.93	2.57	10
12 Ω	46.78	2.57	450
12 Ω	43.70	2.56	880
12 Ω	41.72	2.56	1160
12 Ω	40.00	2.56	1400

Table.3.1 discharging characteristics comparisons

In the discharging module the battery is getting used by the R load of 12 Ω, and the rating of the battery is 24 V 10Ah, hence the discharging for 10% is 23.3 minutes. A bi-directional DC-DC converter provides the required bidirectional power flow for battery charging and discharging. The duty cycle of the converter controls charging and discharging based on the state of charge of the battery and direction of the current.[1]

4. TWO - QUADRANT BIDIRECTIONAL DC/DC CONVERTER (PWM)

This circuit is used in the project as such to provide both the charging and the discharging options together through the buck and the boost operation.

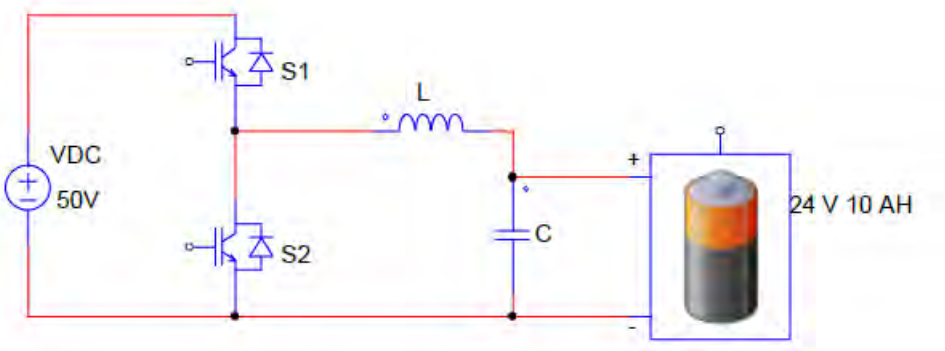

Figure 4.1. Basic Non-isolated Bidirectional Converter

The basic 2 quadrant bi-directional DC-DC converter is simulated with normal PWM technique.

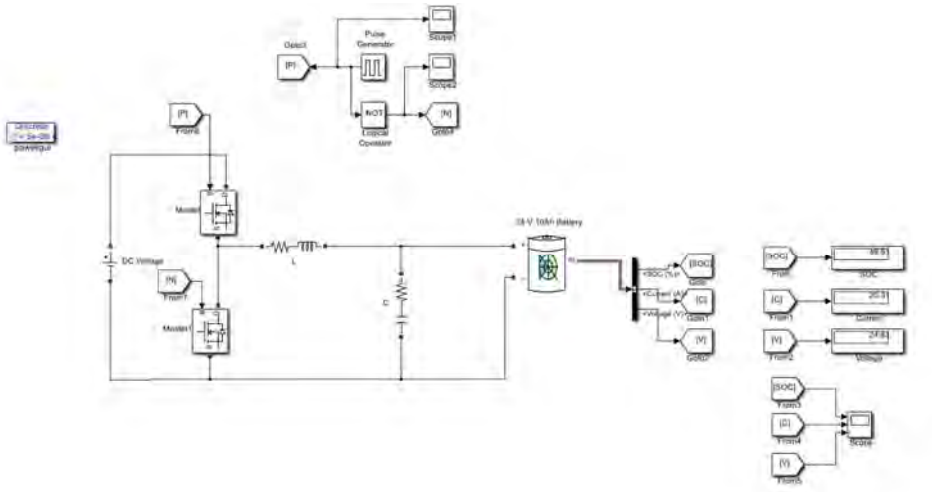

Figure 4.2. Simulation of 24 V,10 Ah, through basic non-isolated bidirectional converter

A. Buck mode (Forward Operation/Charging):

In Buck mode, the output voltage is less than the input voltage. To charge the battery from the DC input voltage, switch S1 is triggered and S2 is kept off as shown in Figure. 4.1 When switch S1 is ON, the input current rises and flows through S1 and L. When S1 is OFF, the inductor current falls until the next cycle. The energy stored in inductor L is supplied for charging the battery.[2]

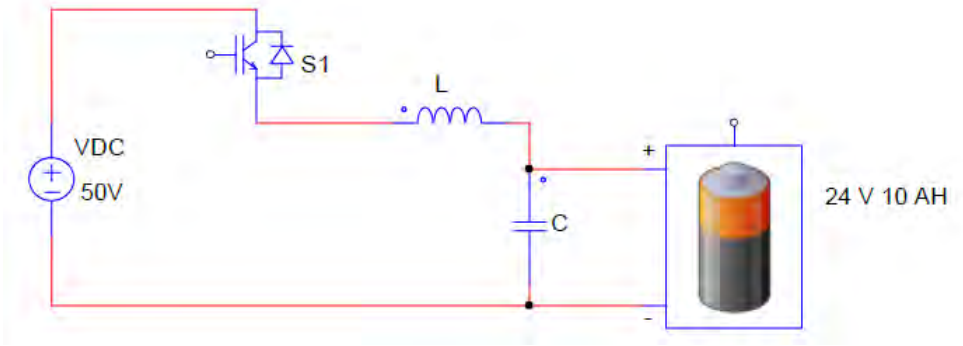

Figure 4.3. Buck Mode Operation.

The DC voltage is assumed to be 51 V and battery voltage is 24 V The design of Buck converter is as shown below:

i) Duty cycle

The duty cycle of the switch with estimated efficiency of 95% is given by equation.

$$D = \frac{Vout}{Vin * \eta} = \frac{24}{50 * 0.9} = 0.54$$

Input Voltage	SOC (in %)	Current (in amp)	Time (in sec)
50	50.8	6.88	90
50	53.12	6.87	140
50	55.16	6.68	370
50	57.79	7.54	419
50	60.54	7.25	465

Table 4.1. charging characteristics (BDC- PWM)

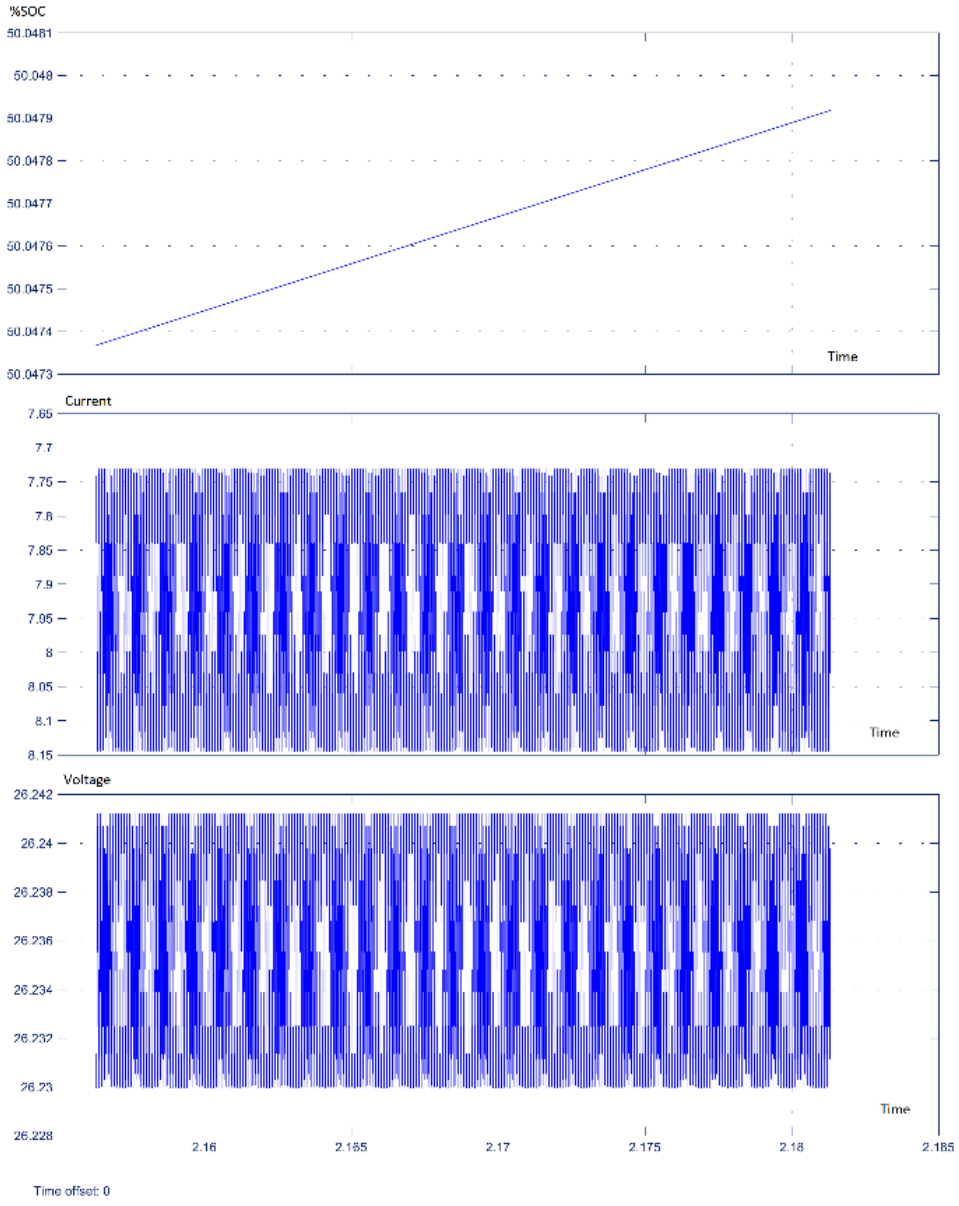

Figure 4.4. Simulation of 24 V,10 Ah, through basic non-isolated bidirectional converter.

The Figure 4.4 Shows the graph of discharging in buck mode. In the discharging module the battery is getting used and the rating of the battery is 24 V 10Ah, hence the discharging for 10% is 7.73 minutes.

B. Boost mode (Backward Operation/Discharging)

In Boost mode, the output voltage is more than the input voltage. The battery discharges power to the load with switch S2 is triggered and S1 is off. The operation of this mode is shown by Figure 4.1. When switch S2 is ON, the input current rises through inductor L and S2. When S2 is OFF, the inductor current falls until the next cycle. The energy stored in inductor L flows through the load.[2]

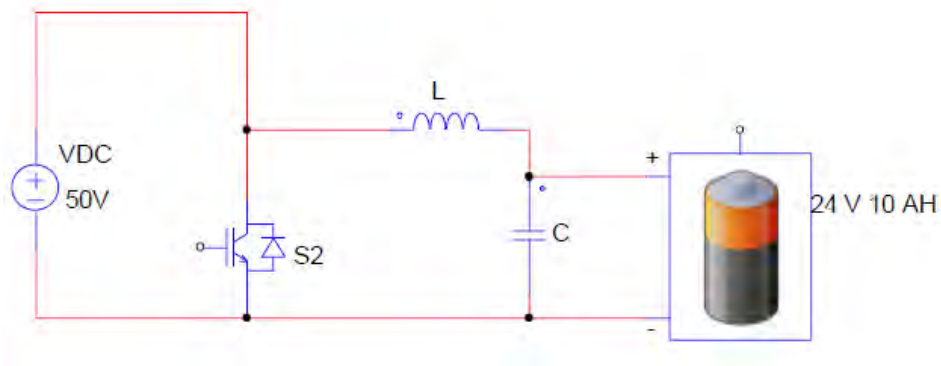

Figure 4.4. Boost mode operation.

$$D = 1 - \frac{Vin * \eta}{Vout} = \frac{50 * 0.9}{24} = 0.54$$

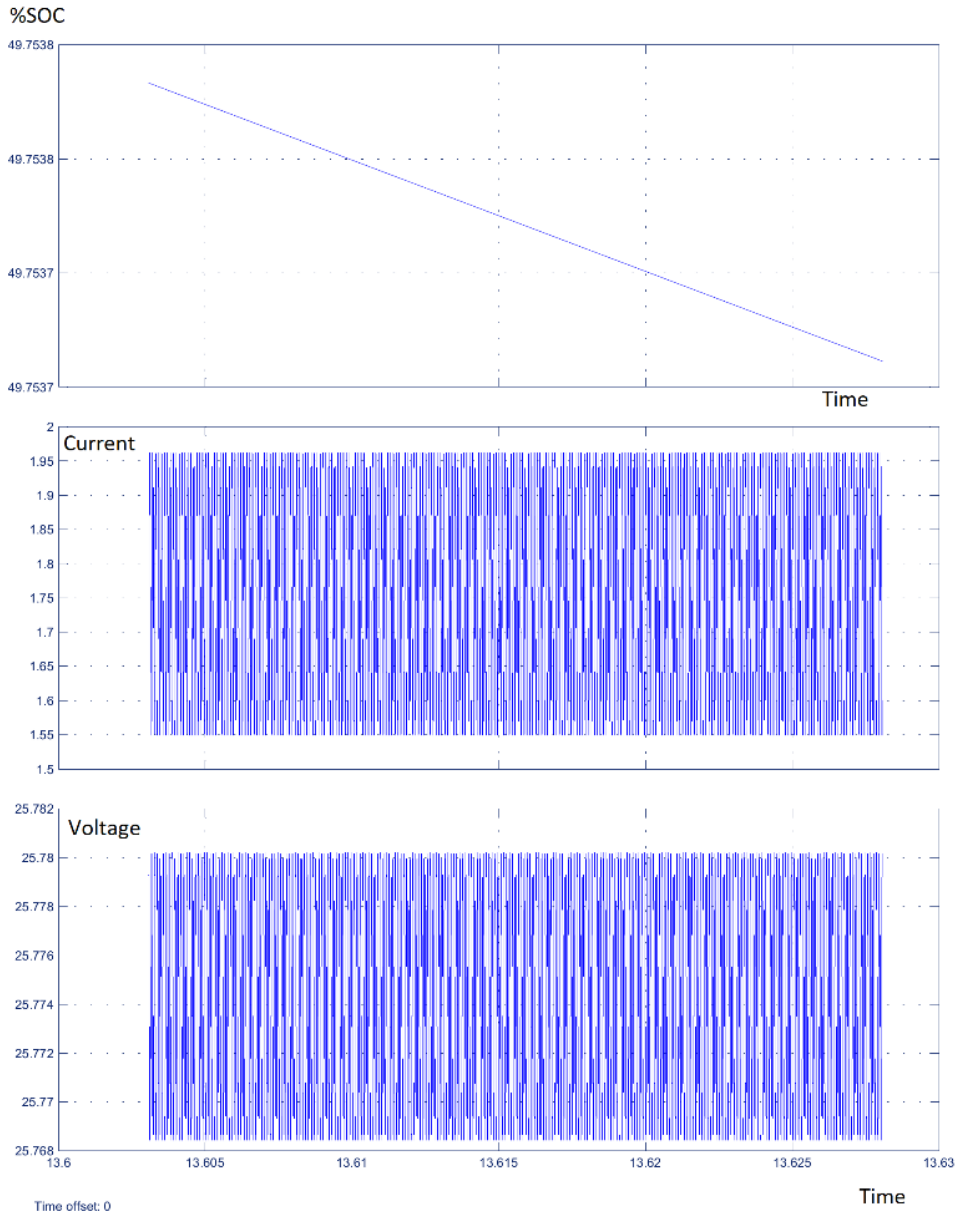

Figure 4.5. Simulation of 24 V,10 Ah, through basic non-isolated bidirectional converter

Input Voltage	SOC (in %)	Current (in amp)	Time (in sec)
50	50.8	3.8	90

50	45.6	3.7	140
50	43.70	3.71	622
50	41.72	3.6	809
50	40.00	3.5	905

Table 4.2 discharging characteristics (BDC-PWM)

The Figure 4.5 Shows the graph of charging in boost mode. In the discharging module the battery is getting used and the rating of the battery is 24 V 10Ah, hence the discharging for 10% is 15.73 minutes.[12]

5. TWO QUADRANT BIDIRECTIONAL DC/DC CONVERTER (SPWM)

The Sinusoidal PWM (SPWM) control is the most efficient PWM Control Technique, the sinusoidal AC voltage reference is compared with the high-frequency triangular carrier wave in real time. After comparing, the switching states for each pole can be determined based on the following:[12]

- Voltage reference > triangular carrier: upper switch is ON
- Voltage reference < triangular carrier: lower switch is ON.

The same comparison is shown in Figure 5.1 The sinusoidal waveform is compared with the repetitive triangular carrier waveform of a switching frequency of 10kHZ.

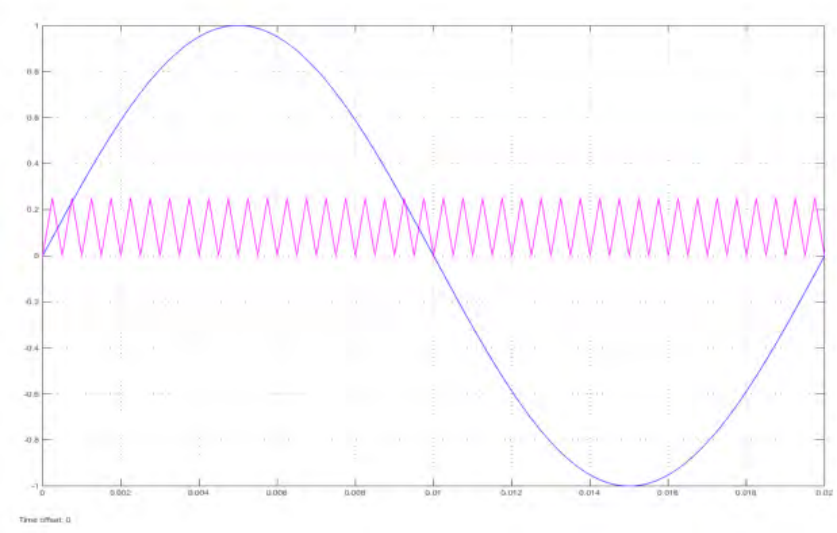

Figure 5.1. SPWM Career Signal Comparison (POD)

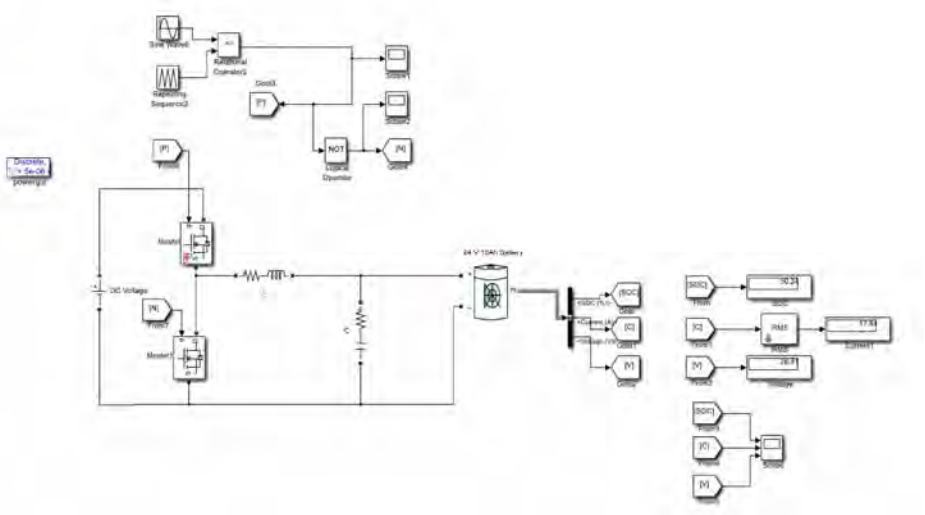

Figure 5.2. Simulation of 24 V,10 Ah, through basic non-isolated bidirectional converter (SPWM Control).

Finally, the various comparisons are done for the type of control techniques used in the circuit. Hence this clarifies that the SPWM control technique will definitely save the effective time in charging. This can be further helpful for charging the battery. [12]

Type of Control	SOC (in %) for 10%	Mode	Time (in sec)
PWM	50.8 to 60.54	Charging	465
SPWM	50.12 to 60.81	Charging	358
PWM	50.3 to 40.14	Discharging	905
SPWM	50.3 to 40.14	Discharging	1204

Table 5.1 Comparisons of different control techniques

Switching Device	IGBT
Input Voltage	50 volts (D.C)
Output Voltage	26 volts (D.C)
Output Current	1.9 Amp
Output Power	49.4W
Switching Frequency	10kHz

Capacitance	1000μF
Magnetizing Inductance	1mH

Table 5.2. Circuit parameters of the dc-dc converter (PWM)

6. CONCLUSION

In this paper the basic behaviour of the charging and discharging module of the lithium-ion battery is designed and simulated to understand and to realize the battery response as in how much constant voltage and the current is required.

Analysing this data, a basic two quadrant non-isolated bidirectional DC/DC converter is simulated with constant PWM and SPWM Control techniques. The reading of the simulation is than compared for determination of faster response from the SPWM technique. This paper will be helpful for researchers and scholars in the field of battery charging and battery management system for EV's

7. REFERENCES

[1] Manu Jain, M. Daniele, and Praveen K. Jain, "A Bidirectional DC–DC Converter Topology for Low Power Application" IEEE TRANSACTIONS ON POWER ELECTRONICS, VOL. 15, NO. 4, JULY 2000.

[2] Ned Mohan, Tore M. Undeland, William P. Robbins, "Power Electronics: Converters, Applications, and Design", Wiley; Third edition (16 January 2007).

[3] Sunny Kumar, Maheswarapu Sydulu, "Bidirectional DC-DC Converter for Integration of Battery Energy Storage System with DC Grid" in International Journal of Industrial Electronics and Electrical Engineering, ISSN: 2347-6982 Volume- 2, Issue- 3, March-2014.

[4] Daniel Celius Zacharek, Filip Sundqvist, "Design of Bidirectional DC/DC Battery Management System for Electrical Yacht" LiTH-ISY-EX-ET--18/0475—SE.

[5] Lizhi Zhu, "A novel soft-commutating isolated boost full-bridge ZVS-PWM dc-dc converter for bi-directional high power SCEECS 2012 applications"2004 35th annual IEEE power electronics specialists conference.

[6] Shigenori Inoue, Hirofumi Akagi, "A bi-directional dc–dc converter for an energy storage system with galvanic isolation" IEEE transactions on power electronics, vol. 22, no. 6, November 2007.

[7] M. Jain, M. Daniele, and P. K. Jain, "A bidirectional dc-dc converter topology for low power application," IEEE Trans. Power Electron., vol.15, no. 4, pp. 595–606, Jul. 2000.

[8] A. D. Swingler and W. G. Dunford, “Development of a bi-directional dc/dc converter for inverter/charger applications with consideration paid to large signal operation and quasi-linear digital control,” IEEE Power Electronics Specialists Conf. (PESC), 2002, vol. 2, pp.961–966.

[9] Y. Hu, J. Tatler, and Z. Chen, “A bi-directional dc/dc power electronic converter for an energy storage device in an autonomous power system,” in Proc. Power Electron. Motion Cont. Conf. (IPEMC), 2004, vol. 1, pp. 171–176.

[10] Chan, C.C. "An overview of electric vehicle technology,”. Proc. of the IEEE, vol. 81, no. 9, pp. 1202-1213, Sept. 1993.

[11] Haghbin, S, Khan, K., Lundmark, S, Alaküla, M., Carlson, O, Leksell, M.; Wallmark, O, “Integrated chargers for EV’s and PHEV’s examples and new solutions,” Electrical Machines (ICEM), 2010 XIX International Conference on, pp. 1-6. Sep. 2010.

[12] Power Electronics D. Hart (McGraw Hill, 2010) BBS

[13] W. Yu, H. Qian, and J. S. Lai, “Design of high-efficiency bidirectional DCDC converter and high-precision efficiency measurement,” IEEE Trans. Power Electron., vol. 25, no. 3, pp. 650–658, (2010)

1

Implementation of advanced 3 in 1 smart meter using GSM module

Deepa K.R, Ashwini Kumari P, Jhansi K, Chaitra A S, Ravishankar H, Swetha G
deepa.kr@reva.edu.in

School of Electrical and Electronics Engineering,REVA University,Bangalore, India 560064

Abstract

Due to the COVID-19 pandemic, humans confronted the problem with electrical billing Machine. The system generated billing gadget is set in this sort of way that its far taken either month-to month/bimonthly. But, this time the bill has been generated after 65 to 67 days due to COVID-19 lockdown. So there has been a soar inside the slab costs, this made customers to be charged greater than what's to be paid. To overcome this problem, proposed advanced 3 in 1 smart meter utilizing GSM. This paper aims at timely measurement of electricity, gas and water in smart way, Whose objective is to gather the meter perusing consequently sending messages from the Modem to remote mobile phone where the process of noting down the meter readings is easier and accurate. Besides, the consumer can access the notification regarding the scenario with power from any place. GSM recipient consists of data set that functions as a charging point that is connected to a system from the opposite end. Occasionally from the GSM empowered energy meter's pursued live meter is directed back to the charging point. Proposed system measures electricity as well includes a water and gas billing system. The framework exhibited its ability to monitor the Energy utilization, send the notification to

An Edited Volume, 1–9.

the mobile phones when the breaking point is approached, using effectively by rebooting, just by getting to a GSM-based cell phone.

Keywords: GSM-based energy meter, GSM-based Water billing meter, Gas Leakage Detection, Automatic meter reading (AMR).

1.1 Introduction

Life's content is maintained by an indispensable requirement that is electricity. For around 10 years advanced energy meter innovations have been explored. Over the decades, a lot of advancements took place that decreased hefty and complex meters to simple measuring and billing meters by improving highlights, determination [1]. Nowadays, due to the immense distinction in energy creation and utilization, energy consumption and energy conveyance have gotten a major subject for conversation [2]. Then again, customers are likewise not happy with the administrations of force organizations [3]. More often than not they have grumblings in regards to factual mistakes in the month-to-month bills. Advanced precise billing smart meter scan undoubtedly take readings, significantly decline the bill of a client by cautioning the client with an alarm message prior to multiplying the unit charge and lessen the squandering of force. At present, the meter consists of a round about metal strip that pivots and as per that revolution; energy consumption is calculated. But, the consumption of energy is the main working of the meter. With this are aiming to get the month-to-month energy utilization from a distant place to an incorporated office [4]. Along these lines, we can decrease the human endeavors expected to record the meter readings which are recorded by visiting every home exclusively till today. It's difficult to screen the changing most outrageous interest of users in the circulation organizations of the current billing system. The user is confronting issues like getting due bills for charges that have effectively been paid just as helpless dependability of power supply and quality regardless of whether the bills are paid consistently. The solution for this load of issues is to monitor the customer's heap on a convenient premise, which will have held to guarantee exact charging, track the greatest interest, and checking set value [5-9]. These are generally the features to be considered for arranging a capable energy charging framework. Similarly, Water distribution and its control over the billing cycle is one of the most challenging tasks for the government [10]. Municipal Corporation. Water Distribution System is a manual system and it is difficult to monitor the consumption of water centrally. The existing

system fails to monitor the quantity of water. This proposed system i.e., the advanced 3 in 1 smart meter is fully automated. Where it receives real-time data of consumption and can control the valve to restrict the flow of water. Consumers can interact with the mobile application to monitor the usage and for payment of bills or to stop or start the service. And these water meters are connected via GSM which will take the data from that meter and send it to the server. It also consists of Flow Sensor, Micro controller [11, 12, 13], and GSM module. This system enables respective departments to access the meter recordings monthly, avoiding the traditional practice. The value will be set previously; when this value gets closer the user receives the message of alert in a verbal format via GSM.A Smart Meter works by estimating the electrical flow stream and voltage at standard stretches and afterward adding this up to ascertain the force Ute- lazed savvy Meter works by estimating the electrical flow stream and voltage at ordinary spans and afterward adding this up to figure the force utilized. Additionally, for gas, the stream is estimated at customary stretches. This information can be seen on your mobile application and sent to your supplier. This meter not only calculates the consumption of gas but also detects and prevents the leakage of gas. Various communications technologies might be utilized in various types of premises for the Home Area Network to convey and various advances will be utilized in various pieces of the nation to permit the Wide Area Network to send information to and from the organization giving the correspondences.

1.2 Methodology

The current framework presents another technique for Programmed meter perusing electronically and communicating to base camp for additional handling and consumers. This aids in lessening the human mistakes that happen in the current meter perusing frameworks blend of both technologies: GSM networks and embedded systems. The proposed system consists of three main components: Electricity, Water and Gas. Allow us to think about an illustration of Electricity; here we are associating the Energy Meter between main supply and load, by which Microcontroller will be able to measure the energy units consumed by the consumer. When the various appliances of the household consume energy, the energy meter reads the reading continuously and this consumed load can be seen on meter. We can see that the LED on meter continuously blinks which counts the meter reading and observed that the LED of the meter constantly sq units , which checks the meter perusing. The units are checked based on the number of times it blinks. Typically, 3200

flickers are one unit. In this task, we are attempting to create, a framework where PIC16F877A goes about as the fundamental regulator, which constantly monitors the advanced building meter. According to the flickering of the LED on this meter, the PIC16F877A will gauge the unit utilization. The deliberate perusing with the estimation of the expense will be consistently shown on the web that we have developed. Communication medium depends on the current GSM network. The Meter billing and control operations will be performed simply using the Short Messaging System service that is available over GSM. For this, no alteration or even customization is required in the actual network. The threshold value can be set according to the user's necessity. At the point when the users perusing will be close reaching the set edge esteem it's anything but a warning worth to the customer Via GSM. Above limit, esteem warning builds mindfulness among the buyer about this energy. Similarly, Gas and flow meters are used to check how much amount of gas and water has been used based on that bill has been generated. The Micro controller processes the measure of energy, water, and gas burned through. Then, at that point, the determined quantities are sent immediately by means of GSM to the main station and the essential updates are performed.

1.3 Block Diagram

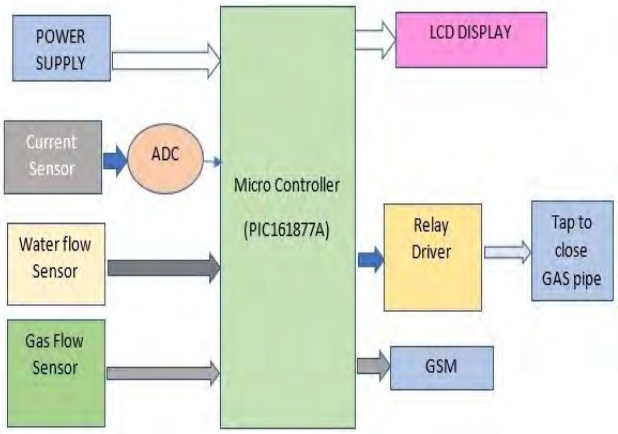

Figure 1.1 Block Diagram of the proposed system.

The micro-controller used in this is PIC16f877A to which the power supply is connected. The current sensor, water flow sensor, and gas sensor are

connected to the micro controller, where the current sensor is connected via ADC. Once the operation takes place the reading of the current, water, and gas is displayed on the LCD which is again connected to the micro controller, when there is a gas leakage, the gas sensor will detect and send it to the micro controller, where the relay driver helps to increase the voltage and closes the tap of gaspipe , all these information will be sent to the mobile phone via GSM. Fig 1.1 shows the block diagram of the proposed system.

1.4 Flowchart

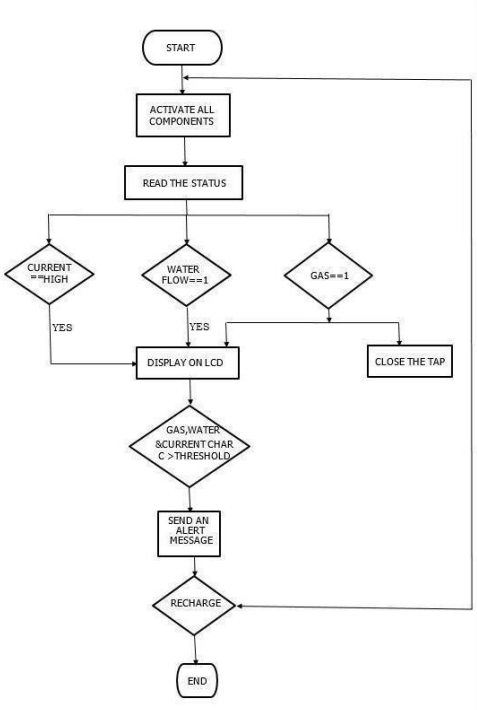

Figure 1.2 Flow Chart of the proposed system.

In fig 1.2, it explains the working of the system. The system starts and activates all the components as soon as it is switched on. It reads the status, if the electricity, water, and gas are higher than the previously set threshold value then it will be displayed on the LCD and also sends an alert message to

our phones via GSM if it exceeds the set values the flow of the current, water, and gas will stop. If the gas leakage is detected it will close the pipe.

1.5 Hardware Components

Table 1.1 Specification of the Components

Sl. No	**Components**	**Specification**
1	PIC16F877A	Operating voltage : 2 to 5.5 Program Memory: 14KB CPU Speed (MIPS): 5 MIPS RAM Bytes: 368
2	Power supply	Output voltage: 12 V
3	Gas sensor	Detection Range: 100 - 10,000ppm Fast Response Time: ¡ 10s Heater Voltage: 5.0V
4	LCD	Display: 16×2 characters Operating Temp : (0-5 0C) Power supply: 5.0 V
5	Water Level Sensors	Voltage Range: 5 to 18V DC Max current draw: 15mA at 5V Flow Rate: 1 to 30 Liters/Minute. Max water pressure: 2.0 MPa
6	Current sensors	Supply Voltage: 4.5V 5.5V DC Measure Current Range: 30A 30A Sensitivity: 100mV/A.
7	GSM Modem SIM 300	Operating Voltage: 7 15V

1.6 Software Components

In this paper, we have used embedded C programming and MPLAB IDE, and PICkit 2 software.

1.7 Results

The paper aims at, generate billing system and notify the status of electricity, water, and gas. The electricity bill will be generated automatically every month and will be updated to the concerned department through GSM and

the bill generated will be sent to consumers through SMS. Similar to the electricity bill the water and gas bills are generated. The amount of water consumed by the customers will be recorded in the meter and the meter sends the information to the concerned department through GSM and they, in turn, send the bill to the consumers. Currently, in most parts of India, the gas will be delivered in cylinders to the consumers. In the coming future, gas pipelines will be established similar to water and the gas will be delivered through these pipes. Then the consumption of the gas must be recorded using a meter. So, this advanced meter is automated to send the gas usage details to the concerned department and they in turn send to the consumers through GSM. Another advantage of this advanced meter is the detection of gas leakage in the pipelines and taking preventive measures before the issue gets serious. System facilitates inbuilt prepaid billing system for future, Where the supply can be stopped immediately as and when the amount is over. Fig 1.3 shows the hardware set up of advanced 3 in 1 smart meter and fig 1.4 shows the message delivered to consumer notifying the status of recharging, running out of cost, renew electricity bill and gas leakage detected.

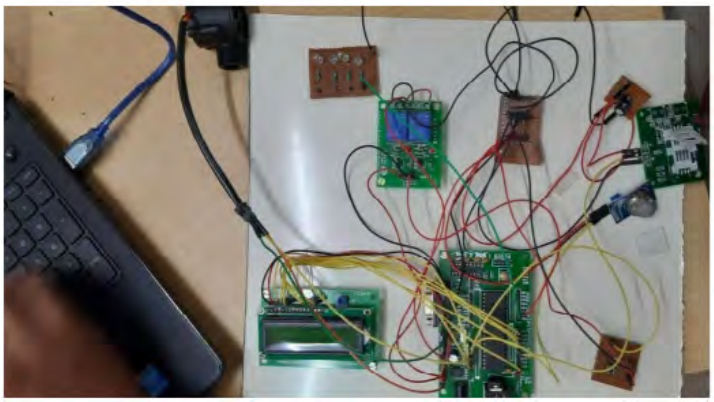

Figure 1.3 Proposed hardware system

1.8 Conclusion

The proposed system considers the existing issues and builds an efficient and effective advanced 3 in 1 smart meter for generating electricity, water and gas bill automatically every month and will be updated to the concerned department through GSM and the bill generated will be sent to consumers

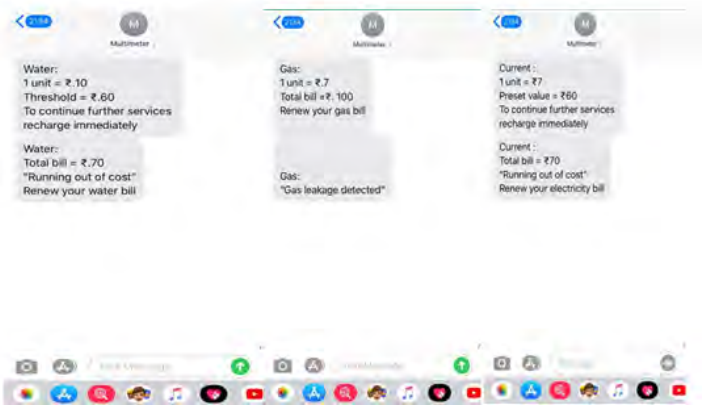

Figure 1.4 Message delivered to consumer

through SMS. This metering system enhances the efficiency and effectiveness and timely data availablity to consumer. Along with this, Detection and Prevention of Gas Leakage are also carried out as an additional necessity by the system. To conclude that, there can be no conclusion to the human race's constant striving for Excellence and the evolution of technology. The future advancements of this unassuming thought of our own can be the acknowledgment of a solitary chip arrangement that will impregnate inside itself a force re-estimating unit, alongside a GSM-based module. This will not only reduce the size of the meter but will also make it more robust and commercially available. The tedious job of Energy Management at each sub- station can also be simplified by using this smart metering system, the conglomerated the modern technologies of SIM cards and meters into a single unit believing that this will revolutionize the power scenario in our country.

References

[1] Kumari, P. Ashwini, and P. Geethanjali. "Parameter estimation for photovoltaic system under normal and partial shading conditions: A survey." Renewable and Sustainable Energy Reviews 84 (2018): 1-11.

[2] Kumari, P. Ashwini, and P. Geethanjali. "Artificial Neural Network-Based Smart Energy Meter Monitoring and Control Using Global System for Mobile Communication Module." In Soft Computing for Problem Solving, pp. 1-8. Springer, Singapore, 2020.

[3] Brinda, S., Vishal Kumar Sah, Jaladi Harish, U. Akshay, Vishal Deo Mahto, and Swetha Umapathy. "Smart Energy Meter." International Journal of Engineering Science and Com-

puting 8, no. 3 (2018).W.-K. Chen, Linear Networks and Systems (Book style). Belmont, CA: Wadsworth, 1993, pp. 123–135.

[4] Indra, Win Adiyansyah, Fatimah Bt Morad, Norfadzlia Binti Mohd Yusof, and Siti Asma Che Aziz. "GSM-Based Smart Energy Meter with ArduinoUno." International Journal of Applied Engineering Research 13, no. 6(2018): 3948-3953.

[5] Chandwani, K. S., Abhaya Gulhane, Neha Mahakalkar, Rasika Shivhare, and Payal Mankar. "IoT based Water Distribution Control and Monitoring System."

[6] Leelavati, M., and K. Aswini. "Smart Energy Meter with Reading Indication using GSM." IRJET 2 (2015).

[7] Jadhav, A. N., Y. T. Suryavanshi, B. K. Dewar, and M.

[8] M.Kumbhar."Automatic electric meter reading monitoring system using GSM." Inter. Res. J. Eng. Technol 3, no. 5 (2016): 1025-1028.

[9] Chaudhari, Sneha, Purvang Rathod, Ashfaque Shai kh, Darshan Vora, and Jignesha Ahir. "Smart energy meter using Arduino and GSM." In 2017 International Conference on Trends in Electronics and Informatics (ICEI), pp. 598-601. IEEE, 2017.

[10] Pandya, Raj. Mobile and personal communication systems and services. Wiley-IEEE Press, 1999.

[11] Mahfuz, Nagib, Mehen Nigar, and Nawshin Ulfat. "Smart Energy Meter and Digital Billing System for Bangladesh." In 2020 11th International Conference on Computing, Communication and Networking Technologies (ICCCNT), pp. 1-4. IEEE, 2020.

[12] Ouyang, Zengkai, Qing Xu, Shuangshuang Zhao, Jian Liu, Yunan Zhu, and Zhengqi Tian. "Design of Multi- meter Integration Scheme Based on Electricity Information Acquisition System." In 2018 5th IEEE International Conference on Cloud Computing and Intelligence Systems (CCIS), pp. 1053-1055. IEEE, 2018.

[13] Amruta, K., and S. G. Hate. "Implementation of Automatic Meter Reading System Using Wireless Sensor Network." International Journal of Advanced Research in Computer Engineering Technology 2, no. 12 (2013): 3030-3032.